EXPERIMENTAL EVALUATION OF NEW GENERATION AGGREGATE IMAGE MEASUREMENT SYSTEM

A Thesis

by

LESLIE LEIGH GATES

Submitted to the Office of Graduate Studies of
Texas A&M University
in partial fulfillment of the requirements for the degree of

MASTER OF SCIENCE

May 2010

Major Subject: Civil Engineering

EXPERIMENTAL EVALUATION OF NEW GENERATION AGGREGATE

IMAGE MEASUREMENT SYSTEM

A Thesis

by

LESLIE LEIGH GATES

Submitted to the Office of Graduate Studies of
Texas A&M University
in partial fulfillment of the requirements for the degree of

MASTER OF SCIENCE

Approved by:

Chair of Committee,	Eyad Masad
Committee Members,	Amy Epps Martin
	Mahmoud El-Halwagi
Head of Department,	John Niedzwecki

May 2010

Major Subject: Civil Engineering

ABSTRACT

Experimental Evaluation of New Generation Aggregate Image Measurement System.

(May 2010)

Leslie Leigh Gates, B.S., Texas A&M University

Chair of Advisory Committee: Dr. Eyad Masad

The performance of hot mix asphalt, Portland cement concrete, unbound base, and subbase layers in a pavement are significantly affected by aggregate shape characteristics. Classification of coarse and fine aggregate shape properties such as shape (form), angularity, and texture, are important in predicting the performance of pavements. Consequently, there is a need to implement a system that can characterize aggregates without the limitations of the current aggregate classification standards. The Aggregate Image Measurement System (AIMS) was developed as a comprehensive and capable means of measuring aggregate shape properties.

A new design of AIMS will be introduced with several modifications to improve the operational and physical components. The sensitivity, repeatability, and reproducibility are analyzed to evaluate the quality of AIMS measurements. The sensitivity of AIMS is evaluated and found to be good for several operational and aggregate parameters.

Important operational and environmental factors that could affect the AIMS results are identified and appropriate limits are recommended. AIMS is able to control normal variations in the system without affecting the results. A comprehensive analysis is conducted to determine the repeatability and reproducibility of AIMS for multiple users and laboratories. Single-operator and multi-laboratory precision statements are developed for the test method in order to be implemented into test standards.

DEDICATION

This thesis is dedicated to my loving husband, Brian; my mother, Lou Ellen; and my family. Without their love, support, and encouragement, I would not be the person that I am today. This thesis is also dedicated in memory of Lewis C. Norton.

ACKNOWLEDGEMENTS

Many people deserve my appreciation and thanks. I would like to express my special thanks to Dr. Eyad Masad for all of the opportunities that he has provided to me throughout my time at Texas A&M University. I am grateful for his guidance, knowledge, encouragement and support throughout my undergraduate and graduate studies. Additionally, I would like to thank Dr. Amy Epps Martin and Dr. Mahmoud El-Halwagi for serving on my committee and for helping with the review of this thesis.

I would also like to thank the Federal Highway Administration and Highways for LIFE program for funding my research project. Special thanks to Mr. Roger Pyle, Mr. Ed Kaltenbaugh, and Mr. Steve Williams at Pine Instruments Co. for their help with technical and programming issues and testing and data collection process. I would like to thank all of the participating State, Federal, and Canadian laboratories for their help with testing and data collection process.

Also, I would like to thank Enad Mahmoud for his guidance and assistance throughout my research. Special thanks to Stephen Kirksey and Ashlyn Kelbly for their tremendous help in testing, data collecting, and traveling.

TABLE OF CONTENTS

Page

Page

LIST OF FIGURES

Page

Page

Page

Page

Page

Page

LIST OF TABLES

Page

Page

Page

Page

Page

CHAPTER I

INTRODUCTION

Aggregate shape characteristics for fine and coarse aggregates have a significant effect on the performance of hot mix asphalt, Portland cement concrete, unbound base, and subbase layers in a pavement. These physical aggregate characteristics of shape, texture, and angularity affect the overall performance of the pavement by influencing the engineering properties such as workability, durability, shear resistance, stiffness, and fatigue response. Identifying and understanding the influence of the shape characteristics on the behavior of pavements is essential for improving performance. The current standard aggregate test methods are limited in their ability to directly and objectively characterize aggregate shape characteristics.

Many test methods have been developed recently with the objective of measuring these characteristics accurately and rapidly at various research institutions. The test method that has been shown to be the most comprehensive and capable of measuring the aggregate characteristics is the Aggregate Image Measurement System (AIMS).

This thesis follows the style and format of *Journal of Materials of Civil Engineering*.

AIMS was developed to directly measure aggregate shape characteristics that influence pavement performance. The design of AIMS was made to be functional enough to measure the distribution of angularity, texture, and dimensions for a range of aggregate sizes.

This thesis presents the features of a new design of AIMS and a comprehensive evaluation of the quality of the AIMS measurements. The new AIMS system is calibrated to ensure that it yields the same results as the old design. The new system is also analyzed by measuring the sensitivity, repeatability, and reproducibility of the measurements. The sensitivity evaluation is aimed at identifying important operational and environmental factors that might cause significant variability in the AIMS results and establishing appropriate ranges of the parameters in question. The repeatability and reproducibility are quantified by developing two different precision estimates (single-operator and multi-laboratory) of the test method.

OBJECTIVES OF THE STUDY

The primary objective of this thesis is to evaluate the new design of the AIMS. This objective is achieved through the following tasks:

- Identify hardware and software differences between the old and new designs of AIMS.
- Calibrate the two AIMS systems to ensure they are producing similar results.

- Conduct statistical measurements of the sensitivity of AIMS.
- Identify important operational and environmental factors which might cause significant variability in the results to establish appropriate ranges of the parameters in question through a ruggedness analysis.
- Determine the repeatability and reproducibility of AIMS for multiple users and laboratories from an interlaboratory study. The results can then be used to develop precision statements for the test method.

THESIS ORGANIZATION

This thesis is organized into six chapters. Chapter I introduces the problem statement, the objectives, and outline of the thesis. Chapter II consists of a literature review describing the influence of aggregate characteristics on performance of different types of pavements including hot mix asphalt, Portland cement concrete, and unbound layers. A summary of various test methods used for measuring the aggregate shape characteristics is also presented. The review includes a description of the components and the working principles of AIMS. Chapter III describes the new design of AIMS and compares it with the old system. The sensitivity of AIMS was evaluated statistically in terms of operator placement of particles, the ability of AIMS to differentiate between aggregate sources, and the number of particles in a sample to represent an aggregate source. Chapter IV identifies significant operational and environmental factors which might cause significant variability in the results. The results of the ruggedness study conducted following ASTM standards (ASTM C 1067-00 "Conducting a Ruggedness or Screening Program for Test Methods for Construction Materials" and ASTM E 1169-07 "Standard Practice for Conducting Ruggedness Tests") are used to establish appropriate ranges of the parameters in question. Chapter V quantifies the repeatability and reproducibility of AIMS for multiple users and laboratories in order to develop a precision statement for the test method. This statement was found following ASTM C 802–96, "Standard Practice for Conducting an Interlaboratory Test Program to Determine the Precision of Test Methods for Construction Materials" and ASTM C 670–03, "Standard Practice for Preparing Precision and Bias Statements for Test Methods for Construction Materials." Chapter VI includes the conclusions and recommendations of this thesis.

CHAPTER II

LITERATURE REVIEW

INTRODUCTION

This chapter focuses on the significance of aggregate characteristics in influencing pavement performance. Several available test methods that are used for measuring aggregate shape characteristics will be briefly described. An emphasis will be made on the features of the Aggregate Image Measurement System (AIMS).

AGGREGATE PROPERTIES AFFECTING PAVEMENT PERFORMANCE

The performance of a pavement depends primarily on the material composition of the mixture. The performance of hot mix asphalt (HMA) pavements, Portland cement concrete (PCC) pavements, and unbound layers are affected by aggregate shape characteristics. These aggregate shape characteristics are angularity, texture, and particle shape, which can vary widely based on type and source of aggregates and processing techniques (Masad et al. 2007).

Asphalt pavement properties such as shear resistance, fatigue response, skid resistance, workability, and durability, are affected by aggregate shape characteristics (Masad et al. 2007). Aggregate shape properties were found to influence the stiffness and fatigue response of HMA mixtures (Monismith 1970). For thick pavements with a dense gradation, rough textured aggregates were suggested to increase mixture stiffness and fatigue life. Smooth textured aggregates were recommended for thin pavements since these aggregates produce less stiff mixtures resulting in an increased fatigue life (Monismith 1970). The presence of flat and elongated particles affects the durability of HMA mixes because these particles tend to break down during production and construction (Kandhal and Parker 1998).

Coarse aggregate properties affect the performance of PCC pavements in terms of transverse cracking, faulting of joints and cracks, punch outs, and spalling. A high percent of flat and elongated aggregates could cause decreased workability, resulting in voids and incomplete consolidation of the mix. Faulting in jointed concrete pavements and punchouts in continuously reinforced concrete pavements might be caused by the breaking of flat and elongated particles (Meininger 1998). The workability and initial water content of PCC mixes are affected by fine aggregate content and particle shape. These can cause improper consolidation and increased shrinkage (Meininger 1998). Coarse aggregate shape characteristics can also affect workability and initial water content (Kosmatke et at. 2002). As aggregates change from smooth, round particles to rough, angular particles the bond strength between the cement paste and a given coarse aggregate increases (Kosmatke et at. 2002).

Unbound base and subbase layers are also affected by aggregate shape characteristics. A significant correlation was found between resilient modulus and shear resistance of unbound aggregates in base layers and aggregate shape properties (Barksdale and Itani 1994). The shear strength and stiffness of an unbound layer are affected by the aggregate angularity and texture and have a great influence on the pavement performance (Saeed et al. 2001).

TEST METHODS FOR MEASURING AGGREGATE CHARACTERISTICS

The current Superpave® system characterizes shape properties for coarse and fine aggregates using three tests. The coarse aggregate angularity is determined by the number of aggregate fractured faces using ASTM D 5821-95 "Standard Test Method for Determining the Percentage of Fractured Particles in Coarse Aggregate." AASHTO Standard T 304 "Standard Method of Test for Uncompacted Void Content of Fine Aggregate Method A" tests the fine aggregate angularity (FAA) by determining the volume of air voids in a loosely compacted aggregate sample. The percentage of flat and elongated coarse aggregates is determined by ASTM D 4791-05 "Standard Test Method for Flat Particles, Elongated Particles, or Flat and Elongated Particles in Coarse Aggregate."

The current standard tests are laborious and limited in their ability to test a representative sample of aggregates. The current flat and elongated procedure quantifies the percentage of aggregates above a specified dimension ratio instead of measuring the distribution of the particles dimensions (Fletcher et al. 2003). The current Superpave methods do not measure aggregates texture, although it has significance influence on performance (Fletcher et al. 2002). In some cases, the fine aggregate angularity method does not distinguish between poor and high quality fine aggregates (Huber et al. 1998; Chowdhury et al. 2001). These limitations have caused an inconsistency in measuring aggregate shape characteristic and predicting the influence of aggregates on pavement performance (Fletcher et al. 2002).

Presently several test methods are used to characterize shape properties of aggregates. A review of these test methods can be found in reference Al-Rousan (2004). The test methods can be divided into two main categories, direct and indirect, based on the method used to define the aggregate shape characteristics. Direct test methods measure the geometry of the surface of individual aggregates. Indirect test methods measure the bulk properties of aggregates as indications of shape characteristics (Al-Rousan 2004). The test methods studied are shown in Table 2.1 (Al-Rousan 2004).

Table 2.1. Test Methods for Measuring Aggregate Shape Characteristics (Al-Rousan 2004)

Test Method	Direct (D) or indirect (I) method
Uncompacted Void Content of Fine Aggregates AASHTO T304	I
Uncompacted Void Content of Coarse Aggregates AASHTO TP56	I
Compacted Aggregate Resistance (CAR)	I
Percentage of Fractured Particles in Coarse Aggregate ASTM D5821	D
Flat and Elongated Coarse Aggregates ASTM D4791	D
Multiple Ratio Shape Analysis	D
VDG-40 Video grader	D
Buffalo Wire Works PSSDA	D
Camsizer	D
Wipshape	D
University of Illinois Aggregate Image Analyzer (UIAIA)	D
Aggregate Image Measurement System (AIMS)	D
Laser-Based Aggregate Analysis System	D

These test methods were evaluated by Masad et al. (2007) based on the repeatability of the measurements, accuracy, reproducibility, applicability to the various types of aggregates, cost, ease of use, readiness for implementation, portability, and simplicity of interpretation of the results. It was concluded that AIMS is the most comprehensive system capable of measuring the shape characteristics of both coarse and fine aggregates among the other test methods.

AGGREGATE IMAGE MEASUREMENT SYSTEM (AIMS)

AIMS was developed to measure aggregate shape characteristics using a computer controlled motion and image processing and analysis techniques (Masad et al. 2007).

AIMS is capable of capturing the aggregate characteristics over a range of aggregates sizes from 37.5mm (1.5 in) to 0.075mm (ASTM #200 sieve). The direct measurements of aggregates are characterized in terms of shape, angularity, and surface texture. Fig. 2.1 shows the AIMS system.

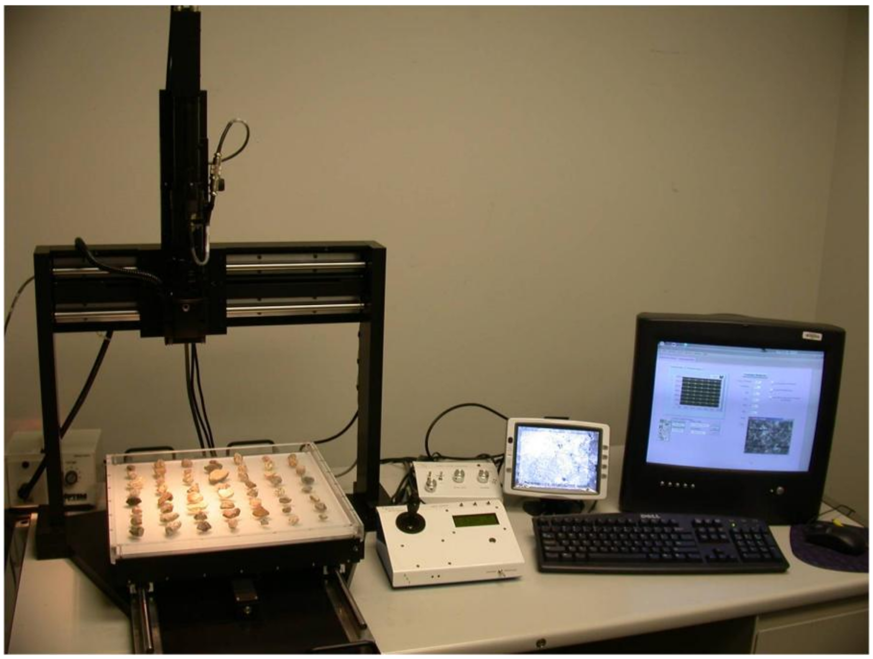

Fig. 2.1. A Picture of AIMS

The aggregates are sieved into size ranges for measurement and analysis. The aggregate size ranges that can by analyzed by AIMS are shown in Table 2.2. The coarse aggregates which are retained on a 4.75mm (ASTM #4) sieve are defined by three dimensional shape, angularity, and texture. The fine aggregates which pass through a 4.75mm (ASTM #4) sieve are represented by two dimensional shape and angularity. In this document, the aggregate ranges will be referred to by the retained size for brevity.

Table 2.2. AIMS Size Ranges for Coarse and Fine Aggregates

Aggregate Type	Aggregates Size Range
Coarse Aggregate	37.5 mm(1.5in) – 25.0mm (1in)
	25.0mm (1in) – 19.0mm (0.75in)
	19.0mm (0.75in) – 12.5mm (0.5in)
	12.5mm (0.5in) – 9.5mm (0.375in)
	9.5mm (0.375in) – 4.75 mm (ASTM #4 sieve)
Fine Aggregate	4.75 mm (ASTM #4 sieve) – 2.36mm (ASTM #8 sieve)
	2.36mm (ASTM #8 sieve) – 1.18mm (ASTM #16 sieve)
	1.18mm (ASTM #16 sieve) – 0.6mm(ASTM #30 sieve)
	0.6mm(ASTM #30 sieve) – 0.3mm (ASTM #50 sieve)
	0.3mm (ASTM #50 sieve) – 0.15mm (ASTM #100 sieve)
	0.15mm (ASTM #100 sieve) – 0.075mm (ASTM #200 sieve)

Coarse aggregates are arranged on a lit aggregate measurement tray with marked grid points at specific distances along the x and y axes, and a digital camera captures images which are analyzed using AIMS SOFTWARE©. The fine aggregate sample is spread randomly on the entire tray.

The aggregate angularity is depicted by measuring the irregularity of a particle surface from a black and white image using a bottom lit tray. The texture index is obtained by analyzing grayscale images captured on a particle surface. The dimensions of the aggregates are obtained during the scanning to measure angularity and texture. The x and y dimensions come from the measurements of the black and white angularity images of the back lit aggregate. The depth of the aggregate or z dimension measurement is obtained from the grayscale texture image as the camera unit focuses on the particle surface (Masad et al. 2007). The aggregate measurement results are listed with some basic statistical values such as mean, standard deviation, and graphical distribution of the measurements (Al-Rousan 2004). Only the black and white angularity images are used to characterize the fine aggregate shape characteristics, since there exists a high correlation between the angularity (measured from the black and white images) and texture (measured from the grayscale images) of the fine aggregates (Masad et al. 2001).

ANALYSIS PRINCIPLES OF AIMS

The shape characteristics evaluated by AIMS for coarse and fine aggregates are obtained by image analysis of the aggregate particles. The measurements of form and angularity are found from the black and white images, while the grayscale images provide information about the texture. Further details of the analysis of these characteristics are provided by Al-Rousan (2004), and a summary is given in this section.

Angularity Index (Gradient Method)

The method used to measure the angularity index is called the gradient method. The gradient method is based on the quantification of the change in the gradient of a particle boundary. This means that at sharp corners of a surface of a particle the direction of the gradient vector changes rapidly while it changes slowly along the outline of the smooth corners of rounded particles. The angularity is calculated based on the average of the change of the inclination of the gradient vectors ($|\Delta\theta|$). The angularity is mathematically represented as shown in Equation 2.1.

$$Angualrity\ Index\ (Gradient\ Method) = \frac{1}{\frac{N}{3} - 1} \sum_{i-1}^{N-3} |\theta_i - \theta_{i-3}| \qquad (2.1)$$

where N is the total number of points on the edge of the particle with the subscript i denoting the i^{th} point on the edge of the particle (Masad et. al 2007).

Texture Index (Wavelet Method)

The texture index describes the relative smoothness or roughness of the aggregate surface. This can be quantified by the local variation in the pixel gray intensity values using the wavelet analysis. Three separate analysis of the particle image gives the texture details in the horizontal, vertical, and diagonal directions for the wavelet analysis. The texture index is computed as the arithmetic mean of squares of the detail coefficients ($D_{i,j}$) at a particular decomposition level. The texture index is given by Equation 2.2.

$$Texture\ Index_n(Wavelet\ Method) = \frac{1}{3N} \sum_{i=1}^{3} \sum_{j=1}^{N} \left(D_{i,j}(x,y)\right)^2 \qquad (2.2)$$

where n is the decomposition level; N is the total number of coefficients in a detailed image of texture; i takes values 1, 2, or 3 for the three detailed images of texture; j is the wavelet coefficient index; and (x, y) is the location of the coefficients in the transformed domain (Al-Rousan 2004 and Masad et. al 2007).

Form Index (2D Form Analysis)

The form index is used to quantify the two-dimensional form. The incremental change in the particle radius is calculated for the form index. The form index is expressed by Equation 2.3.

$$Form\ Index = \sum_{\theta=0}^{\theta=360-\Delta\theta} \frac{|R_{\theta+\Delta\theta} - R_{\theta}|}{R_{\theta}} \tag{2.3}$$

Where at the angle of θ , R_θ is the radius of the particle, and $\Delta\theta$ is the incremental difference in the angle (Masad et al. 2001).

Sphericity Index (3D Form Analysis)

The three-dimensional form analysis is quantified by an index called sphericity. AIMS uses the auto focus camera unit to measure the height of a particle, while the two-dimensional projections are analyzed using eigenvector analysis (Masad 2004). The three dimensions of the particle found using these methods are the longest dimension (d_L), the intermediate dimension (d_I), and the shortest dimension (d_s). Equation 2.4 shows the equation to find sphericity.

$$Sphericity = \sqrt[3]{\frac{d_S * d_I}{d_L^2}} \tag{2.4}$$

SENSITIVITY, REPEATABILITY, AND REPRODUCIBILITY OF AIMS

The repeatability, reproducibility, and sensitivity of AIMS measurements were evaluated by Bathina (2005). Repeatability refers to the level of variation of measuring the characteristics of aggregates by the same operator. This was done for identical and random samples. The variation observed in measurements made by multiple operators of the same set of aggregates is defined as the reproducibility. The sensitivity of AIMS was identified by quantifying the ability of the system to capture the differences in the distribution of shape characteristic results between different aggregate types. These measurements were all conducted using the same unit. The repeatability of AIMS measurements for the same operator was found to have a low coefficient of variation (CV) of 10.9% when measuring random samples and 4.9% when measuring the identical samples. The CV for the reproducibility was found to be 16.3% when the same sample was scanned by three different operators. AIMS was found to be sensitive to the changes in the distribution of shape properties of different aggregate samples (Bathina 2005).

The distribution of the shape characteristics for an aggregate sample is best described by the probability distribution function. Several standard distribution functions were fitted to the distribution of 13 aggregate samples and ranked according to the root mean squared error (RMS) value. The gamma distribution was found to best fit aggregate sample distribution curves (Bathina 2005).

CHAPTER III

IMPROVEMENTS OF THE AGGREGATE IMAGE MEASUREMENT SYSTEM (AIMS)

INTRODUCTION

A new design of AIMS was developed (Fig. 3.1) – which will be, in this report, referred to as AIMS2, while AIMS1 (Fig. 2.1) will refer to the previous system that was available before the initiation of this study. Several improvements were made to the physical components of AIMS to enhance the operational characteristics of the system, reduce human involvement and errors, and enhance the automation of the test procedure. With the development of a new prototype machine, the differences in the two machines needed to be clearly identified and calibrations needed to be done on the new system to confirm that the two systems produce similar results for the same set of aggregates. The sensitivity of AIMS needed to be evaluated in terms of its ability to determine the differences in the distribution between different aggregates and the effect of particle placement. In addition, the number of aggregate particles that need to be scanned by AIMS to represent an aggregate source needed to be studied.

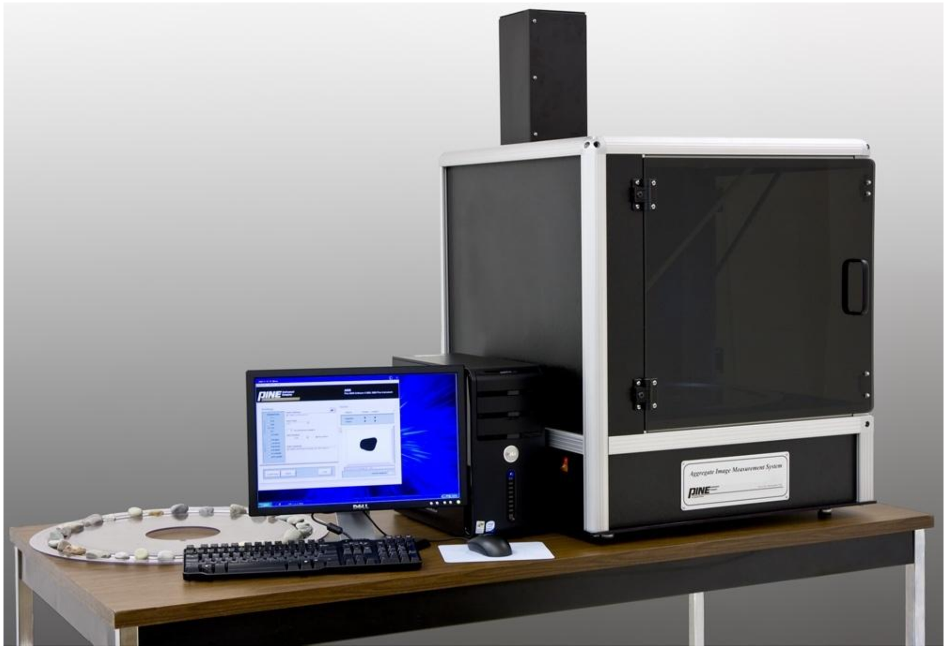

Fig. 3.1. A Picture of AIMS2

IMPROVEMENTS OF AIMS2

Although the physical design and process of capturing images were changed between AIMS1 and AIMS2, the algorithms used for the image analysis were kept the same. The new image acquisition and enclosed unit allowed for many advances that would allow the system to be used as a routine, standard method for aggregate characterization.

For AIMS2, coarse aggregates are placed in the trough of a circular tray. The tray is rotated to move the aggregate under a camera that fixed in the x and y directions. As the back-lit tray rotates, the aggregates are moved below the camera to capture images for the angularity measurements. The positions of the aggregate are recorded so the camera can return to the centroid of the particles for the texture image acquisition. The aggregates images are analyzed using the same computer algorithms as AIMS1. For the fine aggregates, the material is spread evenly in the trough of the tray. The tray moves in the same way as in the coarse aggregate, scanning such that fine aggregate particles are positioned below the camera. An opaque tray was introduced for fine, light colored particles which may be transparent on the clear tray under the bottom light. For the opaque tray, the top light is used to capture the aggregate images, and the image color is inverted for analysis. The system is covered with a nontransparent material to eliminate the effect of exterior light on the images. The interior view of AIMS2 is shown in Fig. 3.2.

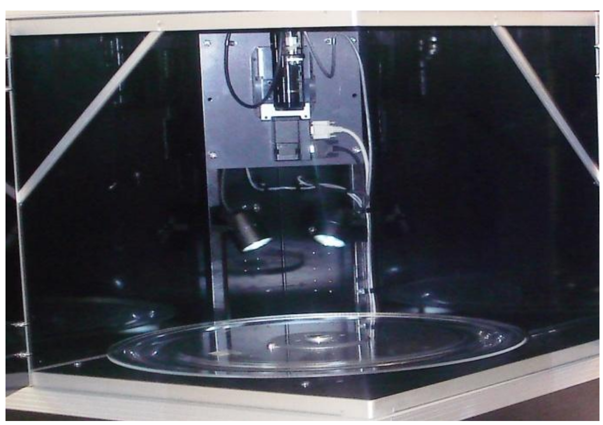

Fig. 3.2. Illustration of AIMS2 System Interior View

The majority of the changes were to the physical components. In addition, there were some changes in image acquisition, physical components, and data outputs. These changes are listed in Table 3.1. The image acquisition camera was changed from an analog camera with an analog video card to a digital camera with a digital firewire interface for improved images. The new camera allowed for the same magnification and maximum resolution as AIMS1 without changing the objective lens. The maximum field of view also remained approximately the same. The multiple oblique LED top lighting allowed for a larger range of light intensities to accommodate for large variations in aggregate color. For AIMS2, the camera is fixed and the aggregate are placed on a rotating trough. This allowed the camera to focus on the aggregate centroid rather than the grid location. AIMS2 was developed to be more automated by integrating many components compared to AIMS1. Additional system calibrations were added to periodically check the system. For fine aggregates, Pine Instruments Co. developed the convex hill analysis which replaced the particle area analysis from AIMS1. The data analysis was the same for AIMS1 and AIMS2. The data output was adjusted to be more user friendly.

Table 3.1. Differences Between AIMS1 and AIMS2 (From Pine Instruments Co.)

	AIMS1	AIMS2
Physical components	Individual components	Integrated system
	VGA analog video camera (640x480)	2mp digital camera (1600 x 1200 multi mode)
	Analog video card	Digital firewire interface
	16x variable magnification microscope	16x variable magnification microscope
	0.50x and 0.25x objective lens	0.25x objective lens
	Max resolution 0.0034mm/px	Max resolution 0.0034mm/px
	Max field of view: 70.4 x 52.8	Max field of view: 72mm x 54mm
	Top Lighting: fiber optic ring	Top Lighting : multiple oblique LEDs
	Linear moving tray	Multiple rotating trays
	4 axis motion (gantry x,y,z, magnification)	3 axis motion (rotation, z, magnification)
	Coarse particle grid	Coarse particle trough
	System not enclosed	System fully enclosed with non transparent sides
Acquisition Software	Texture and height at grid position	Texture and height near centroid
	Texture image mean intensity target: 170	Texture image mean intensity: 175
	Touching particle: particle area analysis	Touching particle: Convex Hull Perimeter Ratio (CHPR)
	Image conditioning: none	Image conditioning: low pass filter
	Particle size filters (Min and Max size filter)	Only minimum particle size filter applied
	No top lighting for translucent fines (used bottom light and clear tray)	Top lighting and opaque tray for translucent fines
	Manual data processing and compilation	Automatic data processing and compilation
	System calibration: none	System Calibration: Magnification, height, resolution, illumination, alignment

Table 3.1. Continued

	AIMS1	AIMS2
Analysis Software and Output	Gradient Angularity (0-10000)	Gradient Angularity (0-10000)
	Texture (0-800)	Texture with shift factor (0-1000)
	Radius Angularity	not used
	Form2D: all sizes (0-20)	Form2D: Fine sizes only (0-20)
	Sphericity I	F&E, F or E distributions
	Sphericity II	Sphericity II

AIMS2 CALIBRATION

The calibrations were done in order to insure that the two systems, AIMS1 and AIMS2, produce similar results for the same set of aggregates. In the development of the new prototype of AIMS2, the resulting parameters from the two systems were compared to each other for a set of 32 coarse aggregate samples and 21 fine aggregate samples. Fifty-six particles were scanned from each aggregate source. The comparison of the angularity of the fine and coarse aggregates is shown in Fig. 3.3. The angularity values of the two AIMS systems are comparable.

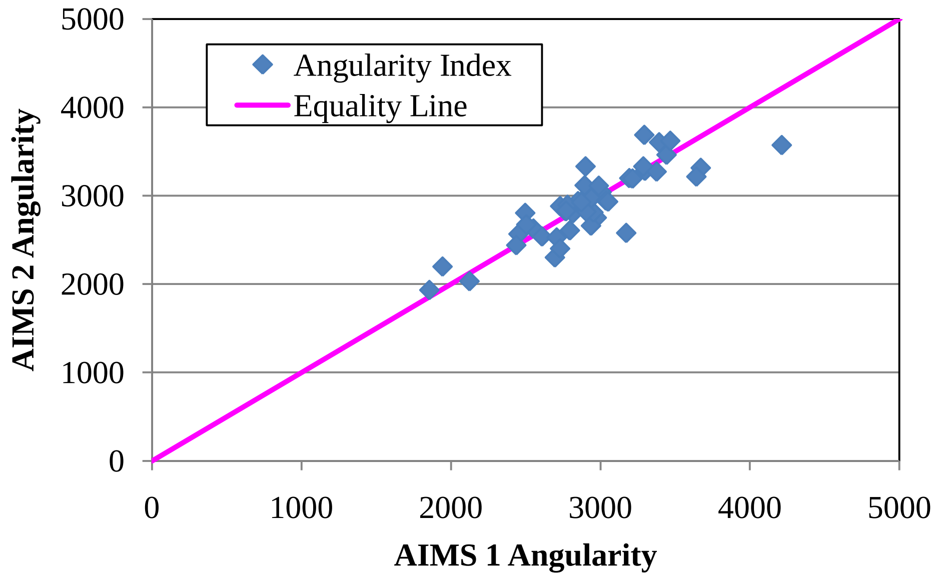

Fig. 3.3 Angularity of AIMS1 and AIMS2

AIMS1 and AIMS2 texture results, shown in Fig. 3.4, rank the aggregates in the same order. However, due to the difference in the cameras and lighting used in AIMS2 and AIMS1, the range of the scale of the texture results of the two systems were different. The scale range for the studied aggregates for AIMS1 was 0 – 600, while the scale for AIMS2 was 0 – 200. It was found that a multiplication shift factor of 2.4563 for the AIMS2 data would provide results comparable to those of AIMS1. The texture values of AIMS1 and AIMS2 after applying the shift factor are shown in Fig. 3.5. The comparison between AIMS1 and AIMS2 results proved that the two systems provide the same ranking of aggregates and give comparable results. Consequently, the classification system developed previously by the TAMU research team for AIMS1 (Mahmoud et al. 2010) can be used to classify aggregates based on AIMS2 results.

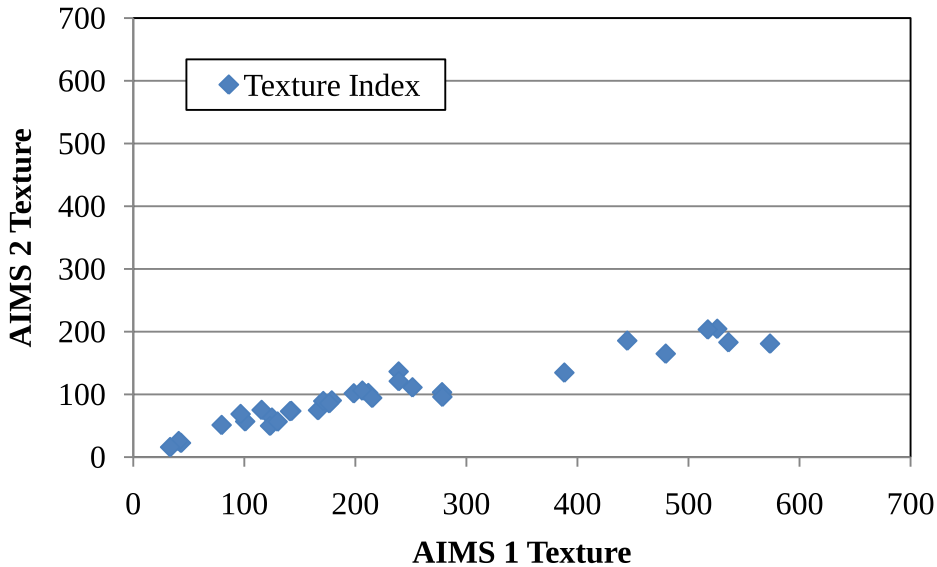

Fig. 3.4. Texture of AIMS1 and AIMS2

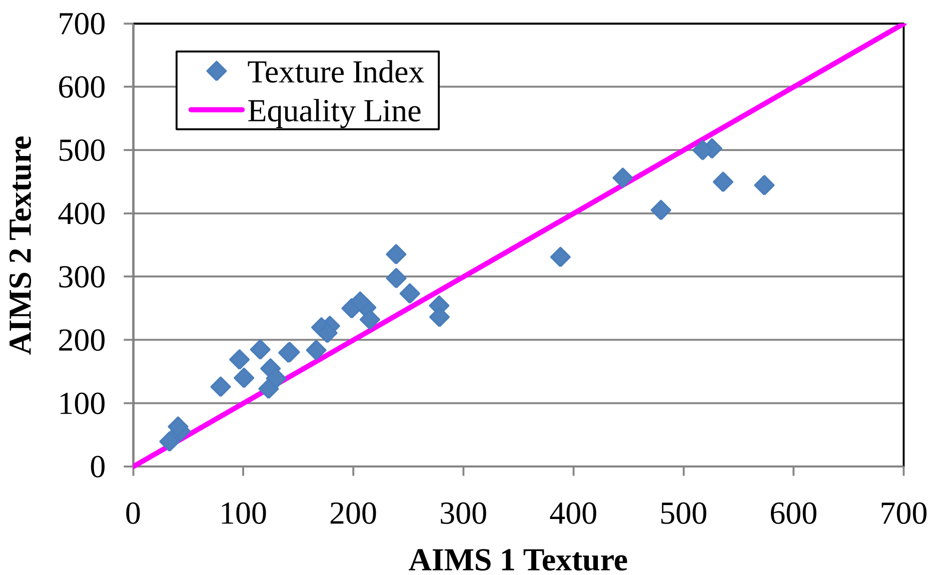

Fig. 3.5. Texture of AIMS1 and AIMS2 Shifted

SENSITIVITY OF AGGREGATE PLACEMENT *

Scanning coarse aggregates using AIMS1 or AIMS2 requires manual placement of particles on the tray to be scanned. On AIMS1, the aggregates are manually placed at specific locations on the AIMS1 tray, while AIMS2 requires aggregates to be manually placed in the trough of the circular tray. Since placement of the particles is not a controlled process, the aggregate particles will inevitably be in different orientations if the placement were repeated by the same operator or done by a different operator. Therefore, it was necessary to study the influence of aggregate placement or aggregate orientation on the variability of the AIMS measurements. The dependence of scan results on these variables was not expected to be significant, but it still needed to be quantified. Since the images used are digital, there are digitization differences between different orientations of an aggregate particle.

Variations in the angularity results were analyzed by conducting scans with aggregates placed in four different positions. The first scan was conducted by placing aggregate

---

particles randomly on their predefined locations. In the second scan, particles were rotated 90^o horizontally at their same average position. The third scan involved inverting the particles so that the underside of each particle was scanned relative to the first scan. The fourth scan involved both turning particles 90^o and inverting them. This allowed the investigation of the separate effects of rotation and inversion, as well as the effect of combined rotation and inversion. The variation of the texture was analyzed due only to particle inversion. The effect of rotation was not considered, because the same surface would be analyzed for texture irrespective of the different horizontal orientation.

Fifteen aggregate samples, each containing 56 particles, consisting of gravel, limestone, shale, and sandstone, were used. Results for angularity are shown in Figs. 3.6, 3.7, and 3.8. Texture analysis results are shown in Fig. 3.9.

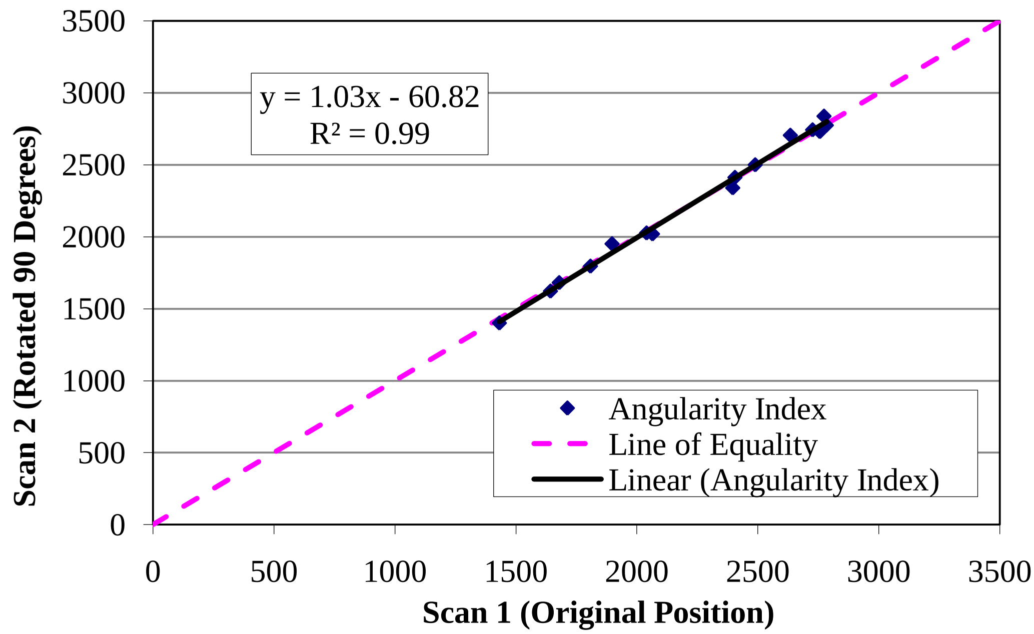

Fig. 3.6. Angularity Results for Particle Rotation

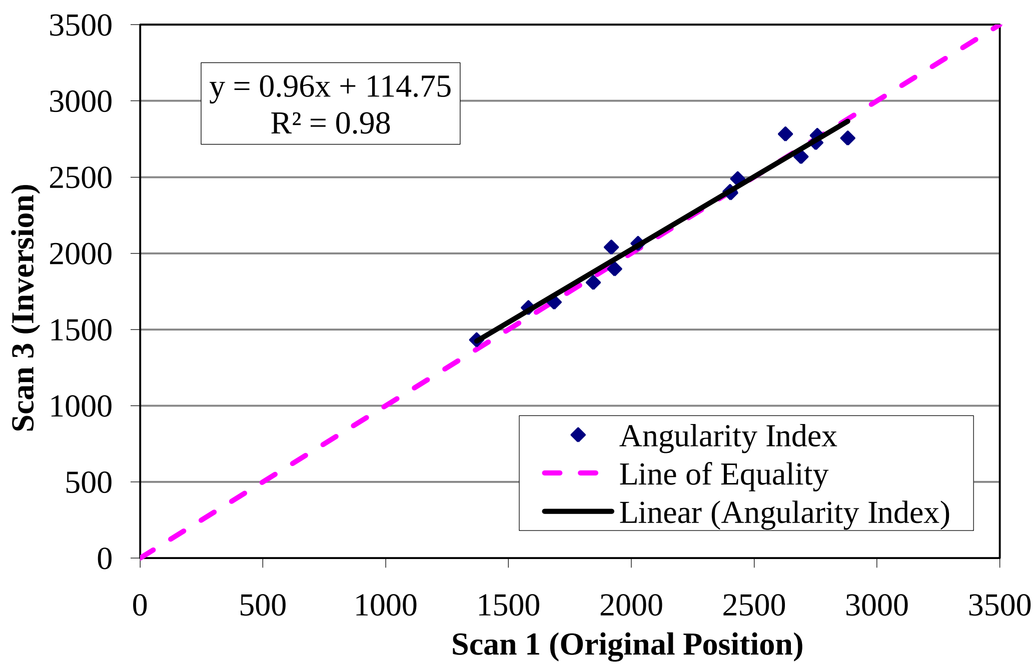

Fig. 3.7. Angularity Results for Particle Inversion

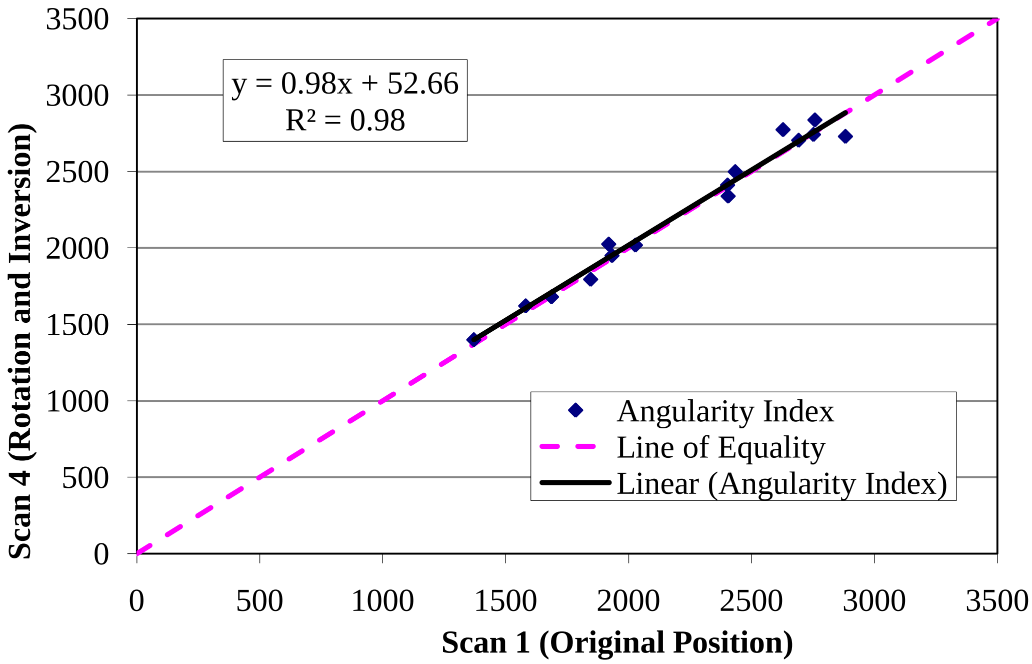

Fig. 3.8. Angularity Results for Particle Rotation and Inversion

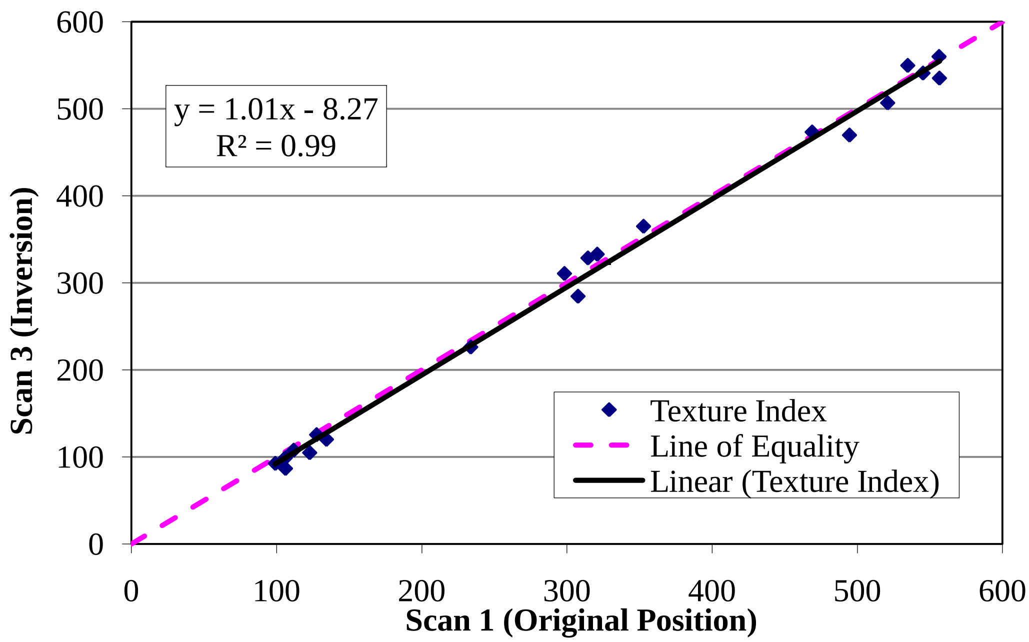

Fig. 3.9. Texture Results for Particle Inversion

The confidence interval (CI) values for the slope and intercept are shown in Table 3.2. The R^2 values are close to unity, agreeing with visual inspection of the graphs. This and the fact that all the CI contained their ideal values of slope = 1 and intercept = 0, indicated that the effect of rotation and inversion of particles on angularity and the effect of inversion were minimal.

Table 3.2 CIs for Aggregate Placement Effect on AIMS Measurements

Placement Variable Considered	Slope CI	Intercept CI
Rotation Effect on Angularity (3.6)	(0.981, 1.07)	(-166, 44)
Inversion Effect on Angularity (3.7)	(0.872, 1.04)	(-75, 304)
Rotation and Inversion Effect on Angularity (3.8)	(0.894, 1.07)	(-150, 255)
Inversion Effect on Texture (Fig. 3.9)	(0.975, 1.05)	(-21, 5)

SENSITIVITY OF AGGREGATE TYPE

A sensitivity test quantifies the ability of the test method to capture the differences of the distribution of aggregate properties within a given sample. A test method is considered sensitive if the measurements of different aggregate samples are monotonic (Bathina 2005). Aggregate samples consisting of specific mixtures of two different aggregates were tested to determine AIMS2 sensitivity. The two aggregates types represented the two diverse shape characteristics (Table 3.3). From previous test results, it was observed that aggregate 1 exhibited low shape, angularity, and texture aggregate characteristics and aggregate 2 exhibited high values of these aggregate characteristics.

Table 3.3 Aggregates Source and Description for Sensitivity Analysis

Aggregate Label	Source	Aggregate Description
1	Texas	Crushed Gravel
2	Oklahoma	Granite

Aggregates 1 and 2 were combined in different proportions into five aggregate samples to evaluate sensitivity. The aggregate samples 1, 2, 3, 4, and 5 comprised of 100 percent of aggregate 1, 75 percent of aggregate 1, 50 percent of aggregate 1, 25 percent of aggregate 1, and 100 percent of aggregate 2, respectively. The mean values of each shape characteristic parameter, angularity, texture, sphericity, and flat or elongated 3:1 ratio, were evaluated independently. The mean values from samples 1, 2, 3, 4, and 5 showed a monotonic pattern as the percent of aggregate 1 and 2 changed for each shape characteristic (Figs. 3.10, 3.11, and 3.12). The percent of flat or elongated 3:1 particles followed a monotonic pattern and becomes constant at about 2% when the percentage of aggregate 1 exceeds 50% (Fig. 3.13).

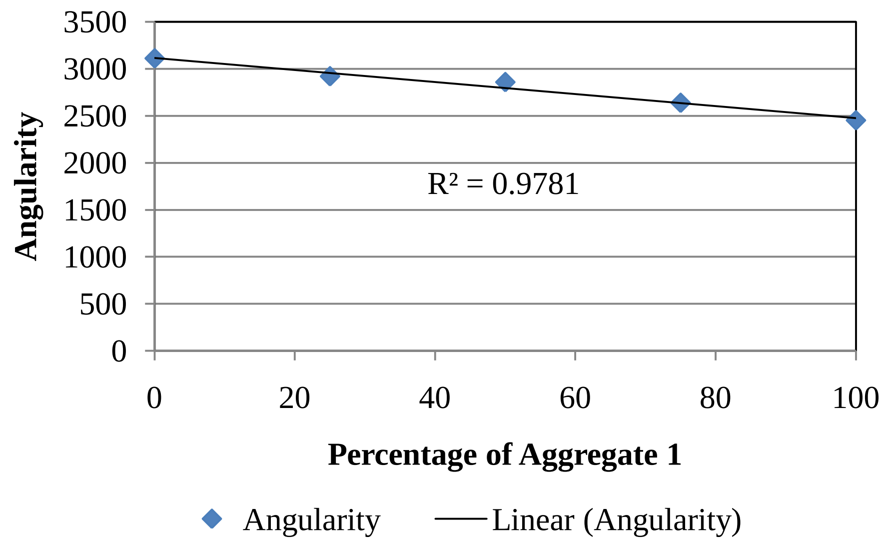

Fig. 3.10. Sensitivity of AIMS2 for Angularity

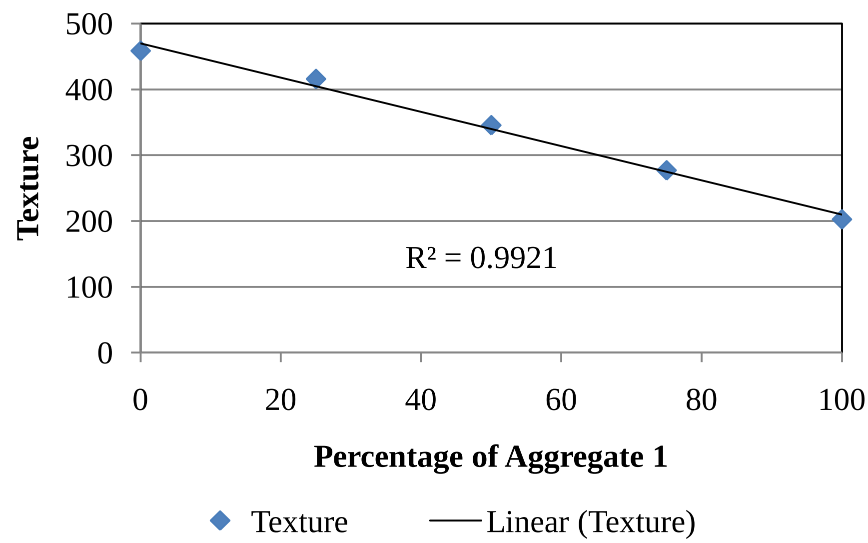

Fig. 3.11. Sensitivity of AIMS2 for Texture

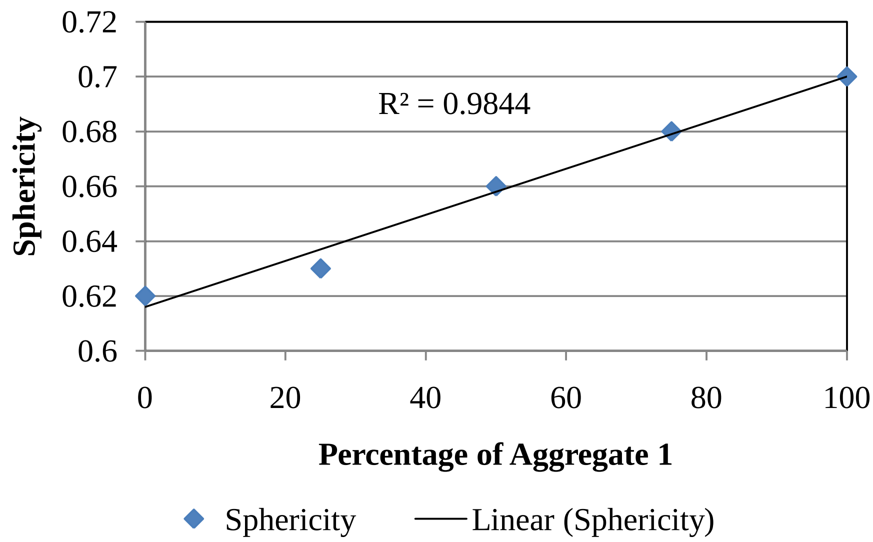

Fig. 3.12. Sensitivity of AIMS2 for Sphericity

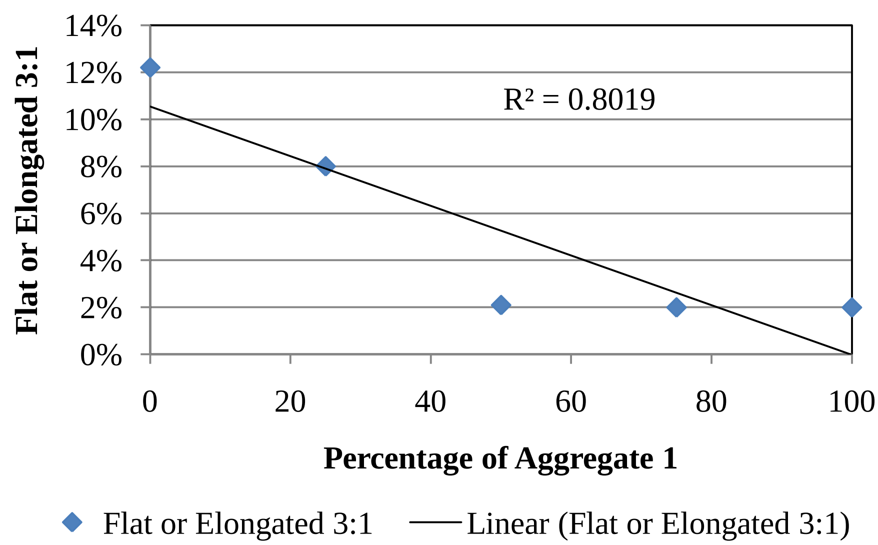

Fig. 3.13. Sensitivity of AIMS2 for Flat or Elongated 3:1 Ratio

Since all of the test parameters of AIMS2 have a monotonic pattern, the sensitivity of the method is defined in terms of the R^2 value for a straight line fit of the data. Table 3.4 shows the sensitivity results for AIMS2.

Table 3.4. Sensitivity Results for AIMS2

Shape Characteristic	Monotonic Pattern	R2 value
Angularity	Yes	0.9781
Texture	Yes	0.9921
Sphericity	Yes	0.9844
Flat or Elongated 3:1	Yes	0.8019

SAMPLE SIZE TO REPRESENT AGGREGATE SOURCE

In the current protocol for AIMS2, the number of particles scanned are 50 coarse aggregates and 150 fine aggregates. These aggregate samples should represent an aggregate source. The results from different sample types and sizes were compared to determine if the sample sizes of 50 coarse aggregates and 150 fine aggregates are sufficient to represent an aggregate source.

The number of particles to represent an aggregate source were analyzed by comparing the cumulative distributions of different samples. Three different aggregates types, granite, limestone, and crushed gravel, were used to determine the appropriate sample size for both coarse and fine aggregates (Table 3.5). One coarse aggregate and one fine aggregate size, shown in Table 3.6, were analyzed for all three aggregate types.

Table 3.5. Aggregate Type for Number of Particles in a Sample

Aggregate Type	Source
Granite	Oklahoma
Limestone	Texas
Crushed Gravel	Texas

Table 3.6. Aggregate Size Range for Number of Particles in a Sample

Aggregate Type	Aggregates Size Range
Coarse Aggregate	25.0mm (1in) – 19.0mm (0.75in)
Fine Aggregate	0.6mm(ASTM #30 sieve) – 0.3mm (ASTM #50 sieve)

It is desirable to use a standard distribution function to describe the cumulative distributions of the shape characteristics of an aggregate sample. The distributions of the aggregate characteristics were found to best follow the gamma distribution (Bathina 2005). The JMP software was used to characterize the aggregate distributions for each sample using the gamma distribution (SAS Institute Inc. 2008). The PDF of the gamma distribution is given by Equation 3.1.

$$f(x) = \frac{1}{\Gamma(\alpha)\sigma^{\alpha}} x^{(\alpha-1)} e^{-x/\sigma} \tag{3.1}$$

Where the shape parameter, $\alpha > 0$ and scale parameter, $\sigma > 0$.

The gamma shape and scale parameters were found for both the coarse and fine aggregates for the three aggregate types. For the coarse aggregates, the number of particles compared were 10, 20, 30, 40, 50, and 60 particles for the angularity and texture characteristics. The number of particles compared for fine aggregates angularity and 2D form characteristics were 110, 120, 130, 140, 150, and 160 particles. A sample size of ten at each for the particle counts was used to determine the point at which the averages of the gamma distribution parameters converge to the average of the source sample. The source sample consisted of 400 coarse and 1500 fine aggregates. In addition, the magnitude of the standard deviation of the gamma parameters decreases. The gamma parameters for the coarse and fine aggregates are shown in Appendix A.

It was of interest to evaluate the variations of the parameters of the gamma distribution as the number of aggregates in the sample increased. The average gamma parameters of the ten samples for each number of aggregates scanned were compared to the average gamma parameters of the stockpile sample. The standard deviation of the gamma parameters showed the variation of the samples decreases when the sample size increases.

The average gamma parameters of the ten samples and one standard deviation variation from the average are shown for each of the particle size samples. The line through all of the particles counts shows the average of the entire source sample. The coarse aggregate (19.0mm (0.75in)) texture and angularity gamma parameters are shown for the three aggregate types. The granite parameters are shown in Figs. 3.14, 3.15, 3.16, and 3.17;

the limestone parameters are shown in Figs. 3.18, 3.19, 3.20, and 3.21; and the crushed gravel aggregate parameters are shown in Figs. 3.22, 3.23, 3.24, and 3.25.

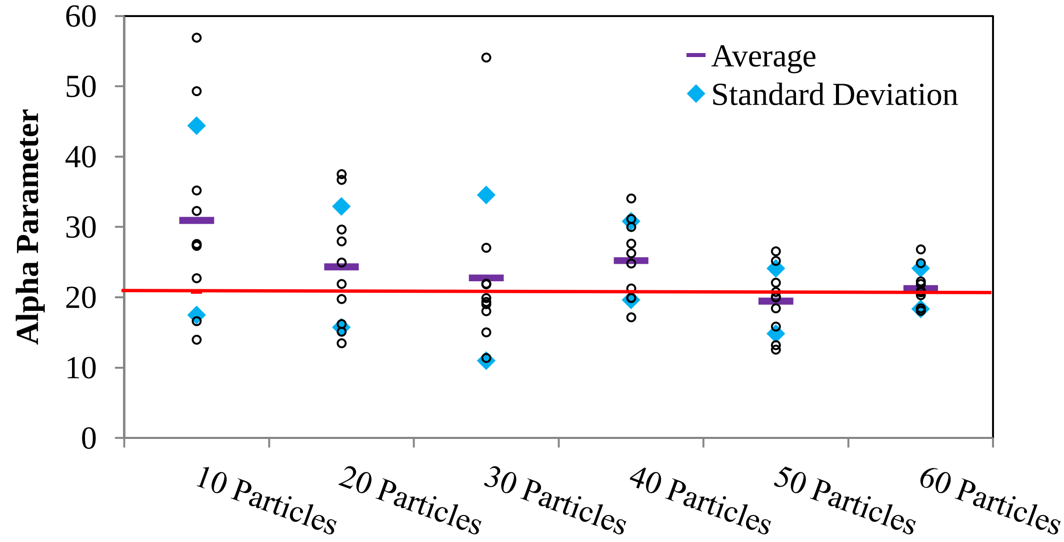

Fig. 3.14. Coarse Aggregate Angularity Alpha Parameter for Granite

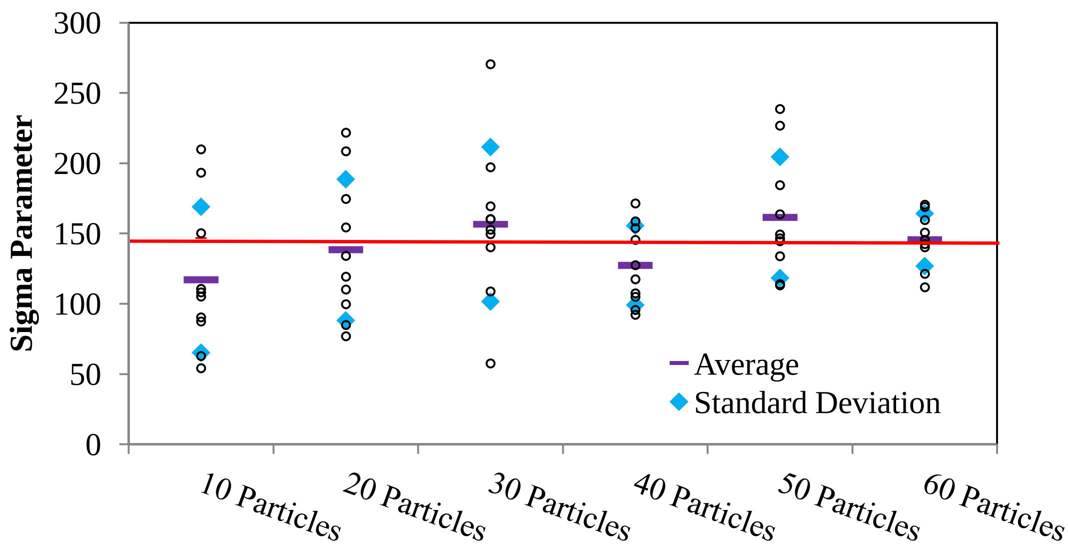

Fig. 3.15. Coarse Aggregate Angularity Sigma Parameter for Granite

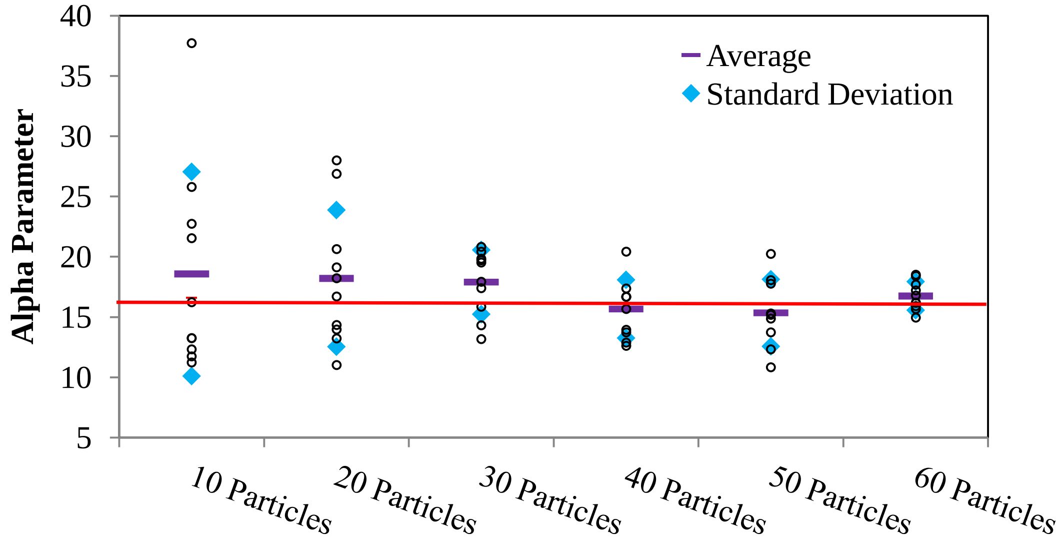

Fig. 3.16. Coarse Aggregate Texture Alpha Parameter for Granite

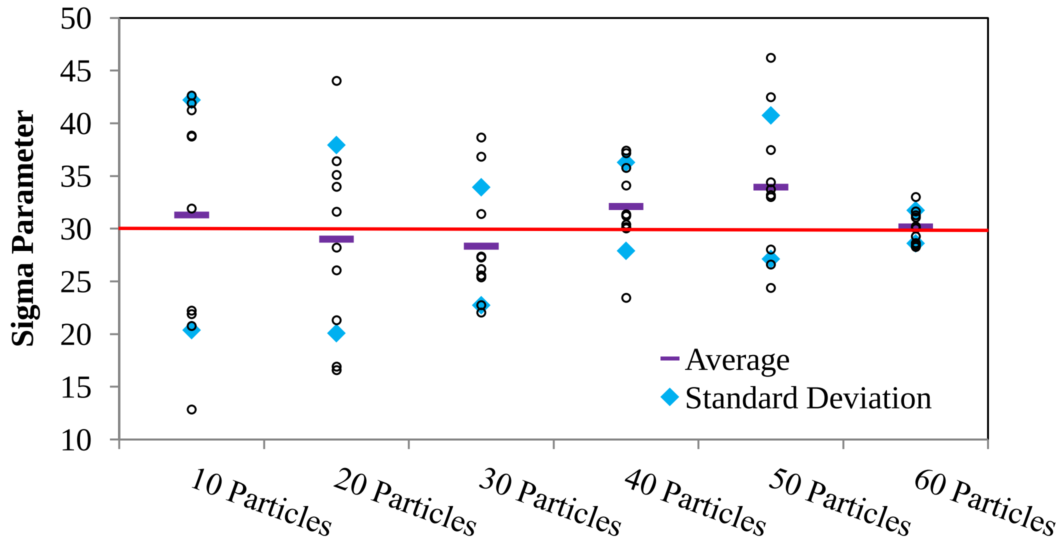

Fig. 3.17. Coarse Aggregate Texture Sigma Parameter for Granite

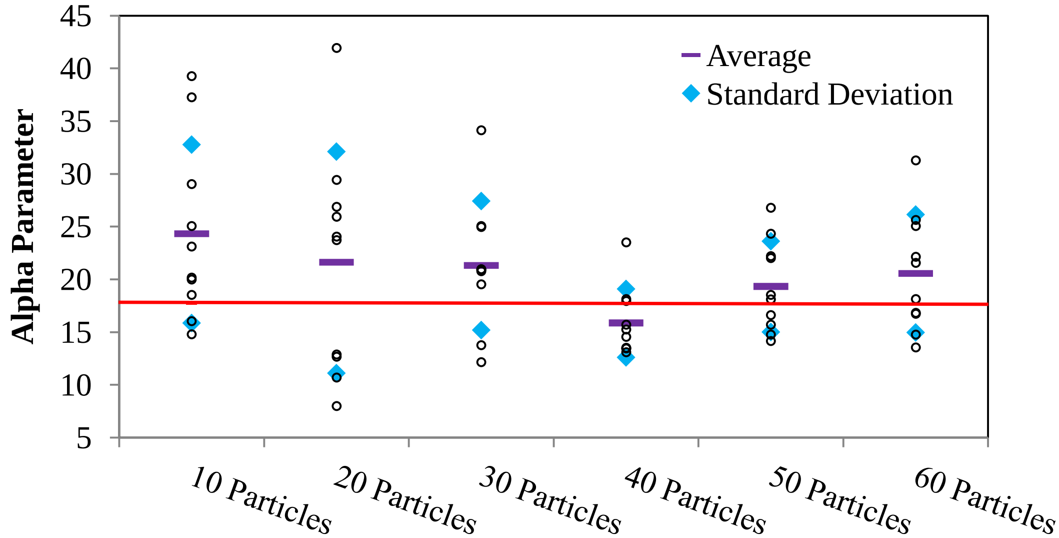

Fig. 3.18. Coarse Aggregate Angularity Alpha Parameter for Limestone

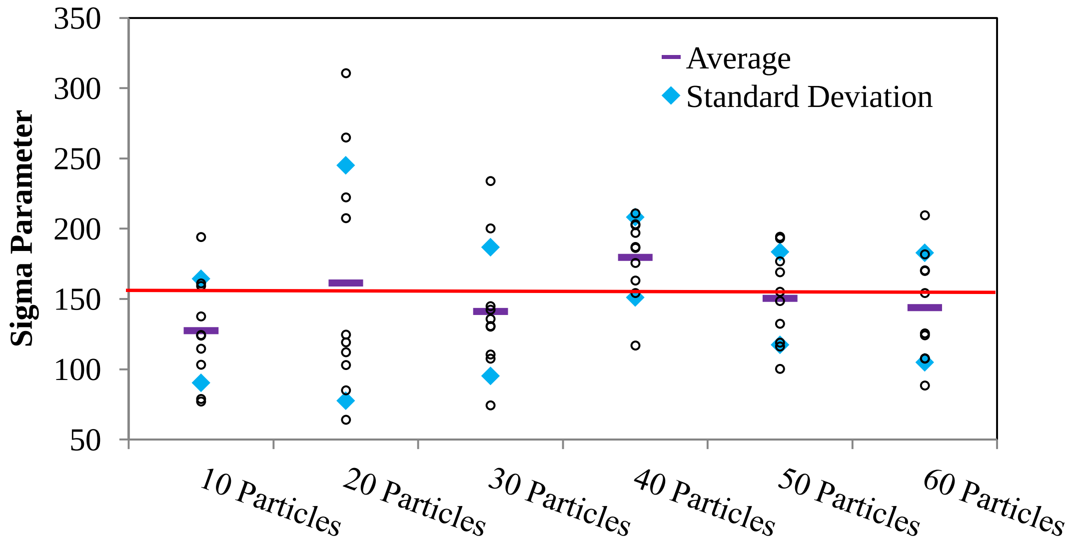

Fig. 3.19. Coarse Aggregate Angularity Sigma Parameter for Limestone

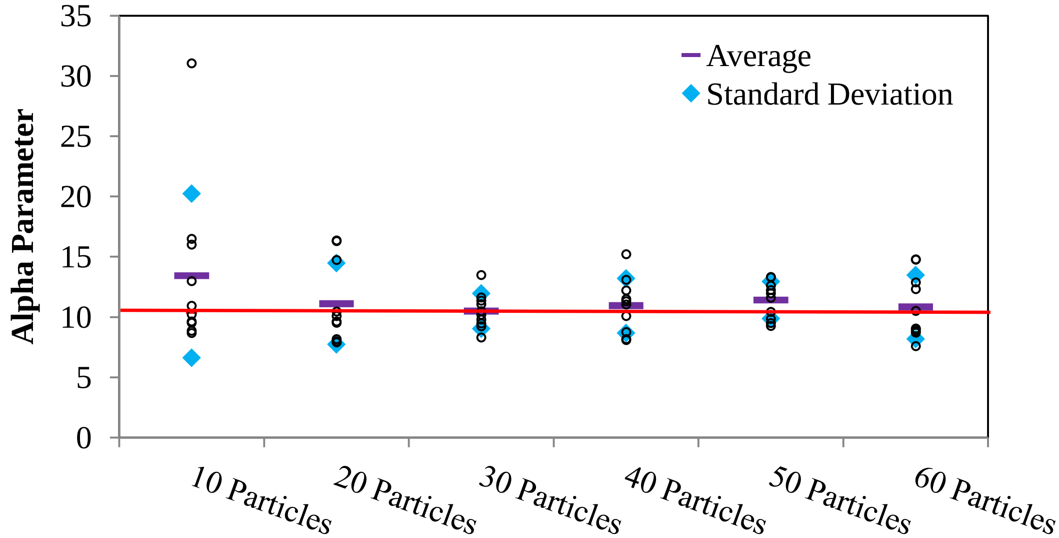

Fig. 3.20. Coarse Aggregate Texture Alpha Parameter for Limestone

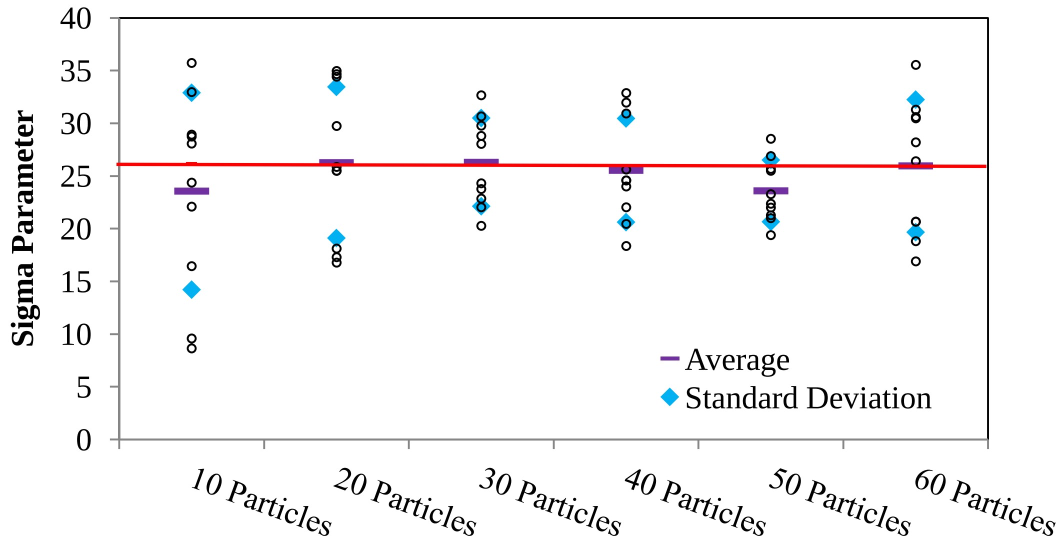

Fig. 3.21. Coarse Aggregate Texture Sigma Parameter for Limestone

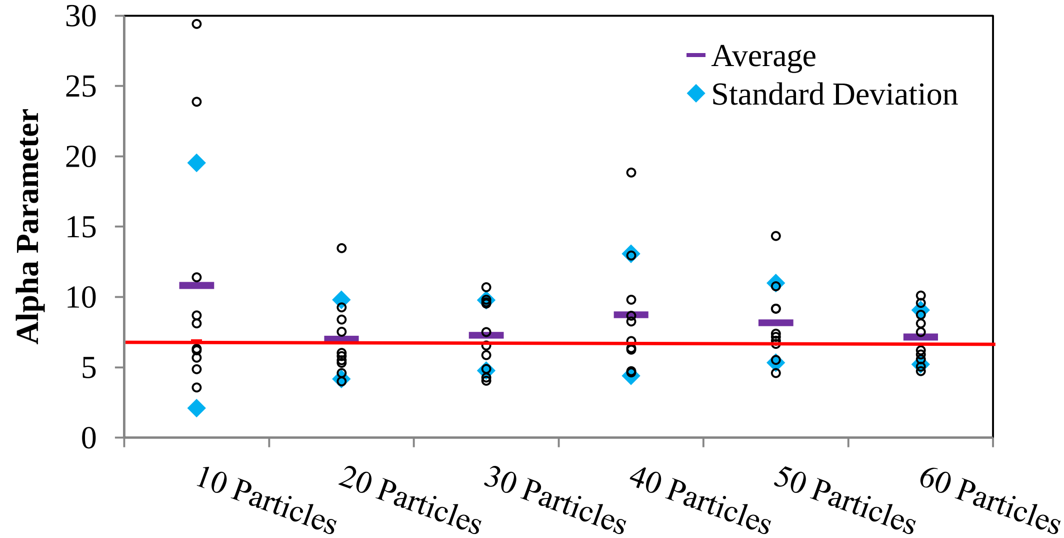

Fig. 3.22. Coarse Aggregate Angularity Alpha Parameter for Gravel

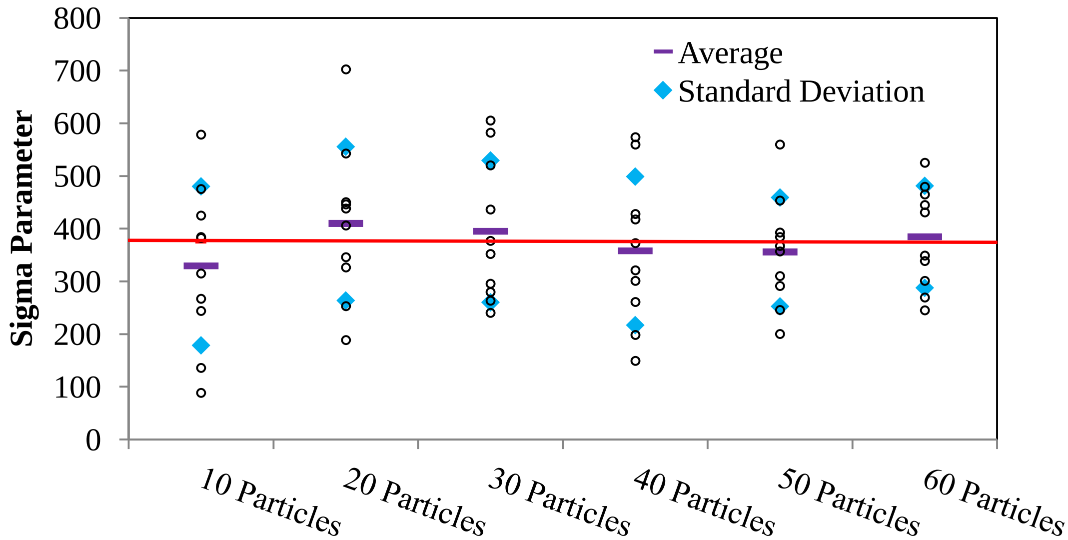

Fig. 3.23. Coarse Aggregate Angularity Sigma Parameter for Gravel

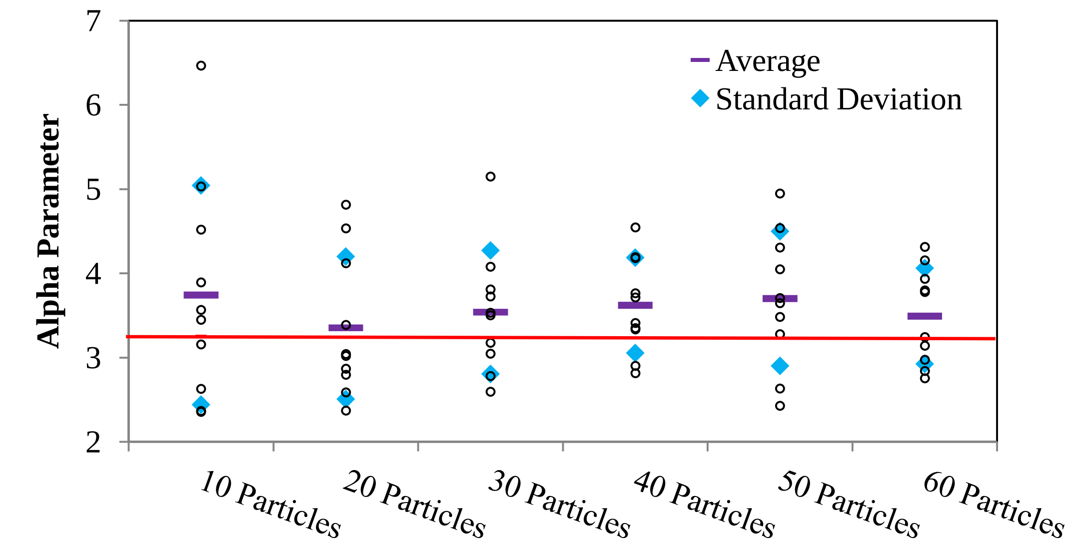

Fig. 3.24. Coarse Aggregate Texture Alpha Parameter for Gravel

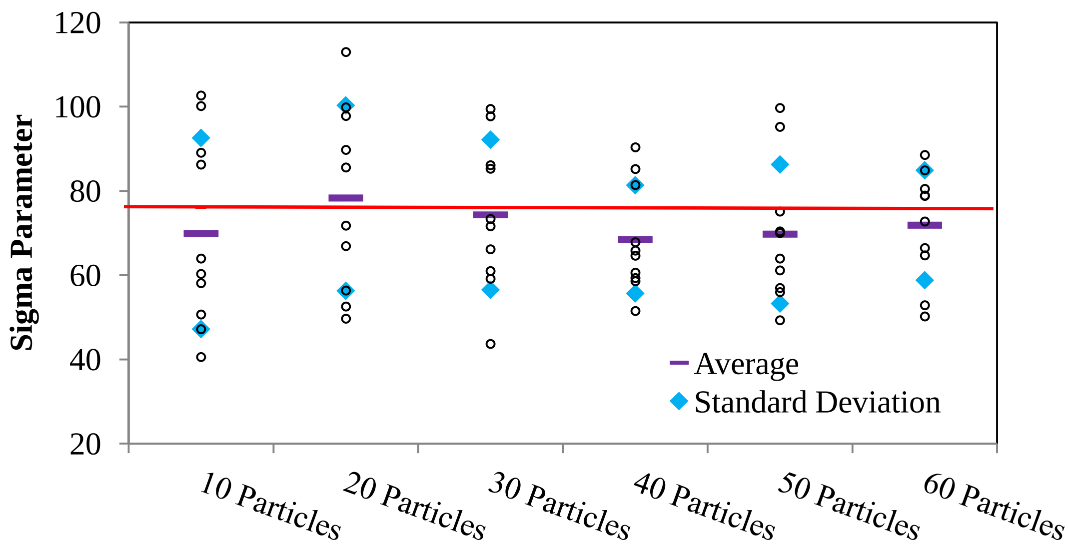

Fig. 3.25. Coarse Aggregate Texture Sigma Parameter for Gravel

The fine aggregate (0.3mm (ASTM #50 sieve)) parameters are shown in Figs. 3.26, 3.27, 3.28, and 3.29 for the granite; Figs. 3.30, 3.31, 3.32, and 3.33 for the limestone; and

Figs. 3.34, 3.35, 3.36, and 3.37 for the crushed gravel aggregates. The alpha and sigma gamma parameter are shown for both the angularity and 2D form.

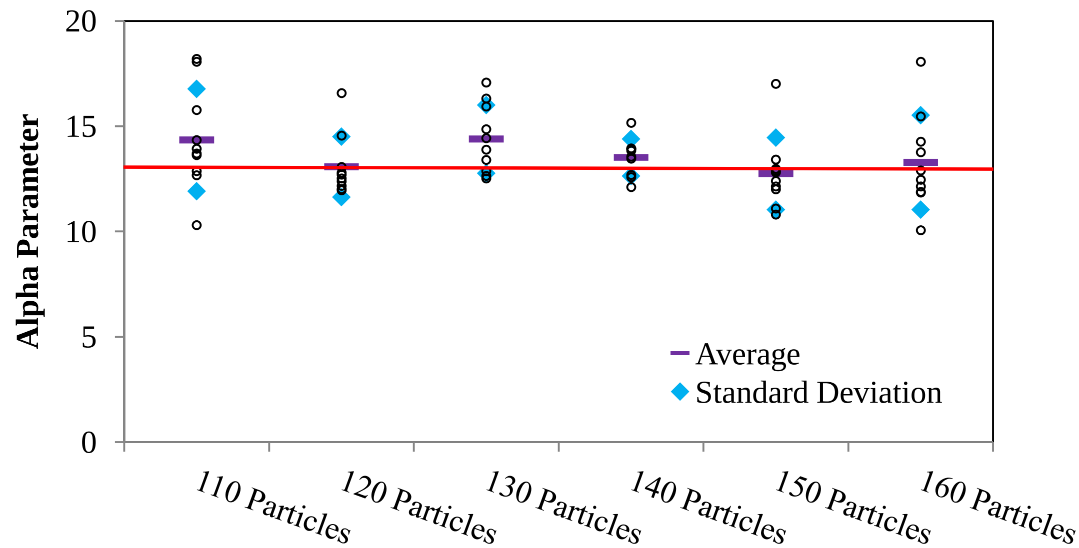

Fig. 3.26. Fine Aggregate Angularity Alpha Parameter for Granite

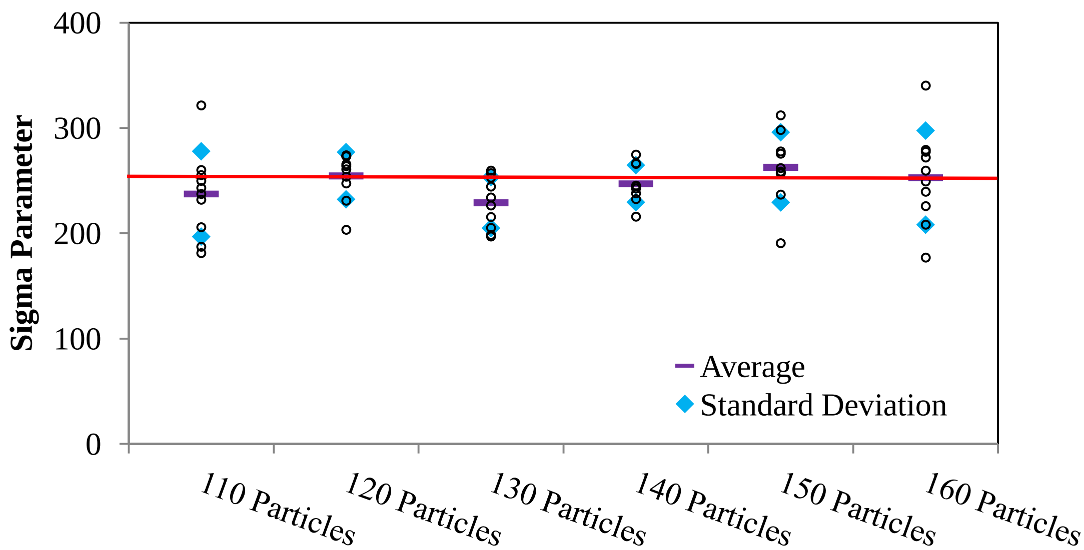

Fig. 3.27. Fine Aggregate Angularity Sigma Parameter for Granite

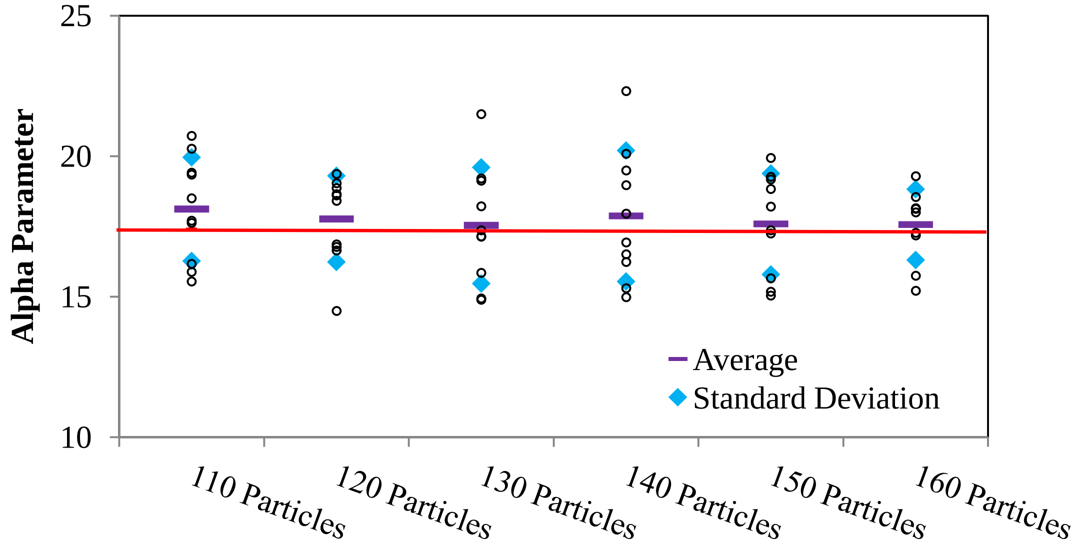

Fig. 3.28. Fine Aggregate 2D Form Alpha Parameter for Granite

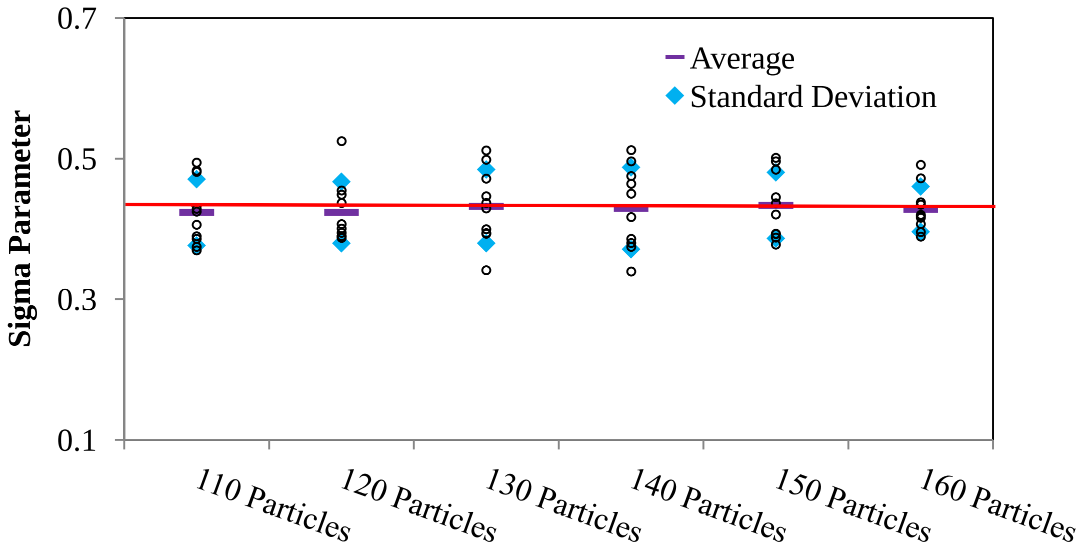

Fig. 3.29. Fine Aggregate 2D Form Sigma Parameter for Granite

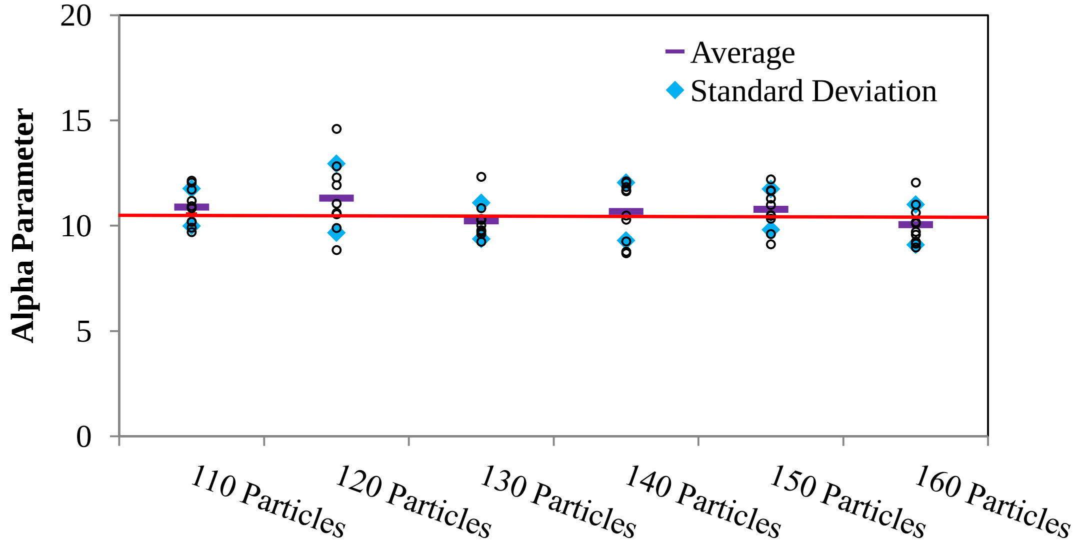

Fig. 3.30. Fine Aggregate Angularity Alpha Parameter for Limestone

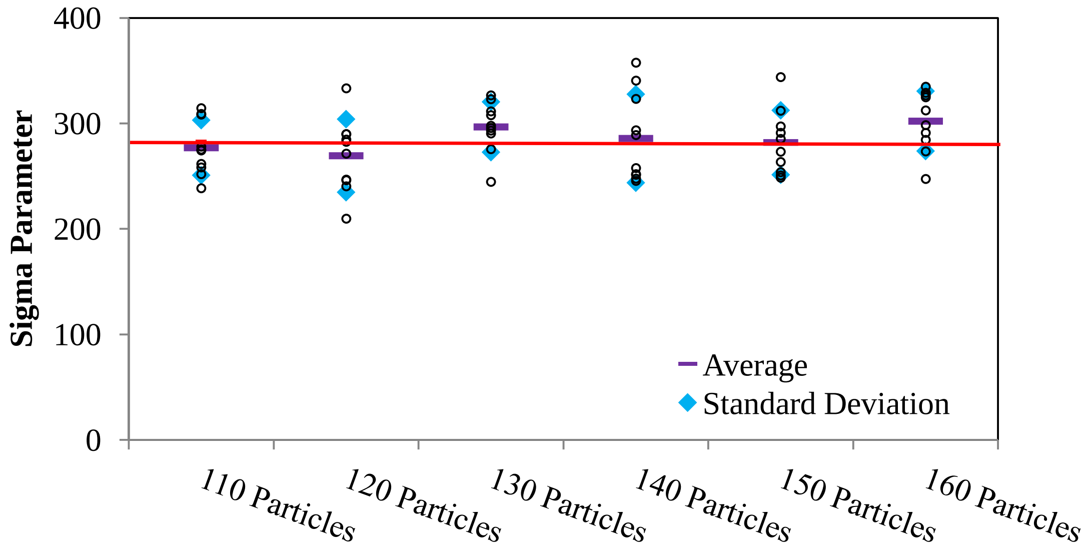

Fig. 3.31. Fine Aggregate Angularity Sigma Parameter for Limestone

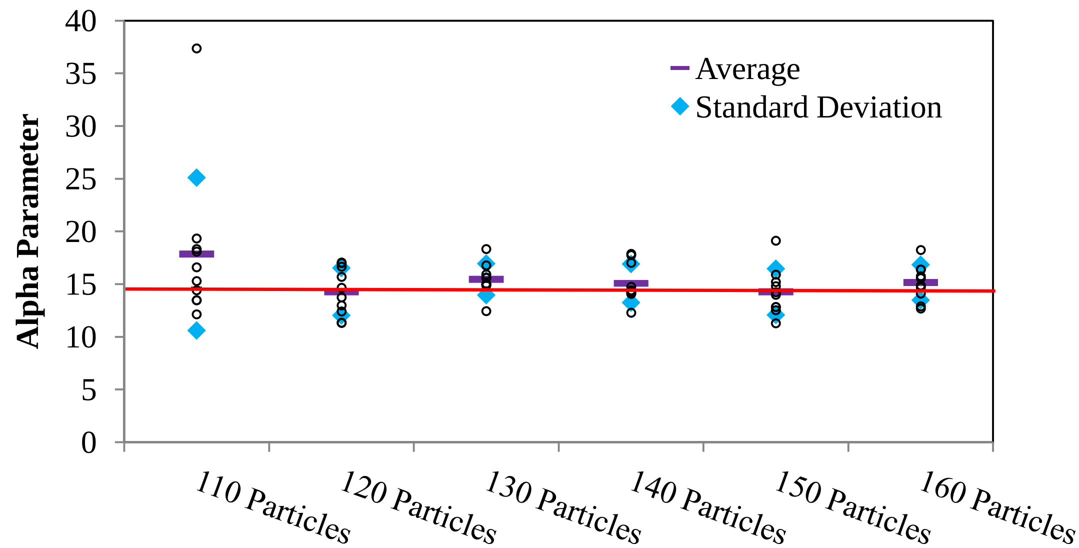

Fig. 3.32. Fine Aggregate 2D Form Alpha Parameter for Limestone

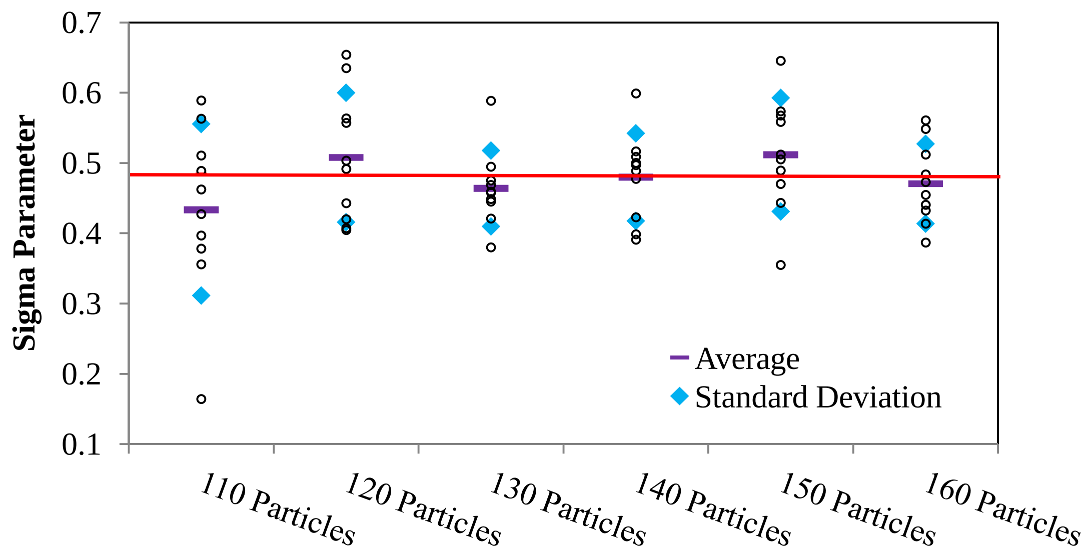

Fig. 3.33. Fine Aggregate 2D Form Sigma Parameter for Limestone

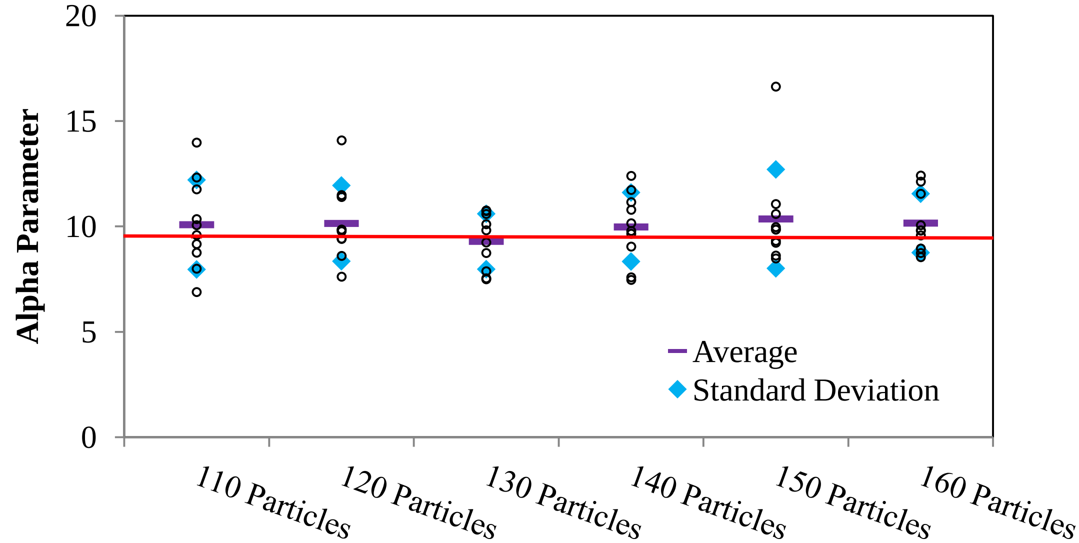

Fig. 3.34. Fine Aggregate Angularity Alpha Parameter for Gravel

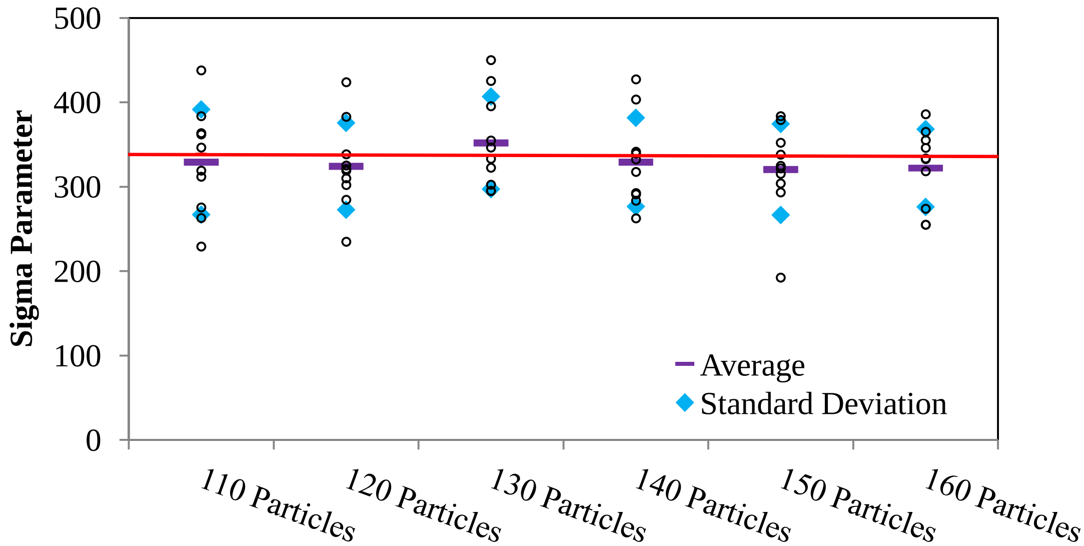

Fig. 3.35. Fine Aggregate Angularity Sigma Parameter for Gravel

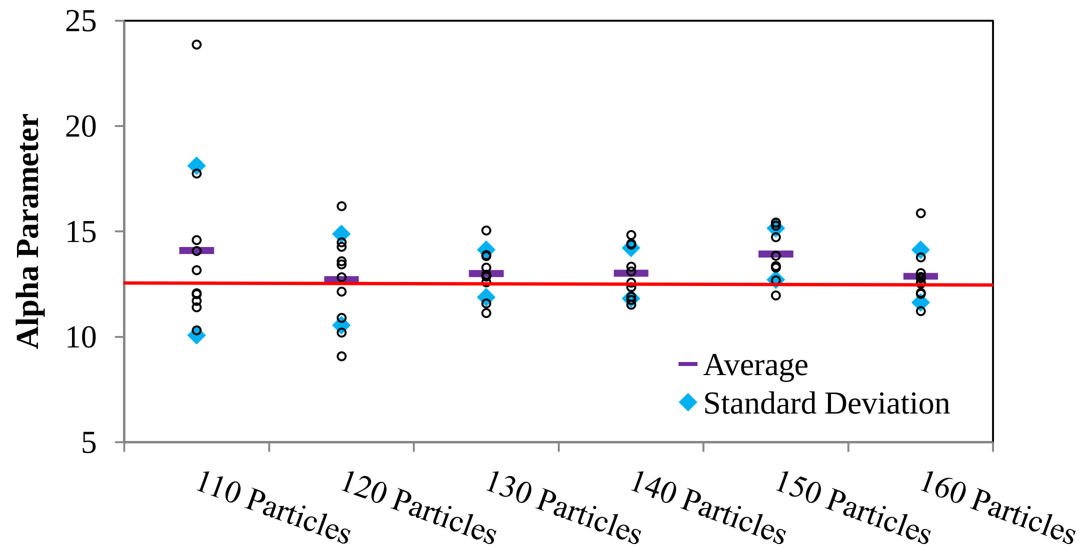

Fig. 3.36. Fine Aggregate 2D Form Alpha Parameter for Gravel

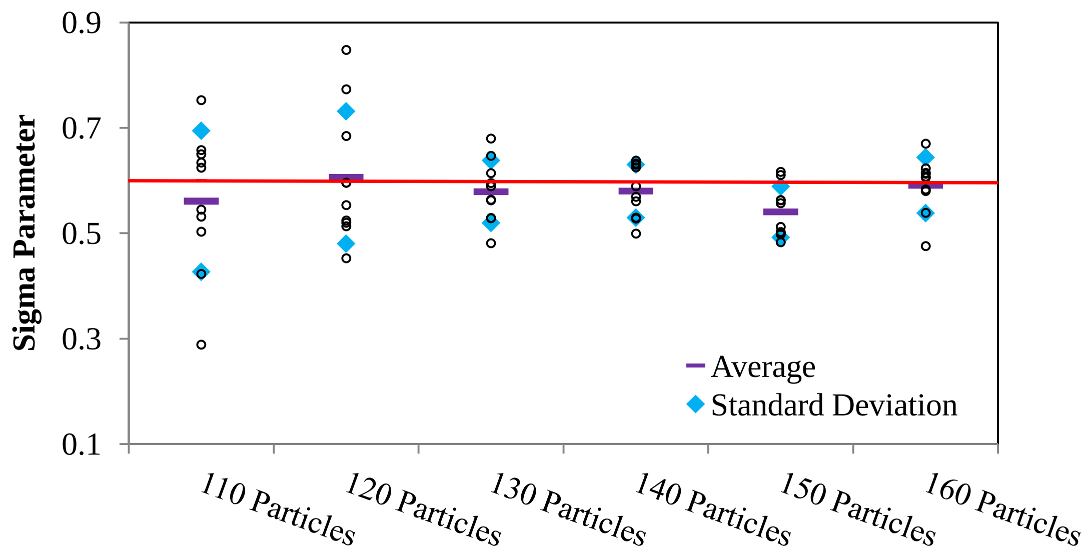

Fig. 3.37. Fine Aggregate 2D Form Sigma Parameter for Gravel

For the coarse aggregates, the average of the alpha and sigma parameter of the gamma distribution converge at approximately 30-40 aggregates for both the angularity and texture shape characteristics for the granite, crushed gravel, and limestone angularity and texture results. The standard deviation also decreases at approximately 30 - 40 aggregates. The average of the shape and scale parameters converges and standard deviation decreases at approximately 130 - 150 aggregates for the angularity and 2D form for all the fine aggregates.

SUMMARY

In this chapter, the results from AIMS1 and AIMS2 were compared. AIMS was also checked for its sensitivity to aggregate placement, number of aggregates, and sample type. AIMS1 and AIMS2 results were found to be comparable in characterizing aggregates. A shift factor was applied to the texture results of AIMS2 to match the scale of AIMS1 texture measurements. The sensitivity of the effect of aggregate placement on AIMS measurements was studied, and the statistical analysis showed that AIMS measurements varied only minimally due to these changes. The relationship of the particle placement had values of R^2 of 0.97 and higher, and the slope and intercept confidence intervals of the best-fit straight lines contained one and zero, respectively. The results of the test method were found to be sensitive to the distribution of the shape properties between different aggregate samples. From the statistical analysis of the AIMS2 sample size, it is recommended that the coarse aggregate sample size be a minimum of 40 aggregates and the fine aggregate sample size be a minimum of 150 to be representative of the aggregate source. The current test protocol of 50 coarse aggregates and 150 fine aggregates in a sample is acceptable. Overall, the two AIMS machines were producing equivalent results and the test method exhibited relatively good sensitivity.

CHAPTER IV

RUGGEDNESS EVALUATION OF AIMS2

INTRODUCTION

Different operational and environmental factors can cause significant variability in the resulting measurements if they are not identified and controlled. A ruggedness study was conducted to determine the sensitivity of the test method due to changes in levels of these important factors. The results of the ruggedness study can be used to establish appropriate ranges for the parameters in questions by determining the effect of worst-case variation in operating conditions within the tested tolerance range. Two different ASTM standards were used to conduct the ruggedness analysis and predict the effect of the factors tested, ASTM C 1067-00 “Conducting a Ruggedness or Screening Program for Test Methods for Construction Materials” and ASTM E 1169-07 “Standard Practice for Conducting Ruggedness Tests.”

Several factors were selected for evaluating the ruggedness of measuring the characteristics of fine and coarse aggregates based on previous experience of the experimental variations that can affect the test results. The high and low limits for each factor were selected based on limits that would reasonably occur in the test if no particular measures were taken to control them. The factors selected were light illumination, tray size or color, door position, ambient light, zoom level, focus, tray height, number of fine aggregates, and Convex Hull Perimeter Ratio (CHPR)value.

The light illumination, used for both coarse and fine aggregates, is the top and bottom lighting required to capture aggregate images. The top light is required to capture aggregate texture images, and the bottom lighting is required to capture the aggregate angularity images. The light intensity limits were selected to be above and below the operational settings.

Each sieve range has a corresponding tray size for the coarse aggregates. The different trays have a specific trough size to align the aggregates under the camera unit. The fine aggregates only use one tray size, but there are two different tray colors. Light colored fine aggregate which may be transparent using the typical bottom light with a clear tray, should use a darker opaque colored tray with the top light to capture the angularity images. The limits chosen for the ruggedness evaluation were the different tray sizes or color.

The AIMS2 system has transparent doors, which are thought to be adequate to block the effects of ambient light while allowing the operator to view the systems progress. Two door positions, completely open or closed, were tested to determine the significance of the door position.

The ambient light was tested to determine the effect of exterior light surrounding the system (i.e. facility lighting system). This is important since the system is supposed to be used in different laboratories, which can have different lighting. The limits, either on or off, were tested for the ambient light.

The zoom level, tray height, and focus are all system parameters which need to be controlled such that these factors do not introduce variability in the results. The zoom level of the camera is used to determine the area captured by the angularity and texture images. The camera unit focuses on the aggregate surface of the coarse aggregate texture image. The tray height is measured from the top of the inside surface of the AIMS2 base. A particle thickness is measured as the difference between the height of a particle surface and the height of the inside surface of the AIMS2 base. The number of fine aggregates was used as a factor to determine if the results are affected by slight changes in the number of aggregates analyzed.

Due to the manual spreading of the fine aggregates onto the tray, some fine aggregates are touching; touching aggregates are analyzed by AIMS2 as a single particle. The CHPR, described in Chapter II, is used to eliminate touching particles that could be analyzed as a single particle.

RUGGEDNESS ANALYSIS USING ASTM C 1067-00

The first ruggedness analysis was carried out according to ASTM C 1067-00 "Conducting a Ruggedness or Screening Program for Test Methods for Construction Materials." This test method was used to detect sources of variation in the test method due to the factors tested.

Seven factors were selected for the fine and coarse aggregates based on previous experience with the experimental factors that could cause significant variation in the test results. The high and low limits for each factor were selected based on limits that could reasonably occur in the test if no particular measures were taken to control them.

EXPERIMENTAL PROCEDURES

Following the ASTM C 1067-00 procedure, 16 scans were performed: two replicate sets of eight determinations each. A determination refers to a certain combination of the values for the factors included in the analysis. Scans 1 through 8 are duplicated for the study to obtain scans 9 through 16 in the analysis. Table 4.1 shows a template of the factors and limits for the scans preformed.

Table 4.1. Template of Ruggedness Scans for ASTM C 1067-00

Replicate Scan Number 1

			Scan Number							
Factor	Low Limit	High Limit	1	2	3	4	5	6	7	8
A	a	A	a	a	a	a	A	A	A	A
B	b	B	b	b	B	B	b	b	B	B
C	c	C	C	c	C	c	C	c	C	c
D	d	D	D	D	d	d	d	d	D	D
E	e	E	e	E	e	E	E	e	E	e
F	f	F	F	f	f	F	F	f	f	F
G	g	G	G	g	g	G	g	G	G	g

Replicate Scan Number 2

			Scan Number							
Factor	Low Limit	High Limit	9	10	11	12	13	14	15	16
A	a	A	a	a	a	a	A	A	A	A
B	b	B	b	b	B	B	b	b	B	B
C	c	C	C	c	C	c	C	c	C	c
D	d	D	D	D	d	d	d	d	D	D
E	e	E	e	E	e	E	E	e	E	e
F	f	F	F	f	f	F	F	f	f	F
G	g	G	G	g	g	G	g	G	G	g

From these scans, an effect factor can be calculated to determine the statistical significance of the limits for each factor. ASTM C1067 contains details about calculations necessary for determining the effect factor. An effect factor $\geq$ 5.59 represents a significant effect with a 5% probability for drawing an erroneous conclusion (ASTM C1067, Section 7.6). If the effect factor is $\leq$5.59 then the factor is considered not significant (NS) with a 95% level of confidence.

Experiment 1 dealt with coarse aggregate, and Experiment 2 was conducted for the analysis of the fine aggregates. The results from Experiment 1 were used as a guide to change the limits of the factors for the coarse aggregates and examine ruggedness under these new limits as part of Experiment 3. Experiment 4 investigated the normal variations within the AIMS2 system for both the coarse and fine aggregates. A summary of these experiments is shown in Table 4.2.

Table 4.2. Summary of Ruggedness Experiments Using ASTM C 1067-00

Experiment	Purpose of the Experiment	Aggregate Sizes
1	Preliminary Study to Determine the Appropriate Limits for a Rugged System	9.5mm (0.375 in)
2	Preliminary Study to Determine the Appropriate Limits for a Rugged System	1.18 mm (ASTM #16 sieve) and 0.60 mm (ASTM #30 sieve)
3	Based on Experiment 1, a Further Investigation of the Limits	9.5mm (0.375in)
4	Investigation of the Normal Variations Within the System	9.5mm (0.375in) and 0.60 mm (ASTM #30)

Experiment 1

Experiment 1 was conducted for the evaluation of the coarse aggregates using the procedure in ASTM C 1067. The analysis was done for two coarse aggregates of the same size (9.5mm (0.375 in)), but different color. Images of particles from the dark colored and light colored aggregate are shown in Fig. 4.1.

Fig. 4.1. Dark and Light 9.5mm (0.375 in) Aggregates Used in Experiment 1

The high and low limits for each factor were selected based on limits that would reasonably occur in the test if no particular measures were taken to control them. The factors and limits chosen for the coarse aggregates are shown in Table 4.3.

Table 4.3. Coarse Aggregate Factors and Limits Used in Experiment 1

Factor	Coarse Aggregate Study Factors:	Low Limit	High Limit
A	Tray size	12.5mm	4.75mm
B	Light illumination (Top and Bottom Light)	-4	+4
C	Door Position	Close	Open
D	Focus	0	+1
E	Zoom level	-5%	+5%
F	Tray Height	-1mm	+1mm
G	Ambient light (On, Off)	On	Off

The limits for the tray size were selected as one tray size above and one tray size below the correct tray size. The light illumination is the top and bottom lighting required to capture the images. The light illumination limits were selected as +4 and -4 from the operational setting to decrease and increase the system lighting. The AIMS2 doors limits were chosen as completely open or completely closed to predict the significance of the door position, which could let some additional ambient light inside the compartment where particles are images. The focus, zoom level, and tray height were used to evaluate the acceptable variability for each factor. The focus was used to find the depth of the aggregate particle when the camera focuses on the particle surface for the texture image. The tray height was the distance from the camera to the tray. The ambient light was used to account for the performance of the doors in eliminating the effect of different intensities of exterior lighting.

It was found that the bottom light during the angularity scans was producing dark shadowed lines around the trough. These dark shadows introduced an additional, uncontrollable error in the test results by reducing the total number of particles scanned especially with the lower light intensities. The coarse aggregates ruggedness study was therefore preformed a second time with different trays. Experiment 1a results discussed hereafter were those that were obtained with the use of trays that produced dark shadowed lines, while Experiment 1b refers to the results from using trays that did not have dark shadowed lines.

Tables 4.4 and 4.5 list the results from AIMS2 for the dark and light coarse aggregates for Experiment 1a. Tables 4.6 and 4.7 list the results for Experiment 1b.

Table 4.4. Results of Dark 9.5mm (0.375 in) Coarse Aggregates Used in Experiment 1a

	Angularity	Texture	Sphericity	Flat or Elongated 3:1
Scan 1	2826.68	265.71	0.65	2.92
Scan 2	2767.43	280.40	0.70	2.33
Scan 3	2756.97	264.41	0.73	2.03
Scan 4	2747.62	270.23	0.64	3.11
Scan 5	2658.89	250.85	0.67	2.79
Scan 6	3135.49	272.17	0.75	1.84
Scan 7	2846.78	272.74	0.73	2.04
Scan 8	2774.34	271.54	0.68	2.56
Scan 9	2763.31	272.66	0.63	3.12
Scan 10	2781.10	272.47	0.71	2.18
Scan 11	2759.57	264.60	0.74	2.00
Scan 12	2762.95	270.94	0.64	3.16
Scan 13	3030.97	282.86	0.65	2.82
Scan 14	2848.53	255.47	0.77	1.76
Scan 15	2756.67	272.36	0.74	2.00
Scan 16	2825.92	269.46	0.68	2.56

Table 4.5. Results of Light 9.5mm (0.375 in) Coarse Aggregates Used in Experiment 1a

	Angularity	Texture	Sphericity	Flat or Elongated 3:1
Scan 1	2434.41	43.74	0.65	2.71
Scan 2	2407.84	42.89	0.69	2.20
Scan 3	2462.07	44.79	0.73	1.98
Scan 4	2507.19	41.70	0.64	3.02
Scan 5	2336.08	37.78	0.64	2.75
Scan 6	2476.93	35.40	0.75	1.78
Scan 7	2448.42	41.28	0.71	2.06
Scan 8	2435.48	43.97	0.67	2.43
Scan 9	2422.70	40.76	0.66	2.68
Scan 10	2453.50	42.10	0.69	2.21
Scan 11	2484.49	44.04	0.73	1.98
Scan 12	2435.96	41.92	0.64	3.01
Scan 13	2807.60	40.11	0.64	2.59
Scan 14	2691.57	40.69	0.69	1.98
Scan 15	2401.64	40.84	0.71	2.05
Scan 16	2407.32	44.07	0.67	2.43

Table 4.6. Results of Dark 9.5mm (0.375 in) Coarse Aggregates Used in Experiment 1b

	Angularity	Texture	Sphericity	Flat or Elongated 3:1
Scan 1	2648.27	263.47	0.65	2.95
Scan 2	2682.28	264.23	0.70	2.35
Scan 3	2722.65	264.35	0.74	2.02
Scan 4	2784.45	260.64	0.63	3.31
Scan 5	2828.15	257.26	0.65	3.07
Scan 6	2850.43	257.84	0.75	1.91
Scan 7	2703.87	258.45	0.72	2.17
Scan 8	2753.98	260.55	0.69	2.56
Scan 9	2628.28	265.41	0.65	2.95
Scan 10	2731.97	265.11	0.70	2.35
Scan 11	2781.50	264.90	0.74	2.02
Scan 12	2732.04	263.02	0.63	3.28
Scan 13	2788.81	256.58	0.65	3.05
Scan 14	2892.87	259.52	0.75	1.95
Scan 15	2719.25	258.93	0.72	2.15
Scan 16	2765.43	261.26	0.68	2.65

Table 4.7. Results of Light 9.5mm (0.375 in) Coarse Aggregates Used in Experiment 1b

	Angularity	Texture	Sphericity	Flat or Elongated 3:1
Scan 1	2429.46	46.98	0.65	2.79
Scan 2	2322.89	45.19	0.68	2.38
Scan 3	2477.50	46.51	0.72	1.99
Scan 4	2481.87	45.55	0.62	3.17
Scan 5	2352.98	42.99	0.63	3.04
Scan 6	2422.59	44.76	0.72	1.95
Scan 7	2459.10	44.29	0.70	2.13
Scan 8	2417.34	44.88	0.67	2.54
Scan 9	2351.49	46.68	0.65	2.79
Scan 10	2421.08	46.39	0.68	2.30
Scan 11	2532.09	46.54	0.73	1.99
Scan 12	2466.29	46.04	0.62	3.16
Scan 13	2376.74	43.32	0.63	2.94
Scan 14	2396.31	44.61	0.72	1.94
Scan 15	2444.22	43.99	0.70	2.14
Scan 16	2414.69	44.06	0.67	2.53

The statistical analysis identified the statistically significant factors for Experiments 1a and 1b. The results found the factors to be significant or not significant (NS). The summary of the analysis for the coarse aggregates is shown in Table 4.8.

Table 4.8. Coarse Aggregates Summary of Results Used in Experiment 1

	Experiment 1a		Experiment 1b		
	Light	Dark	Light	Dark	Factors
Angularity	NS	NS	NS	160.03	Tray size
	NS	NS	96.34	NS	Light illumination
	NS	NS	NS	25.24	Door Position
	NS	NS	NS	408.77	Focus
	NS	NS	NS	NS	Zoom level
	NS	NS	NS	NS	Tray Height
	NS	NS	NS	NS	Ambient light
Texture	19.39	NS	4933.41	20737.60	Tray size
	25.86	NS	NS	NS	Light illumination
	NS	NS	NS	NS	Door Position
	5.89	NS	NS	235.86	Focus
	NS	NS	164.87	220.20	Zoom level
	NS	NS	NS	NS	Tray Height
	6.25	NS	NS	17.65	Ambient light
Sphericity	NS	255.69	8431.15	27870.38	Tray size
	NS	NS	2696.45	606.57	Light illumination
	NS	NS	32.90	NS	Door Position
	NS	NS	NS	NS	Focus
	121.02	56.09	567676.59	210883.99	Zoom level
	4305.08	13049.38	9961142.09	5330850.92	Tray Height
	NS	NS	NS	NS	Ambient light
Flat or Elongated 3:1	876.31	2119.02	8095.51	27942.97	Tray size
	NS	NS	121.76	118.08	Light illumination
	NS	NS	NS	NS	Door Position
	NS	NS	241.74	162.87	Focus
	1375.34	400.86	137713.27	169145.47	Zoom level
	84311.45	122749.74	3483469.88	7088424.96	Tray Height
	25.61	12.01	49.65	424.29	Ambient light

Overall, the angularity and texture variations were significant due to the tray size, light illumination, ambient light, door position, focus, and zoom level. The sphericity and flat or elongated 3:1 results had more significant factors than the angularity and texture results. The tray size, light illumination, door position, focus, zoom level, and tray height affected both the sphericity and flat or elongated results. The ambient light affected only the flat or elongated results. Since the ambient light had a statistical significance on the results, but the AIMS2 door position did not, it was concluded the AIMS2 doors were not shedding the exterior light as designed. As will be discussed later, this led to changing the doors to be non-transparent that and this allow ambient light into the system.

Experiment 2

Four fine aggregates were used in the analysis of Experiment 2. The four aggregates consisted of both a dark and light colored aggregates in two sieve ranges, 1.18 mm (ASTM #16 sieve) and 0.60 mm (ASTM #30 sieve). These aggregates are shown in Figs. 4.2 and 4.3. The fine aggregate factors and limits are listed in Table 4.9.

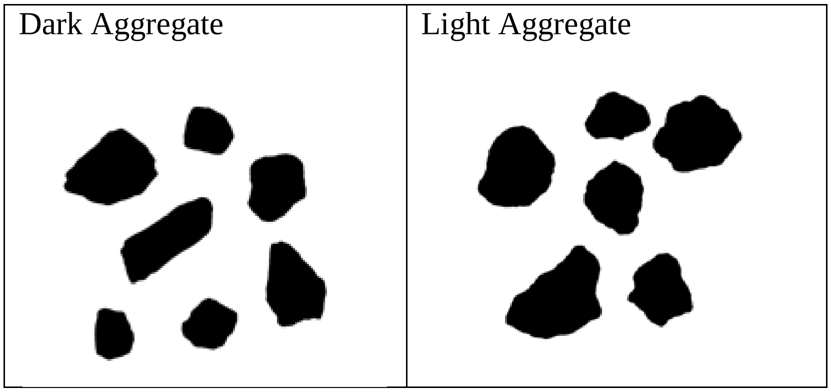

Fig. 4.2. Dark and Light1.18 mm (ASTM #16 Sieve) Aggregates Used in Experiment 2

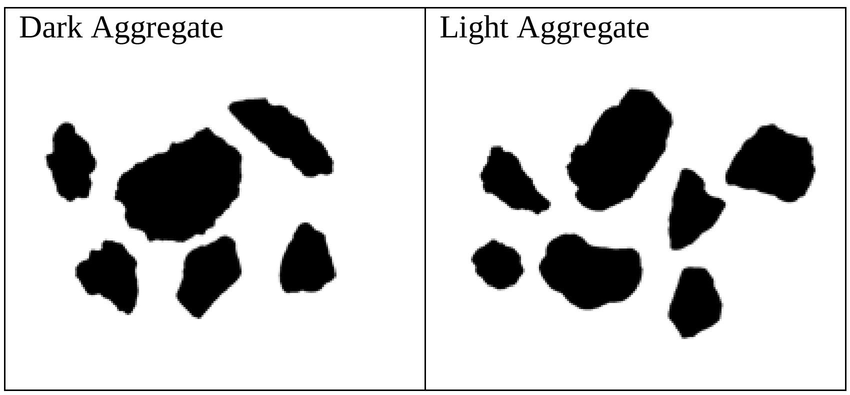

Fig. 4.3. Dark and Light 0.60 mm (ASTM #30 Sieve) Aggregates Used in Experiment 2

Table 4.9. Fine Aggregate Factors and Limits Used in Experiment 2

Factor	Fine Aggregate Study Factors:	Low Limit	High Limit
A	Tray color	Clear Tray	Opaque Tray
B	Light illumination (Top and Bottom Light)	Top -4 Bottom 0	Top +4 Bottom +4
C	Door Position	Closed	Open
D	CHPR	0	0.02
E	Zoom level	-5%	+5%
F	Particle Count	-25	+25
G	Ambient light	On	Off

One tray size is used for all the fine aggregates, but the user must select the tray color, either clear or opaque, depending on the aggregate size and color. The top or bottom lighting for the fine aggregates is directly related to the tray color; the bottom is used if the tray color is clear and the top light is used if the tray color is opaque. For the clear tray, the bottom light was not able to analyze the images at -4 as was used for the coarse aggregates, therefore the limits were changed to 0 and +4 as shown in Table 4.9. The top lighting was kept at the same limits of +4 and -4. The particle count was added to determine the effect of analyzing more or less than the operational number of particles. The CHPR value was used to eliminate touching particles that could be captured and analyzed as a single particle. The results for the dark and light fine aggregates are shown in Tables 4.10, 4.11, 4.12, and 4.13.

Table 4.10. Results of Dark 1.18 mm (ASTM #16 Sieve) Fine Aggregates Used in Experiment 2

	Angularity	2D Form
Scan 1	2733.38	7.01
Scan 2	2773.50	6.90
Scan 3	2749.41	7.06
Scan 4	2728.83	7.15
Scan 5	4232.48	8.84
Scan 6	4130.45	8.77
Scan 7	3974.41	8.53
Scan 8	3886.20	8.54
Scan 9	2760.43	7.00
Scan 10	2750.34	6.90
Scan 11	2741.02	7.04
Scan 12	2730.96	7.18
Scan 13	3933.64	8.46
Scan 14	4095.74	8.76
Scan 15	4038.62	8.74
Scan 16	3984.80	8.70

Table 4.11. Results of Light 1.18 mm (ASTM #16 Sieve) Fine Aggregates Used in Experiment 2

	Angularity	2D Form
Scan 1	3361.02	7.62
Scan 2	3395.39	7.56
Scan 3	3450.58	7.77
Scan 4	3364.33	7.69
Scan 5	3518.22	7.75
Scan 6	3502.52	7.84
Scan 7	3418.22	7.63
Scan 8	3493.94	7.65
Scan 9	3336.29	7.57
Scan 10	3326.40	7.57
Scan 11	3392.10	7.84
Scan 12	3367.07	7.66
Scan 13	3505.06	7.72
Scan 14	3520.79	7.84
Scan 15	3464.49	7.62
Scan 16	3498.74	7.63

Table 4.12. Results of Dark 0.60 mm (ASTM #30 Sieve) Fine Aggregates Used in Experiment 2

	Angularity	2D Form
Scan 1	3865.54	8.07
Scan 2	4035.04	8.34
Scan 3	3888.82	7.94
Scan 4	3940.66	8.19
Scan 5	4257.11	8.72
Scan 6	4524.45	9.00
Scan 7	4448.05	8.69
Scan 8	4488.10	8.74
Scan 9	3932.82	8.13
Scan 10	4021.97	8.23
Scan 11	3816.84	7.91
Scan 12	3923.79	8.03
Scan 13	4267.24	8.74
Scan 14	4566.33	8.95
Scan 15	4444.20	8.95
Scan 16	4506.22	8.76

Table 4.13. Results of Light 0.60 mm (ASTM #30 Sieve) Fine Aggregates Used in Experiment 2

	Angularity	2D Form
Scan 1	3476.30	7.29
Scan 2	3529.06	7.23
Scan 3	3512.45	7.27
Scan 4	3490.71	7.26
Scan 5	3251.36	7.38
Scan 6	3361.33	7.49
Scan 7	3215.62	7.44
Scan 8	3144.88	7.42
Scan 9	3518.83	7.26
Scan 10	3518.01	7.31
Scan 11	3503.70	7.27
Scan 12	3518.25	7.23
Scan 13	3230.41	7.36
Scan 14	3351.78	7.57
Scan 15	3159.08	7.47
Scan 16	3180.98	7.48

The factors which could cause significant variation based on the limits tested, were identified for the fine aggregates. The summary of the analysis is shown in Table 4.14. The tray color was significant in affecting angularity and 2D form results for both aggregate colors and all sizes. All of the seven factors were significant for either the angularity or the 2D form for one or more of the four fine aggregate samples tested. Since both the AIMS2 door and the ambient light were significant, the AIMS2 doors seem to be assisting to some extent in shedding exterior light. However, replacing the doors to non-transparent should decrease or eliminate the influence of ambient light.

Table 4.14. Fine Aggregates Summary of Results Used in Experiment 2

	1.18 mm (ASTM #16 Sieve)		0.60 mm (ASTM #30 Sieve)		
	Dark	Light	Dark	Light	Factors
Angularity	533994.64	1826.07	952321.83	125990.04	Tray color
	NS	NS	NS	387.33	Light illumination
	NS	NS	4796.95	15.10	Door Position
	NS	27.78	331.31	293.74	CHPR
	NS	NS	13.70	NS	Zoom level
	NS	NS	349.59	75.06	Particle Count
	NS	8.94	60.90	13.52	Ambient light
2D Form	241891.77	103.93	32755.39	7789.89	Tray color
	NS	NS	28.00	NS	Light illumination
	NS	NS	45.84	5.76	Door Position
	6.44	9028.55	NS	NS	CHPR
	NS	384.09	NS	34.92	Zoom level
	NS	77.40	NS	32.19	Particle Count
	NS	NS	NS	9.89	Ambient light

Experiment 3

Additional analyses were performed on the coarse aggregates from Experiment 1 (Fig. 4.1) to determine the appropriate limits that would not affect the AIMS2 results. In Experiment 3, some of the previous factors from Experiment 1 were removed and the limits of the remaining factors were tightened. A "dummy factor" was introduced to put in place of the removed factors. These "dummy factors" did not change any of the settings. AIMS2 doors factors were not included in Experiment 3 since it was important to focus on the remaining factors. Table 4.15 lists the Experiment 3 coarse aggregate factors and limits. The results of the 9.5mm (0.375in) coarse aggregates are shown in

Tables 4.16 and 4.17 for the dark and light aggregates, respectively. The effect factors were found to determine the significance of the factors tested. The summary of the effect factors is shown in Table 4.18.

Table 4.15. Coarse Aggregate Factors and Limits Used in Experiment 3

Factor	Coarse Aggregate Adjusted Study Factors:	Low Limit	High Limit
A	Tray size	9.5mm	4.75mm
B	Light illumination (Top light and Bottom light)	-4	+4
C	"Dummy Factor"	0	0
D	"Dummy Factor"	0	0
E	"Dummy Factor"	0	0
F	Tray Height	-0.5mm	+0.5mm
G	Ambient light	On	Off

Table 4.16. Results of Dark 9.5mm (0.375 in) Coarse Aggregates Used in Experiment 3

	Angularity	Texture	Sphericity	Flat or Elongated 3:1
Scan 1	2703.54	261.97	0.65	2.97
Scan 2	2570.88	261.76	0.69	2.43
Scan 3	2741.46	261.72	0.70	2.41
Scan 4	2732.39	262.35	0.66	2.88
Scan 5	2630.47	270.62	0.66	2.85
Scan 6	2539.57	268.44	0.69	2.41
Scan 7	2714.99	270.44	0.70	2.36
Scan 8	2688.32	268.80	0.67	2.79
Scan 9	2642.89	260.08	0.65	2.93
Scan 10	2656.08	262.86	0.69	2.44
Scan 11	2689.69	261.48	0.70	2.40
Scan 12	2733.28	263.37	0.66	2.89
Scan 13	2625.65	268.98	0.66	2.81
Scan 14	2608.40	269.83	0.69	2.43
Scan 15	2737.52	268.91	0.70	2.35
Scan 16	2722.96	268.96	0.66	2.81

Table 4.17. Results of Light 9.5mm (0.375 in) Coarse Aggregates Used in Experiment 3

	Angularity	Texture	Sphericity	Flat or Elongated 3:1
Scan 1	2329.30	41.40	0.64	2.94
Scan 2	2374.09	41.29	0.68	2.42
Scan 3	2434.67	41.28	0.68	2.38
Scan 4	2443.27	42.03	0.65	2.86
Scan 5	2349.79	40.99	0.65	2.82
Scan 6	2328.91	42.29	0.68	2.40
Scan 7	2408.62	40.77	0.68	2.36
Scan 8	2371.11	40.71	0.65	2.76
Scan 9	2303.40	41.79	0.64	2.96
Scan 10	2373.15	41.59	0.68	2.44
Scan 11	2406.42	40.98	0.68	2.40
Scan 12	2403.76	41.64	0.65	2.88
Scan 13	2345.61	41.50	0.64	2.88
Scan 14	2325.77	41.20	0.67	2.43
Scan 15	2406.41	40.74	0.69	2.34
Scan 16	2373.41	42.02	0.65	2.78

Table 4.18. Coarse Aggregates Summary of Results Used in Experiment 3

	Experiment 3		
	Light	Dark	Factors
Angularity	64.12	NS	Tray size
	7308.12	337.25	Light illumination
	NS	NS	"Dummy Factor"
	9.66	NS	"Dummy Factor"
	293.44	NS	"Dummy Factor"
	37.33	NS	Tray Height
	NS	NS	Ambient light
Texture	NS	13151.15	Tray size
	NS	NS	Light illumination
	NS	NS	"Dummy Factor"
	NS	NS	"Dummy Factor"
	NS	NS	"Dummy Factor"
	NS	NS	Tray Height
	NS	NS	Ambient light
Sphericity	27.87	5344.64	Tray size
	1602.37	3849.15	Light illumination
	NS	NS	"Dummy Factor"
	7.79	NS	"Dummy Factor"
	NS	11.26	"Dummy Factor"
	847660.40	7085309.92	Tray Height
	NS	21.33	Ambient light
Flat or Elongated 3:1	3753.97	746.50	Tray size
	5271.79	207.21	Light illumination
	7.01	NS	"Dummy Factor"
	NS	NS	"Dummy Factor"
	NS	NS	"Dummy Factor"
	11256827.41	2005250.58	Tray Height
	480.54	42.50	Ambient light

The angularity results of both aggregates (light and dark) showed significant variation with only changes in the light illumination. Several factors for the light aggregate angularity were significant including tray size, tray height, and two "dummy factors". The texture results have significant variations due to changes in the tray size only. The sphericity and flat or elongated 3:1 results were affected by changes in the tray size, light illumination, tray height, ambient light, and two "dummy factors".

Experiment 4

Since there were some "dummy factors" shown to be significant in Experiment 3, Experiment 4 was conducted using all factors as "dummy factors." This was done to determine if the normal variations within the AIMS2 system were rugged. The dark 9.5mm (0.375in) (Fig. 4.1) coarse aggregates and light and dark 0.60 mm (ASTM #30) (Fig. 4.3) fine aggregates were used in Experiment 4. In addition, the doors were changed to non-transparent which no longer allowed ambient light into the system. Table 4.19 lists the factors and the limits for Experiment 4. These were the same for the coarse and fine aggregates. The results from Experiment 4 for the coarse and fine aggregates are shown in Tables 4.20, 4.21, and 4.22. The summary of the effect factors is shown in Table 4.23 for the coarse aggregates and Table 4.24 for the fine aggregates.

Table 4.19. Coarse and Fine Aggregate Factors and Limits Used in Experiment 4

Factor	Coarse and Fine Aggregate Factors:	Low Limit	High Limit
A	"Dummy Factor"	0	0
B	"Dummy Factor"	0	0
C	"Dummy Factor"	0	0
D	"Dummy Factor"	0	0
E	"Dummy Factor"	0	0
F	"Dummy Factor"	0	0
G	"Dummy Factor"	0	0

Table 4.20. Results of Dark 9.5mm (0.375in) Coarse Aggregates Used in Experiment 4

	Angularity	Texture	Sphericity	Flat or Elongated 3:1
Scan 1	2731.88	656.32	0.66	2.78
Scan 2	2751.49	657.16	0.66	2.79
Scan 3	2719.72	660.84	0.66	2.78
Scan 4	2722.21	657.90	0.67	2.73
Scan 5	2680.50	659.98	0.66	2.77
Scan 6	2697.37	658.39	0.67	2.75
Scan 7	2728.48	662.15	0.66	2.78
Scan 8	2747.92	661.14	0.66	2.77
Scan 9	2702.50	661.24	0.66	2.77
Scan 10	2747.12	663.30	0.66	2.76
Scan 11	2706.37	660.57	0.66	2.77
Scan 12	2719.17	657.08	0.66	2.75
Scan 13	2709.70	657.85	0.66	2.76
Scan 14	2677.41	661.83	0.66	2.76
Scan 15	2730.12	661.51	0.67	2.75
Scan 16	2660.21	658.07	0.67	2.73

Table 4.21. Results of Dark 0.60 mm (ASTM #30 Sieve) Fine Aggregates Used in Experiment 4

	Angularity	2D Form
Scan 1	3841.29	7.83
Scan 2	3727.50	7.72
Scan 3	3900.22	7.74
Scan 4	3772.68	7.79
Scan 5	3761.00	7.80
Scan 6	3775.48	7.82
Scan 7	3712.38	7.73
Scan 8	3810.79	7.78
Scan 9	3737.36	7.76
Scan 10	3815.72	7.74
Scan 11	3897.90	7.82
Scan 12	3800.96	7.73
Scan 13	3845.72	7.73
Scan 14	3851.68	7.79
Scan 15	3884.05	7.76
Scan 16	3892.99	7.74

Table 4.22. Results of Light 0.60 mm (ASTM #30 Sieve) Fine Aggregates Used in Experiment 4

	Angularity	2D Form
Scan 1	3330.09	6.91
Scan 2	3241.78	6.91
Scan 3	3293.31	6.94
Scan 4	3306.61	6.95
Scan 5	3318.89	6.96
Scan 6	3359.40	6.95
Scan 7	3351.62	6.95
Scan 8	3326.83	6.94
Scan 9	3324.90	6.95
Scan 10	3380.49	6.95
Scan 11	3376.37	6.95
Scan 12	3375.59	6.96
Scan 13	3362.93	6.95
Scan 14	3410.54	6.95
Scan 15	3334.68	6.93
Scan 16	3359.42	6.92

Table 4.23. Coarse Aggregates Summary of Results Used in Experiment 4

	Experiment 4	
	Dark	Factors
Angularity	NS	"Dummy Factor"
	NS	"Dummy Factor"
	NS	"Dummy Factor"
	NS	"Dummy Factor"
	NS	"Dummy Factor"
	NS	"Dummy Factor"
	NS	"Dummy Factor"
Texture	NS	"Dummy Factor"
	NS	"Dummy Factor"
	NS	"Dummy Factor"
	NS	"Dummy Factor"
	NS	"Dummy Factor"
	NS	"Dummy Factor"
	NS	"Dummy Factor"
Sphericity	NS	"Dummy Factor"
	NS	"Dummy Factor"
	NS	"Dummy Factor"
	NS	"Dummy Factor"
	NS	"Dummy Factor"
	NS	"Dummy Factor"
	NS	"Dummy Factor"
Flat or Elongated 3:1	NS	"Dummy Factor"
	NS	"Dummy Factor"
	NS	"Dummy Factor"
	NS	"Dummy Factor"
	NS	"Dummy Factor"
	NS	"Dummy Factor"
	NS	"Dummy Factor"

Table 4.24. Fine Aggregates Summary of Results Used in Experiment 4

	Experiment 4		
	Dark	Light	Factors
Angularity	NS	NS	"Dummy Factor"
	NS	NS	"Dummy Factor"
	NS	NS	"Dummy Factor"
	NS	NS	"Dummy Factor"
	NS	NS	"Dummy Factor"
	NS	NS	"Dummy Factor"
	NS	NS	"Dummy Factor"
2D Form	NS	NS	"Dummy Factor"
	NS	NS	"Dummy Factor"
	NS	NS	"Dummy Factor"
	NS	NS	"Dummy Factor"
	NS	NS	"Dummy Factor"
	NS	NS	"Dummy Factor"
	NS	NS	"Dummy Factor"

All of the “dummy factors” for the coarse and fine aggregates showed no significance in the results of the system. It can be concluded that AIMS2 is able to control normal variation in the factors, and this normal variation does not present a statistically significant influence on the results.

SUMMARY OF ASCE ASTM C 1067-00 RUGGEDNESS

The ASTM C 1067-00 ruggedness study led to identifying significant factors affecting the AIMS2 results. The AIMS2 transparent doors were not able to control the effect of ambient lighting changes as originally predicted, so the doors were replaced with non-transparent doors. The new doors were designed to block any ambient light which was shown to be affecting the results. When all “dummy factors” were used and all of the limits were selected to their correct values, AIMS2 was able to control the normal variations in the system such that the AIMS2 controlled factors have no statistical significant effect on the results.

From the results of Experiments 1 and 2 discussed in this report, some factors were thought to be interacting with each other. This could cause factor effects to be artificially significant. ASTM C 1067-00 assumes that any interactions among factors tested are negligible and therefore not included in the test procedure. However, if the effect of the interactions are not negligible, the estimates of the effect could include be skewed due to interactions. Therefore, it was decided to conduct an additional ruggedness study using ASTM E 1169-07 to have a better understanding of the interaction of the factors.

RUGGEDNESS ANALYSIS USING ASTM E 1169-07

Another ruggedness study was conducted with a new set of ranges to identify factors that significantly influence the measurements provided by the AIMS2 and to estimate possible interaction between factors. The study was carried out in accordance with ASTM E 1169-07, “Standard Practice for Conducting Ruggedness Tests.” ASTM E 1169-07 differs from the ASTM C 1067, since ASTM E 1169 is able to identify interactions which may arise from the interference of the individual factors.

EXPERIMENTAL PROCEDURES

The ruggedness test required 16 total scans of seven factors and specified high and low limits. The last eight scans (scans 9 through 16) are an inverse of the first eight scans (scans 1 through 8). This means that the low limits in scans 1 to 8 are used as the high limits in scans 9 to 16 and vice versa. Table 4.25 shows a template of the 16 scans and the limit levels (high or low) of each factor for all the scans.

Table 4.25. Template of Ruggedness Scans for ASTM E 1169-07

Replicate Scans Number 1

			Scan Number							
Factor	Low Limit	High Limit	1	2	3	4	5	6	7	8
A	a	A	A	a	a	A	a	A	A	a
B	b	B	B	B	b	b	B	b	B	b
C	c	C	C	C	C	c	c	C	c	c
D	d	D	d	D	D	D	d	d	D	d
E	e	E	E	e	E	E	E	e	e	e
F	f	F	f	F	f	F	F	F	f	f
G	g	G	g	g	G	g	G	G	G	g

Duplicate Scans

			Scan Number							
Factor	Low Limit	High Limit	9	10	11	12	13	14	15	16
A	a	A	a	A	A	a	A	a	a	A
B	b	B	b	b	B	B	b	B	b	B
C	c	C	c	c	c	C	C	c	C	C
D	d	D	D	d	d	d	D	D	d	D
E	e	E	E	E	e	e	e	E	E	E
F	f	F	F	f	F	f	f	f	F	F
G	g	G	G	G	g	G	g	g	g	G

The calculated effect of each factor as explained in ASTM E 1169-07 is used to determine the statistical significance of the factor on the results. As discussed earlier, the ASTM E 1169-07 method considers the interactions between factors in the test as oppose to the ASTM C 1067-00 method. If the effect of one factor depends on the level of another factor, then these two factors interact. As a general rule, factors only interact when factors have large effects or statistical significance by themselves. The suffix –I is used to indicate the two factor interaction. For example, the position of the door and the intensity of the ambient light may be interacting in causing error in the test results or a false increase in a factor's effect. If an interaction is found, and both the door position and ambient light have large effects, then the interaction is mostly likely caused by these two factors. In this case, the door position and ambient light will typically be found to be statistically significant. If for the interaction there are no possible factors with large individual effects, then the cause of the interaction may be unclear. The unclear interactions could be caused by more than one set of two factor interactions. The list of possible two factor interactions for each interaction effect is shown in Table 4.26. ASTM E 1169-07 contains the required details to calculate the effect factor and interaction for the different main factors.

Table 4.26. Possible Cause of Interactions for ASTM E 1169-07

Interaction	Possible Causes		
A-I	BF	CD	EG
B-I	AF	CG	DE
C-I	AD	BG	EF
D-I	AC	BE	FG
E-I	AG	BD	CF
F-I	AB	CE	DG
G-I	AE	BC	DF

In order to determine the significant factors and interaction, effect factors are plotted on a half-normal plot. A half-normal plot is an analytical test for revealing the presence of outliers by comparing the residuals from the data to the expected observed values from a normal distribution. Both the residuals and expected values are ordered. Points from the plot usually align along a straight line. The values that do not fall along the line and are in the top right of the plot are considered outliers. The half normal plot is much like a normal probability plot, except the outliers of the sample appear only in to upper right corner of the plot instead of at both ends (Devore 2004).

A linear line to represent the standard error for the estimates is drawn through the smallest effects, which are linearly oriented. Potential significant effect factors are those which fall farthest to the right of the standard error line. The statistical significance of factors that lie close, but are to the right of the standard error line were considered to be unclear.

Several experiments were conducted using both coarse and fine aggregates with different limits until the method was concluded to be rugged. Experiments 5 and 6 dealt with coarse aggregate, while Experiments 7 and 8 were for the fine aggregates. Experiment 9 was conducted to further investigate the influence of narrowing the limits of factors used in Experiment 6 on the aggregate height measurements. Replicate measurements of the aggregate height dimensions were compared to determine the ability of AIMS2 to produce replicate measurements for different types and sizes of coarse aggregates in Experiment 10. A summary of the experiments is shown in Table 4.27.

Table 4.27. Summary of Ruggedness Experiments Using ASTM E 1169-07

Experiment	Purpose of the Experiment	Aggregate Sizes
5	Study to Determine the Appropriate Limits for a Rugged System	9.5mm (0.375 in) and 4.75mm (ASTM #4 sieve)
6	Based on Experiment 5, a Further Investigation of the Limits	9.5mm (0.375 in) and 4.75mm (ASTM #4 sieve)
7	Study to Determine the Appropriate Limits for a Rugged System	1.18 mm (ASTM #16 sieve) and 0.15 mm (ASTM #100 sieve)
8	Based on Experiment 7, a Further Investigation of the Limits	1.18 mm (ASTM #16 sieve) and 0.15 mm (ASTM #100 sieve)
9	Further Investigation of the Limits that Affect the Aggregate Height Measurements from Experiment 6	9.5mm (0.375 in) and 4.75mm (ASTM #4 sieve)
10	Comparison of Replicate Height Measurements Gather by AIMS2	25.0mm (1.0 in) to 4.75mm (ASTM #4 sieve)

Experiment 5

Experiment 5 was carried out on two different coarse aggregates (a dark colored aggregate and a light colored aggregate) with a size of 9.5mm (0.375in) (Fig. 4.4). Table 4.28 lists the factors and limits chosen for this experiment.

Fig. 4.4. Dark and Light 9.5mm (0.375 in) Aggregates Used in Experiment 5

Table 4.28. Coarse Aggregate Factors and Limits Used in Experiment 5

Factor	Coarse Aggregate Study Factors:	Low Limit	High Limit
A	Light Illumination	-1	+1
B	Tray Height	-0.25mm	+0.25mm
C	Tray Size	4.75mm	9.5mm
D	Door Position	Open	Closed
E	Ambient Light	Off	On
F	Zoom Level	-1%	+1%
G	Focus (DOF)	1%	0%

The limits of the light illumination were selected as +1 and -1 light intensity from the operational setting which are used to decrease and increase the light illumination setting of the system. The limits for the tray size were selected as the correct tray size, 9.5mm, and one tray size below the correct tray size of 4.75mm. The ambient light, either on or off, was included in order to consider the performance of the doors in eliminating the effect of changes in exterior lighting. The position of the door limits were selected as completely closed or completely open. The focus, zoom level, and tray height limits were chosen to evaluate the acceptable variability for each factor.

Table 4.29 summarizes the texture, angularity, and sphericity results for the dark coarse aggregate. The light coarse aggregate results are summarized in Table 4.30.

Table 4.29. Results of Dark 9.5mm (0.375in) Coarse Aggregates Used in Experiment 5

	Angularity	Texture	Sphericity
Scan 1	2755.46	649.97	0.683
Scan 2	2634.78	650.33	0.673
Scan 3	2615.31	661.51	0.692
Scan 4	2680.15	667.60	0.702
Scan 5	2677.53	661.01	0.679
Scan 6	2703.25	658.79	0.699
Scan 7	2701.79	660.62	0.686
Scan 8	2649.91	659.61	0.700
Scan 9	2648.56	664.01	0.694
Scan 10	2693.35	657.70	0.702
Scan 11	2695.93	664.36	0.682
Scan 12	2623.58	654.00	0.677
Scan 13	2697.51	653.63	0.703
Scan 14	2647.31	657.26	0.681
Scan 15	2664.08	655.03	0.697
Scan 16	2714.22	658.51	0.672

Table 4.30. Results of Light 9.5mm (0.375in) Coarse Aggregates Used in Experiment 5

	Angularity	Texture	Sphericity
Scan 1	2369.09	108.08	0.663
Scan 2	2270.35	105.52	0.660
Scan 3	2319.58	108.62	0.682
Scan 4	2487.44	102.65	0.691
Scan 5	2407.35	100.73	0.668
Scan 6	2368.62	104.98	0.680
Scan 7	2467.20	102.23	0.676
Scan 8	2433.93	102.35	0.688
Scan 9	2420.17	101.37	0.684
Scan 10	2439.31	102.18	0.694
Scan 11	2493.94	101.67	0.673
Scan 12	2352.91	106.55	0.664
Scan 13	2366.58	107.07	0.688
Scan 14	2399.35	102.62	0.672
Scan 15	2353.66	106.14	0.677
Scan 16	2417.20	107.34	0.664

Figs. 4.5, 4.6, and 4.7 show the half-normal plot for the dark aggregate angularity, texture, and sphericity, respectively, while the light aggregate plots are shown in Figs. 4.8, 4.9, and 4.10.

From the half-normal plots of the dark aggregate, three factors were shown to be statistically significant, one for each of the shape characteristics. Light illumination, Factor A, appears to affect the angularity results (Fig. 4.5); tray size, Factor C, appears to be statistically significant for the texture results (Fig. 4.6); and the sphericity results are affected by tray height, Factor B (Fig. 4.7).

The factors tested appear to affect the light coarse aggregate results more than the dark colored aggregate results. The angularity results were affected by tray size (Factor C) and light illumination (Factor A), and by several interaction factors, Factor C-I, F-I, and B-I (Fig. 4.8). The most likely cause for the large C-I interaction factor was the AD interaction since A (light illumination) and D (door position) have large main effects. The interaction AB (light illumination and tray height) or CE (tray size and ambient light) was most likely the cause for the large F-1 factor; the interaction AF (light illumination and zoom level) was most likely the cause of the large B-1 factor. The significance of Factors D (door position), F (zoom level), A-1, and E-1 were unclear. Factor C, tray size, appears to be statistically significant for the texture results (Fig. 4.9). It was not clear whether the zoom level, Factor F, has a significant effect on the texture results or not. The sphericity results appears to be affected by Factors B, C, A, and F which were tray height, tray size, light illumination, and zoom level, respectively (Fig. 4.10).

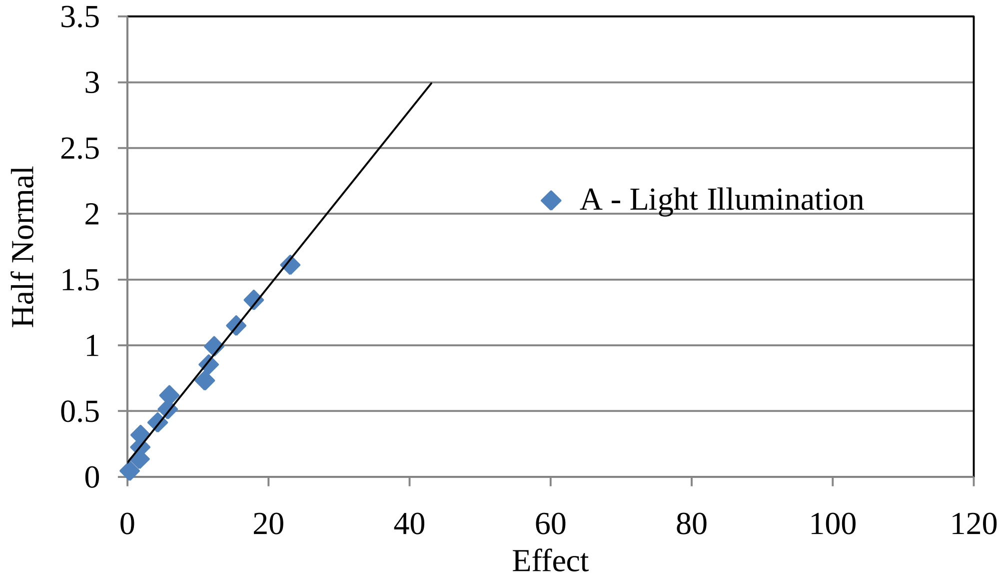

Fig. 4.5. Half-Normal Plot of the Angularity of the Dark 9.5mm (0.375in) Coarse Aggregate Used in Experiment 5

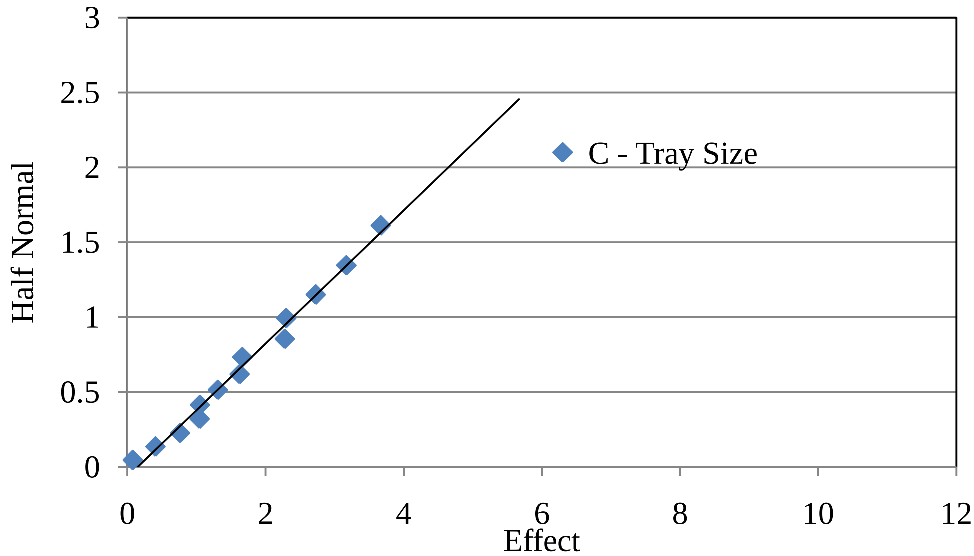

Fig. 4.6. Half-Normal Plot of the Texture of the Dark 9.5mm (0.375in) Coarse Aggregate Used in Experiment 5

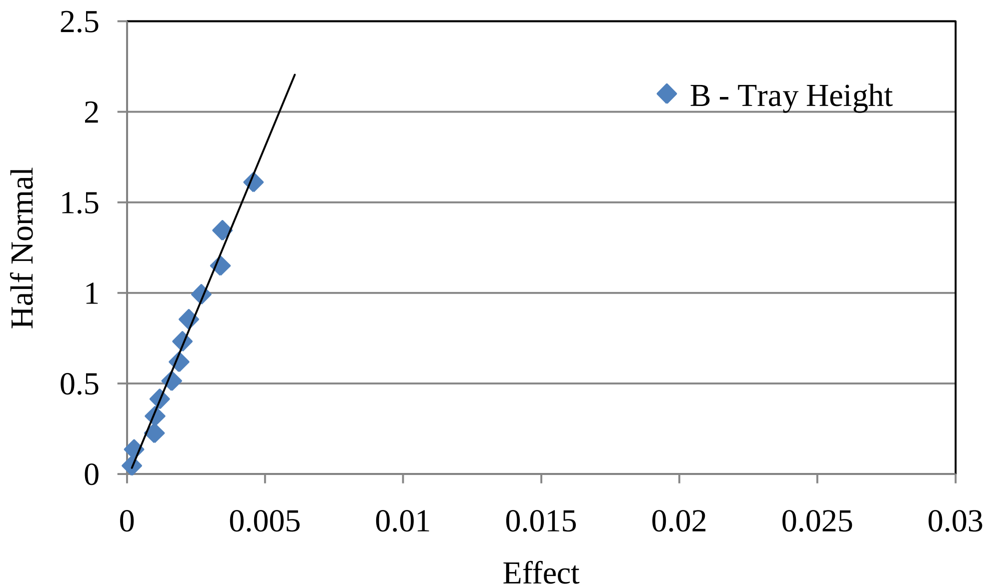

Fig. 4.7. Half-Normal Plot of the Sphericity of the Dark 9.5mm (0.375in) Coarse Aggregate Used in Experiment 5

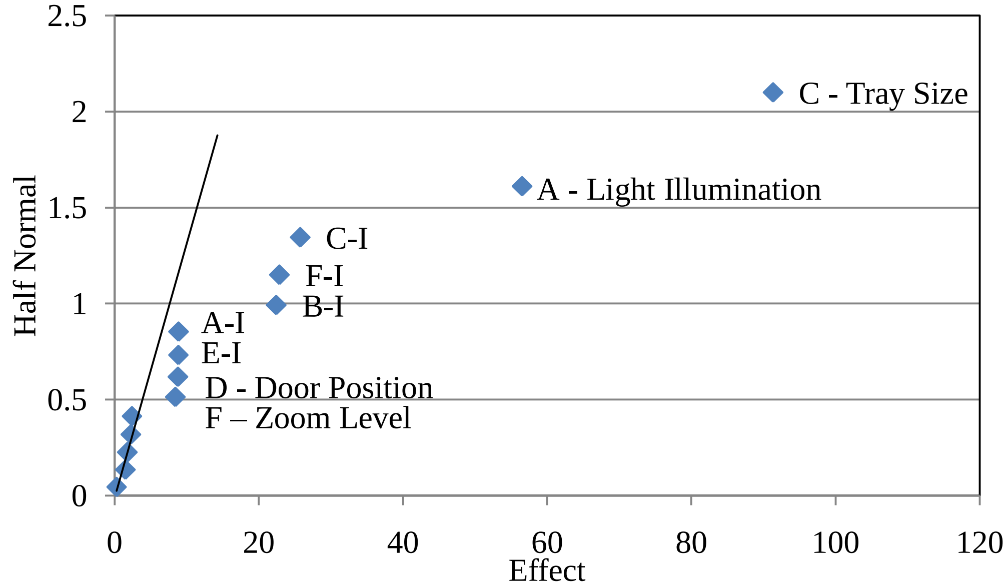

Fig. 4.8. Half-Normal Plot of the Angularity of the Light 9.5mm (0.375in) Coarse Aggregate Used in Experiment 5

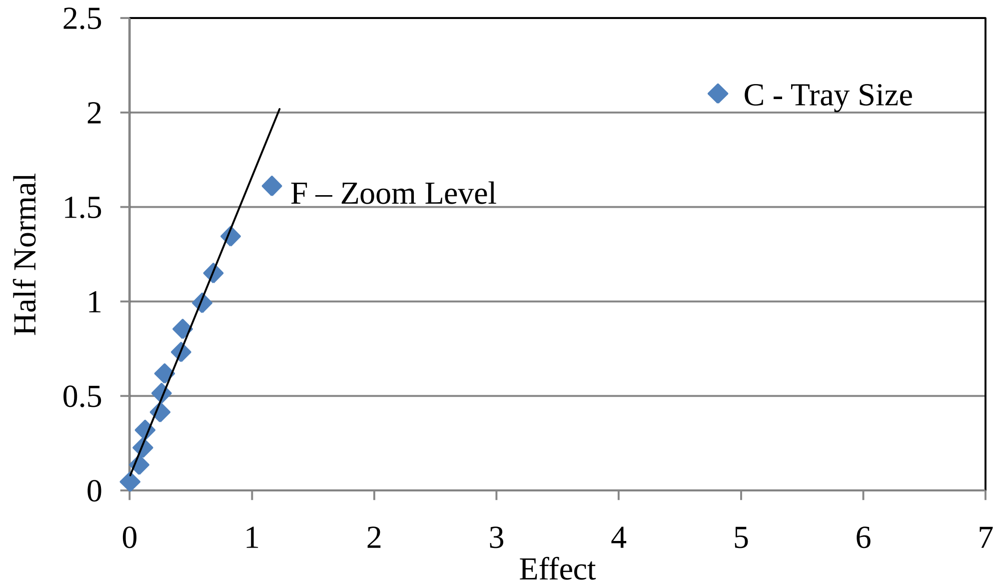

Fig. 4.9. Half-Normal Plot of the Texture of the Light 9.5mm (0.375in) Coarse Aggregate Used in Experiment 5

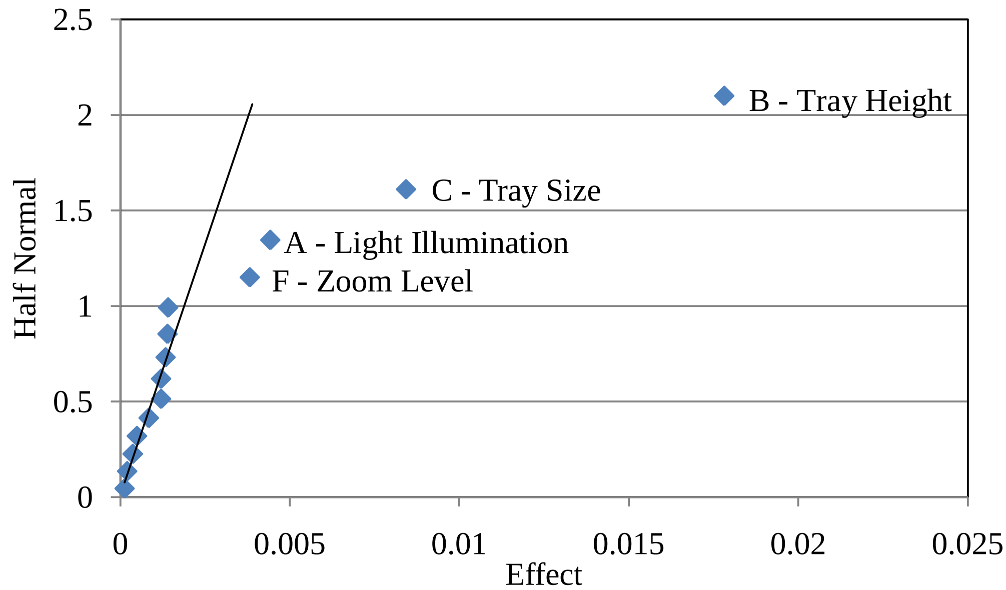

Fig. 4.10. Half-Normal Plot of the Sphericity of the Light 9.5mm (0.375in) Coarse Aggregate Used in Experiment 5

An additional coarse aggregate size 4.75mm (ASTM #4 sieve) was tested to confirm the results of the 9.5mm size aggregate (0.375in). Since more of the factors tested were significant for the light colored aggregate than the dark colored aggregate, only a light colored aggregate was tested (Fig. 4.11). The factors and limits were the same as for the 9.5mm (0.375in) aggregates (Table 4.28). Since the aggregate size tested changed from 9.5mm (0.375in) to 4.75mm (ASTM #4 sieve), the tray size limits with respect to the aggregate size were different. For the 9.5mm (3/8in) aggregate, the trays used were the correct size (9.5mm) and one tray size smaller (4.75mm). For the 4.75mm (ASTM #4 sieve), the trays used were the correct size (4.75mm) and one tray size larger (9.5mm). Table 4.31 shows a summary of the texture, angularity, and sphericity results.

Fig. 4.11. Light 4.75mm (ASTM #4 Sieve) Aggregates Used in Experiment 5

Table 4.31. Results of Light 4.75mm (ASTM #4 Sieve) Coarse Aggregate Used in Experiment 5

Scan	Angularity	Texture	Sphericity
Scan 1	2810.54	161.75	0.628
Scan 2	2688.51	160.94	0.619
Scan 3	2761.23	160.40	0.646
Scan 4	2775.79	163.57	0.602
Scan 5	2719.65	161.70	0.576
Scan 6	2744.61	157.84	0.654
Scan 7	2759.47	161.88	0.584
Scan 8	2620.12	162.98	0.596
Scan 9	2770.68	162.44	0.593
Scan 10	2788.08	163.88	0.605
Scan 11	2748.26	161.48	0.581
Scan 12	2695.06	162.04	0.615
Scan 13	2789.61	163.93	0.653
Scan 14	2678.55	164.21	0.577
Scan 15	2710.44	155.26	0.644
Scan 16	2805.75	155.61	0.625

The half-normal plots for the angularity, texture, and sphericity are shown in Figs. 4.12, 4.13, and 4.14, respectively.

The light 4.75mm (ASTM #4 sieve) aggregates were affected by several of the same factors that affected the light and dark 9.5mm (3/8 in) aggregates. The light illumination (Factor A) was statistically significant for the angularity results (Fig. 4.12). For the texture results (Fig. 4.13), the main factors of tray size (Factor C) and zoom level (Factor F) were statistically significant. The interaction Factors F-I and E-I were also statistically significant, which were caused most likely by the interactions CE (tray size and ambient light) and CF (tray size and zoom level), respectively. The sphericity results were affected by Factor C (tray size), Factor B (tray height), Factor A (light illumination), and G-I. The G-I interaction was probably caused by the interaction BC (tray size and tray height) (Fig. 4.14).

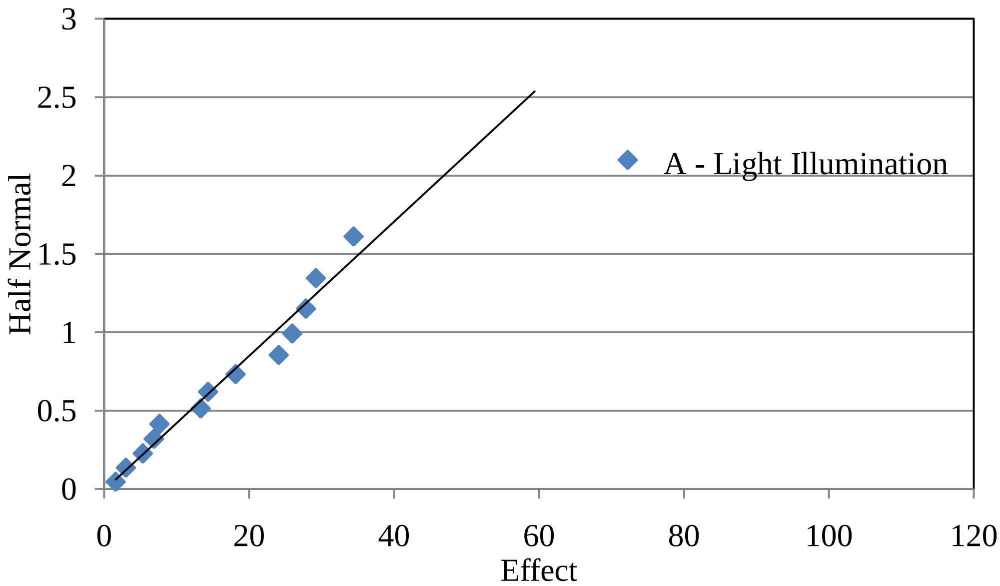

Fig. 4.12. Half-Normal Plot of the Angularity of the Light 4.75mm (ASTM #4 Sieve)

Coarse Aggregate Used in Experiment 5

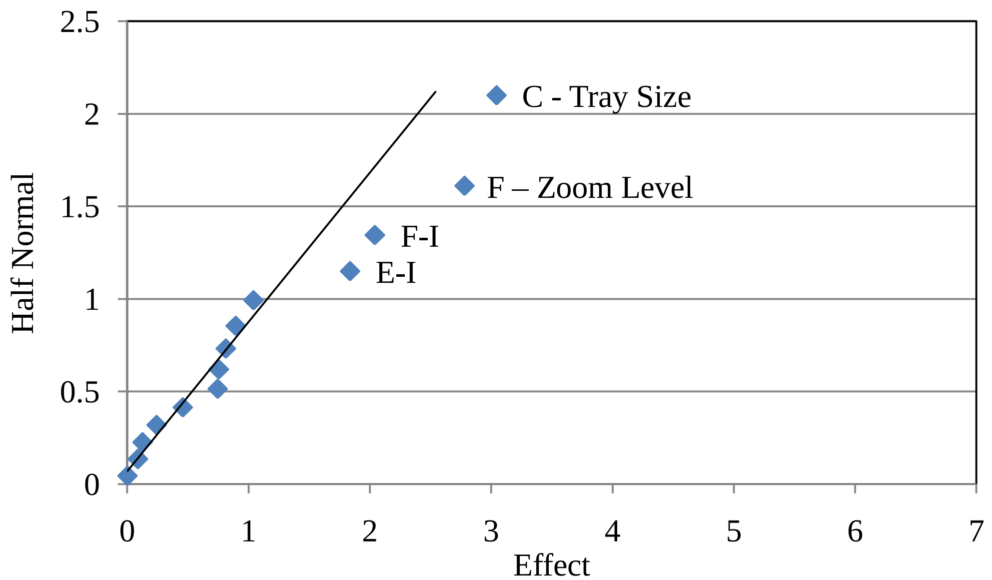

Fig. 4.13. Half-Normal Plot of the Texture of the Light 4.75mm (ASTM #4 Sieve)

Coarse Aggregate Used in Experiment 5

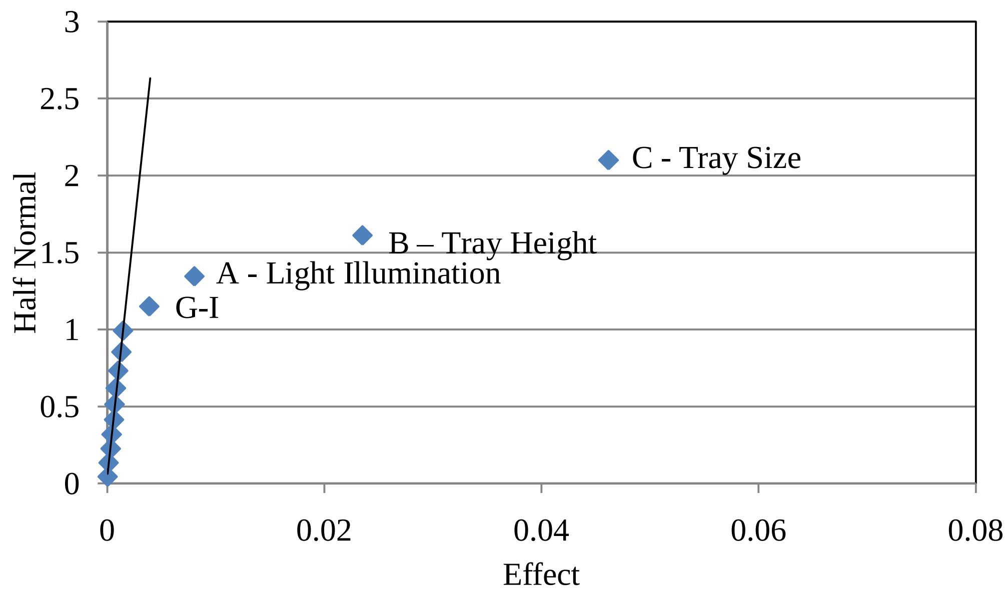

Fig. 4.14. Half-Normal Plot of the Sphericity of the Light 4.75mm (ASTM #4 Sieve) Coarse Aggregate Used in Experiment 5

Overall for the 9.5mm (3/8in) and 4.75 (ASTM #4 sieve) coarse aggregates, light illumination (Factor A), tray height (Factor B), tray size (Factor C), and zoom level (Factor F) were statistically significant using the limits tested. Other factors that appeared to be statistical significant were C-I (AD), F-I (AB or CE), B-I (AF), F-I (CE), D-I (CF), and G-I (BC).

Experiment 6

This experiment was carried out to further investigate acceptable ranges for the factors that were found to be statistically significant in affecting the coarse aggregates based on the results of Experiment 5. These factors are light illumination (Factor A), tray height

(Factor B), and zoom level (Factor F). The new, tighter, factor ranges are shown in Table 4.32. For Experiment 6, the same two aggregates as in Experiment 5 (Fig. 4.4) were tested: a dark colored 9.5mm (0.375 in) and a light colored 9.5mm (0.375 in) aggregate. The summary of the results for the angularity, texture, and sphericity are shown in Tables 4.33 and 4.34.

Table 4.32. Coarse Aggregate Factors and Limits Used in Experiment 6

Factor	Coarse Aggregate Study Factors:	Low Limit	High Limit
A	Light illumination	-1	0
B	Tray Height	-0.10mm	0.10mm
C	Tray Size	4.75mm	9.5mm
D	Door Position	Open	Closed
E	Ambient Light	Off	On
F	Zoom Level	-0.5%	+0.5%
G	Focus (DOF)	1%	0%

Table 4.33. Results of Dark 9.5mm (0.375 in) Coarse Aggregate Used in Experiment 6

	Angularity	Texture	Sphericity
Scan 1	2633.74	635.27	0.680
Scan 2	2679.19	639.65	0.678
Scan 3	2622.26	635.84	0.685
Scan 4	2655.28	631.71	0.687
Scan 5	2719.17	630.36	0.677
Scan 6	2669.10	633.06	0.684
Scan 7	2678.98	630.07	0.680
Scan 8	2678.43	624.20	0.689
Scan 9	2743.88	634.66	0.684
Scan 10	2637.89	620.24	0.688
Scan 11	2676.12	630.75	0.682
Scan 12	2660.87	634.31	0.679
Scan 13	2701.93	634.88	0.687
Scan 14	2709.30	632.69	0.681
Scan 15	2659.13	631.22	0.685
Scan 16	2689.69	635.59	0.677

Table 4.34. Results of Light 9.5mm (0.375 in) Coarse Aggregate Used in Experiment 6

	Angularity	Texture	Sphericity
Scan 1	2462.38	106.35	0.666
Scan 2	2388.29	103.94	0.666
Scan 3	2417.29	105.75	0.670
Scan 4	2337.13	101.59	0.683
Scan 5	2444.97	100.00	0.676
Scan 6	2390.14	104.24	0.672
Scan 7	2379.26	100.83	0.677
Scan 8	2343.70	100.86	0.684
Scan 9	2358.73	100.76	0.682
Scan 10	2367.75	100.63	0.685
Scan 11	2364.89	100.46	0.677
Scan 12	2471.44	103.52	0.666
Scan 13	2482.36	105.35	0.674
Scan 14	2391.33	100.95	0.679
Scan 15	2357.64	103.94	0.671
Scan 16	2446.15	104.02	0.665

The half-normal plots for the 9.5mm (0.375 in) dark aggregate are shown in Figs. 4.15, 4.16, and 4.17 for angularity, texture, and sphericity, respectively. The 9.5mm (0.375 in) light aggregate plots are shown in Figs. 4.18, 4.19, and 4.20.

As result of using tighter ranges, the statistical significance of Factor A (light illumination), Factor B (tray height), and Factor F (zoom level) decreased or was no longer significant. The texture and sphericity results were both affected by Factor C (tray size), as shown in Figs. 4.16 and 4.17. Factor D, door position, was also found to be statistically significant for the texture results (Fig. 4.16).

The light colored aggregate texture and sphericity results were affected by Factor C, (tray size) (Figs. 4.19 and 4.20), and sphericity results were affected by Factor B (tray height) (Fig. 4.20). No interaction factors were found to be statistically significant in Experiment 6. This was most likely due to the decrease in the effects of the main factors.

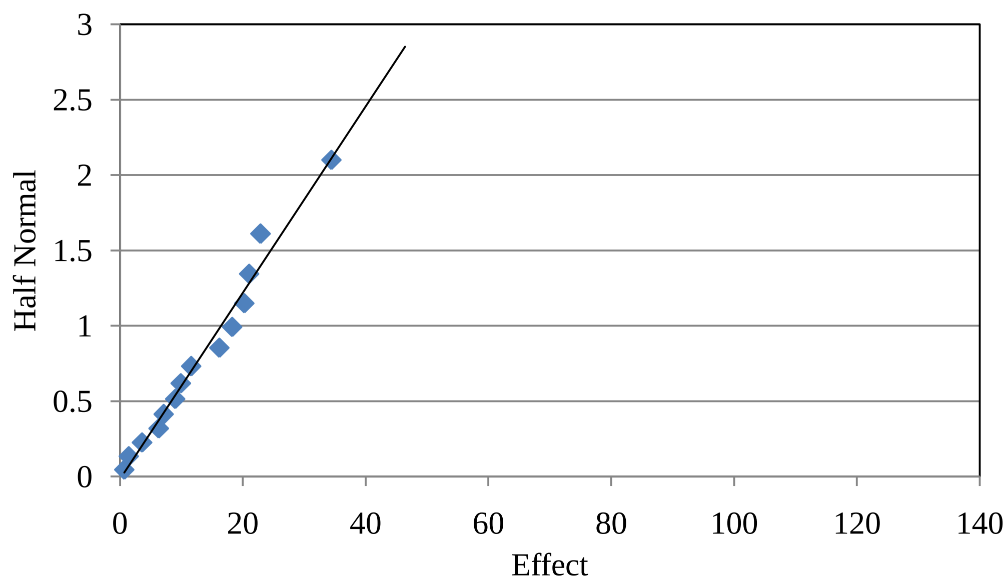

Fig. 4.15. Half-Normal Plot of the Angularity of the Dark 9.5mm (0.375in) Coarse Aggregate Used in Experiment 6

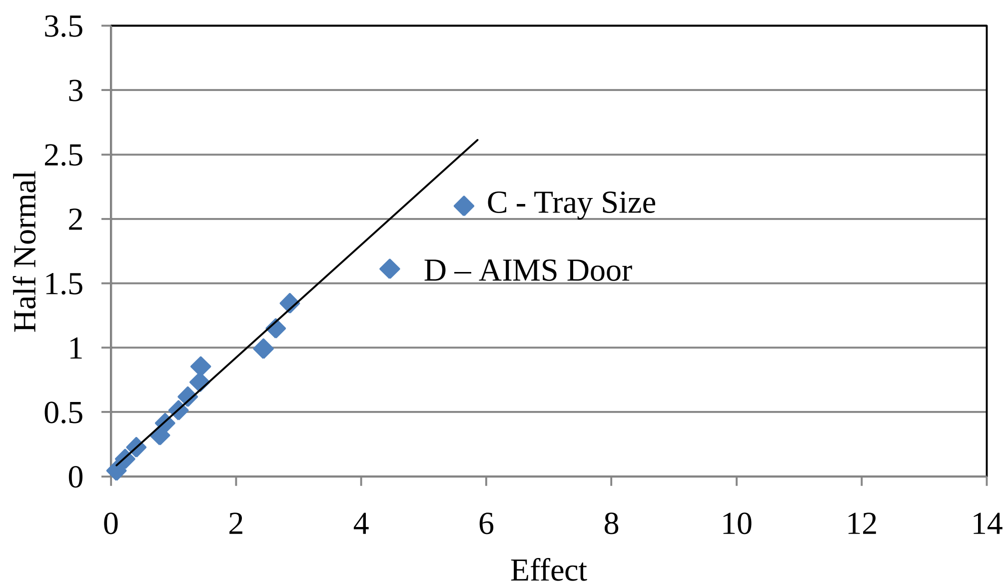

Fig. 4.16. Half-Normal Plot of the Texture of the Dark 9.5mm (0.375in) Coarse Aggregate Used in Experiment 6

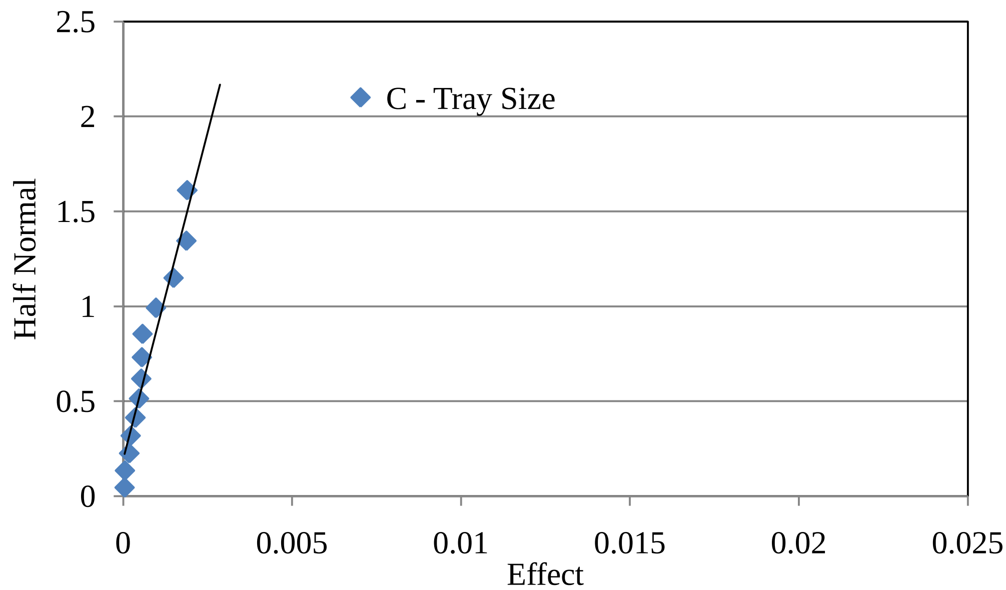

Fig. 4.17. Half-Normal Plot of the Sphericity of the Dark 9.5mm (0.375in) Coarse Aggregate Used in Experiment 6

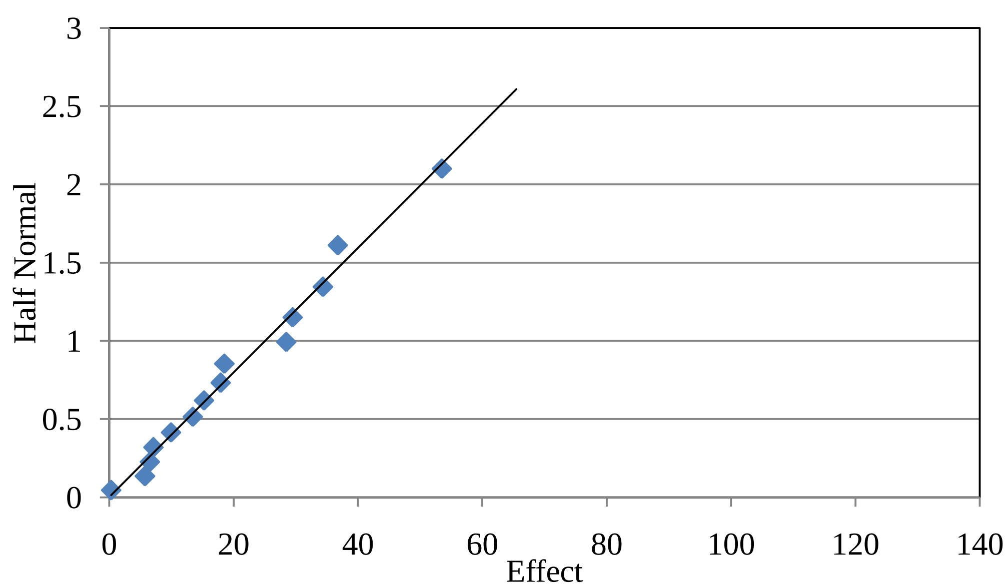

Fig. 4.18. Half-Normal Plot of the Angularity of the Light 9.5mm (0.375in) Coarse Aggregate Used in Experiment 6

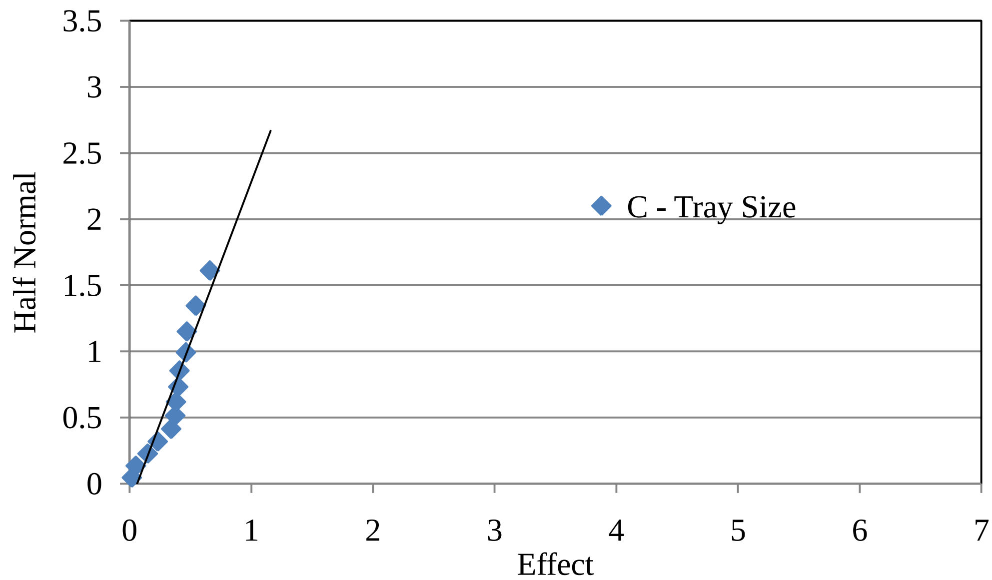

Fig. 4.19. Half-Normal Plot of the Texture of the Light 9.5mm (0.375in) Coarse Aggregate Used in Experiment 6

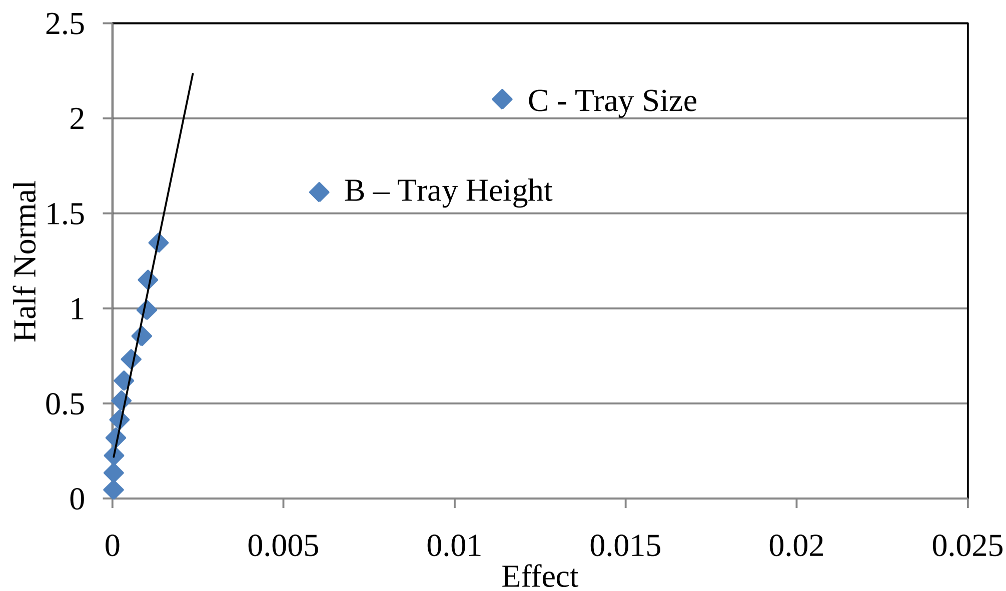

Fig. 4.20. Half-Normal Plot of the Sphericity of the Light 9.5mm (0.375in) Coarse Aggregate Used in Experiment 6

The results from 9.5mm (0.375in) aggregates were confirmed using a light colored 4.75mm (ASTM #4 sieve) aggregate. All the factors remained the same as in Table 4.32. The same light colored 4.75mm (ASTM #4 sieve) aggregate Used in Experiment 5 was used for Experiment 6 (Fig. 4.11). A summary of the angularity, texture, and sphericity results are listed in Table 4.35.

Table 4.35. Results of Light 4.75mm (ASTM #4 Sieve) Coarse Aggregate Used in Experiment 6

	Angularity	Texture	Sphericity
Scan 1	2797.52	162.39	0.637
Scan 2	2818.41	158.53	0.629
Scan 3	2709.42	159.88	0.642
Scan 4	2861.97	161.43	0.592
Scan 5	2860.93	163.56	0.584
Scan 6	2785.88	158.19	0.645
Scan 7	2760.69	166.19	0.583
Scan 8	2779.38	162.63	0.595
Scan 9	2804.20	161.23	0.590
Scan 10	2851.35	163.00	0.597
Scan 11	2838.03	161.50	0.582
Scan 12	2757.61	159.12	0.634
Scan 13	2830.00	158.26	0.645
Scan 14	2801.37	162.29	0.583
Scan 15	2785.70	158.51	0.642
Scan 16	2777.80	157.08	0.635

Figs. 4.21, 4.22, and 4.23 show the half-normal plots of the 4.75mm (ASTM #4 sieve) light aggregates. The results for the 4.75mm (ASTM #4 sieve) light aggregates were the same as the 9.5mm (0.375 in) light aggregate. Factor C (tray size) was statistically

significant for the texture results (Fig. 4.22). The sphericity results were affected by Factor C (tray size) and Factor B (tray height) (Fig. 4.23).

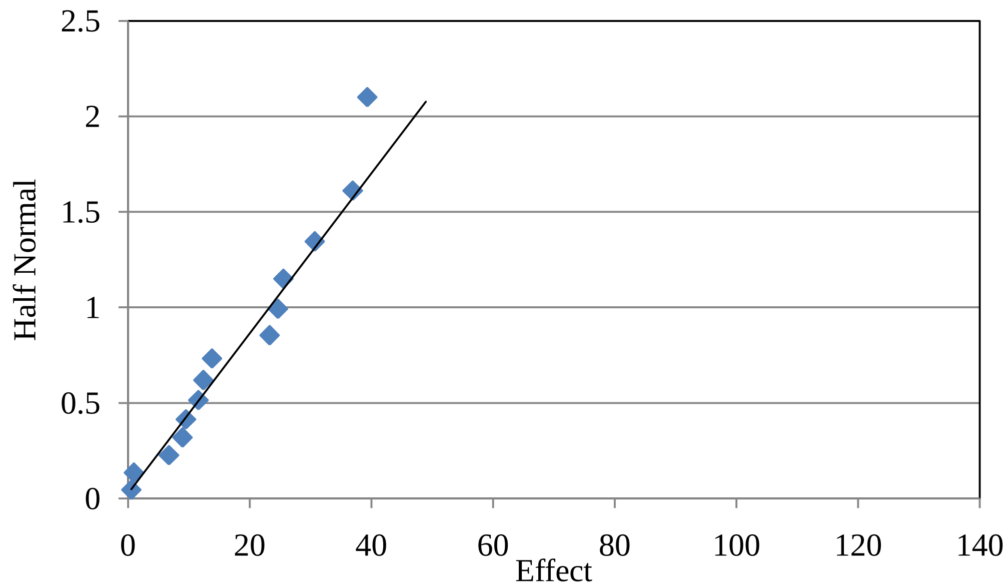

Fig. 4.21. Half-Normal Plot of the Angularity of the Light 4.75mm (ASTM #4 Sieve) Coarse Aggregate Used in Experiment 6

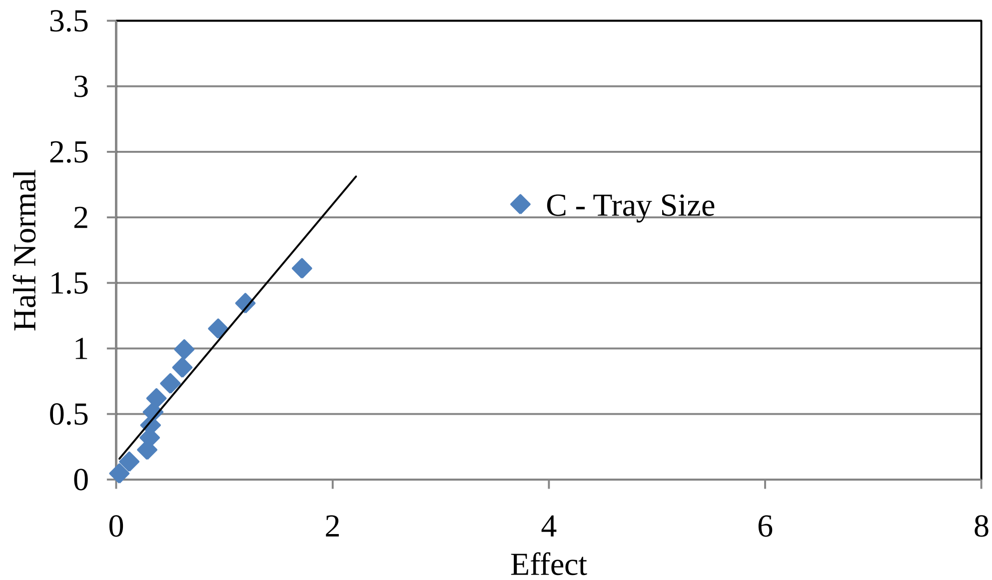

Fig. 4.22. Half-Normal Plot of the Texture of the Light 4.75mm (ASTM #4 Sieve)

Coarse Aggregate Used in Experiment 6

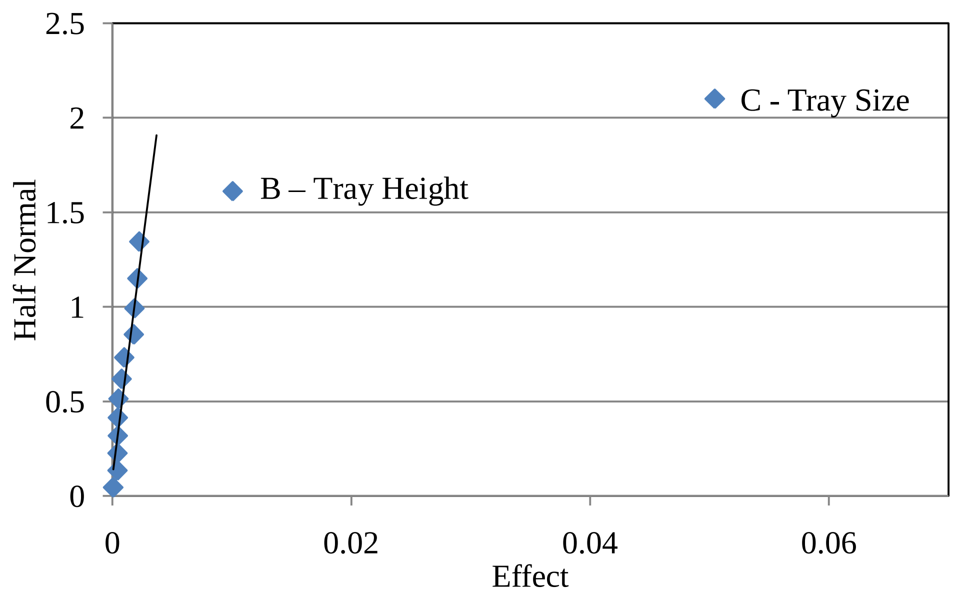

Fig. 4.23. Half-Normal Plot of the Sphericity of the Light 4.75mm (ASTM #4 Sieve)

Coarse Aggregate Used in Experiment 6

Overall tray height (Factor B), tray size (Factor C), and door position (Factor D) were statistically significant using the limits tested. No interaction factors were found to be significant in Experiment 6.

Experiment 7

This experiment was conducted using 2 different fine aggregates, a dark colored and light colored 1.18 mm (ASTM #16 sieve) aggregate (Fig. 4.24). The factors and limits chosen are listed in Table 4.36. Results from the 16 scans for 1.18 mm (ASTM #16 sieve) aggregates are shown in Tables 4.37 and 4.38 for the dark and light colored aggregates, respectively.

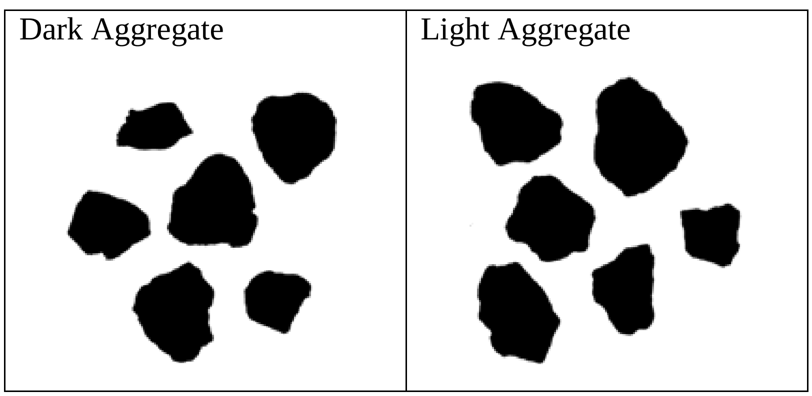

Fig. 4.24. Dark and Light 1.18 mm (ASTM #16 Sieve) Aggregates Used in Experiment 7

Table 4.36. Fine Aggregates Factors and Limits Used in Experiment 7

Factor	Fine Aggregate Factors:	Low Limit	High Limit
A	Light Illumination	-1	+1
B	CHPR	-0.01	0
C	Tray Color	Clear	Opaque
D	Door Position	Open	Closed
E	Ambient Light	Off	On
F	Zoom Level	-1%	+1%
G	Tray Height	-0.25	+0.25

Table 4.37. Results of Dark 1.18 mm (ASTM #16 Sieve) Fine Aggregates Used in Experiment 7

	Angularity	Form 2D
Scan 1	3620.32	8.32
Scan 2	4187.16	8.39
Scan 3	4113.90	7.85
Scan 4	2781.27	7.54
Scan 5	2730.92	7.47
Scan 6	3769.39	8.20
Scan 7	2747.03	7.56
Scan 8	2768.94	7.51
Scan 9	2734.15	7.46
Scan 10	2803.33	7.54
Scan 11	2721.16	7.50
Scan 12	3936.83	8.25
Scan 13	3527.07	8.24
Scan 14	2804.73	7.47
Scan 15	3891.67	8.02
Scan 16	3698.28	8.29

Table 4.38. Results of Light 1.18 mm (ASTM #16 Sieve) Fine Aggregates Used in Experiment 7

	Angularity	Form 2D
Scan 1	3301.83	7.43
Scan 2	3634.56	7.81
Scan 3	3552.14	7.67
Scan 4	3266.17	7.48
Scan 5	3242.04	7.47
Scan 6	3284.80	7.36
Scan 7	3304.95	7.49
Scan 8	3228.74	7.39
Scan 9	3237.06	7.44
Scan 10	3336.02	7.45
Scan 11	3314.50	7.52
Scan 12	3605.44	7.69
Scan 13	3290.79	7.33
Scan 14	3296.94	7.46
Scan 15	3589.77	7.75
Scan 16	3383.13	7.54

Figs. 4.25 and 4.26 show the half-normal plot for the angularity and 2D form, respectively, of the 1.18 mm (ASTM #16 sieve) dark aggregate. Similar plots for the 1.18 mm (ASTM #16 sieve) light aggregate are presented in Figs. 4.27 and 4.28.

The dark aggregate angularity results were affected by Factor C (tray color), Factor A (light illumination), and D-I (Fig. 4.25). The most likely cause of D-I was the interaction between Factors A (tray color) and C (light illumination). Fig. 4.26 shows that the 2D Form results were affected by Factor C (tray color).

For the 1.18 mm (ASTM #16 sieve) light aggregates, Factor C (tray color), Factor D-I, Factor A (light illumination), Factor B (CHPR), and Factor E-I appear to be statistically significant for the angularity results (Fig. 4.27). The interaction between Factors A (light illumination) and C (tray color) most likely was the cause for the significance of D-I. The interaction AG (light illumination and tray height), BD (CHPR and door position), or CF (tray color and zoom level) could be the cause of the larger E-I interaction. The 2D Form results appear to be affected by Factor D-I, Factor A (light illumination), Factor C (tray color), Factor B (CHPR), and Factor F (zoom level) (Fig. 4.28). Again the most likely cause for the large D-I interaction was the AC (light illumination and tray color) interaction.

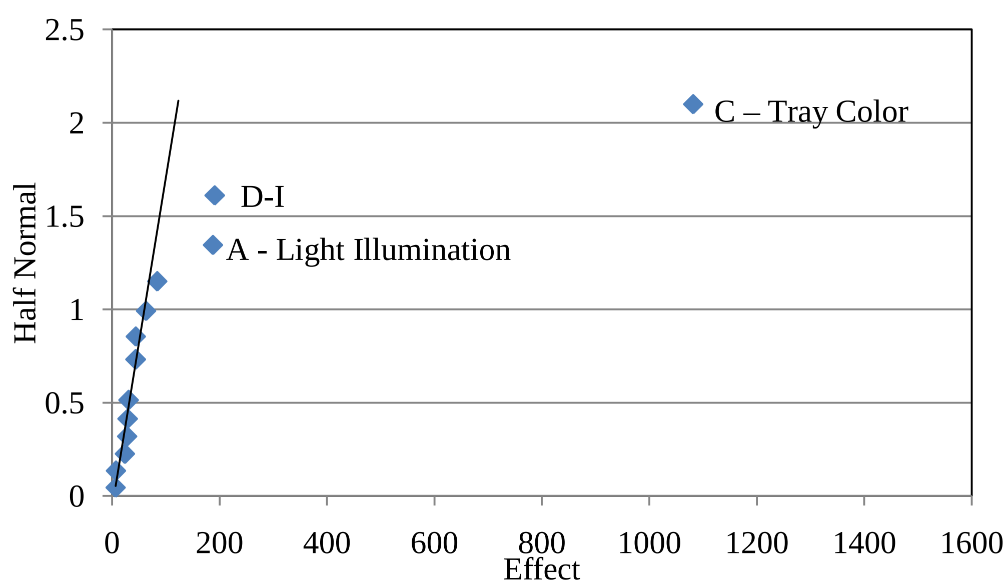

Fig. 4.25. Half-Normal Plot of the Angularity of the Dark 1.18 mm (ASTM #16 Sieve) Fine Aggregate Used in Experiment 7

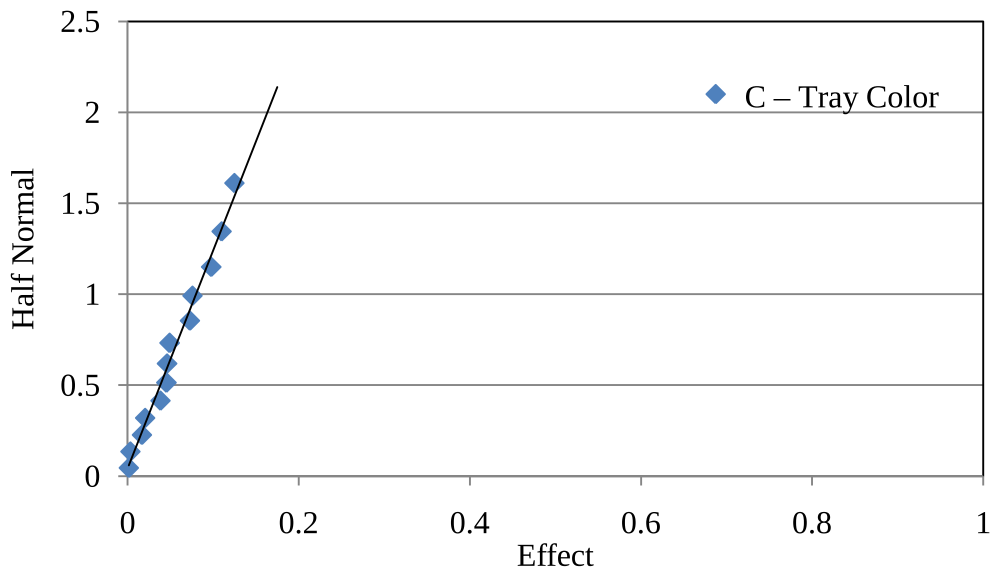

Fig. 4.26. Half-Normal Plot of the 2D Form of the Dark 1.18 mm (ASTM #16 Sieve)

Fine Aggregate Used in Experiment 7

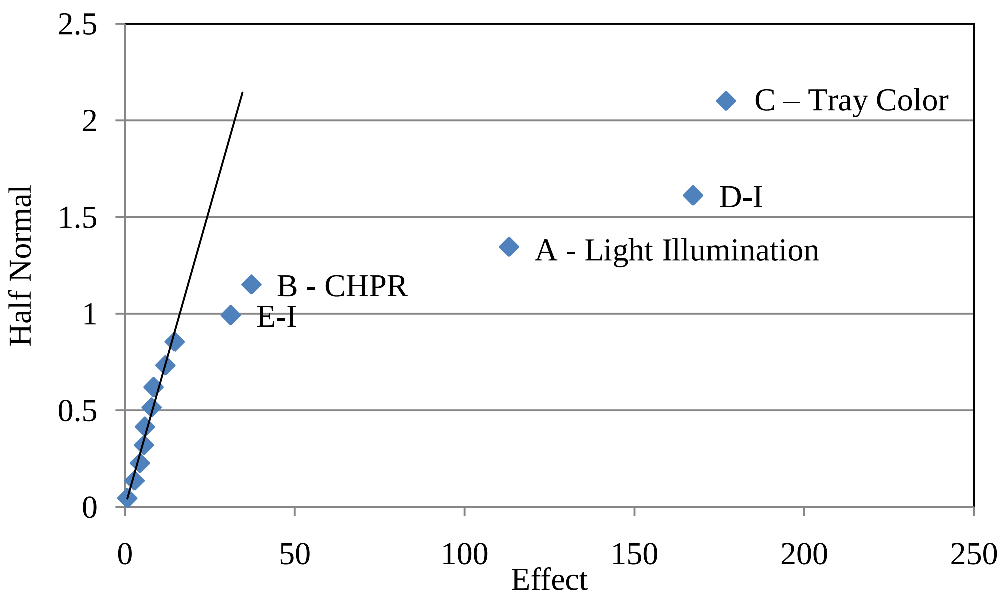

Fig. 4.27. Half-Normal Plot of the Angularity of the Light 1.18 mm (ASTM #16 Sieve)

Fine Aggregate Used in Experiment 7

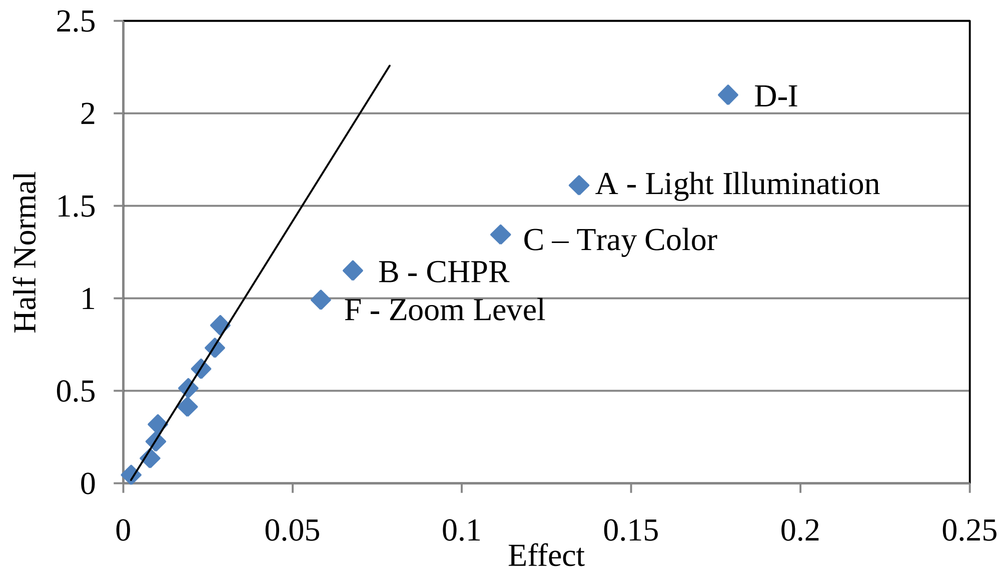

Fig. 4.28. Half-Normal Plot of the 2D Form of the Light 1.18 mm (ASTM #16 Sieve) Fine Aggregate Used in Experiment 7

The factors and limits used for the 1.18 mm (ASTM #16 sieve) fine aggregates were tested on an additional fine aggregate of size 0.15 mm (ASTM #100 sieve) to confirm the results. For 0.15 mm (ASTM #100 sieve) aggregate, only a light colored aggregate (Fig. 4.29) was studied since the light colored aggregates seem to be more affected by the changes in the different factors. Table 4.39 summarizes the angularity and 2D form results.

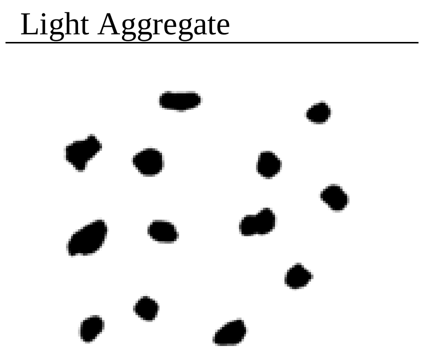

Fig. 4.29. Light 0.15 mm (ASTM #100 Sieve) Aggregates Used in Experiment 7

Table 4.39. Results of Light 0.15 mm (ASTM #100 Sieve) Fine Aggregates Used in Experiment 7

	Angularity	Form 2D
Scan 1	1877.54	6.13
Scan 2	2254.86	6.67
Scan 3	2235.24	6.61
Scan 4	2316.97	6.48
Scan 5	2670.46	6.61
Scan 6	1843.51	6.12
Scan 7	2569.78	6.67
Scan 8	2475.31	6.47
Scan 9	2566.89	6.50
Scan 10	2508.76	6.67
Scan 11	2371.79	6.59
Scan 12	2278.66	6.54
Scan 13	1863.52	6.09
Scan 14	2427.32	6.41
Scan 15	2344.11	6.67
Scan 16	1777.83	5.97

The half-normal plot for the angularity and 2D form for the 0.15 mm (ASTM #100 sieve) aggregate are shown in Figs. 4.30 and 4.31, respectively.

The plot in Fig. 4.30 indicates that tray color (Factor C), light illumination (Factor A), tray height (Factor G), door position (Factor D), Factor D-I, and Factor B-I were statistically significant for the angularity results. The interaction D-I was most likely caused by the interaction AC (light illumination and tray color). The interaction between C and F (tray color and door position) was the most likely cause for the high B-I factor. The effects of Factors G-I and C-I were unclear. The 2D form results were affected by Factor A (light illumination), Factor C (tray color), Factor D-I, and Factor B-I (Fig. 4.31). The interactions D-I and B-I were most likely caused by AC (light illumination and tray color) and CF (tray color and door position), respectively. These interactions were the same as the angularity results. The statistical significance of Factor D (door position) and Factor G-I was unclear.

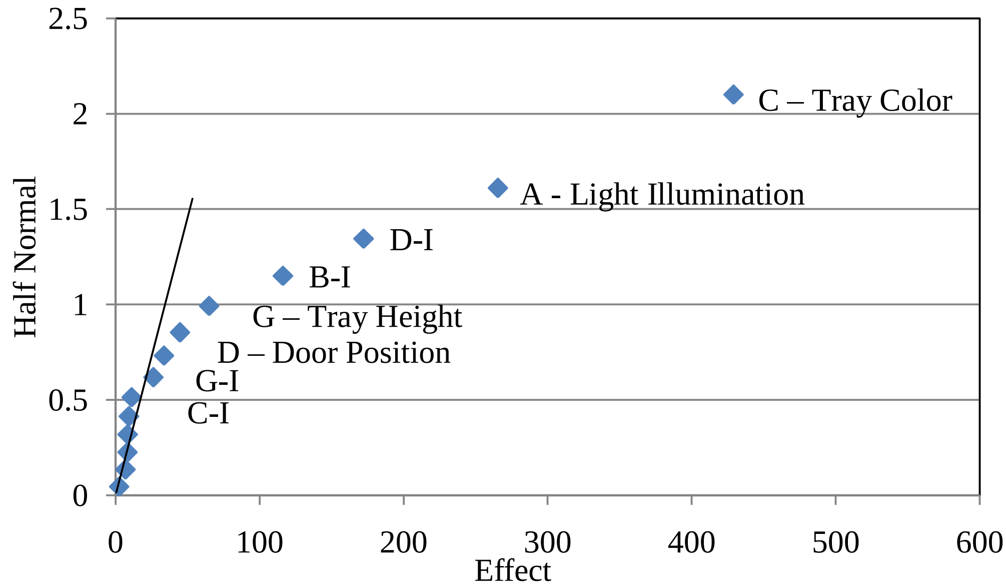

Fig. 4.30. Half-Normal Plot of the Angularity of the Light 0.15 mm (ASTM #100 Sieve)

Fine Aggregate Used in Experiment 7

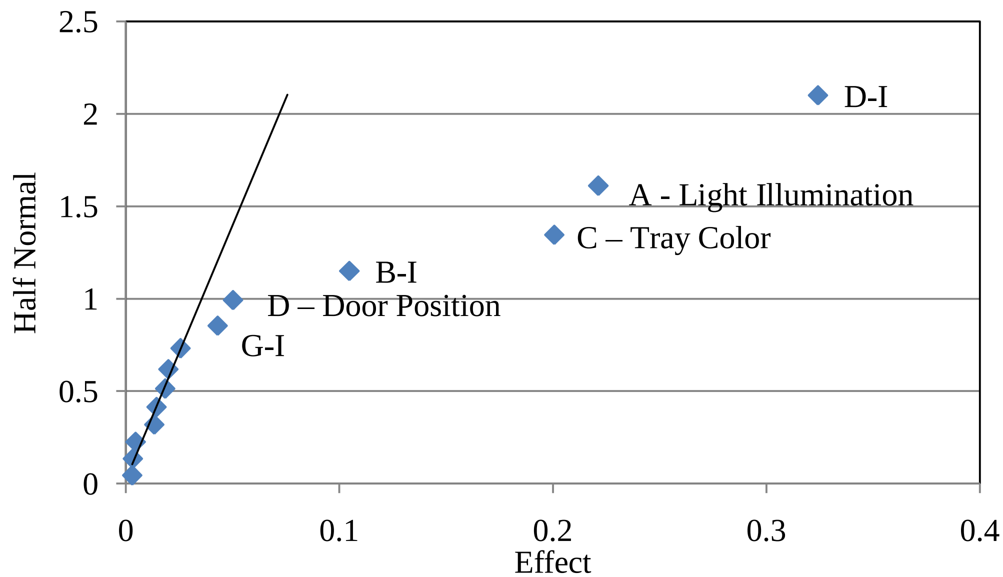

Fig. 4.31. Half-Normal Plot of the 2D Form of the Light 0.15 mm (ASTM #100 Sieve)

Fine Aggregate Used in Experiment 7

In summary, for Experiment 7, Factors A, B, C, D, F, and G (light illumination, CHPR, tray color, door position, zoom level, and tray height) were statistically significant for the limits tested. Other factors that appeared to be significant due to interactions of the main factors were factors D-I (AC), E-I (AG, BD, or CF), and B-I (CG).

Experiment 8

The aim of this experiment was to investigate the effect of tightening the limits of the factors (A, B, F, and G) that showed statistical significance in Experiment 7. Table 4.40 lists the new limits for these factors. The tray color factor was removed and replaced with tray size for the analysis. The same aggregates used in Experiment 7 were used in this experiment, a dark and light colored 1.18 mm (ASTM #16 sieve) aggregate (Fig. 4.24). The results from these two aggregates are shown in Tables 4.41 and 4.42.

Table 4.40. Fine Aggregates Factors and Limits Used in Experiment 8

Factor	Fine Aggregate Factors:	Low Limit	High Limit
A	Light illumination	-1	0
B	CHPR	-0.01	0
C	Tray Size	12.5 mm	19 mm
D	Door Position	Open	Closed
E	Ambient Light	Off	On
F	Zoom Level	-0.5%	+0.5%
G	Tray Height	-0.10mm	+0.10mm

Table 4.41. Results of Dark 1.18 mm (ASTM #16 Sieve) Fine Aggregates Used in Experiment 8

	Angularity	Form 2D
Scan 1	2806.59	7.22
Scan 2	2757.55	7.17
Scan 3	2765.31	7.18
Scan 4	2897.77	7.56
Scan 5	2915.38	7.55
Scan 6	2798.36	7.20
Scan 7	2932.93	7.57
Scan 8	2902.82	7.64
Scan 9	2912.24	7.53
Scan 10	2924.59	7.61
Scan 11	2935.47	7.64
Scan 12	2787.75	7.24
Scan 13	2766.95	7.19
Scan 14	2896.07	7.63
Scan 15	2809.58	7.20
Scan 16	2810.88	7.22

Table 4.42. Results of Light 1.18 mm (ASTM #16 Sieve) Fine Aggregates Used in Experiment 8

	Angularity	Form 2D
Scan 1	3271.76	7.37
Scan 2	3266.46	7.41
Scan 3	3256.10	7.34
Scan 4	3304.98	7.56
Scan 5	3337.61	7.57
Scan 6	3287.02	7.37
Scan 7	3275.73	7.56
Scan 8	3234.57	7.51
Scan 9	3330.38	7.49
Scan 10	3255.30	7.54
Scan 11	3307.82	7.60
Scan 12	3274.35	7.35
Scan 13	3261.85	7.40
Scan 14	3282.11	7.57
Scan 15	3263.61	7.37
Scan 16	3343.92	7.43

The half-normal plot for each shape characteristic parameter (Angularity and 2D Form) of the 1.18 mm (ASTM #16 sieve) dark aggregate are shown in Figs. 4.32 and 4.33. Figs. 4.34 and 4.35 show the half-normal plots for the 1.18 mm (ASTM #16 sieve) light aggregate.

The statistical significance of the factors decreased due to the tighter limits used in this experiment. For angularity and 2D form results of the dark aggregate (Figs. 4.32 and 4.33), the only statistically significant factor was Factor C (tray size).

The light colored aggregate had similar factors as the dark colored aggregate. Factor F (zoom level) appears to be statistically significant for the angularity (Fig. 4.34). On the other hand, Factor C (tray size) was statistically significant for the 2D Form results (Fig. 4.35). No interaction factors were found to be statistically significant in Experiment 8, which was most likely due to the decrease in the effects of the main factors.

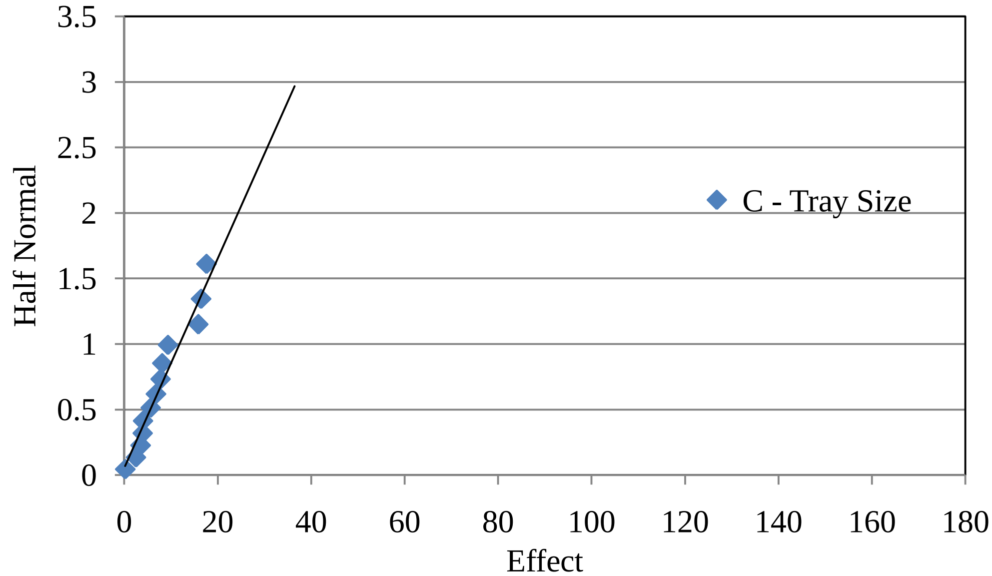

Fig. 4.32. Half-Normal Plot of the Angularity of the Dark 1.18 mm (ASTM #16 Sieve) Fine Aggregate Used in Experiment 8

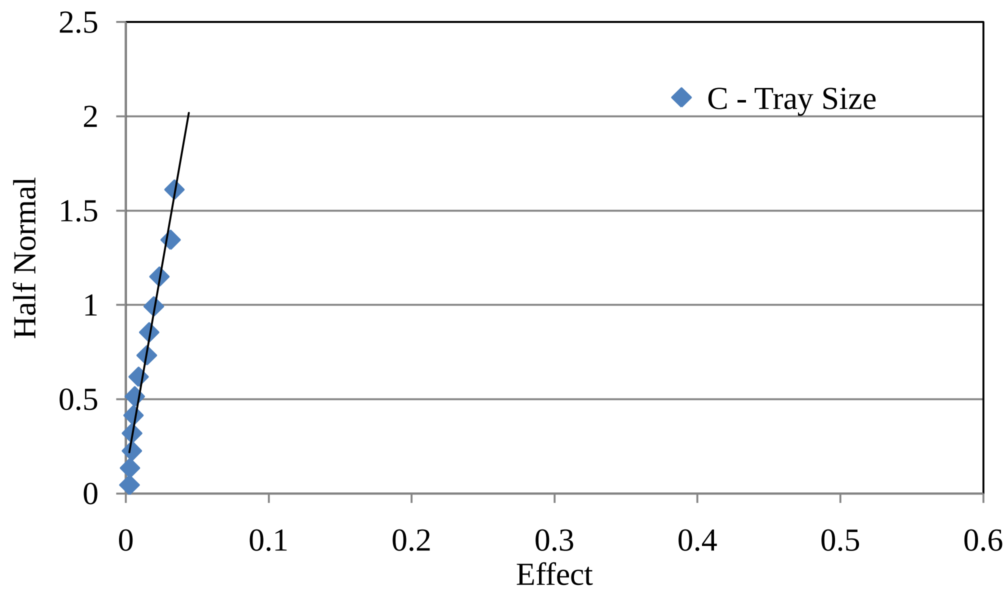

Fig. 4.33. Half-Normal Plot of the 2D Form of the Dark 1.18 mm (ASTM #16 Sieve) Fine Aggregate Used in Experiment 8

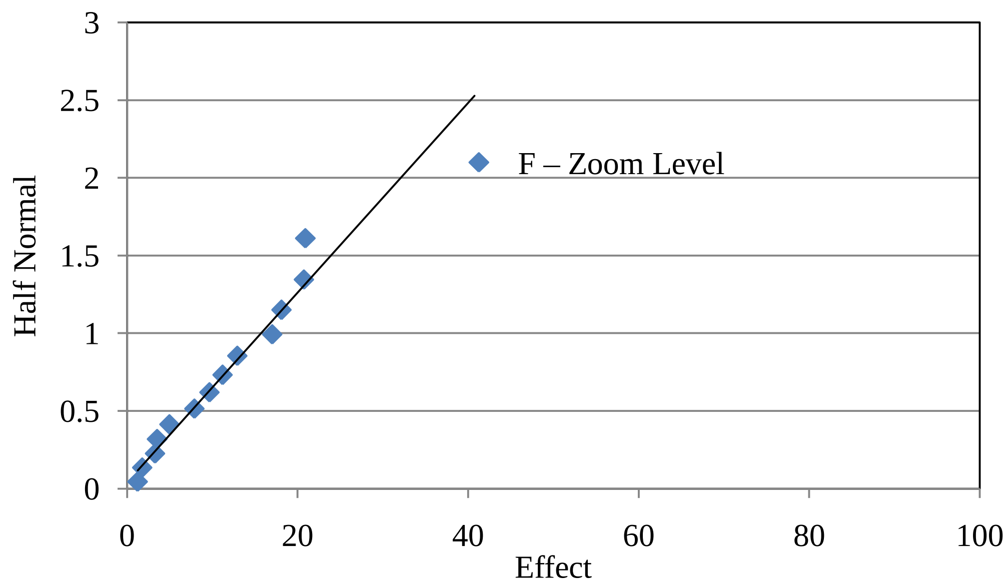

Fig. 4.34. Half-Normal Plot of the Angularity of the Light 1.18 mm (ASTM #16 Sieve) Fine Aggregate Used in Experiment 8

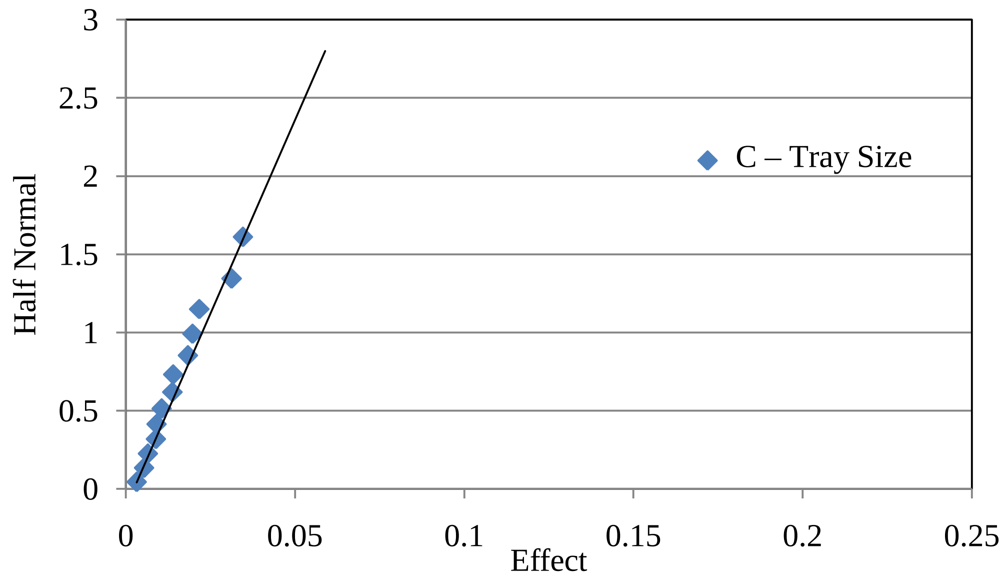

Fig. 4.35. Half-Normal Plot of the 2D Form of the Light 1.18 mm (ASTM #16 Sieve) Fine Aggregate Used in Experiment 8

The light 0.15 mm (ASTM #100 sieve) aggregate (Fig. 4.29) was again used to confirm the result found using the 1.18mm (ASTM #16 sieve) aggregate. The same factors and limits were used for both aggregate sizes (Table 4.40). The summary of the angularity and 2D form results are in Table 4.43.

Table 4.43. Results of Light 0.15 mm (ASTM #100 Sieve) Fine Aggregate Used in Experiment 8

	Angularity	Form 2D
Scan 1	2442.63	6.59
Scan 2	2432.03	6.54
Scan 3	2457.91	6.47
Scan 4	2205.87	6.50
Scan 5	2296.71	6.60
Scan 6	2497.23	6.63
Scan 7	2309.90	6.41
Scan 8	2240.49	6.49
Scan 9	2379.27	6.53
Scan 10	2209.78	6.40
Scan 11	2187.52	6.41
Scan 12	2531.24	6.48
Scan 13	2358.65	6.59
Scan 14	2265.81	6.56
Scan 15	2355.22	6.39
Scan 16	2454.94	6.65

The statistical significance of the factors tested can be determined from the half-normal plots in Figs. 4.36 and 4.37. Factor C (tray size) and Factor G (tray height) were statistically significant for the angularity results in Fig. 4.36. The 2D form results were affected by Factor C (tray size), Factor D-I, and Factor F-I (Fig. 4.37). The interaction AC (light illumination and tray size) was the most likely cause for the high D-I factor. The interaction F-I was most likely caused be the interactions AB (light illumination and CHPR), CE (tray size and ambient light), or DG (door position and tray height). The statistical significance of Factors D, F, and B, which were door position, zoom level, and CHPR, was unclear.

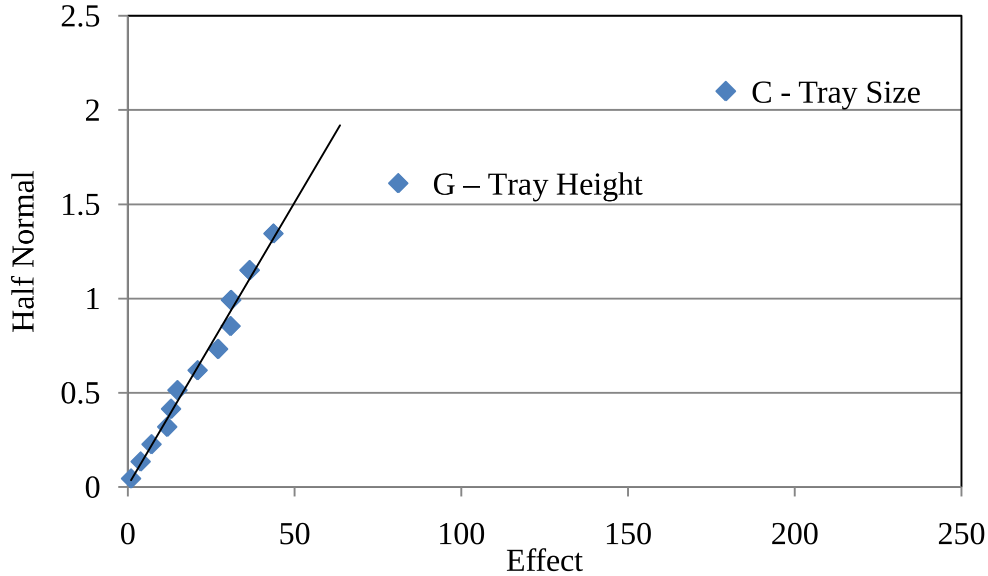

Fig. 4.36. Half-Normal Plot of the Angularity of the Light 0.15 mm (ASTM #100 Sieve)

Fine Aggregate Used in Experiment 8

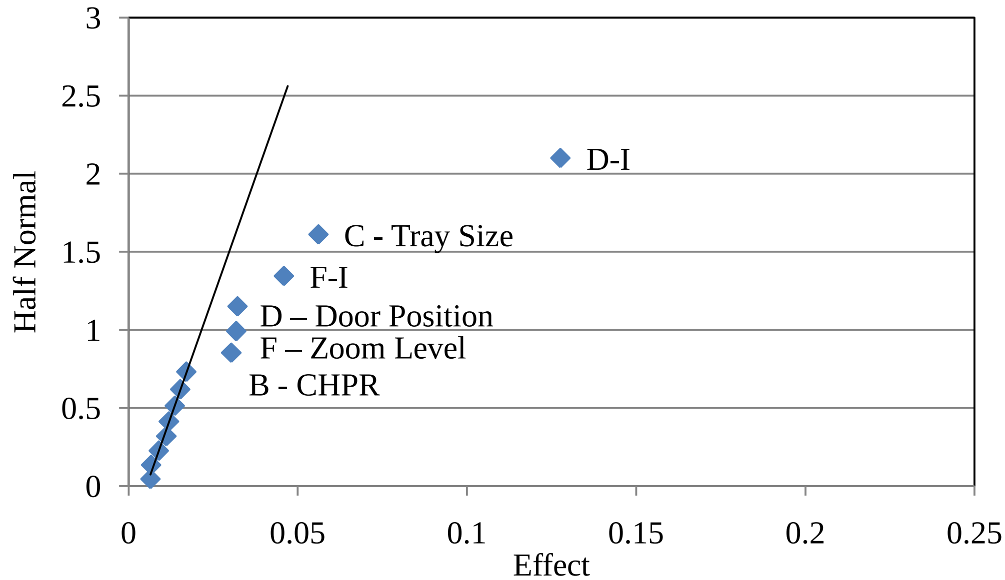

Fig. 4.37. Half-Normal Plot of the 2D Form of the Light 0.15 mm (ASTM #100 Sieve)

Fine Aggregate Used in Experiment 8

Overall for Experiment 8, Factor C (tray size), Factor F (zoom level), and Factor G (tray height), were statistically significant for the limits tested. The other factors that appeared to be significant were Factor D-I (AC) and F-I (AB, CE, or DG).

Experiment 9

Since the tray height was found to affect the sphericity results in Experiment 6, the aggregate height dimension measurements were analyzed. The results of the three coarse aggregates from Experiment 6 were used to further investigate the impact of the tray height. Experiment 6 included two coarse aggregates, one dark and one light, with a size of 9.5mm (0.375in) (Fig. 4.4) and one light colored coarse aggregate with a size of 4.75mm (ASTM #4 sieve) (Fig. 4.11). Table 4.44 lists the factors and limits for Experiment 9, which are from Experiment 6. A list of the height measurement results of the three coarse aggregates are shown in Table 4.45.

Table 4.44. Coarse Aggregate Factors and Limits Used in Experiment 9

Factor	Coarse Aggregate Study Factors:	Low Limit	High Limit
A	Light illumination	-1	0
B	Tray Height	-0.10mm	0.10mm
C	Tray Size	4.75mm	9.5mm
D	Door Position	Open	Closed
E	Ambient Light	Off	On
F	Zoom Level	-0.5%	+0.5%
G	Focus (DOF)	1%	0%

Table 4.45. Results of Coarse Aggregate Used in Experiment 9

	Dark 9.5mm (0.375in) Aggregate	Light 9.5mm (0.375in) Aggregate	Light 4.75mm (ASTM #4 sieve) Aggregate
Scan 1	7.06	6.64	4.55
Scan 2	7.16	6.68	4.47
Scan 3	7.23	6.83	4.69
Scan 4	7.67	6.87	3.76
Scan 5	7.47	6.61	3.66
Scan 6	7.28	6.83	4.75
Scan 7	7.44	6.61	3.58
Scan 8	7.69	6.9	3.82
Scan 9	7.66	6.83	3.77
Scan 10	7.69	6.81	3.83
Scan 11	7.47	6.70	3.59
Scan 12	7.09	6.65	4.52
Scan 13	7.31	6.85	4.71
Scan 14	7.51	6.66	3.62
Scan 15	7.29	6.86	4.70
Scan 16	7.06	6.62	4.54

The half-normal plots for the dark and light 9.5mm (0.375in) aggregates are shown in Figs. 4.38 and 4.39, respectively. The 4.75mm (ASTM #4 sieve) half-normal plot is in Fig. 4.40.

The measured aggregate heights for the dark 9.5mm (3/8in) aggregates are affected by Factor B (tray height) and Factor G (focus) (Fig. 4.38). Factor B (tray height) and Factor C (tray size) are statistically significant for the measured aggregate height for the light 9.5mm (0.375in) and light 4.75mm (ASTM #4 sieve) aggregates (Figs. 4.39 and 4.40). From Experiment 9, the tray height was found to still be statistically significant for the height measurements of the aggregates.

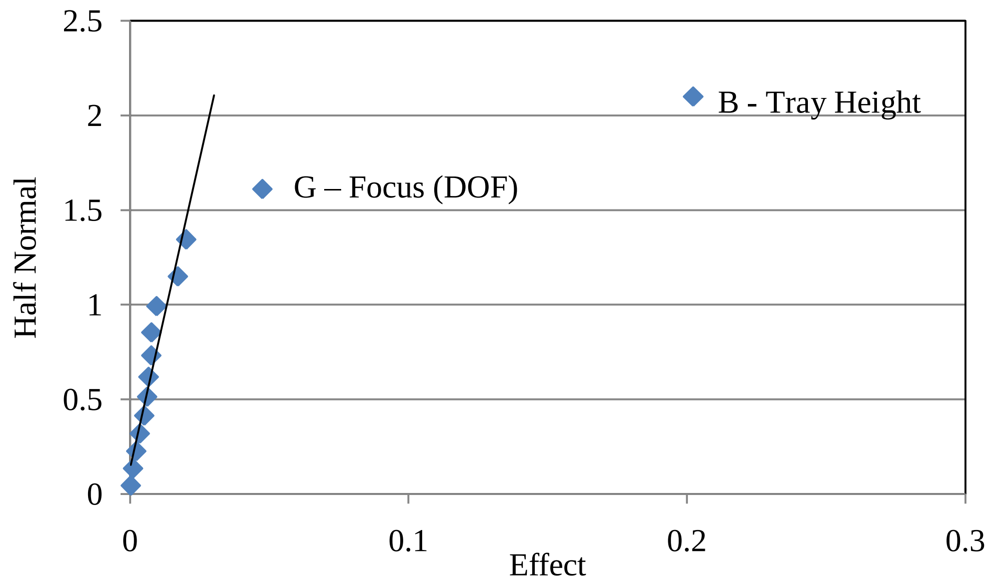

Fig. 4.38. Half-Normal Plot of the Aggregate Height of the Dark 9.5mm (0.375 in) Coarse Aggregate Used in Experiment 9

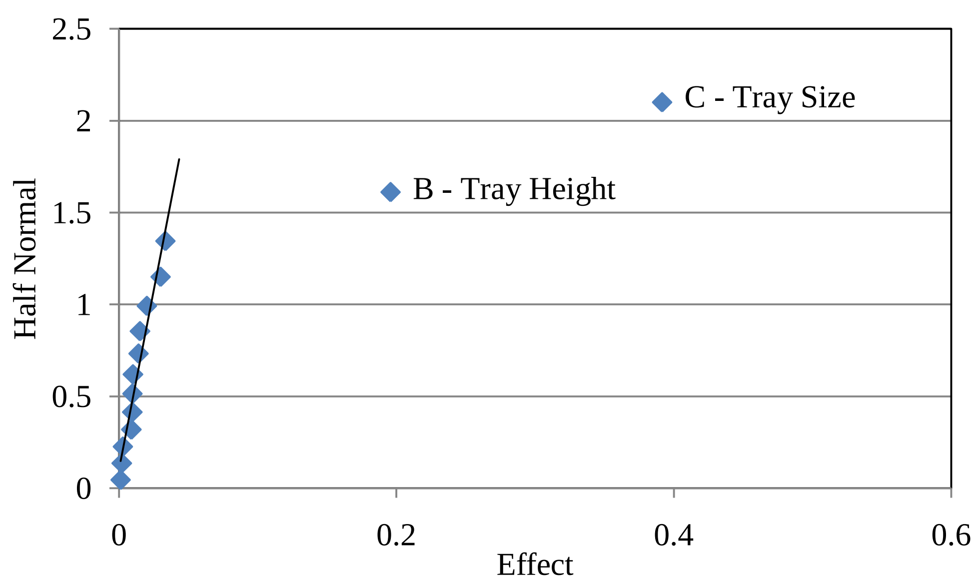

Fig. 4.39. Half-Normal Plot of the Aggregate Height of the Light 9.5mm (0.375in) Coarse Aggregate Used in Experiment 9

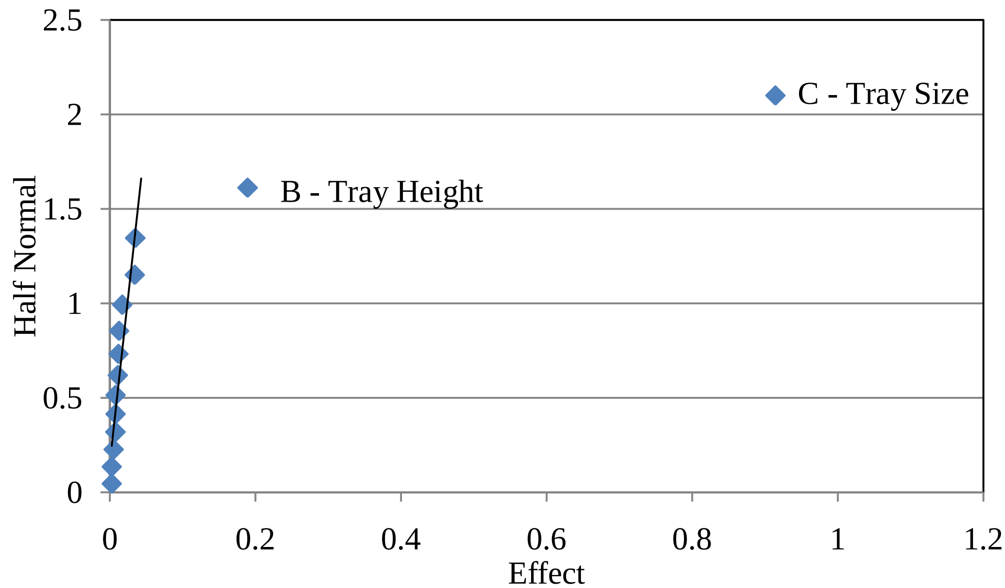

Fig. 4.40. Half-Normal Plot of the Aggregate Height of the Light 4.75mm (ASTM #4 Sieve) Coarse Aggregate Used in Experiment 9

Experiment 10

Although the tray height was shown to be statistically significant for the sphericity and the aggregate height results, this factor might be considered insignificant from an engineering standpoint. It is important to investigate the impact of the significance on the AIMS2 results and the engineering interpretation of these results. In order to investigate this issue, a set of 50 aggregate particles containing a mix of crushed gravel, granite and limestone were scanned three times to determine the difference in AIMS2 results between the three scans of each set. Examples of the comparisons of the height measurements for the 25.0mm (1.0in) aggregate are shown in Figs. 4.41, 4.42, and 4.43

for the three replicate scans. A list of all of the equations for the fitted lines and R^2 values for all of the coarse aggregate sizes is shown in Table 4.46. The data in Table 4.46 show that the measurements are close to the line of equality with very small biases. The values of the confidence interval for the slope either contain or are very close to one, and the values of the confidence interval for the intercepts either contain or are very close to zero (Table 4.47). The high R^2 values show the minimal spread in the data.

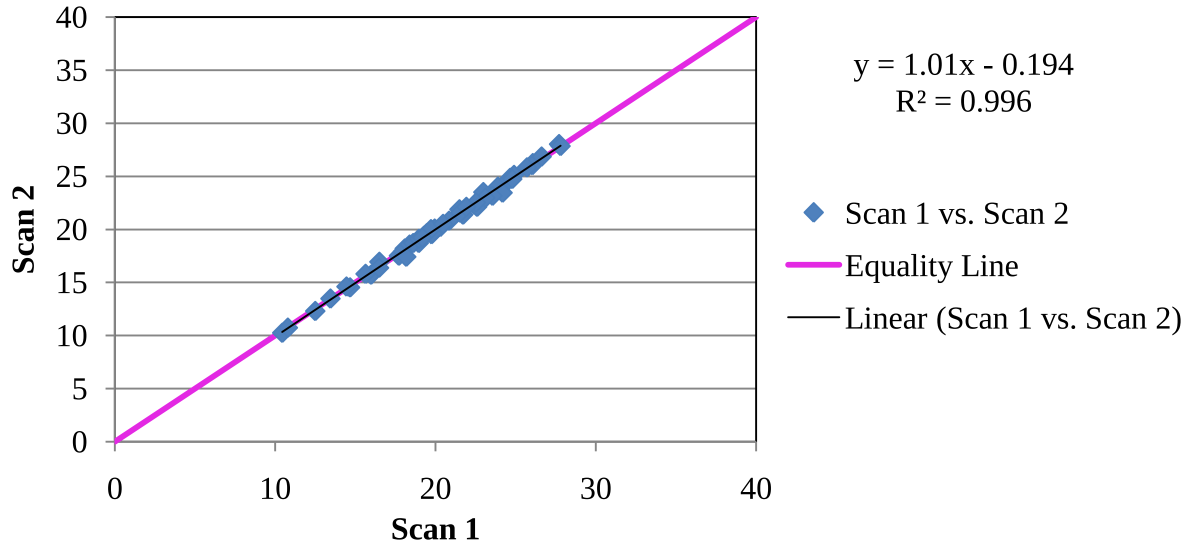

Fig. 4.41. 25.0mm (1.0in) Aggregate Height Measurement for Replicate Scan 1 versus Scan 2

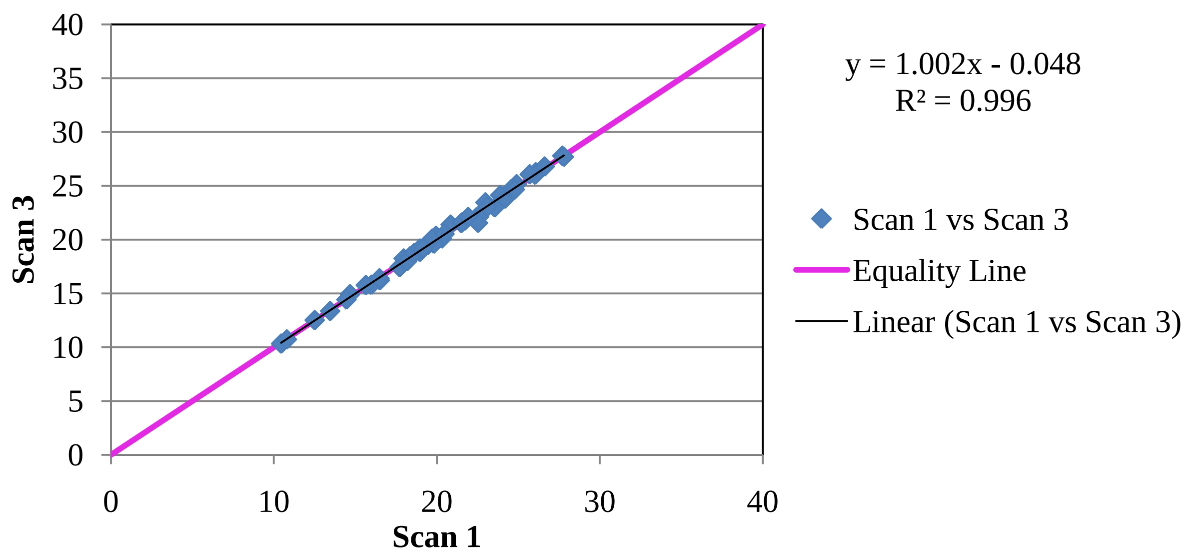

Fig. 4.42. 25.0mm (1.0in) Aggregate Height Measurement for Replicate Scan 1 versus Scan 3

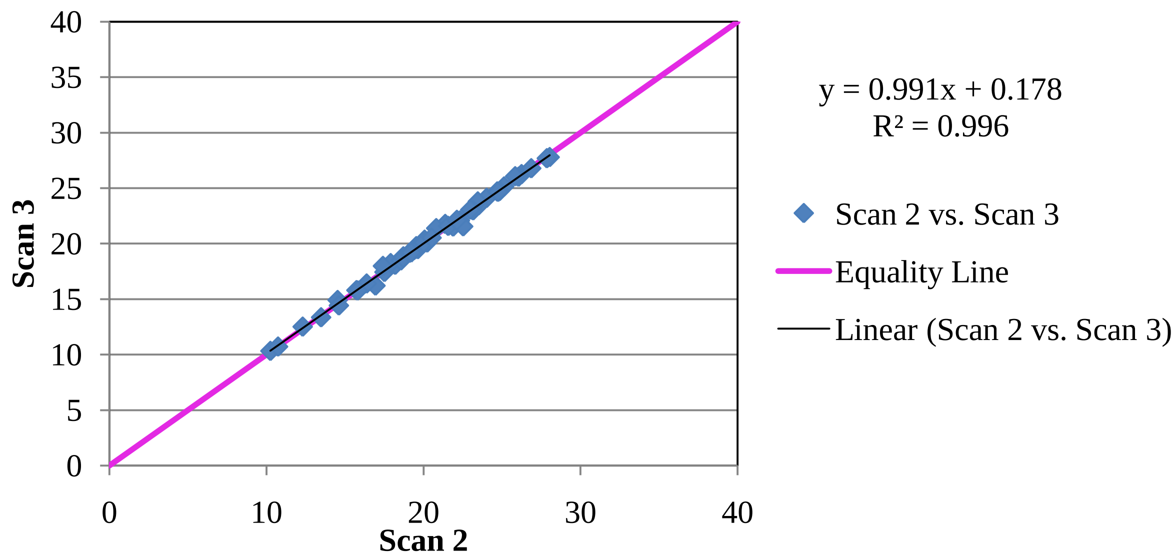

Fig. 4.43. 25.0mm (1.0in) Aggregate Height Measurement for Replicate Scan 2 versus Scan 3

Table 4.46. Linear Model Results for Aggregates Height Measurements

Aggregate Size	Scans Plotted	Best-fit Linear Equation	R^2 Value
25.0mm (1.0 in)	S1* vs. S2*	S1* = 1.01 × S2* - 0.194	0.996
	S1 vs. S3*	S1 = 1.002 × S3* - 0.048	0.996
	S2 vs. S3	S2 = 0.991 × S3 + 0.178	0.996
19.0 (.75in)	S1 vs. S2	S1 = 0.99 × S2 + 0.132	0.992
	S1 vs. S3	S1 = 0.98 × S3 + 0.297	0.989
	S2 vs. S3	S2 = 0.989 × S3 + 0.172	0.996
12.5 (.50in)	S1 vs. S2	S1 = 0.973 × S2 + 0.292	0.995
	S1 vs. S3	S1 = 0.969 × S3 + 0.287	0.996
	S2 vs. S3	S2 = 0.993 × S3 + 0.025	0.995
9.5 (.375in)	S1 vs. S2	S1 = 0.993 × S2 + 0.094	0.986
	S1 vs. S3	S1 = 0.99 × S3 + 0.064	0.97
	S2 vs. S3	S2 = 0.994 × S3 - 0.002	0.976
4.75 (#4 sieve)	S1 vs. S2	S1 = 0.98 × S2 + 0.033	0.958
	S1 vs. S3	S1 = 0.968 × S3 + 0.104	0.961
	S2 vs. S3	S2 = 0.974 × S3 + 0.132	0.975

*S1 = Scan 1, S2 = Scan 2, and S3 = Scan 3

Table 4.47. Confidence Intervals of the Linear Model Results

Aggregate Size	Scans Plotted	Slope CI	Intercept CI
25.0mm (1.0 in)	S1* vs. S2*	(1.001, 1.018)	(-0.375, -0.012)
	S1 vs. S3*	(0.993, 1.012)	(-0.24, 0.144)
	S2 vs. S3	(0.982, 1)	(-0.005, 0.361)
19.0 (.75in)	S1 vs. S2	(0.977, 1.003)	(-0.076, 0.339)
	S1 vs. S3	(0.965, 0.995)	(0.055, 0.54)
	S2 vs. S3	(0.98, 0.998)	(0.032, 0.311)
12.5 (.50in)	S1 vs. S2	(0.963, 0.983)	(0.182, 0.402)
	S1 vs. S3	(0.96, 0.978)	(0.187, 0.386)
	S2 vs. S3	(0.984, 1.003)	(-0.083, 0.132)
9.5 (.375in)	S1 vs. S2	(0.976, 1.01)	(-0.032, 0.22)
	S1 vs. S3	(0.965, 1.016)	(-0.124, 0.252)
	S2 vs. S3	(0.971, 1.016)	(-0.172, 0.168)
4.75 (#4 sieve)	S1 vs. S2	(0.95, 1.01)	(-0.103, 0.169)
	S1 vs. S3	(0.94, 0.996)	(-0.025, 0.232)
	S2 vs. S3	(0.951, 0.996)	(0.029, 0.234)

*S1 = Scan 1, S2 = Scan 2, and S3 = Scan 3

Although the tray height was statistically significant based on the results of Experiments 5 and 6; Experiment 9 showed that the differences in replicate measurements of the same aggregate is minimal. The tray height factor therefore appears not to be affecting the results from a practical aspect and AIMS2 is able to control normal variations in the height dimension measurement of the aggregates.

SUMMARY

The ruggedness study following ASTM C 1067-00 identified several factors that were found to be statistically significant in affecting the AIMS2 results. The transparent doors were not able to control the changes in ambient lighting, therefore these were replaced with non-transparent doors. The non-transparent doors were found to block the ambient light completely. There was concern that the results of the factors may be skewed due to the effect of interactions between the factors. Therefore, the ruggedness analysis was also conducted using the ASTM E 1169-07 procedure, which allows for the identification of the effects of the main factors and interactions between these factors. The ruggedness study following ASTM E 1169-07 led to the identification of several significant factors that could affect the AIMS2 shape characteristics. Consequently, limits were proposed for these factors in order to eliminate their influence on the measured characteristics. The factors and limits listed in Table 4.48 are the recommended controls for the factors in order to ensure the ruggedness of the AIMS2 measurements. As long as these limits are achieved by the system, AIMS2 can control normal variations related to the factors without significantly changing the results.

Table 4.48. Recommendations for AIMS2 to be Rugged

Aggregate Factors	Recommended Limits
Light Illumination	-1 and 0
Tray Size	Use Correct Tray Size Specified for Each Aggregate Size
Tray Color	Opaque Tray for #100 and #200 aggregates unless the system is not able to capture images of dark particles
Door Position	Closed
Ambient Light	Not Significant
Focus (DOF)	A maximum variation of 1% from the settings
CHPR	Value should be fixed as currently in the AIMS2 software
Zoom Level	A variation -0.5% and +0.5% from the settings
Tray Height	AIMS2 is able to control normal variation but tight calibrations are needed following the manufacture’s procedure

CHAPTER V

INTERLABORATORY STUDY (ILS)

INTRODUCTION

The Interlaboratory Study (ILS) was conducted to determine the repeatability and reproducibility of AIMS2 for multiple users and laboratories. The ILS was carried out in accordance with ASTM C 802 – 96, "Standard Practice for Conducting an Interlaboratory Test Program to Determine the Precision of Test Methods for Construction Materials." The ILS results were used to develop a precision statement for the test method using ASTM C 670 – 03, "Standard Practice for Preparing Precision and Bias Statements for Test Methods for Construction Materials."

ILS provides two different precision estimates of the test method; single-operator precision (within-laboratory precision) and multi-laboratory precision (between-laboratory precision). The single-operator precision provides an estimate of the variance that may be expected between duplicate measurements of the same sample made by the same operator in the same laboratory. The multi-laboratory precision gives an estimate of the differences that may be expected between measurements of the same material made in different laboratories by different users. The single-operator and multi-laboratory precision statements were determined in this study for the following outputs of the AIM2S system: angularity, texture, 2D Form, sphericity, and flat or elongated 3:1 ratio.

AGGREGATES SOURCES AND SIZES

Three different aggregates (crushed gravel, limestone, and granite) were used for all sizes except that a sandstone source was used instead of granite for the size passing the 0.15 mm sieve (ASTM #100 sieve) and retained on the 0.075mm (ASTM #200 sieve). Based on previous characterization of these aggregates, the crushed gravel (CG) has the lowest shape, angularity, and texture characteristics among the three aggregates; the granite (GR) has the highest shape, angularity, and texture characteristics; and the limestone (LS) is in the middle. A list of the materials and sources used in this study are shown in Table 5.1. The coarse and fine aggregates sizes are listed in Table 5.2. Coarse aggregates are defined as those retained on the 4.75 mm sieve (ASTM #4 sieve), while fine aggregates are those passing the 4.75 mm sieve (ASTM #4 sieve). Table 5.2 gives the aggregate size ranges tested.

Table 5.1. Aggregates Source and Sizes for ILS

Label	Source	Aggregate Description	Aggregate Size Range
CG	Texas	Crushed Gravel	38.0mm (1.5 in) – 0.15mm (ASTM #100 sieve)
LS	Texas	Limestone	
GR	Oklahoma	Granite	
CG*	Georgia	Gravel	0.15mm (ASTM #100 sieve) – 0.075mm (ASTM #200 sieve)
LS*	Texas	Limestone	
GR*	Texas	Sandstone	

Table 5.2. Aggregates Size Ranges Used in the ILS

Aggregate Type	Aggregates Size Range
Coarse Aggregate	37.5 mm(1.5in) – 25.0mm (1in)
	25.0mm (1in) – 19.0mm (0.75in)
	19.0mm (0.75in) – 12.5mm (0.5in)
	12.5mm (0.5in) – 9.5mm (0.375in)
	9.5mm (0.375in) – 4.75 mm (ASTM #4 sieve)
Fine Aggregate	4.75 mm (ASTM #4 sieve) – 2.36mm (ASTM #8 sieve)
	2.36mm (ASTM #8 sieve) – 1.18mm (ASTM #16 sieve)
	1.18mm (ASTM #16 sieve) – 0.6mm(ASTM #30 sieve)
	0.6mm(ASTM #30 sieve) – 0.3mm (ASTM #50 sieve)
	0.3mm (ASTM #50 sieve) – 0.15mm (ASTM #100 sieve)
	0.15mm (ASTM #100 sieve) – 0.075mm (ASTM #200 sieve)

As discussed, different aggregates sources were used for the 0.075mm size (ASTM #200 sieve). These were crushed gravel, limestone, and sandstone. For simplicity in this study, the 0.075mm (ASTM #200 sieve) sandstone will be grouped with the granite.

In addition to the average shape characteristics for each sieve range, the AIMS2 software includes a method to determine the weighted average of an aggregate blend for each property. The weighted averaging factors are determined based on aggregate size as described in Appendix B. The hypothetical gradation shown in Table 5.3 was used in determining the shape characteristics of the blend. Since the 0.075mm (ASTM #200 sieve) fine aggregates were not from the same sources as the other aggregates sizes, it was not included in the combined results.

Table 5.3. Gradation Used for Combined Properties

Retained Size	Percent Passing	Percent Retained
37.5mm (1.5in)	100.0%	0.0%
25.0mm (1in)	93.0%	7.0%
19.0mm (0.75in)	85.0%	8.0%
12.5mm (0.5in)	70.0%	15.0%
9.5mm (0.375in)	55.0%	15.0%
4.75 mm (ASTM #4 sieve)	35.0%	20.0%
2.36mm (ASTM #8 sieve)	25.0%	10.0%
1.18mm (ASTM #16 sieve)	15.0%	10.0%
0.6mm(ASTM #30 sieve)	10.0%	5.0%
0.3mm (ASTM #50 sieve)	5.0%	5.0%
0.15mm (ASTM #100 sieve)	0.0%	5.0%
0.075mm (ASTM #200 sieve)	0.0%	0.0%

Each aggregate source was sieved according to the size ranges and randomly separated into samples which were shipped with each AIMS2 machine to the participating laboratories. Each coarse aggregate sample consisted of 60 particles. All of the coarse particles were placed on the tray, and 50 of them were used in the analysis. Approximately 150 grams of each fine aggregate size, 2.36mm (ASTM #8 sieve) to 0.15mm (ASTM #100 sieve), and 50 grams of 0.075mm (ASTM #200 sieve) aggregate were sent to the laboratories. A fine aggregate sample was spread onto the tray, and 150 aggregate particles were used for the analysis.

Eight AIMS2 machines were used in this study. Given the number of participating laboratories (32 labs), three to four laboratories used the same exact machine and tested the same samples. This procedure satisfied the number of materials and participating laboratory requirements of ASTM C 802-96. Testing began with successfully calibrating the machines according to manufacturer instructions. The user was instructed to scan the two replicate measurements on different days to provide meaningful replicate values. Data from each test was automatically saved into computer files.

DATA ANALYSIS

Following careful examination of the procedure followed to conduct measurements, three laboratories' data were removed from the ILS study due to user error by not following manufacturer and procedure instructions. The within-laboratory and between-laboratory variances were calculated using data from the remaining 29 laboratories. A list of the raw data is show in Appendix C.

With an additional analysis of the raw data images, several 4.75 mm (ASTM #4 sieve) texture images were found to be of the aggregate edge instead of the aggregate surface. Fig. 5.1 shows two texture images, one image including the aggregate edge and one image of the aggregate surface. The image of the edge of the aggregate contains both the surface of the aggregate and the surface of the tray. If several images are of the aggregate edge are within a sample data, these images can affect the AIMS2 results, in particularly the texture values. The images with aggregate edges were removed manually, and the results were recalculated for the remaining images. The remaining coarse aggregate sizes were checked, and the images did not have the same problems as the 4.75 mm (ASTM #4 sieve) aggregates.

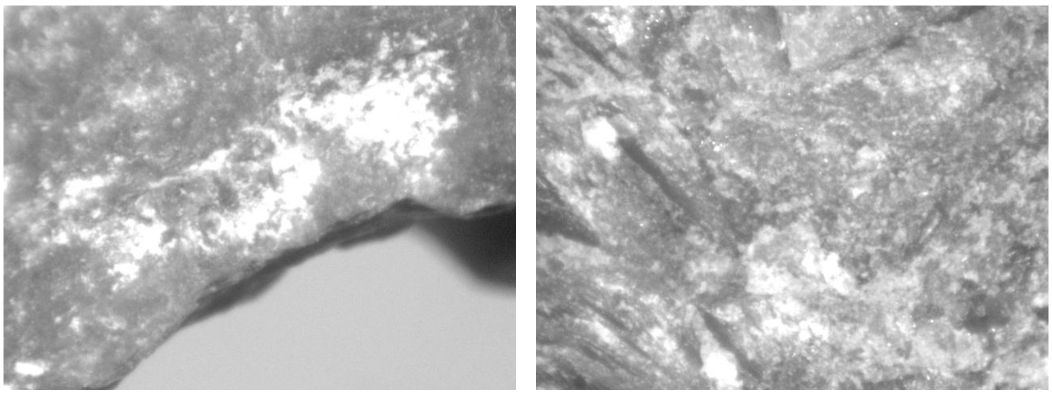

Fig. 5.1. Texture Image with and without Aggregate Edge

The data were checked for agreement of variances and interactions between material and laboratories. ASTM C 802-96 assumes that different laboratories have the same within-laboratory variances. The variance of the each laboratory was checked for an agreement of variances based on the ratio of the largest variance to the sum of variances. The laboratories with the variances above the upper 5% level were eliminated to bring the variances into agreement. The interactions between laboratory and material were checked by plotting the averages values obtained by each laboratory to aggregate type. A similar pattern of change was found from one material to another which indicated little to no interaction between laboratory and materials. An example of the analysis results of all 29 laboratory data is shown in Fig. 5.2 for the angularity measurement of 25.0mm (1in) size aggregates.

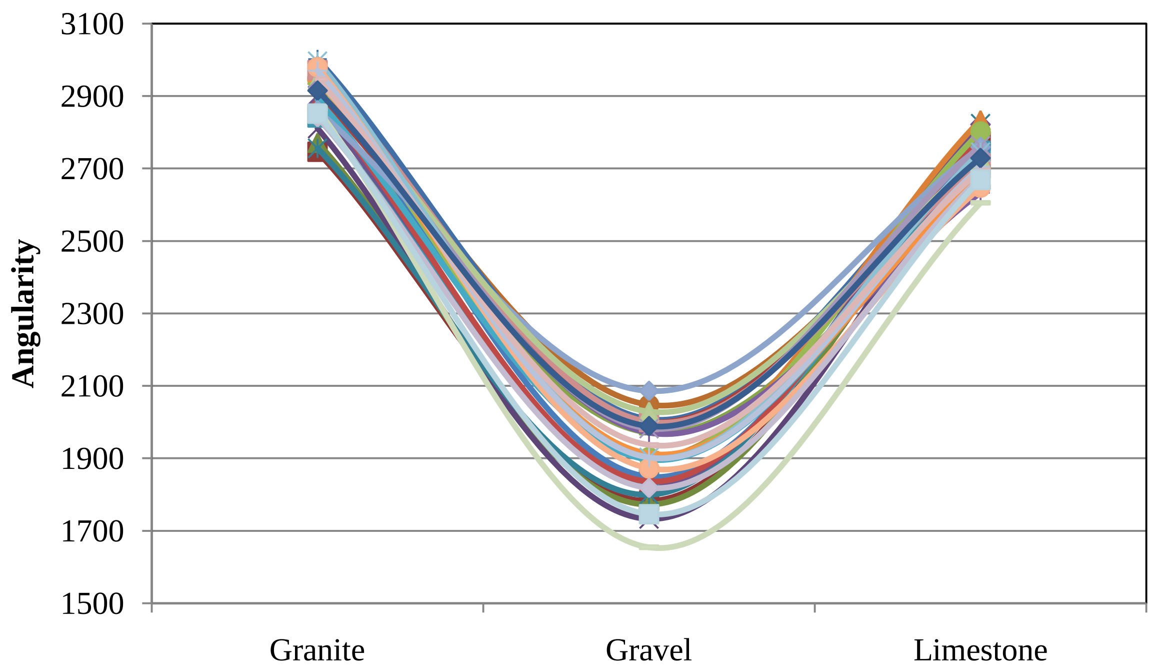

Fig. 5.2. Interaction Check for Angularity versus Material for 25.0mm (1 in) Aggregates

The components of variance, variances, standard deviations, and coefficient of variations were calculated for each shape property for each aggregate type. The components of variance are the estimated amount of variation that can be attributed to the effects of the experiment from the factor tested (Devore 2004). The averages, components of variance, and variances of the crushed gravel, limestone, and granite are shown in Tables 5.4, 5.5, and 5.6, respectively. The standard deviation and coefficient of variation of the crushed gravel, limestone, and granite are shown in Tables 5.7, 5.8 and 5.9, respectively. The combined data results for the weighted aggregate blend are listed in Tables 5.10 and 5.11.

It should be noted that the analysis was conducted on the flat or elongated 3:1 ratio instead of the 5:1 ratio because the aggregate samples had a few or no particles that exceeded the 5:1 ratio. For example, for the 25.0mm (1in) and 4.75 mm (ASTM #4 sieve) aggregates, it was found during the analysis that any small variation in measurements even by one particle would translate to a very high coefficient of variation if the 5:1 ratio was used. The coefficient of variation reported for the flat or elongated 3:1 ratio were calculated based on the average percent of particles that have a ratio less than (not more than) 3:1.

Table 5.4. Averages, Components of Variance, and Variances of Gravel for All Aggregate Sizes.

Aggregate Shape Characteristic	Aggregate Size	Average	Components of Variance		Variance	
			Within-Laboratory	Between-Laboratory	Within-Laboratory	Between-Laboratory
Angularity	25 (1.0")	1895.6	3795.7	9033.3	3795.7	12829.0
	19 (3/4")	2609.1	7630.1	8597.4	7630.1	16227.5
	12.5 (1/2")	2777.9	5511.7	8718.2	5511.7	14229.9
	9.5 (3/8")	2563.5	3038.2	20105.9	3038.2	23144.1
	4.75 (#4)	2275.5	4403.8	14193.3	4403.8	18597.2
	2.36 (#8)	2667.3	7588.7	1311.3	7588.7	8900.0
	1.18 (#16)	3076.3	3482.6	1894.0	3482.6	5376.6
	0.6 (#30)	3237.1	8033.0	824.2	8033.0	8857.2
	0.3 (#50)	3179.5	12085.8	10815.3	12085.8	22901.1
	0.15 (#100)	2735.1	13011.2	10529.8	13011.2	23541.0
	0.075 (#200)	2251.8	31135.2	12453.6	31135.2	43588.8
Texture	25 (1.0")	224.7	78.1	155.4	78.1	233.5
	19 (3/4")	249.8	221.8	165.4	221.8	387.3
	12.5 (1/2")	233.6	161.4	103.6	161.4	264.9
	9.5 (3/8")	227.5	143.6	213.2	143.6	356.8
	4.75 (#4)	180.8	185.0	173.0	185.0	358.1
Sphericity	25 (1.0")	0.7	0.0	0.0	0.0	0.0
	19 (3/4")	0.7	0.0	0.0	0.0	0.0
	12.5 (1/2")	0.7	0.0	0.0	0.0	0.0
	9.5 (3/8")	0.68	0.0000	0.0001	0.0000	0.0001
	4.75 (#4)	0.70	0.0001	0.0003	0.0001	0.0004
Flat or Elongated 3:1	25 (1.0")	0.58%	0.0000	0.0002	0.0000	0.0002
	19 (3/4")	0.76%	0.0001	0.0001	0.0001	0.0002
	12.5 (1/2")	1.12%	0.0001	0.0002	0.0001	0.0003
	9.5 (3/8")	3.83%	0.0003	0.0014	0.0003	0.0016
	4.75 (#4)	3.22%	0.0005	0.0007	0.0005	0.0012
2D Form	2.36 (#8)	6.7	0.0264	0.0043	0.0264	0.0307
	1.18 (#16)	7.4	0.0289	0.0067	0.0289	0.0357
	0.6 (#30)	7.8	0.0335	0.0097	0.0335	0.0432
	0.3 (#50)	7.6	0.0440	0.0334	0.0440	0.0774
	0.15 (#100)	7.4	0.0462	0.0264	0.0462	0.0727
	0.075 (#200)	8.5	0.1465	0.0799	0.1465	0.2265

Table 5.5. Averages, Components of Variance, and Variances of Limestone for All Aggregate Sizes.

Aggregate Shape Characteristic	Aggregate Size	Average	Components of Variance		Variance	
			Within-Laboratory	Between-Laboratory	Within-Laboratory	Between-Laboratory
Angularity	25 (1.0")	2730.7	3746.2	1704.9	3746.2	5451.1
	19 (3/4")	2746.4	5320.3	2813.7	5320.3	8134.0
	12.5 (1/2")	2702.3	4158.7	4364.5	4158.7	8523.2
	9.5 (3/8")	2705.6	4695.5	1237.7	4695.5	5933.1
	4.75 (#4)	2706.5	4656.6	1643.3	4656.6	6299.8
	2.36 (#8)	2913.9	5244.4	-155.9	5244.4	5088.5
	1.18 (#16)	2948.6	3762.9	5953.5	3762.9	9716.4
	0.6 (#30)	3006.6	3610.8	5327.9	3610.8	8938.6
	0.3 (#50)	2914.5	10183.6	8965.8	10183.6	19149.4
	0.15 (#100)	2412.9	11688.2	17729.0	11688.2	29417.2
	0.075 (#200)	2798.3	124617.2	209763.9	124617.2	334381.0
Texture	25 (1.0")	275.4	143.7	198.9	143.7	342.6
	19 (3/4")	268.6	84.4	157.5	84.4	241.8
	12.5 (1/2")	257.3	103.0	108.1	103.0	211.2
	9.5 (3/8")	225.6	93.1	93.2	93.1	186.3
	4.75 (#4)	139.1	31.4	86.3	31.4	117.7
Sphericity	25 (1.0")	0.7	0.0	0.0	0.0	0.0
	19 (3/4")	0.7	0.0	0.0	0.0	0.0
	12.5 (1/2")	0.68	0.0001	0.0001	0.0001	0.0002
	9.5 (3/8")	0.68	0.0001	0.0001	0.0001	0.0002
	4.75 (#4)	0.67	0.0001	0.0002	0.0001	0.0003
Flat or Elongated 3:1	25 (1.0")	0.83%	0.0001	0.0001	0.0001	0.0002
	19 (3/4")	0.31%	0.0000	0.0000	0.0000	0.0001
	12.5 (1/2")	0.97%	0.0002	0.0000	0.0002	0.0002
	9.5 (3/8")	2.04%	0.0003	0.0003	0.0003	0.0006
	4.75 (#4)	4.11%	0.0005	0.0006	0.0005	0.0011
2D Form	2.36 (#8)	7.3	0.0294	0.0134	0.0294	0.0428
	1.18 (#16)	7.5	0.0436	0.0088	0.0436	0.0524
	0.6 (#30)	7.4	0.0208	0.0279	0.0208	0.0487
	0.3 (#50)	7.2	0.0377	0.0376	0.0377	0.0753
	0.15 (#100)	7.0	0.0715	0.0131	0.0715	0.0846
	0.075 (#200)	8.8	0.1805	0.1919	0.1805	0.3724

Table 5.6. Averages, Components of Variance, and Variances of Granite (Sandstone for 0.075 mm size) for All Aggregate Sizes.

Aggregate Shape Characteristic	Aggregate Size	Average	Components of Variance		Variance	
			Within-Laboratory	Between-Laboratory	Within-Laboratory	Between-Laboratory
Angularity	25 (1.0")	2901.4	3012.5	3479.6	3012.5	6492.2
	19 (3/4")	2985.9	5617.4	3750.5	5617.4	9367.9
	12.5 (1/2")	3117.7	3003.9	5429.6	3003.9	8433.5
	9.5 (3/8")	3193.4	3916.6	6345.0	3916.6	10261.6
	4.75 (#4)	3061.0	8969.4	2738.1	8969.4	11707.5
	2.36 (#8)	3330.8	4573.7	331.6	4573.7	4905.3
	1.18 (#16)	3373.1	6988.0	1074.0	6988.0	8062.0
	0.6 (#30)	3428.1	8080.1	9902.4	8080.1	17982.5
	0.3 (#50)	3436.1	9438.5	47278.8	9438.5	56717.2
	0.15 (#100)	3182.0	14401.6	15384.8	14401.6	29786.3
	0.075 (#200)	2845.4	115989.5	14255.0	115989.5	130244.5
Texture	25 (1.0")	471.8	100.4	132.3	100.4	232.7
	19 (3/4")	476.5	68.6	246.7	68.6	315.3
	12.5 (1/2")	465.0	169.6	205.2	169.6	374.8
	9.5 (3/8")	463.2	97.4	381.4	97.4	478.8
	4.75 (#4)	363.5	120.8	276.5	120.8	397.3
Sphericity	25 (1.0")	0.7	0.0	0.0	0.0	0.0
	19 (3/4")	0.6	0.0	0.0	0.0	0.0
	12.5 (1/2")	0.6	0.0	0.0	0.0	0.0
	9.5 (3/8")	0.62	0.0000	0.0002	0.0000	0.0002
	4.75 (#4)	0.68	0.0000	0.0002	0.0000	0.0002
Flat or Elongated 3:1	25 (1.0")	6.81%	0.0005	0.0025	0.0005	0.0030
	19 (3/4")	9.66%	0.0004	0.0027	0.0004	0.0032
	12.5 (1/2")	7.91%	0.0006	0.0008	0.0006	0.0013
	9.5 (3/8")	5.72%	0.0007	0.0010	0.0007	0.0017
	4.75 (#4)	5.19%	0.0011	0.0001	0.0011	0.0012
2D Form	2.36 (#8)	7.6	0.0169	0.0152	0.0169	0.0321
	1.18 (#16)	7.7	0.0258	0.0329	0.0258	0.0587
	0.6 (#30)	7.9	0.0302	0.0238	0.0302	0.0540
	0.3 (#50)	8.0	0.0147	0.0563	0.0147	0.0710
	0.15 (#100)	7.9	0.0401	0.0266	0.0401	0.0667
	0.075 (#200)	9.5	0.2947	0.0373	0.2947	0.3320

Table 5.7. Averages, Standard Deviation, and Coefficient of Variation of Gravel

Aggregate Shape Characteristic	Aggregate Size	Average	Standard Deviations		Coefficients of Variation	
			Within-Laboratory	Between-Laboratory	Within-Laboratory	Between-Laboratory
Angularity	25 (1.0")	1895.6	61.6	113.3	3.3	6.0
	19 (3/4")	2609.1	87.4	127.4	3.3	4.9
	12.5 (1/2")	2777.9	74.2	119.3	2.7	4.3
	9.5 (3/8")	2563.5	55.1	152.1	2.2	5.9
	4.75 (#4)	2275.5	66.4	136.4	2.9	6.0
	2.36 (#8)	2667.3	87.1	94.3	3.3	3.5
	1.18 (#16)	3076.3	59.0	73.3	1.9	2.4
	0.6 (#30)	3237.1	89.6	94.1	2.8	2.9
	0.3 (#50)	3179.5	109.9	151.3	3.5	4.8
	0.15 (#100)	2735.1	114.1	153.4	4.2	5.6
	0.075 (#200)	2251.8	176.5	208.8	7.8	9.3
Texture	25 (1.0")	224.7	8.8	15.3	3.9	6.8
	19 (3/4")	249.8	14.9	19.7	6.0	7.9
	12.5 (1/2")	233.6	12.7	16.3	5.4	7.0
	9.5 (3/8")	227.5	12.0	18.9	5.3	8.3
	4.75 (#4)	180.8	13.6	18.9	7.5	10.5
Sphericity	25 (1.0")	0.7	0.0	0.0	1.1	2.4
	19 (3/4")	0.7	0.0	0.0	1.0	2.3
	12.5 (1/2")	0.69	0.0066	0.0133	0.9574	1.9202
	9.5 (3/8")	0.68	0.0069	0.0114	1.0096	1.6730
	4.75 (#4)	0.70	0.0107	0.0205	1.5294	2.9281
Flat or Elongated 3:1	25 (1.0")	0.58%	0.0066	0.0148	0.6631	1.4909
	19 (3/4")	0.76%	0.0099	0.0124	0.9989	1.2523
	12.5 (1/2")	1.12%	0.0099	0.0167	1.0057	1.6901
	9.5 (3/8")	3.83%	0.0161	0.0406	1.6777	4.2236
	4.75 (#4)	3.22%	0.0232	0.0346	2.3940	3.5730
2D Form	2.36 (#8)	6.7	0.1624	0.1752	2.4326	2.6235
	1.18 (#16)	7.4	0.1701	0.1888	2.2868	2.5379
	0.6 (#30)	7.8	0.1830	0.2079	2.3469	2.6666
	0.3 (#50)	7.6	0.2098	0.2783	2.7553	3.6536
	0.15 (#100)	7.4	0.2150	0.2696	2.8944	3.6288
	0.075 (#200)	8.5	0.3828	0.4759	4.5283	5.6292

Table 5.8. Averages, Standard Deviation, and Coefficient of Variation of Limestone

Aggregate Shape Characteristic	Aggregate Size	Average	Standard Deviations		Coefficients of Variation	
			Within-Laboratory	Between-Laboratory	Within-Laboratory	Between-Laboratory
Angularity	25 (1.0")	2730.7	61.2	73.8	2.2	2.7
	19 (3/4")	2746.4	72.9	90.2	2.7	3.3
	12.5 (1/2")	2702.3	64.5	92.3	2.4	3.4
	9.5 (3/8")	2705.6	68.5	77.0	2.5	2.8
	4.75 (#4)	2706.5	68.2	79.4	2.5	2.9
	2.36 (#8)	2913.9	72.4	71.3	2.5	2.4
	1.18 (#16)	2948.6	61.3	98.6	2.1	3.3
	0.6 (#30)	3006.6	60.1	94.5	2.0	3.1
	0.3 (#50)	2914.5	100.9	138.4	3.5	4.7
	0.15 (#100)	2412.9	108.1	171.5	4.5	7.1
	0.075 (#200)	2798.3	353.0	578.3	12.6	20.7
Texture	25 (1.0")	275.4	12.0	18.5	4.4	6.7
	19 (3/4")	268.6	9.2	15.6	3.4	5.8
	12.5 (1/2")	257.3	10.2	14.5	3.9	5.6
	9.5 (3/8")	225.6	9.6	13.7	4.3	6.1
	4.75 (#4)	139.1	5.6	10.8	4.0	7.8
Sphericity	25 (1.0")	0.72	0.0054	0.0155	0.7598	2.1676
	19 (3/4")	0.68	0.0057	0.0165	0.8326	2.4187
	12.5 (1/2")	0.68	0.0074	0.0142	1.0887	2.0887
	9.5 (3/8")	0.68	0.0076	0.0133	1.1196	1.9515
	4.75 (#4)	0.67	0.0100	0.0164	1.5023	2.4658
Flat or Elongated 3:1	25 (1.0")	0.83%	0.0071	0.0127	0.7173	1.2764
	19 (3/4")	0.31%	0.0070	0.0073	0.6990	0.7350
	12.5 (1/2")	0.97%	0.0124	0.0137	1.2473	1.3826
	9.5 (3/8")	2.04%	0.0159	0.0240	1.6281	2.4467
	4.75 (#4)	4.11%	0.0225	0.0326	2.3424	3.4007
2D Form	2.36 (#8)	7.3	0.1715	0.2069	2.3464	2.8304
	1.18 (#16)	7.5	0.2089	0.2289	2.8027	3.0717
	0.6 (#30)	7.4	0.1442	0.2206	1.9395	2.9662
	0.3 (#50)	7.2	0.1941	0.2743	2.6878	3.7988
	0.15 (#100)	7.0	0.2675	0.2909	3.8203	4.1550
	0.075 (#200)	8.8	0.4249	0.6103	4.8284	6.9350

Table 5.9. Averages, Standard Deviation, and Coefficient of Variation of Granite

(Sandstone for 0.075 mm size)

Aggregate Shape Characteristic	Aggregate Size	Average	Standard Deviations		Coefficients of Variation	
			Within-Laboratory	Between-Laboratory	Within-Laboratory	Between-Laboratory
Angularity	25 (1.0")	2901.4	54.9	80.6	1.9	2.8
	19 (3/4")	2985.9	74.9	96.8	2.5	3.2
	12.5 (1/2")	3117.7	54.8	91.8	1.8	2.9
	9.5 (3/8")	3193.4	62.6	101.3	2.0	3.2
	4.75 (#4)	3061.0	94.7	108.2	3.1	3.5
	2.36 (#8)	3330.8	67.6	70.0	2.0	2.1
	1.18 (#16)	3373.1	83.6	89.8	2.5	2.7
	0.6 (#30)	3428.1	89.9	134.1	2.6	3.9
	0.3 (#50)	3436.1	97.2	238.2	2.8	6.9
	0.15 (#100)	3182.0	120.0	172.6	3.8	5.4
	0.075 (#200)	2845.4	340.6	360.9	12.0	12.7
Texture	25 (1.0")	471.8	10.0	15.3	2.1	3.2
	19 (3/4")	476.5	8.3	17.8	1.7	3.7
	12.5 (1/2")	465.0	13.0	19.4	2.8	4.2
	9.5 (3/8")	463.2	9.9	21.9	2.1	4.7
	4.75 (#4)	363.5	11.0	19.9	3.0	5.5
Sphericity	25 (1.0")	0.7	0.0	0.0	0.8	2.9
	19 (3/4")	0.64	0.0054	0.0180	0.8389	2.8273
	12.5 (1/2")	0.62	0.0078	0.0126	1.2580	2.0376
	9.5 (3/8")	0.62	0.0064	0.0148	1.0388	2.3872
	4.75 (#4)	0.68	0.0065	0.0153	0.9542	2.2500
Flat or Elongated 3:1	25 (1.0")	6.81%	0.0222	0.0550	2.3831	5.9008
	19 (3/4")	9.66%	0.0208	0.0562	2.3017	6.2250
	12.5 (1/2")	7.91%	0.0241	0.0366	2.6180	3.9717
	9.5 (3/8")	5.72%	0.0257	0.0407	2.7262	4.3195
	4.75 (#4)	5.19%	0.0332	0.0345	3.4992	3.6437
2D Form	2.36 (#8)	7.6	0.1299	0.1791	1.7012	2.3456
	1.18 (#16)	7.7	0.1606	0.2422	2.0854	3.1457
	0.6 (#30)	7.9	0.1739	0.2325	2.1978	2.9387
	0.3 (#50)	8.0	0.1212	0.2665	1.5243	3.3506
	0.15 (#100)	7.9	0.2003	0.2583	2.5197	3.2500
	0.075 (#200)	9.5	0.5429	0.5762	5.7193	6.0704

Table 5.10. Averages, Components of Variance, and Variances of Combined Properties for the Blend

Aggregate Material	Aggregate Size	Average	Components of Variance		Variance	
			Within-Laboratory	Between-Laboratory	Within-Laboratory	Between-Laboratory
Gravel	Angularity	2878.1	3400.8	4697.5	3400.8	8098.3
	Texture	203.4	44.7	123.9	44.7	168.6
	Sphericity	0.70	0.0001	0.0003	0.0001	0.0003
	Flat or Elongated 3:1	1.52%	0.0000	0.0001	0.0000	0.0002
	2D Form	7.5	0.0124	0.0093	0.0124	0.0217
Limestone	Angularity	2689.8	2715.7	6833.3	2715.7	9549.0
	Texture	183.4	11.0	58.0	11.0	69.0
	Sphericity	0.67	0.0001	0.0001	0.0001	0.0002
	Flat or Elongated 3:1	1.46%	0.0000	0.0000	0.0000	0.0001
	2D Form	7.2	0.0213	0.0109	0.0213	0.0322
Granite	Angularity	3262.2	5341.0	12882.9	5341.0	18223.9
	Texture	399.5	75.2	167.8	75.2	243.0
	Sphericity	0.67	0.0001	0.0001	0.0001	0.0002
	Flat or Elongated 3:1	4.36%	0.0001	0.0001	0.0001	0.0002
	2D Form	7.9	0.0131	0.0109	0.0131	0.0241

Table 5.11. Averages, Standard Deviation, and Coefficient of Variation of Combined Properties for the Blend

Aggregate Material	Aggregate Size	Average	Standard Deviations		Coefficients of Variation	
			Within-Laboratory	Between-Laboratory	Within-Laboratory	Between-Laboratory
Gravel	Angularity	2878.1	58.3	90.0	2.0	3.1
	Texture	203.4	6.7	13.0	3.3	6.4
	Sphericity	0.70	0.0083	0.0183	1.1981	2.6291
	Flat or Elongated 3:1	1.52%	0.0066	0.0138	0.6733	1.4002
	2D Form	7.5	0.1112	0.1472	1.4885	1.9700
Limestone	Angularity	2689.8	52.1	97.7	1.9	3.6
	Texture	183.4	3.3	8.3	1.8	4.5
	Sphericity	0.67	0.0090	0.0151	1.3578	2.2602
	Flat or Elongated 3:1	1.46%	0.0052	0.0084	0.5295	0.8491
	2D Form	7.2	0.1459	0.1794	2.0338	2.4999
Granite	Angularity	3262.2	73.1	135.0	2.2	4.1
	Texture	399.5	8.7	15.6	2.2	3.9
	Sphericity	0.67	0.0092	0.0151	1.3633	2.2521
	Flat or Elongated 3:1	4.36%	0.0103	0.0141	1.0753	1.4739
	2D Form	7.9	0.1146	0.1551	1.4509	1.9645

The standard deviations and coefficient of variations were plotted against the average of each material source. Figs. 5.3 and 5.4 are examples of the standard deviation and coefficient of variations relationships for the angularity measurement of 25.0mm (1in) aggregates.

The precision statement of the data was established by analyzing the relationships of the standard deviations and/or coefficients of variation. The ASTM C 670-96 procedure includes two provisions for the data analysis. One provision is for a constant standard deviation case and the second provision is for a constant coefficient of variation case.

The constant standard deviation case is where pooled within-laboratory standard deviation over all the materials becomes the single-operator standard deviation and the pooled between-laboratory standard deviation becomes the multi-laboratory standard deviation. In the case of a constant coefficient of variation, the average within-laboratory and between-laboratory coefficient of variation becomes the single-operator and the multi-laboratory coefficient of variation, respectively.

Neither of the constant standard deviation or constant coefficient of variation conditions was strictly satisfied in the analysis results. However, from an engineering perspective, the variation of the standard deviation and coefficient of variation is considered small. Therefore, it was decided to determine the precision statements for both a constant standard deviation and a constant coefficient of variation for the single-operator (within-laboratory) and multi-laboratory (between-laboratory) precision.

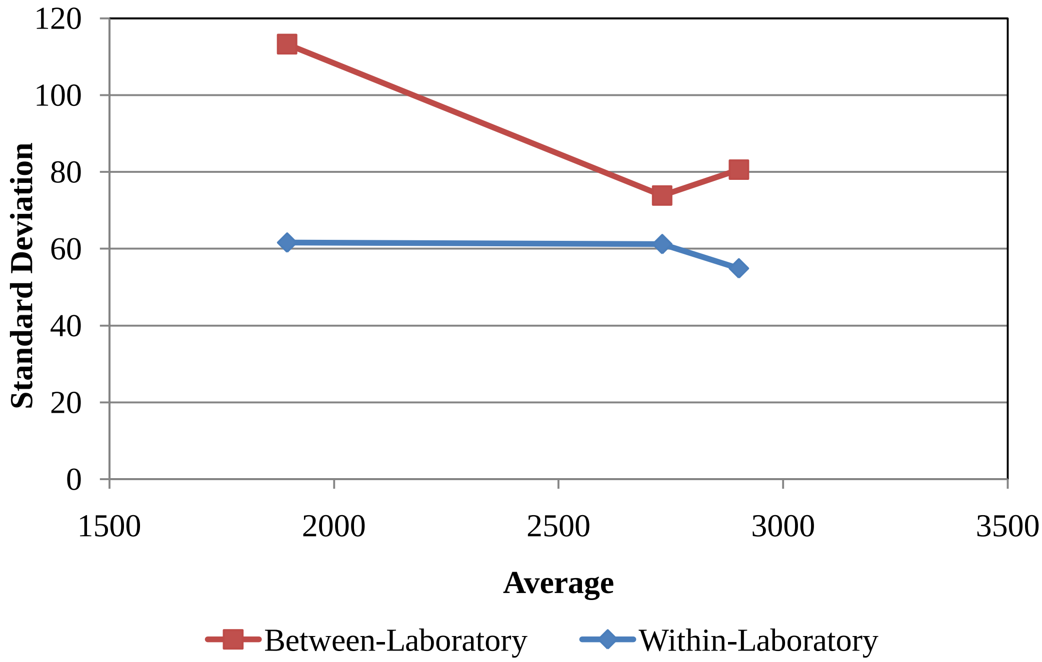

Fig. 5.3. Standard Deviation versus Average Angularity of 25.0mm (1in)

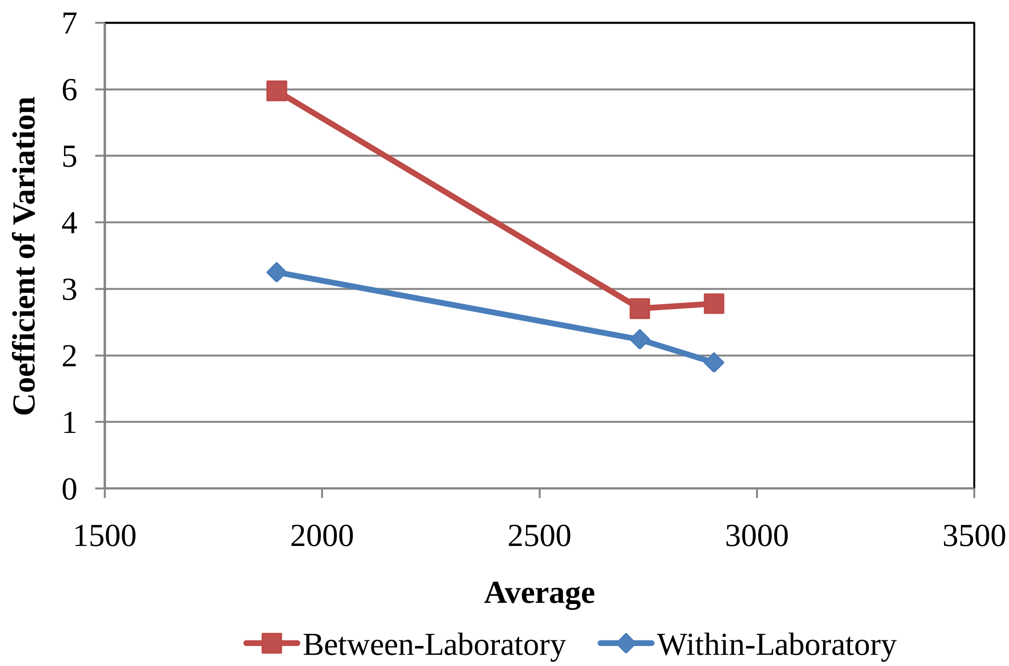

Fig. 5.4. Coefficient of Variation versus Average Angularity of 25.0mm (1in)

The precision statements (1s%) based on the assumption of constant standard deviation are shown in Table 5.12 for the single-operator and multi-laboratory results. The precision statements (1s%) based on the assumption of constant coefficient of variation are shown Table 5.13. The combined results precision statements (1s%) based on the assumptions of constant standard deviation and constant coefficient of variation are shown in Tables 5.14 and 5.15, respectively.

Based on these precisions statements, the results of two properly conducted tests (d2s%) which are tested either by a single-operator or multi-laboratory are not expected to differ more than the values shown in Tables 5.16, 5.17, 5.18, and 5.19. These numbers are based on the calculations described in ASTM C 670-96.

Table 5.12. Precision Statements (1s%) for Constant Standard Deviation

Aggregate Shape Characteristic	Aggregate Size	Standard Deviation	
		Single-Operator	Multi-Laboratory
Angularity	25 (1.0")	59.3	90.9
	19 (3/4")	78.7	106.0
	12.5 (1/2")	65.0	102.0
	9.5 (3/8")	62.3	114.5
	4.75 (#4)	77.5	110.5
	2.36 (#8)	76.2	79.4
	1.18 (#16)	68.9	87.9
	0.6 (#30)	81.1	109.2
	0.3 (#50)	102.8	181.4
	0.15 (#100)	114.2	166.1
	0.075 (#200)	301.0	411.6
Texture	25 (1.0")	10.4	16.4
	19 (3/4")	11.2	17.7
	12.5 (1/2")	12.0	16.8
	9.5 (3/8")	10.6	18.5
	4.75 (#4)	10.6	17.1
Sphericity	25 (1.0")	0.0066	0.0178
	19 (3/4")	0.0061	0.0171
	12.5 (1/2")	0.0073	0.0134
	9.5 (3/8")	0.0070	0.0132
	4.75 (#4)	0.0092	0.0175
Flat or Elongated 3:1	25 (1.0")	0.0140	0.0337
	19 (3/4")	0.0139	0.0335
	12.5 (1/2")	0.0167	0.0245
	9.5 (3/8")	0.0198	0.0360
	4.75 (#4)	0.0271	0.0331
2D Form	2.36 (#8)	0.1556	0.1876
	1.18 (#16)	0.1811	0.2212
	0.6 (#30)	0.1679	0.2206
	0.3 (#50)	0.1793	0.2731
	0.15 (#100)	0.2294	0.2733
	0.075 (#200)	0.4553	0.5570

Table 5.13. Precision Statements (1s%) for Constant Coefficient of Variation

Aggregate Shape Characteristic	Aggregate Size	Coefficient of Variation	
		Single-Operator	Multi-Laboratory
Angularity	25 (1.0")	2.5%	3.8%
	19 (3/4")	2.8%	3.8%
	12.5 (1/2")	2.3%	3.6%
	9.5 (3/8")	2.2%	4.0%
	4.75 (#4)	2.8%	4.2%
	2.36 (#8)	2.6%	2.7%
	1.18 (#16)	2.2%	2.8%
	0.6 (#30)	2.5%	3.3%
	0.3 (#50)	3.2%	5.5%
	0.15 (#100)	4.1%	6.0%
	0.075 (#200)	10.8%	14.2%
Texture	25 (1.0")	3.5%	5.6%
	19 (3/4")	3.7%	5.8%
	12.5 (1/2")	4.1%	5.6%
	9.5 (3/8")	3.9%	6.4%
	4.75 (#4)	4.9%	7.9%
Sphericity	25 (1.0")	0.9%	2.5%
	19 (3/4")	0.9%	2.5%
	12.5 (1/2")	1.1%	2.0%
	9.5 (3/8")	1.1%	2.0%
	4.75 (#4)	1.3%	2.5%
Flat or Elongated 3:1	25 (1.0")	1.3%	2.9%
	19 (3/4")	1.3%	2.7%
	12.5 (1/2")	1.6%	2.3%
	9.5 (3/8")	2.0%	3.7%
	4.75 (#4)	2.8%	3.5%
2D Form	2.36 (#8)	2.2%	2.6%
	1.18 (#16)	2.4%	2.9%
	0.6 (#30)	2.2%	2.9%
	0.3 (#50)	2.3%	3.6%
	0.15 (#100)	3.1%	3.7%
	0.075 (#200)	5.0%	6.2%

Table 5.14. Combined Properties Precision Statements (1s%) for Standard Deviation for the Blend

Aggregate Shape Characteristic	Constant Standard Deviation	
	Single-Operator	Multi-Laboratory
Angularity	61.8	109.3
Texture	6.6	12.7
Sphericity	0.0089	0.0162
Flat or Elongated 3:1	0.0077	0.0124
2D Form	0.1249	0.1612

Table 5.15. Combined Properties Precision Statements (1s%) for Constant Coefficient of Variation for the Blend

Aggregate Shape Characteristic	Coefficient of Variation	
	Single-Operator	Multi-Laboratory
Angularity	2.1%	3.6%
Texture	2.4%	4.9%
Sphericity	1.3%	2.4%
Flat or Elongated 3:1	0.8%	1.2%
2D Form	1.7%	2.1%

Table 5.16. Precision Statements of Two Tests (d2s%) for Constant Standard Deviation

Aggregate Shape Characteristic	Aggregate Size	Standard Deviation	
		Single-Operator	Multi-Laboratory
Angularity	25 (1.0")	167.8	257.0
	19 (3/4")	222.5	299.9
	12.5 (1/2")	183.8	288.4
	9.5 (3/8")	176.3	323.9
	4.75 (#4)	219.3	312.4
	2.36 (#8)	215.4	224.5
	1.18 (#16)	194.8	248.5
	0.6 (#30)	229.3	308.9
	0.3 (#50)	290.8	513.2
	0.15 (#100)	322.9	469.7
	0.075 (#200)	851.3	1164.1
Texture	25 (1.0")	29.3	46.4
	19 (3/4")	31.6	50.2
	12.5 (1/2")	34.0	47.6
	9.5 (3/8")	29.8	52.2
	4.75 (#4)	30.0	48.2
Sphericity	25 (1.0")	0.0186	0.0504
	19 (3/4")	0.0172	0.0483
	12.5 (1/2")	0.0206	0.0379
	9.5 (3/8")	0.0198	0.0374
	4.75 (#4)	0.0261	0.0496
Flat or Elongated 3:1	25 (1.0")	0.0396	0.0953
	19 (3/4")	0.0393	0.0948
	12.5 (1/2")	0.0471	0.0694
	9.5 (3/8")	0.0560	0.1018
	4.75 (#4)	0.0765	0.0938
2D Form	2.36 (#8)	0.4402	0.5306
	1.18 (#16)	0.5122	0.6255
	0.6 (#30)	0.4748	0.6238
	0.3 (#50)	0.5070	0.7724
	0.15 (#100)	0.6488	0.7729
	0.075 (#200)	1.2877	1.5756

Table 5.17. Precision Statements of Two Tests (d2s%) for Constant Coefficient of Variation

Aggregate Shape Characteristic	Aggregate Size	Coefficient of Variation	
		Single-Operator	Multi-Laboratory
Angularity	25 (1.0")	7.0%	10.8%
	19 (3/4")	8.0%	10.8%
	12.5 (1/2")	6.4%	10.0%
	9.5 (3/8")	6.3%	11.3%
	4.75 (#4)	8.0%	11.7%
	2.36 (#8)	7.3%	7.6%
	1.18 (#16)	6.1%	7.9%
	0.6 (#30)	7.0%	9.4%
	0.3 (#50)	9.2%	15.5%
	0.15 (#100)	11.7%	17.1%
	0.075 (#200)	30.6%	40.2%
Texture	25 (1.0")	9.8%	15.8%
	19 (3/4")	10.5%	16.4%
	12.5 (1/2")	11.5%	15.8%
	9.5 (3/8")	11.0%	18.0%
	4.75 (#4)	13.7%	22.4%
Sphericity	25 (1.0")	2.5%	7.1%
	19 (3/4")	2.5%	7.1%
	12.5 (1/2")	3.1%	5.7%
	9.5 (3/8")	3.0%	5.7%
	4.75 (#4)	3.8%	7.2%
Flat or Elongated 3:1	25 (1.0")	3.5%	8.2%
	19 (3/4")	3.8%	7.7%
	12.5 (1/2")	4.6%	6.6%
	9.5 (3/8")	5.7%	10.4%
	4.75 (#4)	7.8%	9.8%
2D Form	2.36 (#8)	6.1%	7.4%
	1.18 (#16)	6.8%	8.3%
	0.6 (#30)	6.1%	8.1%
	0.3 (#50)	6.6%	10.2%
	0.15 (#100)	8.7%	10.4%
	0.075 (#200)	14.2%	17.6%

Table 5.18. Combined Properties Precision Statements of Two Tests (d2s%) for Constant Standard Deviation for the Blend

Aggregate Shape Characteristic	Standard Deviation	
	Single-Operator	Multi-Laboratory
Angularity	174.8	309.3
Texture	18.7	35.8
Sphericity	0.0250	0.0459
Flat or Elongated 3:1	0.0217	0.0350
2D Form	0.3533	0.4558

Table 5.19. Combined Properties Precision Statements of Two Tests (d2s%) for Constant Coefficient of Variation for the Blend

Aggregate Shape Characteristic	Coefficient of Variation	
	Single-Operator	Multi-Laboratory
Angularity	5.8%	10.3%
Texture	6.8%	14.0%
Sphericity	3.7%	6.7%
Flat or Elongated 3:1	2.1%	3.5%
2D Form	4.7%	6.1%

The machines were calibrated before each laboratory scanned the materials to eliminate possible sources of error. The 0.075mm (ASTM #200 sieve) had larger than expected single-operator and multi-laboratory standard deviations. After investigation into the possible sources of error, the CHPR value, which is used to eliminate touching particles from the data before it is analyzed, was found to be the source of error (Mahmoud et al. 2010). The limits of the CHPR value were believed to allow several touching particles to be analyzed. This was determined by an inspection of the number of touching particles in the images from the analyzed data. Therefore, the 0.075mm (ASTM #200 sieve) results should be further examined after developing a more robust method to eliminate touching particles. Once such a method is developed, precision statements for the standard deviation and coefficient of variation results will be developed for this size.

SUMMARY

The analysis conducted in this chapter led to the development of precision statements for the different shape indices and parameters given by AIMS2. In general, the experiments gave very reasonable coefficients of variation for the various indices for all sizes except the 0.075mm (ASTM #200 sieve). The results from the constant coefficient of variation should be used to describe the precision statement since the standard deviation results have a slight increasing trend with an increase in average. Therefore, a precision statement based on constant standard deviation will be biased against materials with a low average and work in favor of materials with a high average. Overall, the maximum coefficient of variation was less than 5% for a single operator and less than 8% for multi laboratories when individual sizes were analyzed. The maximum coefficient of variation for the combined results of a blend was less than 3% for a single operator and less than 5% for multi laboratories. These are considered acceptable coefficient of variation values given the natural variation in aggregate samples from the same source.

Further tests will be necessary to determine the proper CHRP calibrated value for the small 0.075mm (ASTM #200 sieve) size in order to remove touching particles in the analysis. The determination of this value is expected to reduce the variations in the measurements conducted on the 0.075mm (ASTM #200 sieve) size, and reduce the precision coefficient of variation reported for this size.

The precision statements from the constant coefficient of variations were combined for aggregates sizes, excluding 0.075mm (ASTM #200 sieve), for each aggregate shape characteristic. The was done by taking the square root of the sum divided by n-1 of the squares of all sizes except 0.075mm (ASTM #200 sieve) for each aggregate shape property with n the number of values summed. The precision statements for the single limit (1s%) and difference of two results (d2s%) are shown in Tables 5.20 and 5.21, respectively.

Table 5.20. Precision Statement (1s%) for Each Shape Characteristic

Aggregate Shape Characteristic	Constant Coefficient of Variation	
	Within-Laboratory	Between-Laboratory
Angularity	2.9%	4.3%
Texture	4.5%	7.1%
Sphericity	1.2%	2.6%
Flat or Elongated 3:1	2.1%	3.4%
2D Form	2.7%	3.5%

Table 5.21. Precision Statement (d2s%) for Each Shape Characteristic

Aggregate Shape Characteristic	Constant Coefficient of Variation	
	Within-Laboratory	Between-Laboratory
Angularity	8.3%	12.2%
Texture	12.7%	20.0%
Sphericity	3.4%	7.4%
Flat or Elongated 3:1	5.9%	9.7%
2D Form	7.7%	10.0%

CHAPTER VI

CONCLUSIONS AND RECOMMENDATIONS

SUMMARY

The performance of hot of hot mix asphalt, Portland cement concrete, unbound base, and subbase layers in a pavement are significantly influenced by both coarse and fine aggregate shape characteristics. Aggregate shape can be described by three independent properties: particle shape, angularity, and texture. The Aggregate Image Measurement System (AIMS) is a computer automated system that was developed to measure aggregate shape properties.

A new prototype of AIMS was introduced with several modifications to improve the operational characteristics, develop the automation of the test procedure, and reduce operator interaction during testing and errors. AIMS1 and AIMS2 were found to have comparable results in characterizing aggregates. The repeatability, reproducibility, and sensitivity of AIMS measurements were analyzed on a wide range of coarse and fine aggregates. The sensitivity of AIMS was analyzed for several operational and systematic parameters. The effect of aggregate placement was found to be minimal, based on finding values of R^2 of 0.97 or higher for the change in aggregate orientation for the angularity and texture. AIMS2 was shown to be sensitive to different aggregate samples for the distribution of all the shape properties. The statistical analysis of the sample size confirms that the current sample size scanned by AIMS2 is acceptable in representing an aggregate source.

The sensitivity analysis from the ruggedness study identified several operational and environmental factors that could affect the AIMS2 results. Limits were proposed for these factors in order to limit their influence on the results. AIMS2 was found to be able to control normal variations without significantly changing the results as long as the proposed limits are obtained.

AIMS2 is highly repeatable and reproducible based on the single-operator and multi-laboratory precision estimates given the natural variation in aggregate samples from the same source. The individual aggregate sizes have a maximum coefficient of variation of less than 5% for a single operator and less than 8% for multi laboratories. The maximum coefficient of variation for the combined results of a blend was less than 3% for a single operator and less than 5% for multi laboratories.

RECOMMENDATIONS

The quality of AIMS measurements were quantified in this thesis. AIMS2 was found to have high repeatability, reproducibility, and sensitivity. The test method along with the results from this study are recommended for implementation into pavement industry standards. The test method can be used to measure the shape, angularity, and texture of aggregates. Linking different aggregate shape properties to performance of different types of pavements is also essential in order to develop new specifications.

In this study, the CHPR valued, which is used to eliminate touching particles from the data before it is analyzed, was believed to be the source of error in the precision statements for the 0.075mm (ASTM #200 sieve) aggregates. Further testing is recommended to determine the proper CHRP calibrated value for the 0.075mm (ASTM #200 sieve) aggregates.

REFERENCES

Al-Rousan, T. M. (2004). “Characterization of aggregate shape properties using a computer automated system.” Ph.D. Dissertation, Texas A&M University, College Station, Texas.

Barksdale, R. D., and Itani, S. Y. (1994). “Influence of aggregate shape on base behavior.” *Transportation Research Record 1227,* Transportation Research Board, Washington, D.C. pp. 171-182.

Bathina, M. (2005). “Quality analysis of the aggregate imaging system (AIMS) measurements.” M.S. Thesis, Texas A&M University, College Station, Texas.

Chowdhury, A., Button, J. W., Kohale, V., and Jahn, D. (2001). “Evaluation of superpave fine aggregate angularity specification,” International Center for Aggregates Research (ICAR) Report 201-1, Texas Transportation Institute, Texas A&M Univ., College Station, Texas.

Devore, J. L. (2004). *Probability and Statistics for Engineering and the Sciences*. Belmont, CA: Thomson.

Fletcher, T., Chandan, C., Masad, E., and Siva Kumar, K. (2002). “Measurements of aggregate texture and its influence on HMA permanent deformation.” *Journal of Testing and Evaluation, American Society for Testing and Materials, ASTM*, 30(6), 524-531

Fletcher, T., Chandan, C., Masad, E., and Siva Kumar, K. (2003). “Aggregate Imaging System (AIMS) for characterizing the shape of fine and coarse aggregates.” *Transportation Research Record 1832*, Transportation Research Board, Washington D.C., 67-77.

Huber, G. A., Jones, J. C., and Jackson, N. M. (1998) “Contribution of fine aggregate angularity and particle shape to Superpave mixture performance.” *Transportation Research Record 1609*, Transportation Research Board, Washington D.C., 28 – 35.

Kandhal, P. S., and Parker, F. Jr. (1998). “Aggregate tests related to asphalt concrete performance in pavements.” *National Cooperative Highway Research Program Report 405*, Transportation Research Board, National Research Council, Washington, D.C.

Kosmatka, S. H., Kerkhoff, B., and Panarese, W. C. (2002). *Design and control of concrete mixtures*. 14th Ed., Portland Cement Association, Skokie, IL.

Masad, E. (2004). “Aggregate Imaging System (AIMS) basics and applications” Report no. FHWA/TX-05/5-1707-01-1, *Texas Department of Transportation and Federal Highway Administration,* Washington, D.C.

Masad, E., Olcott, D., White, T., and Tashman, L. (2001). “Correlation of fine aggregate imaging shape indices with asphalt mixture performance,” *Transportation Research Record 1757,* Transportation Research Board, Washington, D.C., 148-156.

Masad, E., T. Al-Rousan, J. Button, D. Little, and E. Tutumluer, (2007). “Test methods for characterizing aggregate shape, texture, and angularity” *National Cooperative Highway Research Program NCHRP Report 555*, Washington, D.C.

Mahmoud, E., L. Gates, E. Masad, S. Erdoğan, E. Garboczi, (2010). “Comprehensive evaluation of AIMS texture, angularity, and dimensional Measurements” *Journal of Materials in Civil Engineering*, 22(4), 369-379.

Meininger, R. C. (1998). “Aggregate test related to performance of Portland cement concrete pavement.” Final Report, *National Cooperative Highway Research Program Project 4-20A.* Transportation Research Board, National Research Council, Washington, D.C.

Monismith, C. L. (1970). “Influence of shape, size, and surface texture on the stiffness and fatigue response of asphalt mixtures.” *Highway Research Board 109 Special Report,* Transportation Research Board, National Research Council, Washington, D.C., 4–11.

Saeed, A., Hall, J., and Barker, W. (2001) “Performance-related tests of aggregates for use in unbound pavement layers.” Report 453, *National Cooperative Highway Research Program* (NCHRP), Transportation Research Board, National Research Council, Washington, D.C.

SAS Institute Inc. 2008. *JMP® 8Statistics and Graphics Guide*. SAS Institute Inc. 2008, Cary, NC.

APPENDIX A

GAMMA PARAMETERS

Table A-1. Coarse Aggregate Shape and Scale Parameters of the Gamma Distribution

	Granite				Limestone				Gravel			
	Angularity		Texture		Angularity		Texture		Angularity		Texture	
Number of Aggregates	Alpha (α)	Sigma (σ)	Alpha (α)	Sigma (σ)	Alpha (α)	Sigma (σ)	Alpha (α)	Sigma (σ)	Alpha (α)	Sigma (σ)	Alpha (α)	Sigma (σ)
400	20.69	146.88	16.61	29.95	17.70	156.28	10.36	26.19	6.89	374.47	3.26	76.01
10	35.17	87.29	11.24	42.62	16.04	123.98	16.01	9.58	6.21	424.55	3.89	47.16
10	22.70	150.12	21.54	22.23	37.26	78.80	10.22	28.75	23.88	135.57	2.35	102.64
10	16.58	193.19	13.24	38.82	25.06	114.58	31.05	8.64	3.57	578.54	4.52	58.04
10	27.46	110.49	25.79	20.77	20.18	137.56	12.98	22.08	8.12	315.09	6.46	40.51
10	56.90	54.14	11.73	41.24	23.13	124.45	16.48	16.44	8.70	266.68	3.57	63.92
10	13.98	209.91	12.31	41.91	39.27	77.04	10.93	24.37	6.32	384.17	5.03	60.26
10	49.29	62.73	16.23	31.92	14.79	194.00	9.53	28.08	4.86	381.99	2.36	89.06
10	32.25	90.26	13.24	38.74	20.00	159.21	8.86	32.97	5.68	475.40	3.45	50.65
10	27.32	105.15	37.72	12.85	18.53	161.01	9.63	28.93	11.39	244.07	3.16	86.23
10	27.57	108.01	22.73	21.88	29.04	103.13	8.67	35.72	29.40	88.61	2.63	100.10
20	16.21	174.60	11.01	44.03	24.05	124.54	9.52	25.85	7.53	345.57	4.12	49.65
20	21.89	134.11	13.22	35.08	8.00	310.55	7.90	34.41	3.99	702.51	3.02	99.79
20	19.75	154.28	20.63	21.32	10.71	264.92	10.46	25.50	9.27	252.69	2.87	85.52
20	29.64	99.71	16.70	31.60	29.44	85.02	16.29	16.77	13.46	188.54	2.37	97.78
20	24.95	119.11	26.87	16.90	25.95	112.02	10.07	25.48	5.81	406.10	2.79	112.92
20	37.49	76.89	14.34	36.40	41.94	64.12	9.63	29.73	6.02	446.30	4.53	56.32
20	36.69	84.86	18.22	28.19	23.73	119.21	16.34	17.31	8.40	326.15	4.82	52.57
20	13.45	221.77	13.97	33.97	12.87	222.21	8.18	34.96	4.60	542.36	2.59	89.68
20	15.10	208.57	19.12	26.05	12.67	207.45	7.99	34.66	5.33	438.13	3.39	66.84

20	27.94	110.15	28.00	16.58	26.89	102.96	14.72	18.12	5.51	450.06	3.04	71.72
30	19.01	160.21	13.18	38.65	20.89	130.84	13.48	20.28	10.70	240.32	2.78	97.71
30	54.10	57.48	15.87	31.40	24.98	107.41	8.32	30.65	7.52	351.78	4.08	60.95
30	11.35	270.51	19.53	27.25	19.54	144.77	11.63	22.02	9.81	263.45	5.15	43.68
30	18.00	169.29	20.83	22.04	20.77	142.29	11.06	24.29	4.04	605.12	3.53	71.54
30	15.02	197.02	17.41	25.38	20.97	135.81	9.79	28.05	9.61	295.64	3.72	66.11
30	19.34	160.26	17.93	27.35	25.06	110.50	10.18	28.80	4.27	581.79	3.04	86.04
30	19.89	152.60	19.83	26.16	20.95	130.33	9.24	32.65	5.86	436.02	2.59	99.41
30	21.93	140.19	19.69	25.57	13.75	200.12	10.49	23.75	6.55	376.63	3.50	73.30
30	27.04	108.77	20.41	22.73	34.14	74.39	9.46	29.77	9.53	279.44	3.18	85.25
30	21.82	149.61	14.31	36.82	12.16	233.87	11.36	22.84	4.88	520.26	3.81	59.15
40	34.06	92.09	15.68	31.21	13.45	202.55	8.75	30.91	8.67	301.19	3.41	81.37
40	19.88	158.59	12.61	37.39	15.23	186.20	13.09	20.45	9.81	260.69	2.90	65.81
40	26.26	117.46	13.72	34.09	13.46	196.93	8.17	32.88	12.94	198.09	3.33	67.76
40	17.14	171.33	20.42	23.44	13.10	210.97	11.50	23.99	6.25	427.55	4.19	51.44
40	21.26	145.34	16.69	30.03	17.96	154.10	11.05	24.59	6.36	417.31	3.76	64.62
40	27.62	104.81	12.88	37.15	18.14	163.11	12.20	22.04	4.64	559.57	3.71	60.54
40	31.14	95.49	16.68	31.35	15.71	175.52	10.07	25.63	8.25	321.11	2.81	90.31
40	24.80	127.31	13.95	35.77	23.50	116.91	8.10	31.96	6.86	372.46	3.35	85.20
40	29.99	107.41	16.68	30.40	13.51	203.14	15.21	18.37	18.84	148.90	4.54	58.50
40	19.91	153.90	17.37	30.15	14.56	187.01	11.30	24.57	4.74	573.74	4.18	59.26
50	18.41	163.71	15.29	33.00	22.03	132.23	9.26	28.53	7.38	357.02	4.95	49.29
50	13.17	226.77	15.19	33.72	18.54	155.09	11.61	23.28	7.16	392.50	2.43	95.15
50	19.99	149.38	17.77	28.01	24.34	116.09	11.98	22.35	10.77	245.55	3.70	69.95

50	15.85	184.31	13.72	37.48	26.79	100.33	12.24	21.26	4.60	559.79	3.48	70.35
50	25.15	113.01	15.20	34.38	22.21	118.88	9.51	26.90	9.18	290.96	3.28	75.04
50	22.07	133.86	20.24	24.38	18.11	148.50	13.33	19.38	14.33	200.03	4.54	56.92
50	20.77	144.55	10.83	46.20	14.15	194.33	13.30	21.99	5.52	453.39	4.31	55.92
50	12.54	238.50	18.05	26.59	16.62	169.09	10.44	25.68	9.16	309.87	4.05	61.14
50	26.54	113.98	12.31	42.48	15.70	176.68	9.83	25.49	6.67	383.86	2.63	99.68
50	20.04	146.64	14.87	33.19	14.76	193.23	12.61	20.99	6.90	367.13	3.64	63.91
60	26.82	111.79	18.41	28.44	13.55	209.53	14.76	18.82	5.91	444.94	3.80	66.40
60	18.04	168.83	16.20	28.26	25.65	107.56	10.50	26.40	9.58	269.11	3.24	78.86
60	20.87	142.37	14.96	33.00	16.74	170.32	12.31	20.65	5.03	479.45	3.14	78.76
60	20.30	150.56	16.78	30.21	31.26	88.30	14.78	16.91	8.73	300.66	3.78	72.70
60	22.23	140.15	16.18	31.06	21.55	125.42	8.99	30.46	4.74	525.19	2.97	84.87
60	24.83	121.20	17.20	30.02	16.83	169.89	7.58	35.52	8.12	338.44	4.15	52.83
60	18.10	170.43	18.51	28.62	22.15	124.03	8.83	30.59	7.50	348.87	3.94	64.69
60	20.68	145.18	15.68	31.27	14.75	181.79	9.04	28.21	6.20	430.72	2.84	80.46
60	21.89	145.36	17.69	29.27	25.05	107.83	8.70	31.29	5.56	464.93	2.75	88.47
60	18.44	159.50	15.89	31.65	18.12	154.21	12.86	20.67	10.11	245.32	4.31	50.19

Table A-2. Fine Aggregate Shape and Scale Parameters of the Gamma Distribution

	Granite				Limestone				Gravel			
	Angularity		2D Form		Angularity		2D Form		Angularity		2D Form	
Number of Aggregates	Alpha (α)	Sigma (σ)	Alpha (α)	Sigma (σ)	Alpha (α)	Sigma (σ)	Alpha (α)	Sigma (σ)	Alpha (α)	Sigma (σ)	Alpha (α)	Sigma (σ)
800	13.03	253.16	17.42	0.43	10.57	283.59	14.67	0.48	9.48	338.68	12.57	0.60
110	14.35	231.89	18.50	0.41	10.92	274.43	37.35	0.16	9.58	346.23	23.86	0.29
110	15.76	205.77	19.34	0.39	9.69	308.84	18.33	0.38	8.75	361.98	13.16	0.54
110	12.67	260.01	20.27	0.37	11.72	258.17	18.08	0.40	10.34	319.09	14.58	0.50
110	12.87	255.11	20.72	0.37	10.17	314.49	19.34	0.36	12.32	262.85	11.39	0.66
110	18.20	181.14	15.53	0.49	12.14	238.48	15.28	0.46	9.16	363.53	12.07	0.63
110	13.63	249.66	17.63	0.43	10.84	275.17	13.47	0.56	6.89	437.80	11.70	0.65
110	13.93	237.21	15.88	0.48	11.17	261.69	14.42	0.49	11.77	275.45	17.74	0.42
110	13.70	243.03	17.71	0.42	12.05	251.79	13.48	0.51	13.97	228.93	12.03	0.62
110	10.30	321.51	19.41	0.39	9.90	308.43	12.14	0.59	10.07	311.96	10.30	0.75
110	18.06	187.08	16.17	0.48	10.19	278.02	16.59	0.43	7.99	383.46	14.08	0.53
120	12.79	253.57	19.04	0.39	12.81	240.18	12.97	0.56	9.77	338.30	10.20	0.77
120	12.52	265.43	14.49	0.52	10.56	271.15	11.33	0.64	11.39	284.37	12.82	0.60
120	13.06	247.22	16.86	0.44	8.84	333.29	16.98	0.42	9.84	310.02	13.58	0.55
120	12.38	263.81	18.41	0.41	10.60	282.64	13.74	0.50	7.61	423.85	14.27	0.52
120	12.71	260.78	18.60	0.39	9.89	289.74	12.40	0.56	9.85	318.84	13.44	0.52
120	14.55	231.02	18.87	0.39	10.55	289.81	16.66	0.41	9.40	320.88	12.14	0.60
120	12.17	273.05	19.36	0.39	14.60	209.67	14.66	0.49	14.08	234.69	14.48	0.51
120	16.56	203.39	18.65	0.40	11.93	246.78	11.30	0.65	11.48	301.83	9.08	0.85
120	12.01	273.89	16.64	0.45	12.29	246.12	17.04	0.40	8.61	382.59	16.20	0.45

120	11.96	273.15	16.77	0.45	11.04	284.55	15.69	0.44	9.42	324.94	10.90	0.68
130	12.87	257.11	15.85	0.47	9.78	297.77	15.58	0.45	10.73	302.38	12.85	0.60
130	16.31	205.14	17.15	0.45	9.23	323.01	14.98	0.47	10.76	294.58	11.58	0.65
130	14.43	215.36	14.89	0.51	12.32	244.53	15.62	0.46	7.87	395.32	13.29	0.56
130	12.64	259.36	17.14	0.44	10.83	275.67	12.45	0.59	9.82	332.91	12.94	0.56
130	12.52	252.70	17.36	0.43	9.70	326.42	15.91	0.44	8.74	354.77	15.04	0.48
130	13.88	244.41	19.20	0.39	10.28	293.07	15.04	0.46	10.59	295.20	12.59	0.61
130	14.86	226.21	21.49	0.34	10.01	295.49	14.95	0.48	9.24	346.44	13.83	0.53
130	17.06	196.89	18.21	0.40	10.27	307.85	16.78	0.42	10.10	322.29	11.13	0.68
130	13.39	233.99	14.94	0.50	10.31	290.55	18.31	0.38	7.53	450.08	12.90	0.59
130	15.93	198.50	19.13	0.39	9.60	311.27	14.87	0.49	7.49	425.23	13.87	0.53
140	13.93	237.89	16.50	0.48	8.77	340.49	17.88	0.40	7.46	427.20	14.37	0.53
140	13.94	242.54	14.98	0.50	12.05	245.60	17.02	0.42	7.58	403.35	14.83	0.50
140	13.56	244.83	15.30	0.51	11.68	251.22	17.75	0.39	10.15	317.29	13.10	0.57
140	12.10	266.49	18.96	0.39	10.28	288.78	14.26	0.50	9.04	341.42	11.89	0.62
140	13.84	244.20	16.23	0.46	10.48	293.48	14.11	0.51	10.78	290.99	12.57	0.59
140	15.17	215.78	22.31	0.34	8.69	357.64	14.23	0.50	12.39	262.47	12.35	0.63
140	12.57	265.71	16.92	0.45	11.83	247.48	14.08	0.52	9.79	332.33	13.33	0.56
140	13.46	245.22	19.49	0.38	9.26	323.21	12.28	0.60	11.15	292.26	11.75	0.64
140	13.92	232.51	20.08	0.37	11.63	257.51	14.41	0.49	9.65	339.22	14.42	0.53
140	12.69	274.49	17.95	0.42	12.11	251.76	14.75	0.48	11.73	283.39	11.53	0.63
150	12.80	256.57	19.17	0.39	10.47	291.09	14.80	0.49	9.85	321.75	13.35	0.56
150	13.42	236.79	17.25	0.44	10.98	273.10	12.52	0.57	11.06	293.21	15.27	0.48
150	12.13	275.42	18.20	0.42	9.11	343.99	11.28	0.65	9.23	337.90	13.29	0.56

150	11.09	297.96	15.65	0.48	11.66	250.73	15.90	0.44	8.61	383.34	14.73	0.50
150	12.97	257.75	15.17	0.50	9.60	311.89	14.21	0.50	8.47	379.14	15.41	0.50
150	10.80	311.95	19.93	0.38	10.34	297.18	15.19	0.47	9.97	315.05	13.84	0.51
150	17.01	190.63	19.26	0.39	11.68	253.61	13.97	0.51	9.87	324.60	15.42	0.50
150	12.88	258.63	17.36	0.44	11.28	263.25	19.13	0.35	10.59	303.89	11.96	0.61
150	12.39	261.87	18.83	0.39	10.50	285.25	12.84	0.56	9.31	351.98	12.67	0.62
150	12.00	277.80	15.04	0.50	12.20	248.57	12.84	0.57	16.63	192.16	13.33	0.56
160	12.13	271.89	17.18	0.44	8.96	334.86	18.23	0.39	9.82	332.72	13.77	0.54
160	14.27	225.66	19.29	0.39	9.70	312.17	15.56	0.45	10.05	318.32	12.04	0.62
160	18.05	176.99	18.55	0.40	9.24	329.01	16.39	0.41	8.95	354.89	15.86	0.48
160	11.88	279.14	17.28	0.43	10.16	298.40	16.38	0.43	12.12	255.01	13.03	0.61
160	13.76	239.42	18.15	0.42	12.05	247.38	14.88	0.47	8.73	364.75	11.21	0.67
160	10.06	340.13	15.20	0.49	9.57	326.62	12.68	0.56	8.54	385.94	12.59	0.61
160	12.46	259.31	15.74	0.47	10.10	290.92	15.76	0.44	12.41	255.03	12.78	0.58
160	12.90	249.02	18.00	0.42	10.62	284.45	14.12	0.51	11.54	273.85	12.84	0.58
160	15.46	208.11	18.14	0.41	9.14	324.68	12.89	0.55	9.57	345.97	12.08	0.61
160	11.85	277.51	18.13	0.42	11.01	273.47	14.68	0.48	9.80	333.39	12.53	0.61

APPENDIX B

BLENDING CALCULATIONS

From Pine Instruments Co.

This is a proposed procedure and has not yet been approved

Standard Practice for

Determining Aggregate Source Shape Values from Digital Image Analysis Shape Properties

AASHTO Designation: xx-xx

This is a proposed procedure and has not yet been approved

Standard Practice for

Determining Aggregate Source Shape Values from Digital Image Analysis Shape Properties

AASHTO Designation: xx-xx

1. SCOPE

1.1. This standard covers the determination of aggregate source and source blend shape characteristics using gradation analysis and shape properties determined by means of digital image analysis.

1.2. This standard may involve hazardous materials, operations, and equipment. This standard does not purport to address all of the safety problems associated with its use. It is the responsibility of the user of this standard to establish appropriate safety and health practices and determine the applicability of regulatory limitations prior to use.

2. REFERENCED DOCUMENTS

2.1. *AASHTO Standards*:

- T 11 Amount of Material Finer Than 75µm in Aggregate
- T 27 Standard Method of Test for Sieve Analysis of Fine and Coarse Aggregates
- T 84 Standard Method of Test for Specific Gravity and Absorption of Fine Aggregate
- T 85 Standard Method of Test for Specific Gravity and Absorption of Coarse Aggregate
- TP XX Standard Method of Test for Determining Aggregate Shape Properties by Means of Digital Image Analysis

3. TERMINOLOGY

3.1. Aggregate size—material retained on a given sieve size after passing the next larger sieve.

3.1.1. Fine Aggregate—Aggregate material passing 4.75mm (#4) sieve.
sieve sizes: 2.36mm (#8), 1.18mm (#16), 0.60mm (#30), 0.30mm (#50), 0.15mm (#100), 0.075mm (#200)

3.1.2. Coarse Aggregate—Aggregate material retained on 4.75mm (#4) sieve.
sieve sizes: 25.0mm (1”), 19.0mm (3/4”), 12.5mm (1/2”), 9.5mm (3/8”), 4.75mm (#4)

3.2. Shape Properties for each retained sieve (x)

3.2.1. Gradient Angularity (*GA*)—Applies to both fine and coarse aggregate sizes and is related to the sharpness of the corners of 2-dimensional images of aggregate particles. The gradient angularity quantifies changes along a particle boundary with higher gradient values indicating a more angular shape. Gradient angularity has a relative range of 0 to 10000 with a perfect circle having a value of 0.

Gradient Angularity: $$GA = \frac{1}{\frac{n}{3} - 1} \sum_{i=1}^{n-3} \left| \theta_i - \theta_{i+3} \right| \qquad (1)$$

where: θ angle of orientation of the edge points

n is the total number of points

subscript *i* denoting the i[th] point on the edge of the particle.

3.2.2. Texture (or Micro-Texture) (*TX*)—Applies to coarse aggregate sizes only and describes the relative smoothness or roughness of surface features less than roughly 0.5 mm in size which are too small to affect the overall shape. Texture has a relative scale of 0 to 1000 with a smooth polished surface approaching a value of 0.

$$TX = \frac{1}{3N} \sum_{i=1}^{3} \sum_{j=1}^{N} \left(D_{i,j}(x, y) \right)^2 \qquad (2)$$

where:

D = decomposition function

n = decomposition level

N = total number of coefficients in an image

i = 1, 2,or 3 for detailed images

j = wavelet index

x,y = location of the coefficients in transformed domain

3.2.3. Sphericity (*SP*)—Applies to coarse aggregate sizes only and describes the overall three dimensional shape of a particle. Sphericity has a relative scale of 0 to 1. A sphericity value of one indicates a particle has equal dimensions (cubical).

$$SP = \sqrt[3]{\frac{d_S * d_I}{d_L^2}} \qquad (3)$$

where: d_S = particle shortest dimension

d_I = particle intermediate dimension

d_L = particle longest dimension

3.2.4. Form 2D—Applies to fine aggregate sizes only and is used to quantify the relative form from 2-dimensional images of aggregate particles. Form2D has a relative scale of 0 to 20. A perfect circle has a Form 2D value of zero.

$$Form\ 2D = \sum_{\theta=0}^{\theta=360-\Delta\theta} \left[\frac{R_{\theta+\Delta\theta} - R_\theta}{R_\theta} \right] \qquad (4)$$

where: R_θ is the radius of the particle at an angle of θ

Δθ is the incremental difference in the angle

3.2.5. Flat <u>and</u> Elongated—those particles having a ratio of longest dimension to shortest dimension greater than a specified value.

Aggregate particle dimensions in an x, y, z coordinate system

d_S = particle shortest dimension

d_I = particle intermediate

d_L = particle longest dimension

Flatness Ratio (*S/L*): $$Flatness = \frac{d_S}{d_I} \quad (5)$$

Elongation Ratio (*I/L*): $$Elongation = \frac{d_I}{d_L} \quad (6)$$

Flat and Elongated Value (F&E): $$L / S = \frac{d_L}{d_S} \quad (7)$$

3.2.6. Flat <u>or</u> Elongated—those particles having a ratio of intermediate dimension to shortest dimension or longest dimension to intermediate dimension greater than a specified value.

Flat or Elongated (ForE): $$\frac{d_I}{d_S} \text{ or } \frac{d_L}{d_I} > Ratio \quad \text{(i.e.: 1, 2, 3…)} \quad (8)$$

3.2.7. $\%Pass_x$ = % passing sieve x

3.2.8. $\%R_x$ = % retained on sieve x (passing sieve x+1)

4. SIGNIFICANCE AND USE

4.1. Shape, angularity, and surface texture of aggregates have been shown to directly affect the engineering properties of highway construction materials such as hot mix asphalt concrete, Portland cement concrete, and unbound aggregate layers. This standard is used to characterize the combined shape values for an aggregate source from the individual particle shape properties determined by digital image analysis from AASHTO Test Method xx-xx. The aggregate shape characterization includes Gradient Angularity, Form 2D, Sphericity, Texture, and Flat and Elongated value.

Note 1—The National Cooperative Highway Research Program Report 555 provides background information relevant to characterizing aggregate shape, texture and angularity.

4.2. This practice may be used to characterize the shape characteristics of single source aggregate materials and multiple source aggregate material blends.

5. PROCEDURE

5.1. Determine the aggregate sample grading according to AASHTO T27 and the amount finer than 75μm according to AASHTO T11.

5.2. Determine the aggregate sample specific gravities according to AASHTO T84 and T85.

5.3. Determine the material sample shape values for Form 2D, Gradient Angularity, Sphericity, Form Ratios (F&E, F or E), and Texture according to AASHTO TP XX.

6. CALCULATIONS – SINGLE SOURCE

6.1. The material sample is typically characterized by individual evaluation of material retained on each sieve size, passing the next larger sieve. For the purpose of calculating the combined shape values, consider any sizes that contain inadequate percent retained mass to achieve minimum particle count to have the same shape value as the average of the next larger or the next smaller size, whichever is present.

6.2. Calculate the Percent Retained for the aggregate sample on each sieve using the AASHTO T27 results.:

Sieve Sizes (x):

Coarse: 25.0mm(1”), 19.0mm(3/4”), 12.5mm(1/2”), 9.5mm(3/8”), 4.75mm(#4)

Fine: 2.36mm(#8), 1.18mm(#16), 0.60mm(#30), 0.30mm(#50), 0.15mm(#100), 0.075mm(#200)

Percent Passing: $\%Pass_x$ = % passing sieve x

Percent Retained: $\%R_x$ = % retained on sieve x

$$\% R_x = \% Pass_{x+1} - \% Pass_x \qquad (9)$$

6.3. Calculate average particle size, volume, and surface area for each sieve size x for unit mass.

For the purposes of shape characterization, volume and surface area of an average particle is estimated by using a cubical shape with side dimensions estimated by the average of the retained sieve and next larger sieve dimension.

Average Particle Size: $$D_x = \frac{(Sieve_x + Sieve_{x+1})}{2} \text{ (mm)} \qquad (10)$$

Average Particle Surface Area (cubical): $$PSA_x = 6 * D_x^2 \text{ (mm}^2\text{)} \qquad (11)$$

Average Particle Volume (cubical): $$V_x = D_x^3 \text{ (mm}^3\text{)} \qquad (12)$$

6.4. Calculate number of particles per sample unit mass for each sieve size from the size distribution of AASHTO T27 and the respective specific gravities from AASHTO T84 and T85.

Number of particles per sieve size: $$\# P_x = \frac{\% R_x * 1000}{G_{sb} * V_x} \qquad (13)$$

Note 2—A mass of 1 is assumed in *Eq* 13. This calculation determines the weighting factor applied to each sieve size for a material sample, therefore, actual mass is not required.

6.5. Calculate total particle surface area for each sieve size per sample unit mass.

Particle Surface Area (each sieve x) (mm^2): $$SSA_x = PSA_x * \# P_x \qquad (14)$$

6.6. Calculate Sample Surface Area (per unit mass):

Total Surface Area (mm^2): $$TSA = \sum_{x=0.075}^{25.0} SSA_x \qquad (15)$$

Coarse Surface Area (mm^2): $$CSA = \sum_{x=4.75}^{25.0} SSA_x \qquad (16)$$

Fine Surface Area (mm^2): $$FSA = \sum_{x=0.075}^{2.36} SSA_x \qquad (17)$$

6.7. Calculate Sample Particles Count (per unit mass):

Total Particles: $$\# TP = \sum_{x=0.075}^{25.0} \# P_x \qquad (18)$$

\# Coarse Particles: $$\# CP = \sum_{x=4.75}^{25.0} \# P_x \qquad (19)$$

\# Fine Particles: $$\# FP = \sum_{x=0.075}^{2.36} \# P_x \qquad (20)$$

6.8. Calculate Sample Gradient Angularity (weighted by surface area):

Fine Gradient Angularity: $$FGA = \frac{1}{FSA} \sum_{x=0.075}^{2.36} \left[SA_x * GA_x \right] \qquad (21)$$

Coarse Gradient Angularity: $$CGA = \frac{1}{CSA} \sum_{x=4.75}^{25.0} \left[SA_x * GA_x \right] \qquad (22)$$

Overall Gradient Angularity: $$GA = \frac{1}{TSA} \sum_{x=0.075}^{25.0} \left[SA_x * GA_x \right] \qquad (23)$$

6.9. Calculate Sample Fine Aggregate Form 2D (weighted by surface area):

$$Form\ 2D = \frac{1}{FSA} \sum_{x=0.075}^{2.36} \left[SA_x * 2D_x \right] \qquad (24)$$

6.10. Calculate Sample Coarse Aggregate Texture (weighted by surface area):

$$TX = \frac{1}{CSA} \sum_{x=4.75}^{25.0} \left[SA_x * TX_x \right] \qquad (25)$$

6.11. Calculate Sample Coarse Aggregate Sphericity (weighted by particle count):

$$SP = \frac{1}{\# CP} \sum_{x=4.75}^{25.0} \left[\# P_x * SP_x \right] \qquad (26)$$

6.12. Calculate Sample Sphericity Range Distribution (weighted by particle count):

% of Particles with Sphericity ≤ 0.3 :

$$SP(0.3) = \frac{1}{\# CP} \sum_{x=4.75}^{25.0} \left[\# P_x * SP(0.3)_x \right] \qquad (27)$$

% of Particles with Sphericity 0.3 < SP ≤ 0.7 :

$$SP(0.7) = \frac{1}{\# CP} \sum_{x=4.75}^{25.0} \left[\# P_x * SP(0.7)_x \right] \qquad (28)$$

% of Particles with Sphericity 0.7 < SP ≤ 1.0 :

This is a proposed procedure and has not yet been approved

$$SP(1.0) = \frac{1}{\#CP} \sum_{x=4.75}^{25.0} \left[P_x * SP(1.0)_x \right] \qquad (29)$$

6.13. Calculate sample weighted percentages of coarse aggregate Flat and Elongated Values (weighted by mass fraction) at the following ratios: ≥1:1, >2:1, >3:1, >4:1, >5:1

$$\% \, d_L/d_S \geq 1: \quad \% L/S(\geq 1) = \sum_{x=4.75}^{25.0} \left[\frac{\% R_x * \% L/S(\geq 1)_x}{100} \right] \qquad (30)$$

$$\% \, d_L/d_S > 2: \quad \% L/S(> 2) = \sum_{x=4.75}^{25.0} \left[\frac{\% R_x * \% L/S(> 2)_x}{100} \right] \qquad (31)$$

$$\% \, d_L/d_S > 3: \quad \% L/S(> 3) = \sum_{x=4.75}^{25.0} \left[\frac{\% R_x * \% L/S(> 3)_x}{100} \right] \qquad (32)$$

$$\% \, d_L/d_S > 4: \quad \% L/S(> 4) = \sum_{x=4.75}^{25.0} \left[\frac{\% R_x * \% L/S(> 4)_x}{100} \right] \qquad (33)$$

$$\% \, d_L/d_S > 5: \quad \% L/S(> 5) = \sum_{x=4.75}^{25.0} \left[\frac{\% R_x * \% L/S(> 5)_x}{100} \right] \qquad (34)$$

6.13.1. Calculate the sample weighted percentages of Coarse Aggregate Flat <u>or</u> Elongated (weighted by mass fraction) at the following ratios: ≥1:1, >2:1, >3:1, >4:1, >5:1

$$\% \, d_I/d_S \text{ or } d_L/d_I \geq 1: \quad \% ForE(\geq 1) = \sum_{x=4.75}^{25.0} \left[\frac{\% R_x * \% ForE(\geq 1)_x}{100} \right] \qquad (35)$$

$$\% \, d_I/d_S \text{ or } d_L/d_I > 2: \quad \% ForE(> 2) = \sum_{x=4.75}^{25.0} \left[\frac{\% R_x * \% ForE(> 2)_x}{100} \right] \qquad (36)$$

$$\% \, d_I/d_S \text{ or } d_L/d_I > 3: \quad \% ForE(> 3) = \sum_{x=4.75}^{25.0} \left[\frac{\% R_x * \% ForE(> 3)_x}{100} \right] \qquad (37)$$

$$\% \, d_I/d_S \text{ or } d_L/d_I > 4: \quad \% ForE(> 4) = \sum_{x=4.75}^{25.0} \left[\frac{\% R_x * \% ForE(> 4)_x}{100} \right] \qquad (38)$$

$$\% \, d_I/d_S \text{ or } d_L/d_I > 5: \quad \% ForE(> 5) = \sum_{x=4.75}^{25.0} \left[\frac{\% R_x * \% ForE(> 5)_x}{100} \right] \qquad (39)$$

7. CALCULATIONS – MULTIPLE SOURCE BLEND

7.1. Use the calculations in this section to estimate the shape characteristics of multiple material source blends. Each source must be sampled and characterized according to Section 6 calculations.

7.2. Determine Blend Composition Percentages

$\%AS_n$ = Percent Aggregate Source n

$$\sum_{i=1}^{n} \% AS_i = 100 \qquad (40)$$

where: n = # of aggregate sources

7.3. Calculate Blend Surface Area

Blend Total Surface Area (each sieve):

()

$$SSA_{Blend\_x} = \sum_{i=1}^{n} \sum_{x=0.075}^{37.5} \left[\frac{\% AS_i * SSA_{ix}}{100} \right]$$

where: x= 0.075 to 25.0 mm

n= # of aggregate sources

Total Surface Area Blend (all sieves x = 0.075 to 25.0 mm)

$$TSA_{Blend} = \sum_{x=0.075}^{25.0} SSA_{Blend\_x} \qquad (41)$$

Coarse Surface Area Blend (sieve x = 4.75 to 25.0):

$$CSA_{Blend} = \sum_{x=4.75}^{25.0} SSA_{Blend\_x} \qquad (42)$$

Fine Surface Area Blend (sieve x =0.075 to 2.36):

$$FSA_{Blend} = \sum_{x=0.075}^{2.36} SSA_{Blend\_x} \qquad (43)$$

7.4. Calculate number of particles per blend unit mass for each sieve size:

$$\# P_{Blend\_x} = \sum_{i=1}^{n} \sum_{x=0.075}^{25.0} \left[\frac{\% AS_i * \# P_{ix}}{100} \right] \qquad (44)$$

7.5. Calculate number of particles per blend unit mass

Total Particle Count Blend:

$$\# TP_{Blend} = \sum_{x=0.075}^{25.0} \# P_{Blend\_x} \qquad (45)$$

Coarse Particles Blend:

$$\# CP_{Blend} = \sum_{x=4.75}^{25.0} \# P_{Blend\_x} \qquad (46)$$

Fine Particles Blend:

$$\# FP_{Blend} = \sum_{x=0.075}^{2.36} \# P_{Blend\_x} \qquad (47)$$

7.6. Calculate Blend Gradient Angularity for each size x = 0.075 to 25.0 mm and combined (weighted by surface area):

$$GA_{Blend\_x} = \frac{1}{SSA_{Blend\_x}} \left[\sum_{i=1}^{i} \left[\frac{\% AS_i * SSA_{ix} * GA_{ix}}{100} \right] \right] \qquad (48)$$

Blend Fine Gradient Angularity:

$$FGA_{Blend} = \frac{1}{FSA_{Blend}} \left[\sum_{x=0.075}^{2.36} SSA_{Blend\_x} * GA_{Blend\_x} \right] \qquad (49$$

Blend Coarse Gradient Angularity:

$$CGA_{Blend} = \frac{1}{CSA_{Blend}} \left[\sum_{x=4.75}^{25.0} \left(SSA_{Blend\_x} * GA_{Blend\_x} \right) \right] \quad (50)$$

Blend Overall Gradient Angularity:

$$GA_{Blend} = \frac{1}{TSA_{Blend}} \left[\sum_{x=0.075}^{25.0} \left(SSA_{Blend\_x} * GA_{Blend\_x} \right) \right] \quad (51)$$

7.7. Calculate Blend Fine Aggregate Form 2D for each size x = 0.075 to 2.36 mm and combined (weighted by surface area):

$$Form\ 2D_{Blend\_x} = \frac{1}{SSA_{Blend\_x}} \left[\sum_{i=1}^{n} \left[\frac{\%\ AS_i * SSA_{ix} * 2D_{ix}}{100} \right] \right] \quad (52)$$

Blend Form 2D:

$$Form\ 2D_{Blend} = \frac{1}{FSA_{Blend}} \left[\sum_{x=0.075}^{2.36} \left(SSA_{Blend\_x} * 2D_{Blend\_x} \right) \right] \quad (53)$$

7.8. Calculate Blend Texture for each size x = 4.75 to 25.0 mm and combined (weighted by coarse aggregate surface area):

$$TX_{Blend\_x} = \frac{1}{SSA_{Blend\_x}} \left[\sum_{i=1}^{n} \left[\frac{\%\ AS_i * SSA_{ix} * TX_{ix}}{100} \right] \right] \quad (54)$$

Blend Texture:

$$TX_{Blend} = \frac{1}{CSA_{Blend}} \left[\sum_{x=4.75}^{25.0} \left(SSA_{Blend\_x} * TX_{Blend\_x} \right) \right] \quad (55)$$

7.9. Calculate Average Blend Sphericity for each size 4.75 to 25.0 and blend (weighted by coarse particle count):

$$SP_{Blend\_x} = \frac{1}{\#\ P_{Blend\_x}} \left[\sum_{i=1}^{n} \left[\frac{\%\ AS_i *\#\ P_{ix} * SP_{ix}}{100} \right] \right] \quad (56)$$

Blend Sphericity:

$$SP_{Blend} = \frac{1}{\#\ CP_{Blend}} \left[\sum_{x=4.75}^{25.0} \left(\#\ P_{Blend\_x} * SP_{Blend\_x} \right) \right] \quad (57)$$

7.10. Calculate Blend Sphericity Distribution for each sieve 4.75 to 25.0 mm and blend (weighted by coarse particle count):

% of Particles with Sphericity ≤ 0.3 (Blend):

$$SP(0.3)_{Blend\_x} = \frac{1}{\#P_{Blend\_x}}\left[\sum_{i=1}^{n}\left[\frac{\%AS_i * \#P_{ix} * SP(0.3)_{ix}}{100}\right]\right] \tag{58}$$

$$SP(0.3)_{Blend} = \frac{1}{\#CP_{Blend}}\left[\sum_{x=4.75}^{25.0}\left(\#P_{Blend\_x} * SP(0.3)_{Blend\_x}\right)\right] \tag{59}$$

% of Particles with Sphericity 0.3 < SP ≤ 0.7 (Blend):

$$SP(0.7)_{Blend\_x} = \frac{1}{\#P_{Blend\_x}}\left[\sum_{i=1}^{n}\left[\frac{\%AS_i * \#P_{ix} * SP(0.7)_{ix}}{100}\right]\right] \tag{60}$$

$$SP(0.7)_{Blend} = \frac{1}{\#CP_{Blend}}\left[\sum_{x=4.75}^{25.0}\left(\#P_{Blend\_x} * SP(0.7)_{Blend\_x}\right)\right] \tag{61}$$

% of Particles with Sphericity 0.7 < SP ≤ 1.0 (Blend):

$$SP(1.0)_{Blend\_x} = \frac{1}{\#P_{Blend\_x}}\left[\sum_{i=1}^{n}\left[\frac{\%AS_i * \#P_{ix} * SP(1.0)_{ix}}{100}\right]\right] \tag{62}$$

$$SP(1.0)_{Blend} = \frac{1}{\#CP_{Blend}}\left[\sum_{x=4.75}^{25.0}\left(\#P_{Blend\_x} * SP(1.0)_{Blend\_x}\right)\right] \tag{63}$$

7.11. Calculate combined Flat and Elongated Values for each sieve 4.75 to 25.0 mm and blend (weighted by mass fraction):

% $d_L/d_S \geq 1$ (Blend):

$$\%L/S(\geq 1)_{Blend\_x} = \left[\sum_{i=1}^{n}\left[\frac{\%AS_i * \%R_{ix} * \%L/S(\geq 1)_{ix}}{100^2}\right]\right] \tag{64}$$

$$\%L/S(\geq 1)_{Blend} = \left[\sum_{x=4.75}^{25.0}\left(\%L/S(\geq 1)_{Blend\_x}\right)\right] \tag{65}$$

% $d_L/d_S > 2$ (Blend):

$$\%L/S(> 2)_{Blend\_x} = \left[\sum_{i=1}^{n}\left[\frac{\%AS_i * \%R_{ix} * \%L/S(> 2)_{ix}}{100^2}\right]\right] \tag{66}$$

$$\%L/S(> 2)_{Blend} = \left[\sum_{x=4.75}^{25.0}\left(\%L/S(> 2)_{Blend\_x}\right)\right] \tag{67}$$

% $d_L/d_S > 3$ (Blend):

$$\%L/S(> 3)_{Blend\_x} = \left[\sum_{i=1}^{n}\left[\frac{\%AS_i * \%R_{ix} * \%L/S(> 3)_{ix}}{100^2}\right]\right] \tag{68}$$

$$\%L/S(> 3)_{Blend} = \left[\sum_{x=4.75}^{25.0}\left(\%L/S(> 3)_{Blend\_x}\right)\right] \tag{69}$$

% d_L/d_S > 4 (Blend):

$$\%L/S(>4)_{Blend\_x} = \left[\sum_{i=1}^{n}\left[\frac{\%AS_i * \%R_{ix} * \%L/S(>4)_{ix}}{100^2}\right]\right] \quad (70)$$

$$\%L/S(>4)_{Blend} = \left[\sum_{x=4.75}^{25.0} \%L/S(>4)_{Blend\_x}\right] \quad (71)$$

% $d_L/d_S \leq 5$ (Blend):

$$\%L/S(>5)_{Blend\_x} = \left[\sum_{i=1}^{n}\left[\frac{\%AS_i * \%R_{ix} * \%L/S(>5)_{ix}}{100^2}\right]\right] \quad (72)$$

$$\%L/S(>5)_{Blend} = \left[\sum_{x=4.75}^{37.5} \%L/S(>5)_{Blend\_x}\right] \quad (73)$$

7.12. Calculate Flat <u>or</u> Elongated Values for each sieve 4.75 to 25.0 mm and blend (weighted by mass fraction):

% d_I/d_S <u>or</u> $d_L/d_I \geq 1$: (Blend):

$$\%ForE(\geq 1)_{Blend\_x} = \left[\sum_{i=1}^{n}\left[\frac{\%AS_i * \%R_{ix} * \%ForE(\geq 1)_{ix}}{100^2}\right]\right] \quad (74)$$

$$\%ForE(\geq 1)_{Blend} = \left[\sum_{x=4.75}^{25.0} \%ForE(\geq 1)_{Blend\_x}\right] \quad (75)$$

% d_I/d_S <u>or</u> $d_L/d_I > 2$: (Blend):

$$\%ForE(>2)_{Blend\_x} = \left[\sum_{i=1}^{n}\left[\frac{\%AS_i * \%R_{ix} * \%ForE(>2)_{ix}}{100^2}\right]\right] \quad (76)$$

$$\%ForE(>2)_{Blend} = \left[\sum_{x=4.75}^{25.0} \%ForE(>2)_{Blend\_x}\right] \quad (77)$$

% d_I/d_S <u>or</u> $d_L/d_I > 3$: (Blend):

$$\%ForE(>3)_{Blend\_x} = \left[\sum_{i=1}^{n}\left[\frac{\%AS_i * \%R_{ix} * \%ForE(>3)_{ix}}{100^2}\right]\right] \quad (78)$$

$$\%ForE(>3)_{Blend} = \left[\sum_{x=4.75}^{25.0} \%ForE(>3)_{Blend\_x}\right] \quad (79)$$

% d_I/d_S <u>or</u> $d_L/d_I > 4$: (Blend):

$$\%ForE(>4)_{Blend\_x} = \left[\sum_{i=1}^{i}\left[\frac{\%AS_i * \%R_{ix} * \%ForE(>4)_{ix}}{100^2}\right]\right] \quad (80)$$

$$\% ForE\ (>4)_{Blend} = \left[\sum_{x=4.75}^{25.0} \% ForE\ (>4)_{Blend\_x}\right] \tag{81}$$

% d_I/d_S <u>or</u> $d_L/d_I > 5$: (Blend):

$$\% ForE\ (>5)_{Blend\_x} = \left[\sum_{i=1}^{n}\left[\frac{\% AS_i * \% R_{ix} * \% ForE\ (>5)_{ix}}{100^2}\right]\right] \tag{82}$$

$$\% ForE\ (>5)_{Blend} = \left[\sum_{x=4.75}^{25.0} \% ForE\ (>5)_{Blend\_x}\right] \tag{83}$$

8. REPORT

8.1. Report the following information:
A sample report format is presented in Appendix X1

8.1.1. Project name

8.1.2. Date of the analysis

8.1.3. Material sample identifications: type, source, size, gradation.

8.1.4. Number of particles analyzed for each size.

8.1.5. Material shape property mean and standard deviation. Graphical representations of the property distributions may be included.

9. PRECISION AND BIAS

9.1. *Precision*—This practice uses data generated from other testing methods to develop cumulative information, therefore the precision of the values generated in this practice are established by the precision of the standards used to collect the raw data.

9.2. *Bias*—Since there is no accepted reference device suitable for determining the bias in this method, no statement of bias is made.

10. KEYWORDS

10.1. aggregate; angularity; consensus property, shape, texture, form, elongation

Appendix X1: Sample Report

Stockpile Information

Date:	2/5/09
Project:	41_Granite_1
Technician:	mjg
Workbook Name:	41_Granite1_AIMS_Stockpile_v3.6.xlsm
Description:	

Gsb(Coarse)= 2.500

Gsb (Fine)= 2.500

	Include	Estimate	Nominal Sieve 25 Size	% Passing	% Retained
		☐	37.5 (1.5")	100.0%	0.0%
Coarse	☑	☐	25.0 (1.0")	93.0%	7.0%
	☑	☐	19.0 (3/4")	85.0%	8.0%
	☑	☐	12.5 (1/2")	70.0%	15.0%
	☑	☐	9.5 (3/8")	55.0%	15.0%
	☑	☐	4.75 (#4)	35.0%	20.0%
Fine	☑	☐	2.36 (#8)	25.0%	10.0%
	☑	☐	1.18 (#16)	15.0%	10.0%
	☑	☐	0.60 (#30)	10.0%	5.0%
	☑	☐	0.30 (#50)	5.0%	5.0%
	☑	☐	0.15 (#100)	0.0%	5.0%
	☑	☐	0.075 (#200)	0.0%	0.0%
			Passing #200	0.0%	0.0%

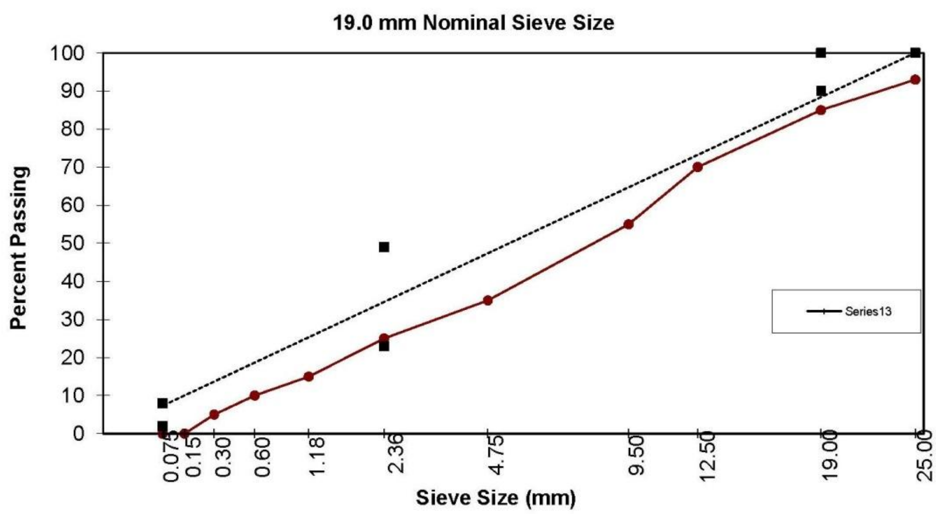

AIMS Stockpile Summary

Project Name:	41_Granite_1	Date:	2/5/09
Workbook:	41_Granite1_AIMS_Stockpile_v3.6.xlsm	Technician:	mjg
Description:			

Combined Properties (weighted)

2D Form (Fine)	7.95	Sphericity (Coarse)	%	Flat & Elongated Ratio (Coarse)	%	Flat or Elongated Ratio (Coarse)	Cum.%
Angularity (Coarse & Fine)	3457.5	Low (≤ 0.3)	0.0%	L/S ≥ 1:1	65.0%	F or E ≥ 1:1	65.0%
Fine Angularity	3501.3	Medium (0.3 - 0.7)	44.3%	L/S > 2:1	48.0%	F or E > 1:2	25.7%
Coarse Angularity	3039.7	High (0.7 - 1.0)	20.7%	L/S > 3:1	23.3%	F or E > 1:3	4.8%
				L/S > 4:1	7.3%	F or E > 1:4	0.8%
Texture (Coarse)	387.6	Sphericity (Coarse)	0.67	L/S > 5:1	2.0%	F or E > 1:5	0.8%

Form2D

Size	Particles in Range	Average	Standard Deviation	Low (≤ 6) #	%	(≤ 6) Cum. %	Medium (6 - 12) #	%	(≤ 12) Cum. %	High (12 - 20) #	%	(≤ 20) Cum. %	Out of Range #
2.36 (#8)	151	7.7	1.9	33	21.9%	21.9%	113	74.8%	96.7%	5	3.3%	100.0%	0
1.18 (#16)	150	7.5	1.8	32	21.3%	21.3%	116	77.3%	98.7%	2	1.3%	100.0%	0
0.60 (#30)	150	8.0	2.1	26	17.3%	17.3%	119	79.3%	96.7%	5	3.3%	100.0%	0
0.30 (#50)	151	8.0	2.2	28	18.5%	18.5%	115	76.2%	94.7%	8	5.3%	100.0%	0
0.15 (#100)	151	8.1	2.0	17	11.3%	11.3%	128	84.8%	96.0%	6	4.0%	100.0%	0
0.075 (#200)	146	8.9	2.8	19	13.0%	13.0%	104	71.2%	84.2%	23	15.8%	100.0%	5

Angularity

Size	Particles in Range	Average	Standard Deviation	Low (≤ 3300) #	%	(≤ 3300) Cum. %	Medium(3300-6600) #	%	(≤ 6600) Cum. %	High(6600-10000) #	%	(≤ 10000) Cum. %	Out of Range #
37.5 (1.5")													
25.0 (1.0")	50	2873.0	493.1	37	74.0%	74.0%	13	26.0%	100.0%	0	0.0%	100.0%	0
19.0 (3/4")	50	2841.5	639.0	41	82.0%	82.0%	9	18.0%	100.0%	0	0.0%	100.0%	0
12.5 (1/2")	50	3138.7	597.3	28	56.0%	56.0%	22	44.0%	100.0%	0	0.0%	100.0%	0
9.5 (3/8")	50	3251.6	694.5	27	54.0%	54.0%	23	46.0%	100.0%	0	0.0%	100.0%	0
4.75 (#4)	50	2963.7	590.8	37	74.0%	74.0%	13	26.0%	100.0%	0	0.0%	100.0%	0
2.36 (#8)	151	3454.8	918.6	71	47.0%	47.0%	79	52.3%	99.3%	1	0.7%	100.0%	0
1.18 (#16)	150	3288.5	802.0	81	54.0%	54.0%	69	46.0%	100.0%	0	0.0%	100.0%	0
0.60 (#30)	150	3642.0	949.7	58	38.7%	38.7%	90	60.0%	98.7%	2	1.3%	100.0%	0
0.30 (#50)	151	3650.0	984.1	62	41.1%	41.1%	89	58.9%	100.0%	0	0.0%	100.0%	0
0.150 (#100)	151	3451.5	1060.6	83	55.0%	55.0%	66	43.7%	98.7%	2	1.3%	100.0%	0
0.075 (#200)	151	2595.7	1241.4	126	83.4%	83.4%	24	15.9%	99.3%	1	0.7%	100.0%	0

AIMS Stockpile Summary

Project Name:	41_Granite_1	Date:	2/5/09
Workbook:	41_Granite1_AIMS_Stockpile_v3.6.xlsm	Technician:	mjg
Description:			

Texture

	Particles	Average	Standard	Low (≤ 260)		(≤ 260)	Medium (260 - 550)		(≤ 550)	High (550 - 1000)		(≤ 1000)	Out of Range
Size	in Range		Deviation	#	%	Cum. %	#	%	Cum. %	#	%	Cum. %	#
37.5 (1.5")													
25.0 (1.0")	50	461.0	84.8	0	0.0%	0.0%	45	90.0%	90.0%	5	10.0%	100.0%	0
19.0 (3/4")	50	480.4	90.5	1	2.0%	2.0%	39	78.0%	80.0%	10	20.0%	100.0%	0
12.5 (1/2")	50	455.5	119.8	1	2.0%	2.0%	41	82.0%	84.0%	8	16.0%	100.0%	0
9.5 (3/8")	50	430.5	128.8	5	10.0%	10.0%	38	76.0%	86.0%	7	14.0%	100.0%	0
4.75 (#4)	50	342.5	135.2	13	26.0%	26.0%	33	66.0%	92.0%	4	8.0%	100.0%	0

Sphericity

	Particles	Average	Standard	Low (≤ 0.3)		(≤ 0.3)	Medium (0.3 - 0.7)		(≤ 0.7)	High (0.7 - 1.0)		(≤ 1.0)	Out of Range
Size	in Range		Deviation	#	%	Cum. %	#	%	Cum. %	#	%	Cum. %	#
37.5 (1.5")													
25.0 (1.0")	49	0.68	0.08	0	0.0%	0.0%	30	61.2%	61.2%	19	38.8%	100.0%	1
19.0 (3/4")	49	0.62	0.09	0	0.0%	0.0%	39	79.6%	79.6%	10	20.4%	100.0%	1
12.5 (1/2")	49	0.62	0.09	0	0.0%	0.0%	37	75.5%	75.5%	12	24.5%	100.0%	1
9.5 (3/8")	50	0.61	0.10	0	0.0%	0.0%	37	74.0%	74.0%	13	26.0%	100.0%	0
4.75 (#4)	50	0.67	0.12	0	0.0%	0.0%	28	56.0%	56.0%	22	44.0%	100.0%	0

Flat and Elongated Distribution

	Particles	L/S ≥ 1:1		L/S > 2:1		L/S > 3:1		L/S > 4:1		L/S > 5:1		Out of Range
Size	in Range	#	%	#	%	#	%	#	%	#	%	#
37.5 (1.5")												
25.0 (1.0")	49	49	100.0%	33	67.3%	9	18.4%	1	2.0%	0	0.0%	1
19.0 (3/4")	49	49	100.0%	42	85.7%	20	40.8%	5	10.2%	1	2.0%	1
12.5 (1/2")	49	49	100.0%	43	87.8%	21	42.9%	6	12.2%	1	2.0%	1
9.5 (3/8")	50	50	100.0%	39	78.0%	25	50.0%	7	14.0%	1	2.0%	0
4.75 (#4)	50	50	100.0%	29	58.0%	12	24.0%	6	12.0%	3	6.0%	0

Flat or Elongated Distribution

	Particles	F or E ≥ 1:1		F or E >2:1		F or E >3:1		F or E >4:1		F or E >5:1		Out of Range
Size	in Range	#	%	#	%	#	%	#	%	#	%	#
37.5 (1.5")												
25.0 (1.0")	49	49	100.0%	12	24.5%	2	4.1%	0	0.0%	0	0.0%	1
19.0 (3/4")	49	49	100.0%	23	46.9%	4	8.2%	0	0.0%	0	0.0%	1
12.5 (1/2")	49	49	100.0%	23	46.9%	4	8.2%	0	0.0%	0	0.0%	1
9.5 (3/8")	50	50	100.0%	24	48.0%	2	4.0%	0	0.0%	0	0.0%	0
4.75 (#4)	50	50	100.0%	15	30.0%	5	10.0%	2	4.0%	2	4.0%	0

AIMS Angularity

Project Name:	41_Granite_1	Date:	2/5/09
Workbook:	41_Granite1_AIMS_Stockpile_v3.6.xlsm	Technician:	mjg
Description:			

Particles in Range	1154
Average	3274.7
Std. Deviation	995.6
Median	3170.6
Mode	3330.1

	#	%		Cum. %
Low (≤ 3300)	651	56.4%	(≤ 3300)	56.4%
Medium (3300 - 6600)	497	43.1%	(≤ 6600)	99.5%
High (6600 - 10000)	6	0.5%	(≤ 10000)	100.0%
Out of Range	0			

	#	%
$-\sigma < n < \sigma$	814	70.5%
$-2\sigma < n < 2\sigma$	1105	95.8%
$-3\sigma < n < 3\sigma$	1144	99.1%
$n < -3\sigma$ or $n > 3\sigma$	10	0.9%

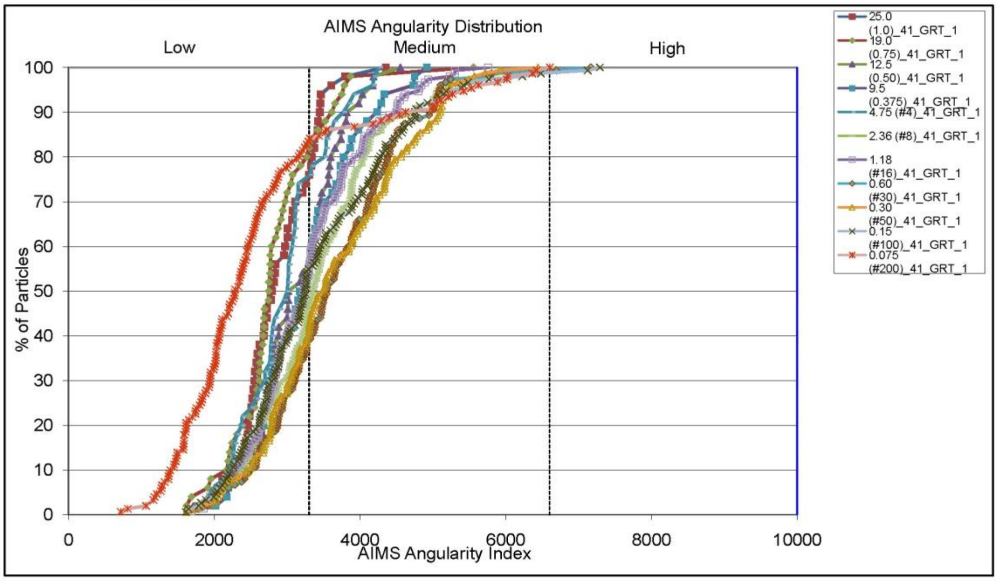

APPENDIX C

ILS DATA

Table C-1. Angularity Results of Gravel for ILS Analysis

Gravel		Angularity										
Laboratory	Scan #	25.0 (1.0")	19.0 (3/4")	12.5 (1/2")	9.5 (3/8")	4.75 (#4)	2.36 (#8)	1.18 (#16)	0.6 (#30)	0.3 (#50)	0.15 (#100)	0.075 (#200)
1	1	1794.4	2778.9	2620.1	2743.5	2122.4	2462.7	3135.1	3218.7	3014.1	2633.3	2121.6
	2	1770.1	2717.2	2784.8	2650.4	2120.8	2668.3	3130.6	3348.8	2855.4	2899.1	2046.7
2	1	1755.8	2705.0	2751.5	2647.5	2197.2	2594.2	3075.8	3266.9	3275.2	2879.5	2226.9
	2	1788.7	2644.3	2801.8	2611.4	2213.7	2726.8	3024.3	3400.4	3148.2	2825.1	2242.0
3	1	1604.0	2857.6	2740.1	2641.4	2129.6	2731.6	3057.2	3284.1	3127.2	2725.6	2362.0
	2	1861.3	2597.3	2732.2	2559.4	2273.2	2614.9	3045.6	3276.4	3127.0	2657.7	2260.0
4	1	1856.4	2499.3	2918.8	2674.2	2215.2	2770.0	2987.0	3226.6	3186.9	2705.4	2432.6
	2	1742.3	2751.0	2735.1	2607.5	2133.1	2737.0	3113.3	3261.8	3069.5	2539.3	2220.3
5	1	2090.9	2662.6	2897.1	2510.2	2462.3	2826.7	3193.4	3186.6	3125.1	2586.4	2291.3
	2	2004.6	2483.3	2867.7	2467.3	2386.1	2803.0	3300.4	3289.9	3026.6	2744.7	2554.9
6	1	2046.9	2599.0	2667.9	2461.5	2225.2	2876.3	3105.5	3168.8	3386.2	2943.0	2263.7
	2	1968.9	2585.9	2854.7	2457.8	2242.4	2611.1	3002.3	3348.8	3353.3	2807.7	2297.7
7	1	2013.4	2604.8	2897.9	2597.8	2275.7	2691.6	3033.9	3262.4	3211.0	2663.3	2347.2
	2	1987.2	2519.6	2845.9	2462.4	2293.5	2700.7	3093.4	3013.2	2912.0	2841.4	2417.4
8	1	2000.8	2598.1	2912.8	2409.9	2321.5	2763.2	3046.2	3273.5	3181.2	2817.1	2504.8
	2	1941.3	2552.4	2912.8	2530.6	2243.0	2642.5	3071.0	3058.3	3337.2	2964.3	2505.9
9	1	1782.4	2635.9	2901.0	2418.9	2036.7	2668.9	3058.6	3269.0	2956.8	2670.4	2164.6
	2	1869.0	2738.9	3079.1	2410.4	1951.8	2662.1	3093.1	3239.1	3036.5	2650.2	2742.0
10	1	1817.0	2599.3	2895.2	2710.6	2173.3	2549.7	3104.7	3350.7	3231.6	2705.6	2374.6
	2	1868.3	2551.9	2870.4	2401.7	2074.9	2713.4	3015.4	3358.2	3173.1	2835.6	2002.8
11	1	1890.2	2543.2	2795.7	2520.4	2027.5	2648.5	3040.8	3228.4	3248.0	2135.6	1639.6
	2	1916.1	2564.0	2806.3	2468.5	2179.8	2572.5	3212.3	3293.3	3233.9	2598.1	2031.3
12	1	1875.2	2580.9	2828.5	2568.4	2034.1	2481.5	2971.3	3208.7	3164.6	2825.1	2268.1

	2	1823.3	2526.0	2875.6	2606.7	2090.6	2670.9	3085.8	3256.4	3335.4	2878.6	2360.2
13	1	1924.2	2392.0	2806.2	2376.3	2203.2	2594.5	3078.0	3306.1	3341.1	2633.9	2596.8
	2	1747.9	2495.4	2971.7	2445.6	2417.9	2735.7	3070.3	3330.2	3275.6	2639.9	2045.4
14	1	1905.6	2416.4	2623.1	2503.0	2382.7	2614.4	3091.6	3190.0	3181.8	2835.6	2257.2
	2	1899.6	2443.4	2813.2	2476.9	2382.1	2679.7	3197.1	3350.3	3120.2	2943.3	2196.2
15	1	1962.3	2625.0	2729.9	2468.8	2254.3	2735.5	3108.5	3296.9	3401.1	2855.4	1970.8
	2	1979.0	2781.0	2710.9	2427.4	2289.8	2647.6	3086.1	3267.2	3349.1	2819.6	2405.2
16	1	1880.5	2847.1	2617.1	2322.1	2279.4	2724.4	3024.6	3116.6	3240.7	2689.8	2229.6
	2	1912.2	2818.4	2589.8	2376.1	2224.2	2627.6	3001.0	3181.4	3393.9	2649.8	2381.1
17	1	1936.3	2735.9	2580.7	2351.5	2259.5	2519.7	3050.1	3166.9	3226.6	2938.8	2523.0
	2	1888.8	2818.5	2537.7	2495.3	2291.5	2594.0	3145.2	3236.4	3150.8	2650.8	2584.0
18	1	1979.3	2666.9	2583.5	2395.0	2299.7	2557.0	3070.4	3214.5	3375.0	2671.9	1960.2
	2	2193.3	2868.0	2707.0	2360.0	2415.6	2763.2	3152.9	3209.2	3225.1	2720.2	2007.3
19	1	2048.8	2421.1	2908.7	2528.8	2489.5	2601.8	3153.2	3253.0	3149.4	2602.4	1966.4
	2	1952.4	2511.6	2834.8	2455.0	2513.6	2739.0	3190.9	3309.5	3001.7	2597.4	2293.1
20	1	2014.1	2505.9	2763.4	2466.0	2399.7	2709.4	3157.9	3258.5	3131.9	2594.0	2177.6
	2	2043.2	2384.2	2835.9	2487.2	2370.4	2627.5	3124.2	3415.5	3260.8	2625.0	2162.5
21	1	1951.3	2359.2	2868.9	2446.9	2421.4	2758.8	3093.7	3304.1	3243.9	2817.0	2168.3
	2	2013.1	2491.9	2816.9	2388.4	2548.2	2673.4	3165.4	3277.0	3266.8	2766.2	2565.0
22	1	1900.3	2651.8	2887.1	2938.1	2179.0	2711.2	2891.2	3182.0	3355.2	2861.0	2309.2
	2	1904.7	2598.7	2872.2	2834.4	2347.6	2495.1	3081.0	3167.0	3294.7	2896.6	2195.5
23	1	1844.7	2519.8	2885.9	2700.7	2258.5	2587.7	3148.7	3363.2	3189.8	2588.3	2008.9
	2	1899.9	2593.6	2752.4	2858.0	2346.3	2384.4	3086.0	3231.5	2996.1	2446.6	1826.1
24	1	1871.7	2667.2	2741.1	2706.0	2312.7	2831.8	2962.5	3277.3	3326.2	2678.1	2451.2
	2	1933.2	2399.3	2782.4	2774.6	2211.6	2761.5	2974.4	3272.3	3257.2	2772.4	2427.6
25	1	1953.1	2603.1	2766.3	2728.2	2371.7	2631.4	2995.7	3119.7	3347.4	2967.4	2209.8
	2	1920.6	2605.1	2826.4	2775.6	2210.1	2621.1	3006.0	3114.1	3211.9	2703.6	2230.8

26	1	1632.7	2711.4	2666.2	2819.7	2241.4	2650.9	2977.1	3155.1	3152.4	2798.8	2299.4
	2	1675.8	2692.9	2709.4	2703.2	2242.5	2688.1	3113.0	3035.3	2801.5	2521.3	2084.7
27	1	1788.0	2718.8	2594.1	2831.0	2225.5	2546.1	3084.8	3323.3	2949.9	2308.5	1719.3
	2	1848.6	2680.5	2575.5	2757.6	2182.7	2638.8	3053.5	2953.7	3014.8	2329.6	1717.6
28	1	1751.1	2779.1	2501.0	2630.2	2268.6	2602.4	2974.9	3304.6	2739.9	2726.1	2151.7
	2	1740.1	2586.6	2743.5	2701.0	2351.0	2714.5	3033.9	3139.0	3173.5	2701.2	2341.3
29	1	1993.0	2547.3	2791.7	2523.3	2388.7	2757.9	3003.0	3120.1	3290.6	3012.8	2253.2
	2	1985.0	2496.5	2731.5	2475.4	2299.2	2786.8	3082.8	3220.7	3256.8	2907.6	2269.3

Table C-2. Angularity Results of Limestone for ILS Analysis

Limestone		Angularity										
Laboratory	Scan #	25.0 (1.0")	19.0 (3/4")	12.5 (1/2")	9.5 (3/8")	4.75 (#4)	2.36 (#8)	1.18 (#16)	0.6 (#30)	0.3 (#50)	0.15 (#100)	0.075 (#200)
1	1	2749.0	2826.6	2802.1	2625.7	2786.4	3356.8	3271.3	3198.1	2905.3	2226.3	2451.3
	2	2802.5	2837.1	2803.7	2695.9	2777.1	3336.6	3263.0	3230.1	2888.6	2146.8	1952.0
2	1	2718.0	2817.4	2968.7	2687.6	2712.8	2917.3	3031.4	3147.8	2927.4	2313.0	2697.2
	2	2861.8	2849.4	2879.3	2596.5	2717.5	2881.7	2884.6	2974.2	2856.4	2417.6	3057.0
3	1	2718.5	2741.6	2762.8	2621.3	2723.6	2949.1	2985.2	2972.5	2893.8	2268.5	3192.5
	2	2781.1	2775.4	2801.1	2567.5	2536.1	2848.9	2930.6	2893.3	2925.9	2469.4	3381.3
4	1	2823.5	2766.0	2793.8	2611.3	2740.2	2855.1	2969.7	3158.7	2969.9	2350.6	2177.6
	2	2824.2	2795.4	2782.4	2592.9	2623.9	2791.7	2928.2	3005.8	2866.1	2358.1	3113.3
5	1	2665.5	2741.6	2702.9	2835.6	2763.5	2874.6	2930.7	3202.9	2947.9	2462.2	4138.6
	2	2748.9	2797.1	2691.7	2667.3	2725.3	2998.1	3108.5	3234.0	3302.8	2412.6	3391.5
6	1	2828.5	2815.8	2727.9	2761.8	2732.5	2747.2	3060.7	2942.4	3011.4	2566.1	2780.3
	2	2707.6	2772.5	2675.9	2669.7	2608.7	2906.7	2894.8	2972.4	2942.5	2439.0	3086.9
7	1	2736.7	2824.9	2637.5	2720.7	2759.0	2878.9	3019.6	3016.5	2959.6	2680.4	3178.9
	2	2718.6	2722.9	2573.1	2670.6	2740.6	3017.1	2936.3	3002.7	2929.3	2948.5	2544.5
8	1	2659.6	2767.8	2804.1	2835.3	2557.6	2847.6	3164.8	2874.8	2664.6	2419.7	3121.5
	2	2638.0	2874.4	2888.2	2835.5	2729.9	2977.8	3034.6	2884.2	2966.3	2500.2	3629.0
9	1	2829.7	2765.6	2538.4	2672.0	2656.8	2922.9	3033.7	3085.1	2789.8	2468.4	3536.3
	2	2813.8	2719.1	2583.5	2718.5	2705.7	2942.4	3007.4	3093.3	2678.1	2338.6	3447.9
10	1	2735.5	2786.3	2644.4	2650.5	2712.1	2923.1	2902.1	3023.1	2851.0	2348.4	2674.7
	2	2761.7	2651.5	2699.7	2785.5	2751.3	2990.8	2910.0	2982.3	2946.8	2420.9	2199.1
11	1	2829.2	2753.4	2685.4	2609.0	2798.1	2898.5	2977.1	2975.3	2981.3	2106.0	3090.4
	2	2838.3	2820.0	2642.8	2742.8	2722.9	2893.2	2917.6	3125.2	3055.7	2482.7	3193.8
12	1	2800.1	2750.8	2640.4	2672.6	2780.3	2794.4	2921.0	3013.0	2931.5	2464.4	2785.2

	2	2748.3	2758.6	2633.3	2680.9	2787.4	3037.3	3004.3	3005.8	3023.0	2536.1	3187.7
13	1	2743.5	2626.3	2728.8	2786.7	2823.2	2900.3	2960.5	3174.7	2953.7	2652.2	2485.8
	2	2825.1	2635.2	2714.8	2686.8	2859.6	3029.8	2917.7	2991.5	2910.3	1759.9	1584.7
14	1	2836.7	2650.2	2670.4	2867.1	2738.9	2862.0	2920.7	2943.4	3046.0	2584.9	2860.7
	2	2767.0	2703.5	2731.9	2659.1	2721.9	3052.4	2987.8	3011.1	2985.0	2637.8	3261.4
15	1	2740.8	2811.3	2805.2	2807.9	2792.2	2938.9	3042.6	2878.2	3007.3	2563.6	2908.2
	2	2525.0	2847.7	2825.4	2672.8	2726.1	2897.3	2958.3	2984.7	2951.7	2430.9	3106.1
16	1	2749.5	2724.9	2722.7	2657.0	2774.8	2895.4	2912.4	2988.7	3046.8	2422.0	2632.4
	2	2628.0	2848.4	2659.6	2787.2	2624.7	2859.7	2936.4	2967.2	2862.6	2371.1	2861.1
17	1	2656.2	2802.8	2788.1	2730.3	2718.0	3065.4	2868.2	2987.8	3030.1	2571.0	3865.4
	2	2702.2	2840.9	2682.0	2691.1	2788.9	2996.3	2970.1	2982.8	2920.1	2679.2	3594.3
18	1	2719.4	3058.2	2521.8	2796.8	2768.6	2809.6	2793.7	3031.4	2769.2	2190.5	2220.2
	2	2799.7	2760.9	2782.2	2729.9	2684.9	2930.0	2897.3	3121.4	2850.6	2232.9	2222.4
19	1	2652.0	2499.2	2726.5	2674.7	2724.6	2742.2	2837.7	3074.0	2974.7	2275.9	2932.0
	2	2776.3	2725.6	2632.4	2590.7	2667.6	2859.3	2887.6	3056.4	2937.3	2200.0	2337.6
20	1	2709.3	2629.3	2719.1	2727.5	2738.9	2947.4	2979.5	3049.2	2968.5	2205.3	2238.8
	2	2745.2	2658.1	2644.6	2772.9	2642.1	2848.3	2972.7	2975.0	2740.7	2360.3	1873.5
21	1	2828.8	2559.8	2772.2	2629.7	2672.0	2931.0	2911.9	2919.7	3017.2	2528.6	2895.5
	2	2697.9	2700.1	2698.7	2790.5	2605.9	2874.5	2967.9	3008.3	3062.5	2446.5	2552.5
22	1	2669.1	2683.9	2616.9	2766.1	2522.2	2935.9	2877.8	2937.8	2505.8	2382.5	1752.1
	2	2820.9	2659.1	2746.9	2847.2	2734.6	2891.6	2940.1	2886.1	2851.6	2288.4	3002.5
23	1	2692.7	2821.0	2565.3	2697.7	2670.9	2893.9	2899.4	2942.2	3036.0	2046.4	2026.8
	2	2602.3	2727.1	2707.7	2595.0	2676.8	2969.2	2923.2	3075.5	2888.6	2101.5	1861.6
24	1	2646.2	2707.5	2690.7	2765.3	2807.7	2943.9	2961.7	2920.3	3130.9	2462.9	3144.0
	2	2763.1	2799.4	2576.1	2738.9	2718.3	2948.9	2912.6	2939.3	3034.1	2614.0	3048.4
25	1	2686.2	2732.2	2647.1	2865.8	2643.8	2795.0	2879.3	2916.6	2896.7	2346.2	2945.6
	2	2702.9	2812.7	2753.4	2744.2	2608.5	2941.6	2851.6	2984.7	2755.5	2638.9	3349.7

26	1	2587.0	2768.3	2649.1	2653.5	2617.0	2981.3	2742.3	2869.0	2959.7	2180.8	1932.0
	2	2623.7	2687.2	2630.7	2694.7	2528.7	2945.5	2862.5	2942.9	2884.8	2475.5	1888.8
27	1	2678.0	2637.6	2596.5	2662.0	2627.8	2886.7	2727.4	2852.0	2519.0	1984.0	1782.6
	2	2672.0	2815.7	2770.1	2664.2	2580.4	2889.5	2887.8	2912.2	2596.0	2148.1	2221.4
28	1	2662.9	2685.1	2577.0	2633.7	2608.5	2896.5	2920.3	2922.8	2799.1	2424.2	3212.9
	2	2675.4	2609.9	2563.4	2738.9	2642.7	2957.2	2840.1	3024.1	2914.6	2359.2	2785.2
29	1	2750.0	2630.8	2779.0	2665.8	2828.8	2964.4	2966.7	3012.2	3039.3	2490.2	3064.0
	2	2707.9	2697.8	2673.5	2607.3	2728.3	3002.3	3018.0	3087.2	2982.8	2641.3	2625.5

Table C-3. Angularity Results of Granite for ILS Analysis

Granite		Angularity										
Laboratory	Scan #	25.0 (1.0")	19.0 (3/4")	12.5 (1/2")	9.5 (3/8")	4.75 (#4)	2.36 (#8)	1.18 (#16)	0.6 (#30)	0.3 (#50)	0.15 (#100)	0.075 (#200)
1	1	2740.5	2823.7	3343.8	3301.6	3261.3	3288.7	3432.4	3396.6	3215.6	3068.5	2266.4
	2	2751.9	2889.6	3191.3	3225.9	3106.5	3391.0	3335.6	3457.5	3375.7	3017.6	2677.1
2	1	2815.5	2913.1	3270.8	3228.2	3086.6	3367.7	3370.2	3488.5	3404.7	2975.0	2525.3
	2	2728.3	3000.4	3322.3	3245.4	3114.2	3429.3	3409.1	3427.1	3371.0	3276.9	2366.3
3	1	2848.5	2914.9	3143.1	3283.8	3127.0	3281.1	3468.5	3402.2	3278.9	3103.6	3127.0
	2	2772.8	2943.2	3229.9	3249.8	3170.7	3332.2	3379.4	3401.7	3245.5	3227.9	2908.6
4	1	2720.5	2933.0	3322.6	3427.0	3183.9	3300.0	3394.1	3588.0	3409.2	3077.2	2666.4
	2	2791.0	2975.4	3286.6	3380.0	3115.9	3274.8	3408.3	3537.9	3432.5	3098.0	3174.9
5	1	2984.5	3308.7	3231.7	3194.4	3066.0	3284.1	3358.5	3965.3	4090.7	3668.5	3323.1
	2	2917.6	2996.5	3136.2	3368.6	3030.6	3361.9	3438.4	3754.3	4087.0	3224.4	3467.2
6	1	2982.2	2995.5	3140.3	3123.7	3137.8	3285.0	3465.7	3335.8	3208.5	3214.2	3338.9
	2	3021.1	3015.8	3183.4	3130.2	3004.5	3297.3	3508.0	3365.0	3235.2	3256.3	2694.6
7	1	2851.2	2996.4	3080.5	3120.8	2928.7	3422.9	3409.2	3320.9	3252.2	3144.9	2836.4
	2	2958.8	2962.4	3048.1	3100.5	3019.0	3263.4	3570.3	3304.5	3287.2	3425.5	3550.4
8	1	2867.4	2935.9	3139.3	3245.1	2982.8	3449.4	3396.8	3329.3	3170.0	3141.1	2776.9
	2	2871.5	2967.9	3154.3	3504.7	3053.0	3368.3	3455.6	3298.4	3165.9	3189.3	3337.8
9	1	2892.1	2890.2	3067.9	3203.9	3100.3	3389.9	3325.9	3525.9	3686.5	3367.5	3017.5
	2	2860.4	3019.0	3142.4	3163.8	3058.9	3331.0	3334.7	3503.7	3551.9	3127.5	3173.6
10	1	2832.1	2926.0	3192.6	3150.6	3183.0	3275.8	3444.1	3443.1	3368.0	3102.6	2942.8
	2	2849.7	2876.2	2983.1	3049.1	3121.2	3189.1	3307.2	3371.3	3512.9	3102.6	2870.5
11	1	2930.0	2955.5	3148.0	3162.9	3006.1	3410.5	3379.4	3397.7	3642.6	3039.1	3065.9
	2	2988.7	2889.7	3134.7	3114.0	3147.8	3289.0	3436.3	3541.3	3477.6	2898.8	2283.0
12	1	2968.9	2912.9	3124.2	3014.8	3184.6	3249.5	3356.5	3437.9	3397.7	2650.2	2474.1

	2	2931.7	2978.8	3105.3	3012.7	3158.3	3253.7	3296.3	3512.9	3329.7	2042.7	1285.7
13	1	2885.2	2901.2	3181.9	3269.6	3063.7	3320.3	3415.7	3443.1	3681.5	3158.3	2453.0
	2	2900.8	2926.0	3201.2	3257.7	3120.1	3300.9	3379.0	3526.4	3604.2	3072.0	3297.1
14	1	3014.1	2927.9	3118.7	3244.5	3138.2	3367.3	3472.8	3392.4	3458.3	3295.6	3470.3
	2	2873.1	2870.2	3112.4	3242.6	3136.5	3251.1	3325.9	3430.1	3490.6	3450.7	3101.6
15	1	2973.0	3087.7	3121.6	3166.8	2937.5	3477.7	3473.9	3498.6	3371.9	2958.1	3059.0
	2	2913.7	3025.9	3202.3	3229.6	2903.9	3247.2	3230.1	3611.8	3436.9	2802.6	2752.8
16	1	2928.3	2965.0	3051.7	3217.7	2753.9	3339.6	3557.1	3372.7	3403.9	3403.2	2797.7
	2	2851.1	3055.2	3063.8	3360.1	2960.3	3328.1	3386.5	3344.5	3332.3	3108.3	2305.5
17	1	3026.0	2924.6	3018.9	3295.3	2921.2	3229.9	3331.3	3074.4	3332.1	3324.0	2763.3
	2	2865.4	2983.8	3085.6	3250.4	2968.5	3327.8	3512.6	3527.6	3402.2	3454.1	2794.4
18	1	2869.0	3017.8	3055.1	3207.0	3037.2	3231.5	3446.9	3539.1	3359.1	2929.9	2464.5
	2	2851.8	2970.1	3190.2	3224.8	2918.9	3367.7	3243.8	3356.8	2967.0	2993.8	2378.7
19	1	2935.3	2968.9	3049.5	3111.3	3086.4	3352.0	3409.0	3484.9	3363.0	3195.6	2478.7
	2	3007.4	3014.2	2995.8	3281.8	2904.5	3271.4	3344.9	3430.7	3468.8	3240.2	2949.3
20	1	3019.2	2934.4	2962.6	3088.5	3024.8	3325.4	3341.0	3426.0	3395.5	3052.6	2454.8
	2	2864.9	2854.1	2973.5	3107.6	2963.8	3335.3	3386.0	3507.6	3340.9	3011.2	2548.1
21	1	2973.2	2958.6	3035.5	3116.8	3045.1	3504.3	3277.0	3427.0	3298.3	3289.0	2750.1
	2	2921.6	2995.7	3009.0	3234.2	3122.5	3365.4	3478.7	3356.5	3424.8	3265.6	2807.0
22	1	2962.2	3171.9	3027.1	2967.1	3054.1	3325.6	3307.2	3319.9	3252.2	3108.3	2244.3
	2	3030.4	2891.8	2974.8	3096.1	3140.9	3298.3	3433.7	3317.2	3205.0	3171.1	3082.8
23	1	2989.9	3142.9	3056.5	3106.9	3126.0	3381.6	3392.9	3486.1	3437.6	3310.4	2665.6
	2	2969.7	3080.6	3091.4	3182.7	3171.0	3439.6	3351.7	3470.7	3458.1	3147.8	2717.6
24	1	2950.2	3035.3	3022.6	3198.4	3078.3	3402.5	3428.9	3278.2	4017.5	3349.4	3122.4
	2	2990.5	3115.7	3105.4	3165.9	3128.9	3322.0	3286.6	3474.8	3962.3	3384.2	3440.4
25	1	2863.2	3108.2	3010.2	3110.3	2904.8	3307.6	3111.8	3240.6	3178.6	3328.5	3221.7
	2	3030.5	2926.4	3108.9	3169.4	3240.6	3166.9	3256.8	3393.8	3144.7	3148.7	2328.3

26	1	2853.0	3183.3	3173.5	3222.8	2933.3	3406.7	3298.4	3343.6	3242.5	2965.0	2298.2
	2	2873.9	3146.3	3067.2	3188.2	3123.7	3292.4	3269.1	3324.6	3250.4	2896.2	3197.8
27	1	2825.9	2968.3	3092.5	3105.5	3028.4	3312.3	3356.8	3049.8	3459.6	2673.1	1957.8
	2	2857.1	3105.7	3048.6	3126.3	2951.8	3315.3	3312.7	3357.1	3763.5	2775.3	1850.1
28	1	2828.9	3048.9	3062.4	3067.8	2975.0	3396.2	3235.0	3260.2	3734.5	3109.7	2967.8
	2	2874.1	3143.8	3055.9	3139.8	3120.1	3324.1	3171.9	3442.2	3896.9	3360.5	3090.9
29	1	2873.0	2841.5	3138.7	3251.6	2963.7	3454.8	3288.5	3642.0	3650.0	3451.5	2595.7
	2	2957.1	2870.0	3238.3	3211.8	3079.6	3331.1	3446.2	3319.6	3310.6	3345.5	2663.9

Table C-4. Texture and Sphericity Results of Gravel for ILS Analysis

Gravel		Texture						Sphericity				
Laboratory	Scan #	25.0 (1.0")	19.0 (3/4")	12.5 (1/2")	9.5 (3/8")	4.75 (#4)		25.0 (1.0")	19.0 (3/4")	12.5 (1/2")	9.5 (3/8")	4.75 (#4)
1	1	205.9	269.9	209.3	236.8	201.3		0.76	0.72	0.69	0.68	0.71
	2	207.2	266.7	218.6	226.4	219.9		0.77	0.71	0.69	0.68	0.71
2	1	201.0	252.9	226.1	244.3	197.9		0.75	0.71	0.69	0.70	0.70
	2	221.0	240.3	220.5	237.8	222.5		0.76	0.71	0.69	0.68	0.72
3	1	210.9	239.2	235.7	242.7	189.3		0.76	0.71	0.69	0.69	0.72
	2	215.4	264.1	242.6	215.0	202.4		0.75	0.71	0.69	0.68	0.70
4	1	221.1	229.5	243.5	234.9	198.6		0.74	0.72	0.68	0.68	0.69
	2	230.7	227.9	206.8	236.7	214.4		0.77	0.71	0.69	0.69	0.70
5	1	196.6	264.1	245.3	204.5	153.2		0.74	0.75	0.68	0.67	0.66
	2	195.2	284.3	202.6	209.6	168.2		0.74	0.73	0.69	0.68	0.65
6	1	211.7	275.5	219.8	218.7	155.5		0.74	0.75	0.68	0.67	0.66
	2	211.2	295.7	220.4	231.8	171.1		0.74	0.73	0.67	0.68	0.67
7	1	207.7	256.5	227.8	218.4	169.8		0.72	0.75	0.68	0.69	0.68
	2	203.8	265.5	221.8	219.2	152.8		0.75	0.74	0.68	0.68	0.68
8	1	208.8	272.3	230.4	222.2	180.6		0.75	0.75	0.67	0.67	0.67
	2	215.2	284.7	217.0	218.2	163.0		0.74	0.74	0.67	0.68	0.68
9	1	232.9	248.4	236.8	257.9	176.6		0.76	0.70	0.69	0.68	0.72
	2	231.6	209.4	243.2	226.9	166.1		0.76	0.69	0.71	0.70	0.70
10	1	249.4	226.7	232.7	241.0	171.4		0.75	0.70	0.71	0.71	0.70
	2	235.6	259.8	223.7	222.9	155.1		0.76	0.71	0.70	0.69	0.71
11	1	213.3	226.2	229.8	241.6	174.6		0.75	0.70	0.69	0.69	0.70
	2	224.4	224.2	236.5	239.5	164.8		0.76	0.69	0.71	0.70	0.73
12	1	225.8	199.2	222.3	235.9	150.8		0.75	0.70	0.71	0.70	0.71

	2	219.9	230.5	216.3	203.9	151.9		0.76	0.70	0.71	0.69	0.70
13	1	219.7	248.0	200.2	233.2	209.0		0.73	0.73	0.69	0.67	0.75
	2	230.9	260.2	216.5	209.8	191.8		0.73	0.73	0.69	0.67	0.73
14	1	224.6	255.7	224.4	200.1	177.0		0.74	0.73	0.69	0.68	0.71
	2	235.1	227.6	233.6	204.9	180.8		0.75	0.72	0.68	0.69	0.72
15	1	220.8	275.8	236.5	249.9	183.5		0.71	0.74	0.69	0.68	0.68
	2	210.2	271.9	233.4	214.5	182.9		0.72	0.73	0.68	0.68	0.69
16	1	229.1	246.0	243.5	231.6	165.3		0.71	0.73	0.68	0.67	0.67
	2	227.1	265.7	243.3	233.9	180.4		0.71	0.75	0.69	0.66	0.68
17	1	241.9	250.1	229.4	229.3	170.3		0.71	0.74	0.69	0.65	0.70
	2	213.7	243.8	232.0	215.0	162.2		0.72	0.73	0.67	0.66	0.68
18	1	202.1	277.6	221.1	223.0	160.6		0.73	0.74	0.68	0.67	0.68
	2	209.1	247.1	232.8	225.5	130.6		0.72	0.75	0.68	0.67	0.68
19	1	223.4	249.8	257.6	211.3	182.4		0.73	0.74	0.71	0.69	0.69
	2	236.3	277.2	235.8	201.7	183.8		0.74	0.75	0.71	0.69	0.68
20	1	231.4	257.3	229.0	200.8	197.4		0.74	0.73	0.71	0.68	0.69
	2	241.2	258.5	219.6	212.6	190.0		0.72	0.74	0.72	0.69	0.69
21	1	217.8	227.5	257.0	196.3	189.0		0.72	0.74	0.72	0.69	0.68
	2	221.9	257.1	262.7	198.6	185.6		0.71	0.73	0.70	0.69	0.68
22	1	238.3	246.6	244.7	262.6	200.9		0.75	0.72	0.68	0.68	0.69
	2	236.4	254.8	273.4	257.2	189.6		0.76	0.73	0.68	0.68	0.70
23	1	251.0	222.5	234.6	262.4	185.6		0.75	0.70	0.68	0.67	0.70
	2	243.7	255.5	271.5	264.7	218.1		0.75	0.71	0.68	0.68	0.69
24	1	250.2	245.8	235.7	244.2	198.5		0.76	0.72	0.69	0.68	0.69
	2	256.1	236.4	238.2	252.8	199.6		0.76	0.73	0.68	0.68	0.70
25	1	227.6	235.0	274.7	240.6	196.3		0.78	0.73	0.69	0.69	0.73
	2	258.5	234.4	253.3	227.0	195.2		0.78	0.73	0.69	0.67	0.71

26	1	235.7	231.0	242.5	251.9	169.8		0.76	0.71	0.69	0.66	0.70
	2	215.0	265.1	241.1	218.8	187.6		0.75	0.71	0.71	0.68	0.71
27	1	235.9	228.3	243.8	220.3	194.7		0.76	0.72	0.70	0.66	0.73
	2	250.9	251.5	234.8	236.4	177.3		0.73	0.72	0.71	0.67	0.72
28	1	230.3	232.1	243.8	236.9	179.9		0.75	0.71	0.70	0.67	0.68
	2	217.2	255.3	220.7	251.1	175.9		0.75	0.73	0.70	0.67	0.70
29	1	233.6	242.1	211.8	182.1	189.5		0.75	0.72	0.69	0.67	0.72
	2	217.3	240.8	247.0	209.7	186.4		0.75	0.73	0.70	0.68	0.73

Table C-5. Texture and Sphericity Results of Limestone for ILS Analysis

Limestone		Texture						Sphericity				
Laboratory	Scan #	25.0 (1.0")	19.0 (3/4")	12.5 (1/2")	9.5 (3/8")	4.75 (#4)		25.0 (1.0")	19.0 (3/4")	12.5 (1/2")	9.5 (3/8")	4.75 (#4)
1	1	300.0	278.5	267.2	221.7	132.4		0.72	0.66	0.68	0.69	0.65
	2	321.2	261.8	260.6	206.4	131.3		0.72	0.68	0.66	0.68	0.65
2	1	275.7	250.1	262.6	207.7	121.0		0.73	0.67	0.67	0.69	0.67
	2	280.3	268.2	252.3	228.4	121.0		0.71	0.66	0.66	0.69	0.68
3	1	297.9	254.0	262.8	221.8	131.6		0.72	0.66	0.68	0.70	0.68
	2	282.9	256.6	277.3	224.2	131.2		0.72	0.66	0.68	0.68	0.67
4	1	277.9	286.3	263.7	216.0	123.8		0.72	0.66	0.65	0.69	0.65
	2	249.6	247.9	270.8	205.8	129.8		0.72	0.66	0.67	0.69	0.64
5	1	279.6	280.3	272.2	244.6	157.1		0.72	0.67	0.65	0.66	0.68
	2	271.0	280.5	273.9	235.9	148.8		0.72	0.69	0.67	0.67	0.66
6	1	293.5	279.8	261.9	242.2	158.1		0.73	0.70	0.67	0.67	0.65
	2	256.6	283.7	265.6	242.9	155.6		0.72	0.70	0.67	0.68	0.65
7	1	274.1	261.6	253.8	244.4	149.4		0.72	0.70	0.66	0.67	0.66
	2	292.5	265.6	266.3	256.4	140.3		0.72	0.70	0.66	0.68	0.67
8	1	282.3	285.9	300.5	241.3	136.9		0.73	0.69	0.65	0.67	0.65
	2	276.5	268.9	268.5	253.9	136.2		0.73	0.70	0.66	0.67	0.65
9	1	258.7	278.5	243.9	216.4	139.1		0.73	0.68	0.67	0.71	0.65
	2	254.6	293.9	249.0	221.3	148.4		0.72	0.67	0.68	0.70	0.65
10	1	265.6	272.9	239.8	211.6	140.1		0.74	0.68	0.68	0.70	0.64
	2	247.4	280.9	261.5	208.6	123.4		0.72	0.68	0.67	0.71	0.64
11	1	279.7	293.5	257.2	236.4	126.3		0.73	0.69	0.67	0.70	0.67
	2	266.6	283.0	255.1	217.2	132.2		0.73	0.69	0.67	0.70	0.65
12	1	253.0	265.7	246.2	207.7	132.2		0.72	0.69	0.67	0.70	0.66

	2	245.9	258.3	236.7	216.3	132.9		0.73	0.68	0.67	0.70	0.64
13	1	249.7	241.4	278.8	230.8	128.8		0.71	0.68	0.69	0.69	0.67
	2	258.1	236.3	263.5	230.9	137.5		0.71	0.69	0.68	0.69	0.67
14	1	256.8	249.1	252.3	224.0	128.8		0.71	0.70	0.69	0.69	0.67
	2	245.2	250.5	259.7	232.3	124.7		0.71	0.68	0.69	0.69	0.68
15	1	281.7	283.8	265.5	212.9	137.9		0.70	0.65	0.69	0.69	0.66
	2	294.1	275.9	274.5	209.2	126.6		0.70	0.66	0.68	0.68	0.65
16	1	292.5	283.1	260.5	221.0	134.0		0.70	0.65	0.67	0.67	0.64
	2	279.6	277.3	239.2	222.8	134.6		0.69	0.65	0.69	0.68	0.65
17	1	312.2	282.9	255.5	220.8	122.8		0.69	0.66	0.68	0.67	0.65
	2	292.8	295.0	258.2	214.4	126.5		0.69	0.66	0.68	0.69	0.66
18	1	272.7	262.4	233.5	212.5	131.9		0.69	0.67	0.65	0.68	0.67
	2	264.6	268.5	223.2	203.1	131.0		0.70	0.66	0.67	0.69	0.65
19	1	301.9	280.0	274.2	206.3	168.9		0.70	0.71	0.69	0.65	0.66
	2	291.6	279.1	289.8	230.0	146.5		0.71	0.72	0.69	0.66	0.67
20	1	266.1	305.9	257.1	241.8	158.8		0.72	0.71	0.69	0.67	0.67
	2	264.1	292.3	246.3	219.9	156.2		0.71	0.71	0.68	0.66	0.66
21	1	263.4	254.2	265.0	230.6	149.5		0.69	0.70	0.68	0.69	0.67
	2	285.4	253.9	251.5	205.5	145.9		0.70	0.70	0.68	0.66	0.66
22	1	267.2	253.5	238.4	230.3	137.9		0.73	0.68	0.70	0.70	0.69
	2	293.6	260.2	262.7	241.1	130.4		0.73	0.67	0.69	0.70	0.68
23	1	283.6	259.0	229.0	219.7	134.4		0.72	0.66	0.69	0.68	0.68
	2	303.9	262.5	258.9	253.3	142.3		0.73	0.67	0.69	0.68	0.66
24	1	302.6	264.4	250.7	251.3	128.8		0.73	0.68	0.68	0.67	0.70
	2	277.0	267.1	255.2	235.6	131.6		0.75	0.68	0.69	0.68	0.68
25	1	270.9	255.4	245.4	237.9	139.1		0.76	0.69	0.70	0.67	0.69
	2	277.5	246.2	253.6	226.4	129.1		0.75	0.70	0.70	0.67	0.70

26	1	291.0	270.0	257.2	217.5	144.5		0.71	0.68	0.69	0.67	0.65
	2	282.5	273.6	239.0	221.2	139.9		0.70	0.68	0.70	0.67	0.67
27	1	279.8	278.2	237.4	228.0	138.8		0.71	0.68	0.70	0.69	0.71
	2	255.5	251.5	236.6	227.2	140.0		0.71	0.68	0.71	0.68	0.67
28	1	263.2	251.9	264.2	216.1	134.9		0.72	0.68	0.72	0.68	0.65
	2	283.5	273.7	260.4	226.7	140.6		0.71	0.70	0.69	0.68	0.64
29	1	244.0	243.7	267.1	222.2	124.4		0.73	0.69	0.68	0.68	0.67
	2	241.2	257.1	247.3	233.9	132.4		0.72	0.69	0.68	0.68	0.69

Table C-6. Texture and Sphericity Results of Granite for ILS Analysis

Granite		Texture						Sphericity				
Laboratory	Scan #	25.0 (1.0")	19.0 (3/4")	12.5 (1/2")	9.5 (3/8")	4.75 (#4)		25.0 (1.0")	19.0 (3/4")	12.5 (1/2")	9.5 (3/8")	4.75 (#4)
1	1	493.3	474.7	485.3	460.4	375.6		0.71	0.66	0.61	0.61	0.66
	2	484.7	457.9	456.5	444.9	350.3		0.71	0.65	0.62	0.59	0.66
2	1	470.5	456.2	470.7	439.3	354.8		0.70	0.65	0.63	0.61	0.68
	2	471.6	459.1	473.6	449.0	351.6		0.71	0.64	0.62	0.60	0.69
3	1	462.8	466.2	473.4	443.7	347.6		0.69	0.64	0.63	0.59	0.70
	2	465.3	452.0	473.4	446.5	356.8		0.70	0.64	0.61	0.60	0.66
4	1	477.7	446.5	443.8	458.7	335.8		0.69	0.65	0.61	0.60	0.66
	2	453.3	473.2	458.6	446.7	368.4		0.70	0.66	0.62	0.61	0.65
5	1	472.6	482.0	474.0	451.3	316.9		0.69	0.64	0.62	0.62	0.69
	2	475.9	477.9	508.7	437.5	338.4		0.70	0.65	0.62	0.61	0.68
6	1	482.2	506.4	490.2	460.9	340.1		0.69	0.66	0.62	0.63	0.68
	2	475.9	518.3	486.1	456.6	347.8		0.69	0.67	0.63	0.64	0.68
7	1	465.4	483.8	481.5	451.1	348.4		0.68	0.67	0.62	0.61	0.69
	2	469.4	476.1	496.6	460.2	351.1		0.69	0.68	0.62	0.63	0.69
8	1	460.3	507.5	476.7	470.4	327.8		0.68	0.66	0.61	0.61	0.65
	2	463.1	507.1	467.1	449.3	347.6		0.69	0.67	0.63	0.63	0.67
9	1	471.0	474.4	451.7	473.1	297.9		0.69	0.62	0.64	0.63	0.68
	2	449.9	474.7	454.1	442.1	341.3		0.68	0.63	0.63	0.64	0.67
10	1	439.4	488.2	460.6	458.9	302.0		0.69	0.62	0.63	0.63	0.67
	2	475.3	493.1	451.3	447.9	342.6		0.69	0.62	0.64	0.64	0.68
11	1	475.0	467.1	462.6	443.5	331.5		0.69	0.61	0.64	0.64	0.68
	2	480.2	491.7	463.0	436.4	327.7		0.70	0.62	0.64	0.63	0.68
12	1	454.2	483.8	448.9	452.0	320.4		0.69	0.61	0.62	0.64	0.70

	2	453.4	492.2	458.4	433.7	348.1		0.70	0.62	0.64	0.63	0.67
13	1	484.7	502.4	474.3	445.1	370.5		0.67	0.62	0.63	0.61	0.67
	2	479.2	488.6	454.6	440.3	346.8		0.66	0.63	0.63	0.61	0.69
14	1	468.0	494.7	457.4	441.9	350.0		0.67	0.61	0.63	0.63	0.68
	2	488.8	508.5	473.6	444.8	367.1		0.66	0.62	0.64	0.63	0.70
15	1	497.5	451.5	445.5	494.0	359.0		0.65	0.63	0.61	0.61	0.67
	2	484.1	471.3	439.8	468.4	350.7		0.65	0.63	0.59	0.60	0.65
16	1	471.5	448.1	440.9	497.6	348.2		0.64	0.63	0.60	0.61	0.66
	2	478.8	444.5	440.0	481.5	360.7		0.65	0.63	0.62	0.59	0.66
17	1	479.5	441.5	454.8	484.0	340.7		0.63	0.63	0.59	0.61	0.64
	2	491.4	455.6	433.0	490.6	337.8		0.64	0.64	0.60	0.60	0.67
18	1	505.9	456.4	442.0	474.5	331.3		0.66	0.65	0.60	0.61	0.67
	2	481.6	435.5	441.3	469.7	348.7		0.66	0.64	0.61	0.61	0.68
19	1	461.7	484.5	471.4	501.5	359.2		0.66	0.65	0.62	0.62	0.68
	2	475.0	474.8	458.7	499.5	362.0		0.66	0.65	0.62	0.64	0.68
20	1	456.1	488.3	495.8	471.4	367.3		0.66	0.63	0.61	0.62	0.68
	2	460.7	476.0	476.9	453.0	363.6		0.66	0.64	0.60	0.62	0.66
21	1	431.4	470.6	454.8	492.3	352.4		0.64	0.64	0.60	0.62	0.65
	2	443.2	464.9	461.9	468.6	355.4		0.65	0.63	0.61	0.62	0.67
22	1	477.0	480.1	460.9	476.6	345.1		0.67	0.65	0.63	0.64	0.69
	2	456.7	478.6	504.7	480.9	377.3		0.68	0.65	0.63	0.64	0.68
23	1	496.9	490.8	477.6	499.7	400.7		0.66	0.63	0.63	0.65	0.69
	2	481.6	484.3	490.7	509.5	384.6		0.66	0.62	0.62	0.64	0.69
24	1	487.9	472.0	500.6	519.6	374.2		0.68	0.64	0.63	0.62	0.69
	2	467.3	476.1	460.3	492.5	376.1		0.67	0.65	0.62	0.62	0.69
25	1	457.0	474.1	487.1	486.0	382.7		0.69	0.67	0.62	0.63	0.72
	2	443.6	477.5	495.1	480.7	380.6		0.69	0.67	0.63	0.64	0.71

26	1	472.5	480.8	479.2	460.2	331.7		0.67	0.62	0.61	0.61	0.67
	2	474.2	476.6	461.3	454.8	320.5		0.68	0.62	0.61	0.61	0.69
27	1	482.9	477.2	447.9	447.3	330.0		0.68	0.61	0.61	0.72	0.70
	2	469.0	470.0	432.0	454.8	319.9		0.69	0.61	0.62	0.62	0.71
28	1	493.6	487.5	451.9	447.6	305.7		0.69	0.63	0.63	0.61	0.67
	2	489.3	486.7	458.5	454.0	334.7		0.68	0.62	0.62	0.61	0.67
29	1	461.0	480.4	455.5	430.5	342.5		0.68	0.62	0.62	0.61	0.67
	2	469.9	475.8	425.1	436.1	375.2		0.68	0.62	0.62	0.62	0.68

Table C-7. Flat or Elongated 3:1and 2D Form Results of Gravel for ILS Analysis

Gravel		Flat or Elongated 3:1						2D Form					
Laboratory	Scan #	25.0 (1.0")	19.0 (3/4")	12.5 (1/2")	9.5 (3/8")	4.75 (#4)		2.36 (#8)	1.18 (#16)	0.6 (#30)	0.3 (#50)	0.15 (#100)	0.075 (#200)
1	1	100.0%	100.0%	100.0%	100.0%	95.8%		6.4	7.5	8.0	7.2	7.3	8.1
	2	100.0%	100.0%	95.9%	98.0%	95.8%		6.6	7.3	8.2	6.9	7.7	8.1
2	1	100.0%	100.0%	98.0%	100.0%	95.8%		6.7	7.5	7.9	7.6	7.5	8.4
	2	100.0%	100.0%	97.9%	100.0%	98.0%		6.7	7.3	8.0	7.5	7.5	8.2
3	1	100.0%	100.0%	100.0%	100.0%	100.0%		6.6	7.7	7.9	7.7	7.3	8.5
	2	100.0%	100.0%	98.0%	98.0%	95.7%		6.8	7.3	8.0	7.4	7.3	8.6
4	1	100.0%	100.0%	98.0%	95.9%	89.6%		6.8	7.5	7.8	7.6	7.7	9.0
	2	100.0%	100.0%	98.0%	100.0%	95.9%		6.8	7.4	7.7	7.5	7.3	8.2
5	1	100.0%	100.0%	100.0%	96.0%	91.7%		6.7	7.8	8.2	7.5	7.5	8.9
	2	100.0%	100.0%	100.0%	98.0%	91.7%		7.2	7.6	8.0	7.3	7.2	9.4
6	1	98.0%	100.0%	100.0%	96.0%	93.8%		6.9	7.5	7.8	7.6	7.7	8.2
	2	100.0%	100.0%	100.0%	96.0%	100.0%		6.6	7.4	7.9	7.8	7.4	8.3
7	1	100.0%	100.0%	100.0%	98.0%	95.8%		6.7	7.7	8.0	7.8	7.3	8.9
	2	100.0%	100.0%	100.0%	100.0%	100.0%		6.7	7.5	7.5	7.3	7.6	9.0
8	1	100.0%	100.0%	100.0%	98.0%	97.9%		6.9	7.4	8.0	7.3	7.2	8.4
	2	100.0%	100.0%	100.0%	96.0%	100.0%		6.6	7.7	7.5	8.0	7.6	8.6
9	1	100.0%	98.0%	100.0%	100.0%	97.9%		6.6	7.4	7.7	7.4	7.2	8.0
	2	100.0%	100.0%	100.0%	98.0%	98.0%		6.6	7.3	7.8	7.4	7.2	9.5
10	1	100.0%	100.0%	100.0%	100.0%	97.8%		6.6	7.4	7.8	7.8	7.6	9.0
	2	100.0%	100.0%	100.0%	98.0%	97.9%		6.8	7.2	8.0	7.6	7.7	8.6
11	1	100.0%	98.0%	100.0%	98.0%	91.1%		6.6	7.4	8.0	7.7	6.5	7.6
	2	100.0%	100.0%	100.0%	100.0%	97.9%		6.4	7.7	7.9	7.6	7.3	8.1
12	1	100.0%	100.0%	100.0%	100.0%	95.7%		6.4	7.3	7.6	7.7	7.6	8.2

	2	100.0%	100.0%	100.0%	98.0%	95.7%		6.8	7.7	7.9	8.0	7.8	8.3
13	1	100.0%	98.0%	100.0%	98.0%	100.0%		6.4	7.3	7.8	8.1	7.4	9.3
	2	98.0%	96.0%	100.0%	96.0%	95.8%		6.7	7.4	7.9	7.9	7.2	8.0
14	1	100.0%	100.0%	98.0%	98.0%	100.0%		6.9	7.3	7.5	7.5	7.5	7.8
	2	100.0%	98.0%	98.0%	100.0%	97.9%		6.5	7.6	8.0	7.3	7.5	8.3
15	1	94.0%	100.0%	95.9%	91.7%	89.6%		6.8	7.8	7.9	7.7	7.4	7.8
	2	98.0%	100.0%	95.9%	87.8%	93.6%		6.4	7.6	7.7	7.6	7.4	8.6
16	1	94.0%	100.0%	93.9%	88.0%	91.1%		6.9	7.3	7.9	7.4	7.6	8.6
	2	96.0%	100.0%	96.0%	84.0%	91.8%		6.8	7.3	7.8	7.9	7.3	8.6
17	1	94.0%	100.0%	96.0%	83.7%	91.8%		6.6	7.6	7.8	8.2	7.9	9.7
	2	95.9%	100.0%	96.0%	83.7%	91.8%		6.9	7.7	8.1	8.1	7.3	9.1
18	1	98.0%	100.0%	95.8%	81.6%	91.8%		6.6	7.6	7.7	8.0	7.7	7.9
	2	95.9%	100.0%	96.0%	95.9%	93.5%		7.0	7.5	7.8	7.6	7.3	8.1
19	1	100.0%	98.0%	100.0%	98.0%	100.0%		6.7	7.7	7.6	7.4	7.4	8.0
	2	100.0%	100.0%	98.0%	95.9%	100.0%		6.7	7.4	7.6	7.3	7.3	8.7
20	1	100.0%	100.0%	98.0%	98.0%	100.0%		6.8	7.4	8.1	7.5	7.4	8.6
	2	100.0%	100.0%	100.0%	98.0%	100.0%		6.6	7.5	7.8	7.9	7.2	8.7
21	1	100.0%	100.0%	100.0%	100.0%	100.0%		6.7	7.2	7.6	8.2	7.5	8.1
	2	100.0%	100.0%	96.0%	98.0%	100.0%		6.6	7.4	7.8	7.6	7.5	8.9
22	1	100.0%	100.0%	100.0%	98.0%	95.9%		6.7	7.4	7.7	7.8	7.9	8.2
	2	100.0%	98.0%	100.0%	93.9%	100.0%		6.5	7.2	8.1	7.5	7.9	8.3
23	1	100.0%	96.0%	100.0%	98.0%	98.0%		6.3	7.6	7.9	7.4	6.9	8.3
	2	100.0%	98.0%	100.0%	94.0%	95.8%		6.3	7.2	7.8	7.4	7.1	7.8
24	1	100.0%	96.0%	98.0%	92.0%	98.0%		6.9	7.1	7.9	7.6	7.3	8.9
	2	100.0%	98.0%	100.0%	94.0%	100.0%		6.8	7.2	7.7	7.9	7.5	8.8
25	1	100.0%	98.0%	100.0%	96.0%	100.0%		6.6	7.3	7.5	7.9	7.7	8.2
	2	100.0%	98.0%	100.0%	96.0%	100.0%		6.5	7.0	7.2	8.2	7.1	8.1

26	1	100.0%	100.0%	100.0%	93.9%	97.9%		6.7	7.2	7.7	7.6	7.5	8.3
	2	100.0%	95.9%	100.0%	95.9%	100.0%		6.7	7.5	7.7	7.4	7.9	8.8
27	1	100.0%	98.0%	98.0%	95.8%	100.0%		6.9	7.9	7.9	7.5	6.8	7.6
	2	100.0%	98.0%	100.0%	93.9%	100.0%		6.8	7.4	7.5	7.3	7.2	7.8
28	1	100.0%	98.0%	100.0%	95.9%	96.0%		6.7	7.5	7.8	7.3	7.5	8.8
	2	98.0%	100.0%	100.0%	96.0%	100.0%		6.9	7.2	7.4	7.6	7.5	9.1
29	1	100.0%	98.0%	100.0%	96.0%	98.0%		6.7	7.3	7.4	7.6	7.7	8.3
	2	100.0%	100.0%	100.0%	96.0%	98.0%		6.6	7.3	7.5	7.4	7.8	8.2

Table C-8. Flat or Elongated 3:1and 2D Form Results of Limestone for ILS Analysis

Limestone		Flat or Elongated 3:1					2D Form					
Laboratory	Scan #	25.0 (1.0")	19.0 (3/4")	12.5 (1/2")	9.5 (3/8")	4.75 (#4)	2.36 (#8)	1.18 (#16)	0.6 (#30)	0.3 (#50)	0.15 (#100)	0.075 (#200)
1	1	98.0%	100.0%	98.0%	100.0%	90.0%	7.7	8.1	7.8	7.3	6.8	8.3
	2	100.0%	100.0%	98.0%	100.0%	92.0%	7.8	7.7	7.7	7.3	6.9	7.4
2	1	98.0%	100.0%	98.0%	100.0%	94.0%	7.3	7.6	7.6	7.2	6.9	8.3
	2	98.0%	100.0%	98.0%	100.0%	96.0%	7.4	7.4	7.5	7.1	7.3	8.7
3	1	100.0%	100.0%	100.0%	100.0%	98.0%	7.4	7.3	7.4	7.2	6.8	9.2
	2	98.0%	100.0%	100.0%	100.0%	94.0%	7.2	7.3	7.2	7.4	7.2	9.5
4	1	100.0%	98.0%	98.0%	100.0%	90.0%	7.2	7.3	7.5	7.1	7.0	8.1
	2	98.0%	100.0%	100.0%	100.0%	88.0%	7.1	7.3	7.2	7.0	7.0	9.3
5	1	100.0%	100.0%	100.0%	100.0%	95.9%	7.3	7.4	8.3	7.8	7.3	9.5
	2	100.0%	100.0%	100.0%	96.0%	95.7%	7.8	7.9	8.0	8.0	6.9	9.5
6	1	100.0%	100.0%	100.0%	100.0%	92.0%	7.2	7.3	7.6	7.4	7.1	9.0
	2	100.0%	100.0%	98.0%	98.0%	98.0%	7.4	7.5	7.7	7.3	6.8	9.7
7	1	100.0%	100.0%	96.0%	100.0%	96.0%	7.2	7.5	7.4	7.2	7.3	9.2
	2	100.0%	100.0%	100.0%	100.0%	98.0%	7.4	7.5	7.6	6.9	7.5	8.2
8	1	100.0%	100.0%	100.0%	100.0%	94.0%	7.1	7.4	7.5	6.9	6.9	9.3
	2	100.0%	100.0%	100.0%	100.0%	94.0%	7.3	8.0	7.3	7.2	7.0	9.7
9	1	100.0%	100.0%	100.0%	98.0%	96.0%	7.5	7.6	7.2	7.2	6.9	9.4
	2	100.0%	100.0%	100.0%	98.0%	96.0%	7.5	7.6	7.5	7.1	7.0	9.3
10	1	100.0%	100.0%	100.0%	98.0%	92.0%	7.5	7.4	7.5	7.1	7.1	8.9
	2	100.0%	98.0%	100.0%	98.0%	91.8%	7.5	7.6	7.5	7.3	7.3	8.4
11	1	100.0%	100.0%	100.0%	100.0%	98.0%	7.1	7.5	7.3	7.5	6.5	9.0
	2	100.0%	100.0%	98.0%	98.0%	94.0%	7.3	7.4	7.6	7.3	7.0	9.2
12	1	100.0%	100.0%	98.0%	98.0%	96.0%	7.2	7.3	7.3	7.2	7.0	8.1

	2	100.0%	100.0%	100.0%	98.0%	94.0%		7.5	7.8	7.5	7.5	7.4	8.8
13	1	100.0%	100.0%	96.0%	98.0%	98.0%		7.3	7.5	7.5	7.3	7.5	8.3
	2	98.0%	98.0%	98.0%	98.0%	94.0%		7.7	7.2	7.3	7.3	6.6	8.0
14	1	100.0%	100.0%	98.0%	100.0%	96.0%		7.2	7.4	7.2	7.2	7.0	9.4
	2	100.0%	100.0%	98.0%	100.0%	98.0%		7.4	7.5	7.3	7.0	7.7	9.5
15	1	96.0%	98.0%	100.0%	98.0%	93.9%		7.1	7.4	7.1	7.3	7.2	8.9
	2	98.0%	100.0%	100.0%	92.0%	96.0%		7.3	7.5	7.3	7.2	7.4	9.2
16	1	100.0%	98.0%	98.0%	94.0%	86.0%		7.3	7.5	7.6	7.7	6.9	8.9
	2	96.0%	100.0%	100.0%	92.0%	92.0%		7.1	7.7	7.6	7.8	6.8	9.0
17	1	98.0%	100.0%	100.0%	92.0%	88.0%		7.7	7.5	7.3	7.0	7.0	9.8
	2	96.0%	100.0%	100.0%	94.0%	94.0%		7.3	7.6	7.5	7.7	7.4	9.4
18	1	98.0%	100.0%	96.0%	98.0%	98.0%		7.3	7.3	7.3	7.1	6.5	7.8
	2	100.0%	100.0%	100.0%	92.0%	90.0%		7.3	7.1	7.5	7.2	6.6	8.3
19	1	100.0%	100.0%	100.0%	98.0%	93.9%		6.8	6.9	7.6	7.2	7.0	9.3
	2	100.0%	100.0%	100.0%	96.0%	98.0%		7.1	7.3	7.3	6.9	6.8	8.9
20	1	100.0%	100.0%	100.0%	98.0%	93.9%		7.2	7.4	7.4	7.0	6.7	8.2
	2	100.0%	100.0%	100.0%	100.0%	96.0%		7.3	7.5	7.3	6.9	6.9	7.7
21	1	98.0%	100.0%	100.0%	98.0%	96.0%		7.3	7.4	7.5	7.6	7.0	8.9
	2	98.0%	98.0%	98.0%	98.0%	98.0%		7.1	7.7	7.5	7.3	7.2	8.6
22	1	100.0%	98.0%	100.0%	100.0%	100.0%		7.2	7.2	7.3	6.6	6.9	7.5
	2	100.0%	98.0%	100.0%	100.0%	96.0%		7.1	7.8	7.5	7.3	6.7	8.9
23	1	100.0%	98.0%	100.0%	94.0%	98.0%		7.2	7.3	7.2	7.2	6.3	8.6
	2	100.0%	100.0%	100.0%	96.0%	98.0%		7.4	7.3	7.6	7.3	6.5	8.1
24	1	100.0%	100.0%	100.0%	98.0%	98.0%		7.3	7.5	7.6	7.3	6.8	9.2
	2	100.0%	100.0%	100.0%	98.0%	98.0%		7.4	7.3	7.7	7.4	7.4	9.1
25	1	100.0%	100.0%	100.0%	100.0%	100.0%		7.5	7.7	7.3	7.0	7.0	8.5
	2	100.0%	100.0%	100.0%	97.9%	100.0%		7.2	7.2	7.3	7.1	7.1	9.6

26	1	98.0%	100.0%	95.9%	100.0%	94.0%		7.2	7.1	7.0	7.4	6.6	8.1
	2	98.0%	100.0%	98.0%	98.0%	98.0%		7.3	7.3	7.3	7.2	7.5	8.1
27	1	95.9%	100.0%	98.0%	98.0%	100.0%		6.9	7.0	7.0	6.6	6.6	7.9
	2	96.0%	100.0%	100.0%	100.0%	100.0%		7.1	7.4	7.4	6.7	7.0	8.5
28	1	98.0%	100.0%	100.0%	96.0%	98.0%		7.4	7.3	7.1	6.7	7.1	9.6
	2	98.0%	100.0%	96.0%	100.0%	94.0%		7.2	7.2	7.3	7.4	6.7	9.0
29	1	100.0%	100.0%	96.0%	94.0%	98.0%		7.1	7.5	7.6	7.1	7.4	9.2
	2	100.0%	100.0%	98.0%	95.9%	98.0%		7.7	7.7	7.4	7.3	7.0	8.5

Table C-9. Flat or Elongated 3:1and 2D Form Results of Granite for ILS Analysis

Granite		Flat or Elongated 3:1						2D Form					
Laboratory	Scan #	25.0 (1.0")	19.0 (3/4")	12.5 (1/2")	9.5 (3/8")	4.75 (#4)		2.36 (#8)	1.18 (#16)	0.6 (#30)	0.3 (#50)	0.15 (#100)	0.075 (#200)
1	1	96.0%	94.0%	98.0%	88.0%	89.8%		7.6	7.9	7.9	7.6	7.7	8.9
	2	95.9%	95.9%	91.8%	93.9%	96.0%		7.5	7.9	7.6	7.9	7.9	9.6
2	1	96.0%	96.0%	96.0%	94.0%	94.1%		7.7	7.7	7.9	7.8	7.7	9.1
	2	98.0%	94.0%	96.0%	90.0%	96.1%		7.8	7.9	8.2	7.9	8.1	9.4
3	1	91.8%	91.8%	93.9%	94.0%	98.0%		7.3	7.4	8.0	7.4	8.0	10.2
	2	96.0%	96.0%	93.9%	86.0%	94.0%		7.6	7.7	7.7	7.7	8.2	9.9
4	1	92.0%	96.0%	96.0%	86.0%	92.0%		7.7	7.8	8.2	7.8	7.7	9.2
	2	94.0%	93.9%	92.0%	90.0%	96.0%		7.7	7.6	7.9	8.1	7.9	10.0
5	1	94.0%	96.3%	90.0%	100.0%	91.8%		7.8	8.0	8.8	8.6	8.1	10.2
	2	95.9%	94.0%	84.0%	96.0%	93.9%		7.8	8.4	8.3	8.5	8.1	9.5
6	1	94.0%	96.0%	87.2%	98.0%	94.0%		7.9	7.9	7.8	7.7	7.7	10.1
	2	93.9%	96.0%	88.0%	100.0%	95.9%		7.7	7.9	7.9	7.6	8.2	9.4
7	1	94.0%	98.0%	88.0%	100.0%	100.0%		7.8	8.0	7.5	7.9	8.0	9.6
	2	93.9%	100.0%	87.8%	100.0%	94.0%		7.7	8.5	7.9	7.9	8.2	9.8
8	1	93.9%	98.0%	88.0%	100.0%	84.0%		8.0	7.9	8.0	7.8	7.9	9.6
	2	95.9%	98.0%	88.0%	100.0%	93.6%		8.0	8.1	7.7	7.8	7.8	9.5
9	1	91.8%	84.0%	91.8%	93.9%	86.0%		7.8	7.8	8.2	8.4	8.4	10.4
	2	94.0%	86.0%	90.0%	93.9%	92.0%		7.5	7.7	8.3	8.1	8.1	10.2
10	1	96.0%	84.0%	96.0%	90.0%	93.9%		7.6	7.6	8.1	7.8	7.9	9.9
	2	98.0%	88.0%	94.0%	91.8%	96.0%		7.4	7.4	8.0	7.9	8.1	9.8
11	1	96.0%	84.0%	93.9%	90.0%	92.0%		8.1	7.5	8.0	8.2	7.6	10.1
	2	96.0%	86.0%	95.9%	94.0%	94.0%		7.4	7.7	8.1	7.8	7.7	9.2
12	1	94.0%	84.0%	98.0%	94.0%	100.0%		7.6	7.6	8.1	8.2	7.4	9.5

	2	98.0%	89.8%	96.0%	90.0%	90.0%		7.5	7.8	8.3	8.2	7.1	7.4
13	1	89.8%	90.0%	94.0%	92.0%	97.9%		7.7	8.0	8.0	8.2	7.9	8.8
	2	94.0%	90.0%	92.0%	90.0%	96.0%		7.6	7.6	8.2	8.1	8.1	10.5
14	1	98.0%	93.9%	90.0%	98.0%	94.0%		7.7	7.9	8.0	7.8	8.1	9.9
	2	98.0%	89.8%	91.7%	98.0%	94.0%		7.7	7.6	7.7	7.8	8.1	9.8
15	1	81.6%	85.7%	94.0%	86.0%	93.8%		7.8	7.8	7.7	7.7	7.9	10.5
	2	78.0%	86.0%	92.0%	94.0%	90.0%		7.6	7.5	8.0	7.7	7.8	10.2
16	1	80.0%	88.0%	90.0%	96.0%	95.9%		7.8	7.8	7.9	8.0	8.5	9.5
	2	83.7%	86.0%	90.0%	92.0%	87.8%		7.5	7.7	8.0	7.9	7.8	9.0
17	1	83.7%	90.0%	88.0%	89.6%	87.0%		7.6	7.7	7.8	8.2	8.1	9.6
	2	80.0%	94.0%	88.0%	94.0%	97.9%		7.5	7.8	7.7	8.2	8.0	9.5
18	1	86.0%	93.9%	87.8%	85.7%	91.8%		7.4	7.6	7.7	7.8	7.9	9.7
	2	88.0%	96.0%	94.0%	90.0%	96.0%		7.5	7.8	7.6	7.4	7.6	9.1
19	1	92.0%	93.8%	96.0%	98.0%	98.0%		7.5	7.5	8.0	8.3	8.2	9.0
	2	83.7%	88.0%	90.0%	92.0%	96.0%		7.4	7.4	8.1	8.2	7.9	9.6
20	1	90.0%	96.0%	86.0%	96.0%	96.0%		7.6	7.8	7.9	7.8	7.9	8.7
	2	93.9%	92.0%	90.0%	92.0%	94.0%		7.4	7.7	7.8	7.8	7.9	9.2
21	1	84.0%	88.0%	86.0%	91.8%	96.0%		7.5	7.4	8.0	7.7	8.0	9.1
	2	89.8%	91.8%	86.0%	90.0%	98.0%		7.4	7.5	7.7	7.8	8.2	9.6
22	1	96.0%	90.0%	98.0%	94.0%	98.0%		7.8	7.9	7.8	7.7	7.8	8.4
	2	100.0%	90.0%	96.0%	96.0%	96.0%		7.9	7.8	8.0	7.8	7.8	10.0
23	1	100.0%	80.0%	87.5%	98.0%	98.0%		8.1	7.7	8.0	7.7	8.5	8.9
	2	96.0%	78.0%	100.0%	96.0%	94.0%		7.7	7.5	7.8	8.4	8.0	9.1
24	1	100.0%	96.0%	98.0%	95.9%	98.0%		7.9	7.5	7.7	8.4	8.1	9.5
	2	100.0%	92.0%	92.0%	96.0%	94.0%		7.8	7.7	8.0	8.3	8.0	10.1
25	1	100.0%	96.0%	95.8%	100.0%	100.0%		7.5	7.7	7.6	7.8	8.2	9.9
	2	98.0%	94.0%	91.7%	98.0%	100.0%		7.5	7.5	7.8	7.8	8.1	8.7

26	1	93.9%	82.0%	96.0%	95.9%	96.0%		7.4	7.6	8.0	7.9	7.9	9.3
	2	94.0%	78.0%	92.0%	96.0%	95.9%		7.5	7.3	7.6	8.0	7.8	9.9
27	1	94.0%	80.0%	90.0%	100.0%	96.0%		7.6	7.6	7.1	8.2	7.6	9.1
	2	96.0%	82.0%	96.0%	98.0%	96.0%		7.5	7.5	8.1	8.2	7.7	8.5
28	1	96.0%	84.0%	96.0%	98.0%	94.0%		7.6	7.3	7.6	8.2	7.9	9.6
	2	94.0%	83.7%	94.0%	98.0%	100.0%		7.8	7.3	7.6	8.3	8.3	9.9
29	1	95.9%	91.8%	91.8%	96.0%	90.0%		7.7	7.5	8.0	8.0	8.1	8.9
	2	98.0%	89.6%	89.8%	94.0%	96.0%		7.2	7.7	7.9	7.7	7.8	9.0

VITA

Leslie Leigh Gates was born in Buffalo Gap, Texas. She was awarded a degree of Bachelor of Science in Civil Engineering in May 2008 from Texas A&M University in College Station, Texas. While working toward her degree, she worked as a research assistant and was supported by the Transportation Scholars Program. She graduated with a Master of Science degree specializing in pavement materials in May 2010 from Texas A&M University.

Leslie L. Gates

c/o

Dr. Eyad Masad

CE/TTI 503-H

3136 TAMU

College Station, TX 77843

lgaggie@gmail.com